frontiers
RESEARCH TOPICS

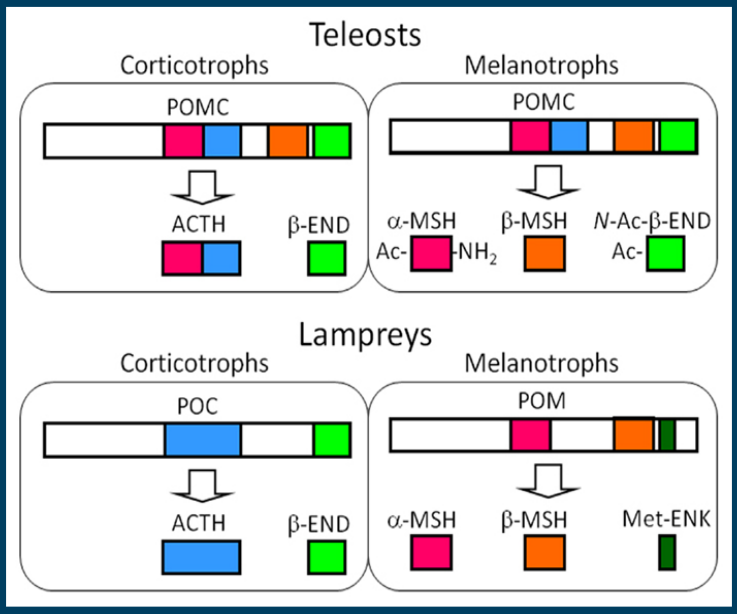

POSTTRANSLATIONAL MODIFICATION OF INTERCELLULAR MESSENGER SYSTEMS

Topic Editors
Sho Kakizawa, Hiroyuki Kaiya and Akiyoshi Takahashi

frontiers in ENDOCRINOLOGY

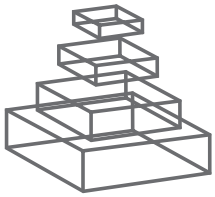

frontiers

ISSN 1664-8714
ISBN 978-2-88919-236-6
DOI 10.3389/978-2-88919-236-6

ABOUT FRONTIERS

Frontiers is more than just an open-access publisher of scholarly articles: it is a pioneering approach to the world of academia, radically improving the way scholarly research is managed. The grand vision of Frontiers is a world where all people have an equal opportunity to seek, share and generate knowledge. Frontiers provides immediate and permanent online open access to all its publications, but this alone is not enough to realize our grand goals.

FRONTIERS JOURNAL SERIES

The Frontiers Journal Series is a multi-tier and interdisciplinary set of open-access, online journals, promising a paradigm shift from the current review, selection and dissemination processes in academic publishing.
All Frontiers journals are driven by researchers for researchers; therefore, they constitute a service to the scholarly community. At the same time, the Frontiers Journal Series operates on a revolutionary invention, the tiered publishing system, initially addressing specific communities of scholars, and gradually climbing up to broader public understanding, thus serving the interests of the lay society, too.

DEDICATION TO QUALITY

Each Frontiers article is a landmark of the highest quality, thanks to genuinely collaborative interactions between authors and review editors, who include some of the world's best academicians. Research must be certified by peers before entering a stream of knowledge that may eventually reach the public - and shape society; therefore, Frontiers only applies the most rigorous and unbiased reviews.
Frontiers revolutionizes research publishing by freely delivering the most outstanding research, evaluated with no bias from both the academic and social point of view.
By applying the most advanced information technologies, Frontiers is catapulting scholarly publishing into a new generation.

WHAT ARE FRONTIERS RESEARCH TOPICS?

Frontiers Research Topics are very popular trademarks of the Frontiers Journals Series: they are collections of at least ten articles, all centered on a particular subject. With their unique mix of varied contributions from Original Research to Review Articles, Frontiers Research Topics unify the most influential researchers, the latest key findings and historical advances in a hot research area!
Find out more on how to host your own Frontiers Research Topic or contribute to one as an author by contacting the Frontiers Editorial Office: researchtopics@frontiersin.org

POSTTRANSLATIONAL MODIFICATION OF INTERCELLULAR MESSENGER SYSTEMS

Topic Editors:
Sho Kakizawa, Kyoto University, Japan
Hiroyuki Kaiya, National Cerebral and Cardiovascular Center Research Institute, Japan
Akiyoshi Takahashi, Kitasato University, Japan

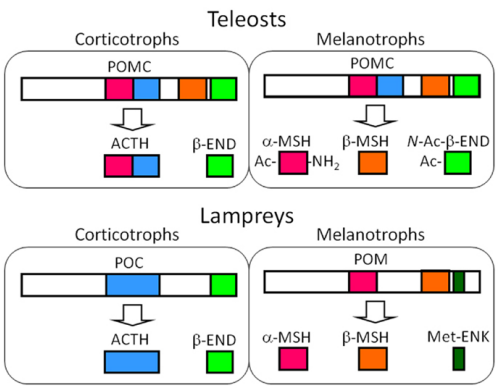

Major POMC-derived peptides in the corticotrophs of the PD and the melanotrophs of the PI in teleost and lamprey pituitary glands based on the results from the barfin flounder (Verasper moseri) (14, 46, 50) and sea lamprey (Petromyzon marinus) (14, 57–59). In the original paper on the sea lamprey POMC, α-MSH, and β-MSH are termed MSH-B and MSH-A, respectively (59). The major products in these cells are common between teleosts and lampreys – ACTH and END in the melanotrophs, and MSHs and opioid peptides, i.e., N-Ac-β-END or Met-ENK. The differences between teleosts and lampreys lie in the genes expressed; identical POMCs are generated in the corticotrophs and melanotrophs of teleosts, as is the case for tetrapods. In contrast, different precursors are generated in lampreys.

[Reproduced with permission from Takahashi and Mizusawa; *Front. Endocrinol.*, 17 October 2013 | doi: 10.3389/fendo.2013.00143]

While it is estimated that the human genome comprises ~27,000 genes, the total number of proteins in the human proteome is estimated at over 1 million. In addition to changes at the transcriptional and mRNA levels, "posttranslational modification of proteins" increases the functional diversity of the proteome. Now, it is increasingly recognized that posttranslational modifications of proteins provide important roles in a wide range of "intercellular signaling pathways", such as endocrine systems. For example, n-octanoyl modification at Ser(3) is essential for ghrelin-induced bioactivities. Moreover, gaseous messengers, such as nitric oxide and hydrogen sulfide, are highly active and affect the functions of target proteins by S-nitrosylation and S-sulfhydration, respectively.

This Research Topic aims to assemble a series of review articles and original research papers on structural analysis or functional significance of posttranslational modification of/by intercellular messengers, including hormonal messengers and gaseous messengers, in animals and plants. The contributing papers may illustrate variety and importance of biological events regulated by posttranslational modification of functional molecules, and become major references for those working in the field of physiology and cell biology.

Table of Contents

frontiers in
ENDOCRINOLOGY

EDITORIAL
published: 05 March 2014
doi: 10.3389/fendo.2014.00027

Posttranslational modification of intercellular messenger systems

Sho Kakizawa[1]*, Hiroyuki Kaiya[2] and Akiyoshi Takahashi[3]

[1] *Department of Biological Chemistry, Graduate School of Pharmaceutical Sciences, Kyoto University, Kyoto, Japan*
[2] *Department of Biochemistry, National Cerebral and Cardiovascular Center Research Institute, Suita, Japan*
[3] *School of Marine Biosciences, Kitasato University, Sagamihara, Japan*
**Correspondence: sho-kaki@pharm.kyoto-u.ac.jp*

Edited and reviewed by:
Cunming Duan, University of Michigan, USA

Keywords: posttranslational modification, hormone, gaseous messenger, endocrine system, receptor

While it is estimated that the human genome comprises ~27,000 genes, the total number of proteins in the human proteome is estimated at over one million. In addition to changes at the transcriptional and mRNA levels, "posttranslational modification of proteins" increases the functional diversity of the proteome. Now, it is increasingly recognized that posttranslational modifications of proteins provide important roles in a wide range of "intercellular signaling pathways," such as endocrine systems. For example, *n*-octanoyl modification at Ser(3) is essential for ghrelin-induced bioactivities. Moreover, gaseous messengers, such as nitric oxide and hydrogen sulfide are highly active and affect the functions of target proteins by S-nitrosylation and S-sulfhydration, respectively.

This Research Topic is aimed to assemble a series of review articles and original research papers on structural analysis or functional significance of posttranslational modification of/by intercellular messengers, including hormonal messengers and gaseous messengers, in vertebrates and invertebrates: posttranslational modification of peptide hormones such as proopiomelanocortin (1, 2), ghrelin (3–5), and hormonal receptors and effectors (6–8). Review articles on gaseous messengers such as hydrogen sulfide (9) and nitric oxide (10) are also included. The contributing papers illustrate variety and importance of biological events regulated by posttranslational modification of functional molecules, and may become major references for those working in the field of physiology and cell biology.

REFERENCES

1. Takahashi A, Mizusawa K. Posttranslational modifications of proopiomelanocortin in vertebrates and their biological significance. *Front Endocrinol* (2013) **4**:143. doi:10.3389/fendo.2013.00143
2. Yasuda A, Jones LS, Shigeri Y. The multiplicity of post-translational modifications in pro-opiomelanocortin-derived peptides. *Front Endocrinol* (2013) **4**:186. doi:10.3389/fendo.2013.00186
3. Riley LG. Different forms of ghrelin exhibit distinct biological roles in tilapia. *Front Endocrinol* (2013) **4**:118. doi:10.3389/fendo.2013.00118
4. Nishi Y, Mifune H, Yabuki A, Tajiri Y, Hirata R, Tanaka E, et al. Changes in subcellular distribution of n-octanoyl or n-decanoyl ghrelin in ghrelin-producing cells. *Front Endocrinol* (2013) **4**:84. doi:10.3389/fendo.2013.00084
5. Kaiya H, Andoh T, Ichikawa T, Amiya N, Matsuda K, Kangawa K, et al. Determination of ghrelin structure in the barfin flounder (Verasper moseri) and involvement of ingested fatty acids in ghrelin acylation. *Front Endocrinol* (2013) **4**:117. doi:10.3389/fendo.2013.00117
6. Satake H, Matsubara S, Aoyama M, Kawada T, Sakai T. GPCR heterodimerization in the reproductive system: functional regulation and implication for biodiversity. *Front Endocrinol* (2013) **4**:100. doi:10.3389/fendo.2013.00100
7. Saito Y, Hamamoto A, Kobayashi Y. Regulated control of melanin-concentrating hormone receptor 1 through posttranslational modifications. *Front Endocrinol* (2013) **4**:154. doi:10.3389/fendo.2013.00154
8. Wakayama N, Katow T, Katow H. Characterization and endocytic internalization of Epith-2 cell surface glycoprotein during the epithelial-to-mesenchymal transition in sea urchin embryos. *Front Endocrinol* (2013) **4**:112. doi:10.3389/fendo.2013.00112
9. Shibuya N, Kimura H. Production of hydrogen sulfide from d-cysteine and its therapeutic potential. *Front Endocrinol* (2013) **4**:87. doi:10.3389/fendo.2013.00087
10. Kakizawa S. Nitric oxide-induced calcium release: activation of type 1 ryanodine receptor, a calcium release channel, through non-enzymatic post-translational modification by nitric oxide. *Front Endocrinol* (2013) **4**:142. doi:10.3389/fendo.2013.00142

Received: 19 February 2014; accepted: 19 February 2014; published online: 05 March 2014.
*Citation: Kakizawa S, Kaiya H and Takahashi A (2014) Posttranslational modification of intercellular messenger systems. Front. Endocrinol. **5**:27. doi: 10.3389/fendo.2014.00027*
This article was submitted to Experimental Endocrinology, a section of the journal Frontiers in Endocrinology.

frontiers in
ENDOCRINOLOGY

REVIEW ARTICLE
published: 15 August 2013
doi: 10.3389/fendo.2013.00100

GPCR heterodimerization in the reproductive system: functional regulation and implication for biodiversity

Honoo Satake*, Shin Matsubara, Masato Aoyama, Tsuyoshi Kawada and Tsubasa Sakai

Suntory Foundation for Life Sciences, Bioorganic Research Institute, Osaka, Japan

Edited by:
Hiroyuki Kaiya, National Cerebral and Cardiovascular Center, Japan

Reviewed by:
T. John Wu, Uniformed Services University of the Health Sciences, USA
Yumiko Saito, Hiroshima University, Japan

****Correspondence:***
Honoo Satake, Suntory Foundation for Life Sciences, Bioorganic Research Institute, 1-1-1 Wakayamadai, Shimamoto, Mishima, Osaka 618-8503, Japan
e-mail: satake@sunbor.or.jp

A G protein-coupled receptor (GPCR) functions not only as a monomer or homodimer but also as a heterodimer with another GPCR. GPCR heterodimerization results in the modulation of the molecular functions of the GPCR protomer, including ligand binding affinity, signal transduction, and internalization. There has been a growing body of reports on heterodimerization of multiple GPCRs expressed in the reproductive system and the resultant functional modulation, suggesting that GPCR heterodimerization is closely associated with reproduction including the secretion of hormones and the growth and maturation of follicles and oocytes. Moreover, studies on heterodimerization among paralogs of gonadotropin-releasing hormone (GnRH) receptors of a protochordate, *Ciona intestinalis*, verified the species-specific regulation of the functions of GPCRs via multiple GnRH receptor pairs. These findings indicate that GPCR heterodimerization is also involved in creating biodiversity. In this review, we provide basic and current knowledge regarding GPCR heterodimers and their functional modulation, and explore the biological significance of GPCR heterodimerization.

Keywords: GPCR, heterodimer, reproduction, diversity hormones

INTRODUCTION

The development of "omics" technologies and ensuring construction of a variety of databases provide vast information regarding primary sequences and functional domains of genes and proteins in diverse organisms, leading to annotation or prediction of biochemical and pharmacological propensities of novel genes and proteins. Even in this post-genomic era, several functions of proteins have yet to be fully elucidated or predicted. One of the most unpredictable and confounding post-translational protein functions is the heterodimerization of G protein-coupled receptors (GPCRs).

Currently, a wide range of GPCRs have been proved to function not only as monomers or homodimers but also as heterodimers formed after translation. It has been shown that GPCR heterodimerization alters or fine-tunes ligand binding, signaling, and internalization of GPCR protomers (1–9). The greatest difficulty in studies on GPCR heterodimers lies in the lack of procedures for the prediction of either GPCR protomer pairs for heterodimerization or the resultant functional alteration of GPCRs. Consequently, high-throughput analysis of GPCR heterodimers (e.g., "GPCR heterodimerome") has not yet been accomplished. Despite this shortcoming, there have been increasing findings regarding the biological and pathological significance of GPCR heterodimerization.

Reproduction is regulated by diverse neuropeptides and hormones, with the receptors belonging to the GPCR family, e.g., melatonin, kisspeptin, neurokinin B (NKB), gonadotropin-inhibitory hormone (GnIH), gonadotropin-releasing hormone (GnRH), luteinizing hormone (LH), follicle-stimulating hormone (FSH), and prostanoids (10–13). In vertebrates, these hormones and neuropeptides play crucial roles in the hypothalamus-pituitary-gonad (HPG) axis (**Figure 1**). Furthermore, various species-specific GPCRs for highly conserved cognate hormones or neuropeptides have been identified (14–18, Kawada et al., forthcoming). Collectively, these findings suggest that GPCR heterodimerization participates in the fine-tuning and diversification of reproductive functions. In this article, we provide an overview of GPCR heterodimerization and discuss the implication of GPCR heterodimers in reproductive functions and their diversification.

GPCR PROTOMERS AS ALLOSTERIC MODULATORS

It is widely accepted that GPCRs can assume various active conformations which enable coupling with distinct G proteins and other associated proteins followed by particular signal transduction cascades (3, 8, 19, 20). Moreover, allosteric effectors interact with GPCRs at binding sites different from those for agonists or antagonists and modulate the conformations of GPCRs, leading to alterations in agonist/antagonist binding affinity or signal transduction (3, 8, 19, 20). Also of significance is that each of the active conformations responsible for individual signaling pathways is not interconvertible (3, 8, 19–21). Combined with experimental evidence that ligand binding and signaling of GPCR protomers are altered via heterodimerization, GPCR heterodimerization is believed to induce protomer-specific modulation (i.e., stabilization or instabilization) of active conformations as an endogenous allosteric modulator. This view is compatible with the fact that a single GPCR protomer acquires diverse biochemical and/or pharmacological properties via heterodimerization with different GPCR partners.

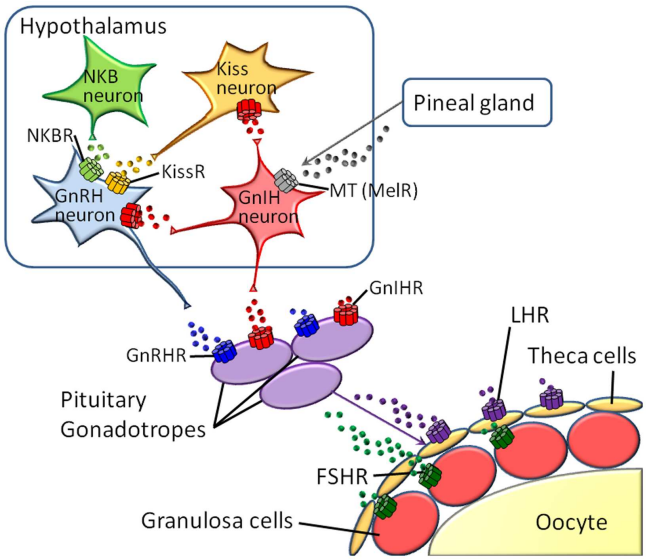

FIGURE 1 | Major GPCRs for neuropeptides or hormones in the hypothalamus-pituitary-gonad (HPG) axis.

TYPICAL FUNCTIONAL CONSEQUENCES OF GPCR HETERODIMERIZATION

Obviously, colocalization of GPCR protomers in a cell is a prerequisite for the formation of the corresponding GPCR heterodimer in native tissues. However, many early studies demonstrated functional alteration of GPCRs only after co-transfection of cultured cells with two GPCRs but not at the level of endogenous co-expression in the same cells in a particular native tissue. Consequently, the biological and physiological significance of such "*in vitro*-only" GPCR heterodimers is highly questionable. Consistent with this, the International Union of Basic and Clinical Pharmacology (IUPHAR) release the paradigm for GPCR heterodimer studies in 2007 (2). First, interaction between GPCR protomers in native tissues should be proved by at least two different experimental procedures including co-immunoprecipitation, fluorescence resonance energy transfer (FRET), or bioluminescence resonance energy transfer (BRET). Second, alteration of biochemical or pharmacological functions of GPCRs should be observed in native tissues or co-transfected cells. Third, biological roles of GPCR heterodimers should be verified using gene-knockout or gene-silenced procedures. At present, meeting all of these criteria is too difficult. Thus, IUPHAR proposed that researchers fulfill at least two of the three criteria. In the following, we focus on GPCR heterodimers which were detected in native tissues (**Table 1**).

G protein-coupled receptor heterodimers are classified into two groups in light of their functions: obligatory and non-obligatory GPCR heterodimers. Obligatory GPCR heterodimers require heterodimerization of GPCR protomers to serve as functional receptors, such as gamma amino butyric acid (GABA) type B receptor and taste receptors. $GABAR_{B1}$ alone is sequestered in the endoplasmic reticulum (ER) due to the presence of an ER retention signal, which is masked by heterodimerization with $GABAR_{B2}$ (22–24). Moreover, the $GABAR_{B1}$ protomer harbors a ligand-binding site, whereas the $GABAR_{B2}$ protomer merely couples to G proteins (22–24). Therefore, the $GABAR_{B1}$ -$GABAR_{B2}$ heterodimer serves as an authentic GABA receptor. Taste receptors also exhibit heterodimerization-dependent pharmacological profiles. The heterodimer between T1R1 and T1R3 is exclusively responsive to umami taste, while the T1R2–T1R3 heterodimer is a specific receptor for sweet taste-inducing molecules (25–27).

Table 1 | Typical functional alteration of GPCRs via heterodimerization.

Heterodimer	Effect
$GABAR_{B1}$–$GABAR_{B2}$	Transition from ER to plasma membrane and function
T1R1–T1R3	Recognition of umami substances
T1R2–T1R3	Recognition of sweet substances
AT1–B2	Increase of IP_3 accumulation induced by angiotensin II or bradykinin
MOR–DOR	Reduction in binding affinity of Met-enkephalin Increase in binding affinity of endomorphin-1 and Leu-enkephalin Shift of coupling of Gz to Gi
KOR–DOR	Enhancement of signaling induced by synthetic KOR agonists
OR1–CB1	Suppression of OR-triggered ERK phosphorylation by a CB1 antagonist Suppression of CB-triggered ERK phosphorylation by a OR1 antagonist
MC3R–GHSR	Increase in cAMP production induced by melanocortin Decrease in ghrelin-induced signaling
D1–D2	Shift of coupling of Gs to Gq/11
MT1–GPR50	Decrease of melatonin-binding, Gi-coupling/signaling, and internalization
NK1–MOR	Alternation of internalization and resensitization profile
R1–R4	Upregulation of ERK phosphorylation via Ca^{2+}-dependent PKCα activation and Ca^{2+}-independent PKCζ activation
R2–R4	Reduction in cAMP production via shift of coupling of Gs to Gi
EP1–β2AR	Dissociation of Gs from bA2R induced by EP1 agonists

GABAR, GABA receptor; T1R, taste receptor; AT1, angiotensin receptor 1; B2 bradykinin receptor 2; MOR, μ-opioid receptor; DOR, δ-opioid receptor; KOR, κ-opioid receptor; OR1, orexin receptor 1; CB1, cannabinoid receptor 1; MC3R, melanocortin receptor 3; GHSR, ghrelin receptor; D1, dopamine receptor 1; MT1, melatonin receptor 1, NK1, tachykinin receptor 1; Ci-GnRHR, Ciona intestinalis GnRH receptor; EP1, prostaglandin E2 receptor 1.

In contrast, non-obligatory GPCR heterodimers are composed of the functional GPCR protomers and modulate the biochemical or pharmacological activities of the protomers (**Table 1**). Non-obligatory GPCR heterodimers account for the major population and exhibit diverse modulatory functions. In human embryonic kidney (HEK) 293 cells expressing the angiotensin II receptor (AT1)-bradykinin receptor (B2) heterodimer, angiotensin II triggered inositol triphosphate (IP_3) accumulation much more potently and effectively than it did in the cells expressing AT1 alone, whereas IP_3 accumulation by bradykinin was slightly weaker in cells expressing the AT1–B2 heterodimer than in the cells expressing only B2 (28). This enhancement was also detected *in vivo*, where AT1 and B2 were shown to form a heterodimer in smooth muscle, omental vessel, and platelets (28, 29).

The opioid receptor family is composed of three subtypes, namely, μ-, δ-, and κ-opioid receptors (MOR, DOR, and KOR), all of which mediate inhibition of cAMP production with different ligand-selectivity (30). Co-expression of MOR and DOR in HEK293 cells resulted in a 10-fold reduction in binding affinity of a synthetic MOR-selective agonist, DAMGO (31). Moreover, the MOR-DOR heterodimer differs in rank order of affinities for endogenous peptide ligands; Met-enkephalin, possessing the highest affinity for MOR among endogenous opioid peptides, exhibited twofold lower affinity to the MOR-DOR heterodimer, while the affinity of endomorphin-1 and Leu-enkephalin to the heterodimer was increased two to threefold, compared to MOR (31). Moreover, heterodimerization of MOR and DOR predominantly induced activation of a pertussis toxin-insensitive G protein, Gz in COS-7 cells, while monomeric or homodimeric MOR and DOR were coupled to a pertussis toxin-sensitive G protein, Gi (32). This is consistent with findings that the binding of ligands to the MOR–DOR heterodimer followed by signal transduction is resistant to pertussis toxin (32). A KOR-selective agonist, U69593, exhibited as potent and efficacious activities at the heterodimer as at KOR, whereas 6′-GNTI was a sixfold more potent agonist for the KOR–DOR heterodimer than for the KOR homodimer (33). More recently, *N*-naphthoyl-β-naltrex-amine (NNTA), a potent antagonist for MOR, was shown to manifest a prominent agonistic activity at MOR–DOR (34). In the mouse tail-flick assay, intrathecal NNTA elicited 100-fold greater antinociception, compared to intracerebroventricular administration (34). These heterodimerization-based pharmacological alterations are expected to provide crucial clues to understand why various *in vivo* pharmacological profiles are inconsistent with those from *in vitro* studies using cells expressing each opioid receptor alone and to develop more specific clinical agents for opioid receptors.

When an orexin receptor OR1 was co-expressed with a cannabinoid receptor CB1 in HEK293 cells, addition of a CB1-specific antagonist, SR-141716A, resulted in the suppression of orexin-triggered phosphorylation of ERK1/2 (35). Likewise, an OR1-specific antagonist, SB-674042, attenuated the ERK phosphorylation activated by a CB1 agonist, WIN55212-2 (35). These data verify the regulatory mechanism by which one GPCR protomer bound to an antagonist modulates the pharmacological profile of another GPCR protomer through heterodimerization.

Melanocortin receptor 3 (MC3R) and ghrelin receptor (GHSR) were found to be co-expressed in a number of neurons in the arcuate nucleus (36, 37). Co-transfection of MC3R and GHSR into COS-7 cells enhanced melanocortin-induced intracellular cAMP accumulation, compared with activation of MC3R in the absence of GHSR, whereas both agonist-independent basal and ghrelin-induced signaling of GHSR were diminished (36). These findings reveal mutual opposite signal modulation by each protomer and suggest that the molecular mechanism underlying a certain agonist-independent active conformation of a protomer is also involved in the regulation of the signaling functionalities of its partner GPCR in a heterodimer. Since MC3R and GHSR play pivotal roles in the orexigenic system, the MC3R–GHSR heterodimer is involved in hypothalamic body weight regulation.

There is increasing evidence for a pathological relevance of GPCR heterodimer. AT1–B2 heterodimer is highly likely to be functionally correlated with preeclampsia. The AT1–B2 heterodimer was more abundant on platelets of preeclamptic women than on platelets of normotensive pregnant women (29). Such increase in the number of heterodimers is due to enhanced expression of B2, as the expression level of B2 was elevated four to fivefold on platelets of preeclamptic women compared to platelets of normotensive pregnant women, whereas expression of AT1 was unchanged (29). Moreover, mobilization of intracellular calcium ions induced by angiotensin II was up-regulated 1.7- to 1.9-fold in platelets of preeclamptic women, compared to normotensive pregnant women (28, 29).

Heterodimerization between dopamine receptor subtypes, D1 and D2, has shown to be implicated in depression. The D1–D2 heterodimer was detected at higher levels in the post-mortem striatum of the patients compared to in normal subjects using co-immunoprecipitation and D1–D2 heteromer-selective antibodies (38). Moreover, dissociation of the D1–D2 heterodimer by an interfering peptide that disrupts the heteromer resulted in substantially reduced immobility in the forced swim test without affecting locomotor activity, and decreased escape failures in learned helplessness tests in rats (38). It should be noted that the heterodimerization between D1 and D2 leads to a drastic shift of G protein coupling; D1 and D2 monomer/homomer are coupled to Gs and Gi, respectively, while Gq/11 is a major G protein-coupled to the D1–D2 heterodimer (39).

More recently, MOR–DOR heterodimer was found to play pivotal roles in the opioid system. An interaction-disrupting peptide fragment for the MOR–DOR heterodimer enhanced morphine analgesia and reduced anti-nociceptive tolerance to morphine in mice (40).

HETERODIMERS AMONG REPRODUCTION – ASSOCIATED GPCRs

MELATONIN RECEPTOR

Melatonin participates in reproductive functions via upregulation of the synthesis and secretion of GnIH in the hypothalamus of mammals and birds (10, 11). Moreover, melatonin receptors were also shown to be expressed in gonads (41), and melatonin significantly decreases testosterone secretion from LH/FSH-stimulated testes of European starlings before breeding (42). Two class A (rhodopsin-like) GPCRs for melatonin, MT1 and MT2, have been

identified in mammals (1, 43). A human orphan GPCR, GPR50, sharing the highest sequence homology with MT1 and MT2, was shown to form a heterodimer with both receptors in HEK293 cells (1, 43). Moreover, heterodimerization of GPR50 with MT1 resulted in a marked reduction of the ability of MT1 to bind to ligands and to couple to G proteins, resulting in decreased in Gi protein-coupled intracellular signaling and β-arrestin – assisted internalization in HEK293 cells, whereas functions of MT2 were not affected (1, 43). These data indicate that GPR50 antagonizes MT1 but not MT2 via heterodimerization. In addition, this is the first report on the functional role of an orphan receptor as a protomer of a GPCR heterodimer.

TACHYKININ RECEPTOR

Tachykinins (TKs) are vertebrate and ascidian multifunctional brain/gut peptides involved in smooth muscle contraction, vasodilation, nociception, inflammation, neurodegeneration, and neuroprotection in a neuropeptidergic endocrine, paracrine fashion (44–48). The mammalian TK family consists of four major peptides: Substance P (SP), Neurokinin A (NKA), NKB, and Hemokinin-1/Endokinins (HK-1/EKs) (EK is a human homolog of mouse and rat HK-1). TK receptors belong to the class A GPCR family. Three subtypes of TK receptors, namely NK1, NK2, and NK3, have been identified in mammals, and several submammalian orthologs have been cloned or suggested by genomic database search. In the ascidian, *Ciona intestinalis*, authentic TK, and its cognate receptor, Ci-TK-I and Ci-TK-R were identified (49, 50). Recently, there are accumulating reports on reproductive roles of TKs as well as the expression of TKs and TK receptors in genital organs of mammals (46, 48, 49, 51–54). In *C. intestinalis*, Ci-TK-I enhances oocyte growth from the vitellogenic stage to the post-vitellogenic stage via upregulation of gene expression and enzymatic activity of several proteases such as cathepsin D, carboxypeptidase B1, and chymotrypsin (55–57). Over the past few years, there has been increasing evidence that NKB plays a central role in the direct enhancement of GnRH synthesis and release in the hypothalamus of mammals, eventually leading to the recognition of novel regulatory function in sexual maturation and reproduction [(58–65)].

Only one tachykinin receptor-relevant heterodimer has thus far been identified. NK1 and an opioid receptor subtype, MOR, were shown to co-exist in pain-processing brain regions, including trigeminal dorsal horn neurons, and to heterodimerize in co-transfected HEK293 cells (66). NK1–MOR heterodimerization altered their internalization and resensitization profile, while ligand binding and signaling intensities of the protomers were not affected. In cells expressing NK1–MOR heterodimer, both DAMGO and SP induced the recruitment of β-arrestin to the plasma membrane and internalization of NK1–MOR heterodimers with β-arrestin into the same endosomal compartment (66). Recent studies also verified that other tachykinin receptors, such as NK3, are co-localized with various GPCRs including kisspeptin receptors and opioid receptors (59). Consequently, tachykinin receptors are expected to form heterodimers with a wide variety of GPCRs, which, in turn, are potentially involved in the molecular mechanisms underlying novel reproductive functions.

GnRH RECEPTOR

Gonadotropin-releasing hormones are hypothalamic decapeptides that regulate the HPG axis to control reproduction by releasing gonadotropins, FSH, and LH from the pituitary in vertebrates (**Figure 1**). The endogenous receptors, GnRHRs, which belong to the Class A GPCR family, have also been shown to possess species-specific paralogs forms in vertebrates. Type I GnRHRs, which completely lack a C-terminal tail region, are restricted to humans, rodents, and cows (14–16, 67, 68). Type II GnRHRs, which bear a C-terminal tail, are widely distributed throughout almost all vertebrates, whereas the type II *gnrhr* gene is silenced due to a deletion of functional domains or interruption of full-length translation by the presence of a stop codon in humans, chimpanzees, cows, and sheep (14–16, 67, 68). To date, no convincing evidence for heterodimerization of GnRHRs in native tissues has been provided.

Gonadotropin-releasing hormones have also been identified in a wide range of invertebrates that lack a pituitary (Kawada et al., forthcoming). To date, seven GnRH peptides (tGnRH-3 to -8 and Ci-GnRH-X) and four GnRH receptor subtypes (Ci-GnRHR-1 to -4) have been identified in *C. intestinalis* (69–71). Molecular phylogenetic analysis indicates that Ci-GnRHR2 (R2), R3, and R4 are *Ciona*-specific paralogs of R1 generated via gene duplication (70, 72). Only R1 activated IP_3 generation followed by intracellular Ca^{2+} mobilization in response to tGnRH-6, whereas R2 and R3 exclusively stimulate cAMP production in response to multiple tGnRHs; tGnRH-6, -7, and -8 exhibited near-equipotent cAMP production via R2, which was 100-fold more potent than tGnRH-3, -4, and -5. tGnRH-3 and -5 specifically triggered R3-mediated cAMP production (70, 73–75). R4 is devoid of binding to any tGnRHs or of activating any signaling pathways (70). Recently, we have shown that the orphan paralog, R4, is responsible for the fine-tuning of the GnRHergic signaling via heterodimerization with R1. The R1–R4 heterodimer elicited a 10-fold more potent Ca^{2+} mobilization than R1 monomer/homodimer in a tGnRH-6-selective manner, while cAMP production by R1 was not modulated via heterodimerization with R4 (73). The R1–R4 heterodimer potentiated translocation of both Ca^{2+}-dependent PKCα by tGnRH-6 and Ca^{2+}-independent PKCζ by tGnRH-5 and -6, eventually leading to upregulation of ERK phosphorylation, compared with R1 alone (73). These results provide evidence that the species-specific GnRHR orphan paralog, R4, serves as an endogenous modulator for the fine-tuning of the activation of PKC subtype-selective signal transduction via heterodimerization with R1. R4 was also shown to heterodimerize with R2 specifically in test cells of vitellogenic oocytes (74). Of particular interest is that the R2–R4 heterodimer in HEK293 cells decreased cAMP production in a non-ligand selective manner via a shift from activation of Gs protein to Gi protein by R2, compared with R2 monomer/homodimer (74). Considering that R1–R4 elicited a 10-fold more potent Ca^{2+} mobilization than R1 monomer/homodimer in a ligand selective manner but did not affect cAMP production, these results indicate that R4 regulates differential GnRH signaling cascades via heterodimerization with R1 and R2 as an endogenous allosteric modulator. Collectively, these studies suggest that heterodimerization among GnRHR paralogs, including the species-specific orphan receptor subtype, is involved in rigorous and diversified GnRHergic signaling in a protochordate lacking an HPG axis.

LH RECEPTOR

Luteinizing hormone is a central pituitary peptide hormone responsible for gonadal maturation (**Figure 1**). A single GPCR for LH has been identified in mammals. Although no LH receptor-containing GPCR heterodimer has been detected, studies on LH homodimers suggests that LH can also serve as a multifunctional protomer in various GPCR heterodimers. Co-expression of a ligand-binding-deficient LH receptor mutant and a signaling-deficient LH receptor mutant resulted in the restoration of normal gonadal and genital function in transgenic mice, indicating that LH receptor functions as a dimer *in vivo* (76).

PROSTAGLANDIN RECEPTOR

Prostanoids consist of prostaglandin (PG) D, PGE_2, $PGF_{2\alpha}$, PGI_2, and thromboxane A_2 and are responsible for a variety of actions in various tissues including the relaxation and contraction of various types of smooth muscles, pain transmission, fever generation, and sleep induction (77). Numerous studies have also proved that ovulation, corpus luteum development and regression are mediated by PGs (78–80). To date, eight GPCRs for PGs have been identified in mammals. Heterodimerization of a PGE_2 receptor, EP1, with β2 adrenergic receptor (β2AR) caused considerable reduction in cAMP production by β2AR *via* enhancement of the dissociation of Gs protein from β2AR in the presence of endogenous or synthetic EP1 agonists in primary cultures of airway smooth muscle or COS-7 cells (81). Of importance in the functional regulation by the GPCR heterodimer is that EP1 have a direct inhibitory effects on bronchodilatory signaling but rather modulates the function of the β2AR. These findings strongly suggest that the heterodimerization of β2AR with EP1 causes the β2-agonist resistance found in asthma (81).

EFFECTS OF GPCR HETERODIMERIZATION ON DIVERSIFICATION OF ANIMAL SPECIES AND BIOLOGICAL FUNCTION

G protein-coupled receptors are largely categorized into two groups. The first group consists of GPCRs conserved as authentic "homologs" in various species, and the second one includes species-specific GPCRs. The latter is further classified into GPCRs for species-specific ligands and subtypes of GPCRs for highly conserved ligands in various species. For instance, *C. intestinalis* GnRH receptors consists of four GPCRs as stated above: R1, R2, R3, and R4. Phylogenetic tree and biochemical analyses proved that R1 is structurally and functionally homologous to vertebrate GnRH receptors, whereas R2, R3, and R4 are *C. intestinalis*-specific paralogs that occurred via gene duplication in the *Ciona* evolutionary lineage (70, Kawada et al., forthcoming). Likewise, species-specific GnRHR-III has been identified in teleost species (14, 15), and lamprey has also three GnRHRs which are genetically independent of teleost GnRHR subtypes (16). Such species-specific GPCR paralogs are thought to determine the functional diversity and physiological regulatory systems, because GPCR paralogs can form species-specific GPCR heterodimers, which, if expressed in the same cells, control the unique expansion and fine-tuning of GPCR-mediated signaling pathways (**Figure 2**), as shown for *C. intestinalis* GnRHRs (73, 74). In other words, heterodimerization involving species-specific GPCRs is highly likely to contribute to the evolution and diversification of organisms to a large extent.

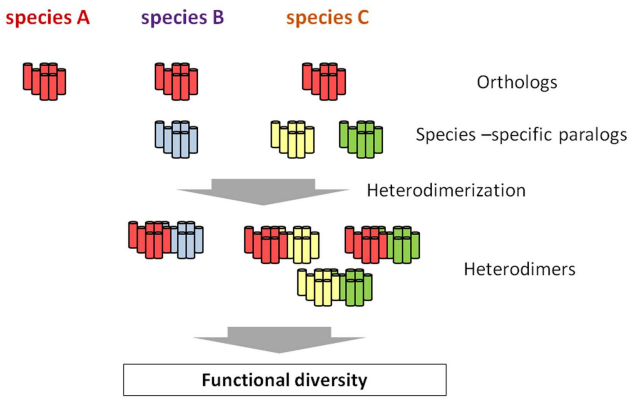

FIGURE 2 | Hypothetical scheme of the emergence of functional diversity *via* species-specific GPCR heterodimerization. All the species conserve the authentic orthologous GPCR (red), whereas species B and C possess one or two additional species-specific paralogs, respectively (blue, yellow, and green). While no heterodimer involving the orthologous GPCR is formed, species-specific GPCR heterodimers occur in species B and C. such species-specific heterodimers are highly likely to be closely related functional diversity of a certain GPCR family, ultimately leading to the evolution and diversification of organisms to a large extent.

CONCLUSION AND PERSPECTIVES

To date, GPCR heterodimerization has attracted keen attentions in light of biochemical and pharmacological features of GPCRs and the development of drugs with high selectivity, given that GPCR heterodimerization has been explored almost exclusively in mammals, except for *C. intestinalis* GnRHRs. Nevertheless, recent studies in various fields suggest that GPCR heterodimerization plays crucial roles in the regulation of the HPG axis and the evolution and diversification of reproductive functions. In this regard, of special interest is whether kisspeptin receptors or GnIH receptors heterodimerize with any GPCRs. Moreover, heterodimerization involving species-specific GPCR paralogs is expected to be responsible for the emergence of unique physiological functions in the respective organisms. Accordingly, combined with the fact that GPCRs form corresponding heterodimers after translation, investigation of GPCR heterodimerization in non-mammalian organisms will provide novel insight into the generation of biodiversity directed by a post-translational protein interaction.

In keeping with this issue, of particular interest is the clarification of the *in vivo* functional correlation between GPCR heterodimerization and biological events. Real-time imaging of GPCR heterodimerization could enable the visualization of biological functions of GPCR heterodimers of interest. Although this experimental strategy is unlikely to be applied to mammals, organisms equipped with transparent or semi-transparent skins, including ascidian, medaka, or zebrafish, are useful for live-imaging of GPCR heterodimers (50). Such studies are currently in progress in our laboratory.

ACKNOWLEDGMENTS

This study was in part financially supported by JSPS (to Honoo Satake, Masato Aoyama, and Tsuyoshi Kawada).

REFERENCES

1. Levoye A, Dam J, Ayoub MA, Guillaume JL, Couturier C, Delagrange P, et al. The orphan GPR50 receptor specifically inhibits MT1 melatonin receptor function through heterodimerization. *EMBO J* (2006) **25**:3012–23. doi:10.1038/sj.emboj.7601193
2. Pin JP, Neubig R, Bouvier M, Devi L, Filizola M, Javitch JA, et al. International Union of Basic and Clinical Pharmacology. LXVII. Recommendations for the recognition and nomenclature of G protein-coupled receptor heteromultimers. *Pharmacol Rev* (2007) **59**:5–13. doi:10.1124/pr.59.1.5
3. Satake H, Sakai T. Recent advances and perceptions in studies of heterodimerization between G protein-coupled receptors. *Protein Pept Lett* (2008) **15**:300–8. doi:10.2174/092986608783744207
4. Milligan G. G protein-coupled receptor hetero-dimerization: contribution to pharmacology and function. *Br J Pharmacol* (2009) **158**:5–14. doi:10.1111/j.1476-5381.2009.00169.x
5. Del Burgo LS, Milligan G. Heterodimerisation of G protein-coupled receptors: implications for drug design and ligand screening. *Expert Opin Drug Discov* (2010) **5**:461–74. doi:10.1517/17460441003720467
6. Kamal M, Jockers R. Biological significance of GPCR heteromerization in the neuro-endocrine system. *Front Endocrinol (Lausanne)* (2011) **2**:2. doi:10.3389/fendo.2011.00002
7. Tadagaki K, Jockers R, Kamal M. History and biological significance of GPCR heteromerization in the neuroendocrine system. *Neuroendocrinology* (2012) **95**:223–31. doi:10.1159/000330000
8. Goupil E, Laporte SA, Hébert TE. Functional selectivity in GPCR signaling: understanding the full spectrum of receptor conformations. *Mini Rev Med Chem* (2012) **12**:817–30. doi:10.2174/138955712800959143
9. Borroto-Escuela DO, Romero-Fernandez W, Garriga P, Ciruela F, Narvaez M, Tarakanov AO, et al. G protein-coupled receptor heterodimerization in the brain. *Methods Enzymol* (2013) **521**:281–94. doi:10.1016/B978-0-12-391862-8.00015-6
10. Tsutsui K, Ubuka T, Bentley GE, Kriegsfeld LJ. Gonadotropin-inhibitory hormone (GnIH): discovery, progress and prospect. *Gen Comp Endocrinol* (2012) **177**:305–14. doi:10.1016/j.ygcen.2012.02.013
11. Ubuka T, Son YL, Tobari Y, Tsutsui K. Gonadotropin-inhibitory hormone action in the brain and pituitary. *Front Endocrinol (Lausanne)* (2012) **3**:148. doi:10.3389/fendo.2012.00148
12. Christensen A, Bentley GE, Cabrera R, Ortega HH, Perfito N, Wu TJ, et al. Hormonal regulation of female reproduction. *Horm Metab Res* (2012) **44**:587–91. doi:10.1055/s-0032-1306301
13. Franceschini I, Desroziers E. Development and aging of the kisspeptin-GPR54 system in the mammalian brain: what are the impacts on female reproductive function? *Front Endocrinol (Lausanne)* (2013) **4**:22. doi:10.3389/fendo.2013.00022
14. Okubo K, Nagahama Y. Structural and functional evolution of gonadotropin-releasing hormone in vertebrates. *Acta Physiol (Oxf)* (2008) **193**:3–15. doi:10.1111/j.1748-1716.2008.01832.x
15. Lindemans M, Janssen T, Beets I, Temmerman L, Meelkop E, Schoofs L. Gonadotropin-releasing hormone and adipokinetic hormone signaling systems share a common evolutionary origin. *Front Endocrinol (Lausanne)* (2011) **2**:16. doi:10.3389/fendo.2011.00016
16. Sower SA, Decatur WA, Joseph NT, Freamat M. Evolution of vertebrate GnRH receptors from the perspective of a basal vertebrate. *Front Endocrinol (Lausanne)* (2012) **3**:140. doi:10.3389/fendo.2012.00140
17. Kanda S, Oka Y. Structure, synthesis, and phylogeny of kisspeptin and its receptor. *Adv Exp Med Biol* (2013) **784**:9–26. doi:10.1007/978-1-4614-6199-9_2
18. Gopurappilly R, Ogawa S, Parhar IS. Functional significance of GnRH and kisspeptin, and their cognate receptors in teleost reproduction. *Front Endocrinol (Lausanne)* (2013) **4**:24. doi:10.3389/fendo.2013.00024
19. Fanelli F, De Benedetti PG. Update 1 of: computational modeling approaches to structure-function analysis of G protein-coupled receptors. *Chem Rev* (2011) **111**:R438–535. doi:10.1021/cr100437t
20. Fuxe K, Borroto-Escuela DO, Marcellino D, Romero-Fernandez W, Frankowska M, Guidolin D, et al. GPCR heteromers and their allosteric receptor-receptor interactions. *Curr Med Chem* (2012) **19**:356–63. doi:10.2174/092986712803414259
21. Milligan G, Smith NJ. Allosteric modulation of heterodimeric G-protein-coupled receptors. *Trends Pharmacol Sci* (2007) **12**:615–20. doi:10.1016/j.tips.2007.11.001
22. Kaupmann K, Malitschek B, Schuler V, Heid J, Froestl W, Beck P, et al. GABA(B)-receptor subtypes assemble into functional heteromeric complexes. *Nature* (1998) **396**:683–7. doi:10.1038/25360
23. Duthey B, Caudron S, Perroy J, Bettler B, Fagni L, Pin JP, et al. A single subunit (GB2) is required for G-protein activation by the heterodimeric GABA(B) receptor. *J Biol Chem* (2002) **277**:3236–41. doi:10.1074/jbc.M108900200
24. Pin JP, Kniazeff J, Liu J, Binet V, Goudet C, Rondard P, et al. Allosteric functioning of dimeric class C G-protein-coupled receptors. *FEBS J* (2005) **272**:2947–55. doi:10.1111/j.1742-4658.2005.04728.x
25. Nelson G, Hoon MA, Chandrashekar J, Zhang Y, Ryba NJ, Zuker CS. Mammalian sweet taste receptors. *Cell* (2001) **106**:381–90. doi:10.1016/S0092-8674(01)00451-2
26. Nelson G, Chandrashekar J, Hoon MA, Feng L, Zhao G, Ryba NJ, et al. An amino-acid taste receptor. *Nature* (2002) **416**:199–202. doi:10.1038/nature726
27. Xu H, Staszewski L, Tang H, Adler E, Zoller M, Li X. Human receptors for sweet and umami taste. *Proc Natl Acad Sci USA* (2004) **101**:14258–63. doi:10.1073/pnas.0404384101
28. AbdAlla S, Lother H, Quitterer U. AT1-receptor heterodimers show enhanced G-protein activation and altered receptor sequestration. *Nature* (2000) **407**:94–8. doi:10.1038/35024095
29. AbdAlla S, Lother H, el Massiery A, Quitterer U. Increased AT(1) receptor heterodimers in preeclampsia mediate enhanced angiotensin II responsiveness. *Nat Med* (2001) **7**:1003–9. doi:10.1038/nm0901-1003
30. Kieffer BL. Opioids: first lessons from knockout mice. *Trends Pharmacol Sci* (1999) **20**:19–26. doi:10.1016/S0165-6147(98)01279-6
31. Gomes I, Jordan BA, Gupta A, Trapaidze N, Nagy V, Devi LA. Heterodimerization of mu and delta opioid receptors: a role in opiate synergy. *J Neurosci* (2000) **20**:RC110.
32. Fan T, Varghese G, Nguyen T, Tse R, O'Dowd BF, George SR. A role for the distal carboxyl tails in generating the novel pharmacology and G protein activation profile of mu and delta opioid receptor hetero-oligomers. *J Biol Chem* (2005) **280**:38478–88. doi:10.1074/jbc.M505644200
33. Waldhoer M, Fong J, Jones RM, Lunzer MM, Sharma SK, Kostenis E, et al. A heterodimer-selective agonist shows in vivo relevance of G protein-coupled receptor dimers. *Proc Natl Acad Sci USA* (2005) **102**:9050–5. doi:10.1073/pnas.0501112102
34. Yekkirala AS, Lunzer MM, McCurdy CR, Powers MD, Kalyuzhny AE, Roerig SC, et al. N-naphthoyl-beta-naltrexamine (NNTA), a highly selective and potent activator of μ/kappa-opioid heteromers. *Proc Natl Acad Sci USA* (2011) **108**:5098–103. doi:10.1073/pnas.1016277108
35. Ellis J, Pediani JD, Canals M, Milasta S, Milligan G. Orexin-1receptor-cannabinoid CB1 receptor heterodimerization results in both ligand-dependent and -independent coordinated alterations of receptor localization and function. *J Biol Chem* (2006) **281**:38812–24. doi:10.1074/jbc.M602494200
36. Rediger A, Piechowski CL, Yi CX, Tarnow P, Strotmann R, Grüters A, et al. Mutually opposite signal modulation by hypothalamic heterodimerization of ghrelin and melanocortin-3 receptors. *J Biol Chem* (2011) **286**:39623–31. doi:10.1074/jbc.M111.287607
37. Rediger A, Piechowski CL, Habegger K, Grüters A, Krude H, Tschöp MH, et al. MC4R dimerization in the paraventricular nucleus and GHSR/MC3R heterodimerization in the arcuate nucleus: is there relevance for body weight regulation? *Neuroendocrinology* (2012) **9**:277–88. doi:10.1159/000334903
38. Pei L, Li S, Wang M, Diwan M, Anisman H, Fletcher PJ, et al. Uncoupling the dopamine D1-D2 receptor complex exerts antidepressant-like effects. *Nat Med* (2010) **16**:1393–5. doi:10.1038/nm.2263
39. Rashid AJ, So CH, Kong MM, Furtak T, El-Ghundi M, Cheng R, et al. D1-D2 dopamine receptor heterooligomers with unique pharmacology are coupled to rapid activation of Gq/11 in the striatum. *Proc Natl Acad Sci USA* (2007) **104**:654–9. doi:10.1073/pnas.0604049104
40. He SQ, Zhang ZN, Guan JS, Liu HR, Zhao B, Wang HB, et al. Facilitation of μ-opioid receptor activity by preventing δ-opioid receptor-mediated codegradation. *Neuron*

(2011) **69**:120–31. doi:10.1016/j.neuron.2010.12.001
41. McGuire NL, Bentley GE. Neuropeptides in the gonads: from evolution to pharmacology. *Front Pharmacol* (2010) **1**:114. doi:10.3389/fphar.2010.00114
42. McGuire NL, Kangas K, Bentley GE. Effects of melatonin on peripheral reproductive function: regulation of testicular GnIH and testosterone. *Endocrinology* (2011) **152**:3461–70. doi:10.1210/en.2011-1053
43. Levoye A, Dam J, Ayoub MA, Guillaume JL, Jockers R. Do orphan G-protein-coupled receptors have ligand-independent functions? New insights from receptor heterodimers. *EMBO Rep* (2006) **7**:1094–8. doi:10.1038/sj.embor.7400838
44. Severini C, Improta G, Falconieri-Erspamer G, Salvadori S, Erspamer V. The tachykinin peptide family. *Pharmacol Rev* (2002) **54**:285–322.
45. Almeida TA, Rojo J, Nieto PM, Pinto FM, Hernandez M, Martin JD, et al. Tachykinins and tachykinin receptors: structure and activity relationships. *Curr Med Chem* (2005) **11**:2045–81. doi:10.2174/0929867043364748
46. Satake H, Kawada T. Overview of the primary structure, tissue-distribution, and functions of tachykinins and their receptors. *Curr Drug Targets* (2006) **7**:963–74. doi:10.2174/138945006778019273
47. Page NM. Characterization of the gene structures, precursor processing and pharmacology of the endokinin peptides. *Vascul Pharmacol* (2006) **45**:200–8. doi:10.1016/j.vph.2005.08.028
48. Satake H, Aoyama M, Sekiguchi T, Kawada T. Insight into molecular and functional diversity of tachykinins and their receptors. *Protein Pept Lett* (2013) **20**:615–27. doi:10.2174/0929866511320060002
49. Satake H, Ogasawara M, Kawada T, Masuda K, Aoyama M, Minakata H, et al. Tachykinin and tachykinin receptor of an ascidian, *Ciona intestinalis*: evolutionary origin of the vertebrate tachykinin family. *J Biol Chem* (2004) **279**:53798–805. doi:10.1074/jbc.M408161200
50. Satake H, Kawada T, Aoyama M, Sekiguchi T, Sakai T. Ascidians: new model orgnanisms for reproductive endocrinology. In: Aimaretti G, Marzullo P, Prodam F editors. *Update on Mechanisms of Hormone Action – Focus on Metabolism, Growth and Reproductions.* Vienna: IN-TECH (2011). p. 313–36.
51. Pennefather JN, Patak E, Ziccone S, Lilley A, Pinto FM, Page NM, et al. Regulation of the stimulant actions of neurokinin a and human hemokinin-1 on the human uterus: a comparison with histamine. *Biol Reprod* (2006) **75**:334–41. doi:10.1095/biolreprod.106.051508
52. Ravina CG, Seda M, Pinto FM, Orea A, Fernandez-Sanchez M, Pintado CO, et al. A role for tachykinins in the regulation of human sperm motility. *Hum Reprod* (2007) **22**:1617–25. doi:10.1093/humrep/dem069
53. Patak E, Pennefather JN, Gozali M, Candenas ML, Kerr K, Exintaris B, et al. Functional characterisation of hemokinin-1 in mouse uterus. *Eur J Pharmacol* (2008) **601**:148–53. doi:10.1016/j.ejphar.2008.10.036
54. Pinto FM, Ravina CG, Subiran N, Cejudo-Román A, Fernández-Sánchez M, Irazusta J, et al. Autocrine regulation of human sperm motility by tachykinins. *Reprod Biol Endocrinol* (2010) **8**:104. doi:10.1186/1477-7827-8-104
55. Aoyama M, Kawada T, Fujie M, Hotta K, Sakai T, Sekiguchi T, et al. A novel biological role of tachykinins as an up-regulator of oocyte growth: identification of an evolutionary origin of tachykininergic functions in the ovary of the ascidian, *Ciona intestinalis*. *Endocrinology* (2008) **149**:4346–56. doi:10.1210/en.2008-0323
56. Aoyama M, Kawada T, Satake H. Localization and enzymatic activity profiles of the proteases responsible for tachykinin-directed oocyte growth in the protochordate, *Ciona intestinalis*. *Peptides* (2012) **34**:186–92. doi:10.1016/j.peptides.2011.07.019
57. Kawada T, Ogasawara M, Sekiguchi T, Aoyama M, Hotta K, Oka K, et al. Peptidomic analysis of the central nervous system of the protochordate, *Ciona intestinalis*: homologs and prototypes of vertebrate peptides and novel peptides. *Endocrinology* (2011) **152**:2416–27. doi:10.1210/en.2010-1348
58. Topaloglu AK, Reimann F, Guclu M, Yalin AS, Kotan LD, Porter KM, et al. TAC3 and TACR3 mutations in familial hypogonadotropic hypogonadism reveal a key role for Neurokinin B in the central control of reproduction. *Nat Genet* (2009) **41**:354–8. doi:10.1038/ng.306
59. Rance NE, Krajewski SJ, Smith MA, Cholanian M, Dacks PA. Neurokinin B and the hypothalamic regulation of reproduction. *Brain Res* (2010) **1364**:116–28. doi:10.1016/j.brainres.2010.08.059
60. Lasaga M, Debeljuk L. Tachykinins and the hypothalamo-pituitary-gonadal axis: an update. *Peptides* (2011) **32**:1972–8. doi:10.1016/j.peptides.2011.07.009
61. Molnár CS, Vida B, Sipos MT, Ciofi P, Borsay BÁ, Rácz K, et al. Morphological evidence for enhanced kisspeptin and neurokinin B signaling in the infundibular nucleus of the aging man. *Endocrinology* (2012) **153**:5428–39. doi:10.1210/en.2012-1739
62. Grachev P, Li XF, Kinsey-Jones JS, di Domenico AL, Millar RP, Lightman SL, et al. Suppression of the GnRH pulse generator by neurokinin B involves a κ-opioid receptor-dependent mechanism. *Endocrinology* (2012) **153**:4894–904. doi:10.1210/en.2012-1574
63. Hrabovszky E, Sipos MT, Molnár CS, Ciofi P, Borsay BÁ, Gergely P, et al. Low degree of overlap between kisspeptin, neurokinin B, and dynorphin immunoreactivities in the infundibular nucleus of young male human subjects challenges the KNDy neuron concept. *Endocrinology* (2012) **153**:4978–89. doi:10.1210/en.2012-1545
64. Gill JC, Navarro VM, Kwong C, Noel SD, Martin C, Xu S, et al. Increased neurokinin B (Tac2) expression in the mouse arcuate nucleus is an early marker of pubertal onset with differential sensitivity to sex steroid-negative feedback than Kiss1. *Endocrinology* (2012) **153**:4883–93. doi:10.1210/en.2012-1529
65. Ruiz-Pino F, Navarro VM, Bentsen AH, Garcia-Galiano D, Sanchez-Garrido MA, Ciofi P, et al. Neurokinin B and the control of the gonadotropic axis in the rat: developmental changes, sexual dimorphism, and regulation by gonadal steroids. *Endocrinology* (2012) **153**:4818–29. doi:10.1210/en.2012-1287
66. Pfeiffer M, Kirscht S, Stumm R, Koch T, Wu D, Laugsch M, et al. Heterodimerization of substance P and mu-opioid receptors regulates receptor trafficking and resensitization. *J Biol Chem* (2003) **278**:51630–7. doi:10.1074/jbc.M307095200
67. Kah O, Lethimonier C, Somoza G, Guilgur LG, Vaillant C, Lareyre JJ. GnRH and GnRH receptors in metazoa: a historical, comparative, and evolutive perspective. *Gen Comp Endocrinol* (2007) **153**:346–64. doi:10.1016/j.ygcen.2007.01.030
68. Millar RP, Pawson AJ, Morgan K, Rissman EF, Lu ZL. Diversity of actions of GnRHs mediated by ligand-induced selective signaling. *Front Neuroendocrinol* (2008) **29**:17–35. doi:10.1016/j.yfrne.2007.06.002
69. Adams BA, Tello J, Erchegyi J, Warby C, Hong DJ, Akinsanya KO, et al. Six novel gonadotropin-releasing hormones are encoded as triplets on each of two genes in the protochordate, *Ciona intestinalis*. *Endocrinology* (2003) **144**:1907–19. doi:10.1210/en.2002-0216
70. Tello JA, River J, Sherwood NM. Tunicate gonadotropin-releasing hormone (GnRH) peptides selectively activate *Ciona intestinalis* GnRH receptors and the green monkey type II GnRH receptor. *Endocrinology* (2005) **146**:4061–73. doi:10.1210/en.2004-1558
71. Kawada T, Aoyama M, Okada I, Sakai T, Sekiguchi T, Ogasawara M, et al. A novel inhibitory gonadotropin-releasing hormone-related neuropeptide in the ascidian, *Ciona intestinalis*. *Peptides* (2009) **30**:2200–5. doi:10.1016/j.peptides.2009.08.014
72. Kusakabe T, Mishima S, Shimada I, Kitajima Y, Tsuda M. Structure, expression, and cluster organization of genes encoding gonadotropin-releasing hormone receptors found in the neural complex of the ascidian *Ciona intestinalis*. *Gene* (2003) **322**:77–84. doi:10.1016/j.gene.2003.08.013
73. Sakai T, Aoyama M, Kusakabe T, Tsuda M, Satake H. Functional diversity of signaling pathways through G protein-coupled receptor heterodimerization with a species-specific orphan receptor subtype. *Mol Biol Evol* (2010) **27**:1097–106. doi:10.1093/molbev/msp319
74. Sakai T, Aoyama M, Kawada T, Kusakabe T, Tsuda M, Satake H. Evidence for differential regulation of GnRH signaling via heterodimerization among GnRH receptor paralogs in the protochordate, *Ciona intestinalis*. *Endocrinology* (2012) **153**:1841–9. doi:10.1210/en.2011-1668
75. Kusakabe TG, Sakai T, Aoyama M, Kitajima Y, Miyamoto Y, Takigawa T, et al. A conserved non-reproductive GnRH system in chordates. *PLoS ONE* (2012) **7**:e41955. doi:10.1371/journal.pone.0041955
76. Rivero-Muller A, Chou YY, Ji I, Lajic S, Hanyaloglu AC, Jonas K, et al. Rescue of defective G protein-coupled receptor function in vivo

by intermolecular cooperation. *Proc Natl Acad Sci USA* (2010) **107**:2319–24. doi:10.1073/pnas.0906695106
77. Narumiya S, Sugimoto Y, Ushikubi F. Prostanoid receptors: structures, properties, and functions. *Physiol Rev* (1999) **79**:1193–226.
78. Matsui M, Miyamoto A. Evaluation of ovarian blood flow by colour Doppler ultrasound: practical use for reproductive management in the cow. *Vet J* (2009) **181**:232–40. doi:10.1016/j.tvjl.2008.02.027
79. Fujimori C, Ogiwara K, Hagiwara A, Rajapakse S, Kimura A, Takahashi T. Expression of cyclooxygenase-2 and prostaglandin receptor EP4b mRNA in the ovary of the medaka fish, *Oryzias latipes*: possible involvement in ovulation. *Mol Cell Endocrinol* (2011) **332**:67–77. doi:10.1016/j.mce.2010.09.015
80. Takahashi T, Fujimori C, Hagiwara A, Ogiwara K. Recent advances in the understanding of teleost medaka ovulation: the roles of proteases and prostaglandins. *Zool Sci* (2013) **30**:239–47. doi:10.2108/zsj.30.239
81. McGraw DW, Mihlbachler KA, Schwarb MR, Rahman FF, Small KM, Almoosa KF, et al. Airway smooth muscle prostaglandin-EP1 receptors directly modulate beta2-adrenergic receptors within a unique heterodimeric complex. *J Clin Invest* (2006) **116**:1400–9. doi:10.1172/JCI25840

Conflict of Interest Statement: The authors declare that the research was conducted in the absence of any commercial or financial relationships that could be construed as a potential conflict of interest.

Received: 06 June 2013; accepted: 31 July 2013; published online: 15 August 2013.
*Citation: Satake H, Matsubara S, Aoyama M, Kawada T and Sakai T (2013) GPCR heterodimerization in the reproductive system: functional regulation and implication for biodiversity. Front. Endocrinol. **4**:100. doi: 10.3389/fendo.2013.00100*
This article was submitted to Frontiers in Experimental Endocrinology, a specialty of Frontiers in Endocrinology.

frontiers in
ENDOCRINOLOGY

REVIEW ARTICLE
published: 17 October 2013
doi: 10.3389/fendo.2013.00143

Posttranslational modifications of proopiomelanocortin in vertebrates and their biological significance

Akiyoshi Takahashi* and Kanta Mizusawa

School of Marine Biosciences, Kitasato University, Sagamihara, Kanagawa, Japan

Edited by:
Sho Kakizawa, Kyoto University, Japan

Reviewed by:
Honoo Satake, Suntory Institute for Bioorganic Research, Japan
Masatomo Tagawa, Kyoto University, Japan

****Correspondence:***
Akiyoshi Takahashi, School of Marine Biosciences, Kitasato University, 1-15-1 Kitasato, Minami-ku, Sagamihara, Kanagawa 252-0373, Japan
e-mail: akiyoshi@kitasato-u.ac.jp

Proopiomelanocortin (POMC) is the precursor of several peptide hormones generated in the pituitary gland. After biosynthesis, POMC undergoes several posttranslational modifications, including proteolytic cleavage, acetylation, amidation, phosphorylation, glycosylation, and disulfide linkage formation, which generate mature POMC-derived peptides. Therefore, POMC is a useful model for the investigation of posttranslational modifications. These processes have been extensively investigated in mammals, primarily in rodents. In addition, over the last decade, much information has been obtained about the posttranslational processing of POMC in non-mammalian animals such as fish, amphibians, reptiles, and birds through sequencing and peptide identification by mass spectrometry. One POMC modification, acetylation, is known to modulate the biological activities of POMC-derived α-melanocyte-stimulating hormone (α-MSH) having an acetyl group at N-terminal through potentiation or inhibition. This bidirectional regulation depends on its intrinsic roles in the tissue or cell; for example, α-MSH, as well as desacetyl (Des-Ac)-α-MSH, stimulates pigment dispersion in the xanthophores of a flounder. In contrast, α-MSH does not stimulate pigment dispersion in the melanophores of the same species, whereas Des-Ac-α-MSH does. Regulation of pigment-dispersing activities may be associated with the subtle balance in the expression of receptor genes. In this review, we consider the posttranslational modifications of POMC in vertebrates from an evolutionary aspect, with a focus on the relationship between acetylation and the biological activities of α-MSH as an important consequence of posttranslational modification.

Keywords: acetylation, pigment-dispersing activity, pars distalis, pars intermedia, pituitary, proopiomelanocortin, melanocyte-stimulating hormone, melanocortin receptor

INTRODUCTION

Proopiomelanocortin (POMC) is a precursor protein of multiple peptide hormones such as adrenocorticotropic hormone (ACTH), melanocyte-stimulating hormone (MSH), endorphin (END), etc. (1). The major tissue that biosynthesizes POMC is the pituitary gland, where POMC is produced in the corticotrophs of the pars distalis (PD) and in the melanotrophs of the pars intermedia (PI) (2, 3). In these cells, POMC is differentially cleaved through tissue-specific proteolysis to generate functional peptides. In corticotrophs, relatively larger peptides such as ACTH are the final products, whereas in melanotrophs, relatively smaller peptides such as α-MSH are generated. In addition to cleavage, POMC and POMC-derived peptides undergo several posttranslational modifications such as acetylation, amidation, phosphorylation, glycosylation, and disulfide linkage formation (4). Therefore, the POMC system is undoubtedly multifunctional, i.e., in addition to the generation of several peptides, various modifications could diversify the biological functions of POMC-derived peptides.

Adrenocorticotropic hormone and MSH are collectively called melanocortin (MC). Their receptor is called the MC receptor (MCR), for which five subtypes (MC1R to MC5R) have thus far been identified (5). The receptors for END are opioid receptors (6, 7). Both receptors are G protein-coupled receptors (GPCRs) with seven transmembrane domains. MCRs are widely distributed throughout animal bodies (8, 9) indicating that POMC-derived peptides have a variety of biological functions. Moreover, posttranslational modification sometimes alters either the binding affinity between the hormonal peptides and their receptors, or the downstream intracellular signal transduction (10). It is thought that the complex POMC network is made up of a variety of peptides with additional modifications and receptor subtypes distributed in many different tissues and organs. Therefore, POMC could be a useful model for investigating posttranslational modifications in endocrine systems.

Posttranslational processing of POMC in mammals is well understood (2, 3). Mammalian POMC is composed of three major segments, *N*-POMC, ACTH, and β-LPH. These segments are divided by the dibasic amino acid residues Arg and Lys, which act as cleavage signals, and contain one MSH sequence whose common sequence is His-Phe-Arg-Trp. The END sequence is always located at the C-terminal end of the β-LPH segment. Therefore, mammalian POMC is described as the 3MSH/1END type. We have investigated the molecular cloning of POMC in non-mammalian species such as birds (11), reptiles (12), and fish, including teleosts, cartilaginous fish, lobe-finned fish, and agnathans (13). Based on the results, we showed the variation in the molecular organization

of POMC; the POMC structures are not always the 3MSH/1END type. Moreover, we found that different POMCs are generated in the PD and PI of the most primitive vertebrates, the lampreys (14), whereas identical POMCs are generated in these lobes in other vertebrates. In addition, we also identified POMC-derived peptides from the pituitary glands in non-mammalian vertebrates.

Herein, we compare the posttranslational modifications of POMC in the corticotrophs and melanotrophs in vertebrates such as birds, reptiles, and fish, which are largely based on the results of our investigations. The results for mammalian and amphibian POMCs will also be summarized. Moreover, we also propose a heteromer hypothesis that would explain the interesting activities of α-MSH in relation to its posttranslational modifications, namely the presence or absence of acetyl groups at the N-terminus.

POSTTRANSLATIONAL PROCESSING OF POMC

MAMMALS

Mammalian POMC is the 3MSH/1END type (1). Posttranslational processing of POMC in the cells of AtT 20/D16v (mouse pituitary epithelial-like tumor cell line) in addition to the PD and PI cells of the pituitary gland has been extensively investigated in mammals such as rodents, including rat and mouse, artiodactyls, including ox and sheep, and humans by peptide isolation/purification and amino acid sequence analysis or by biosynthetic labeling, immunoprecipitation, and sequence analysis (2–4, 15, 16). The results showed that the products from POMC in the PD and PI vary depending on the presence of prohormone convertase 1 and 2 (PC1 and PC2). In the PD, where PC1 is present, pro-γ-MSH, joining peptide (JP), ACTH, and β-LPH are generated; however, in the PI, where PC1 and PC2 are present, pro-γ-MSH is further cleaved to adrenal mitogenic hormone (AMH) and γ-MSH, ACTH is cleaved to generate α-MSH and corticotropin-like intermediate lobe peptide (CLIP), and β-LPH is cleaved to generate *N*-β-LPH, β-MSH, and β-END. α-MSH is produced by way of an intermediate ($ACTH_{1–17}$), and then mature α-MSH is generated after further processing, including removal of C-terminal residues by carboxypeptidase E, formation of a C-terminal amide by peptidyl α-amidating mono-oxygenase, and N-acetylation by POMC *N*-acetyltransferase. Some amount of β-END also undergoes N-terminal acetylation. As adult human pituitary glands lack PI and are only composed of anterior lobes containing the PD and pars tuberalis (17), POMC is predominantly processed into pro-γ-MSH, JP, ACTH, and β-LPH.

BIRDS

Similar to human pituitary glands, adult avian pituitary glands are composed of only the PD (18). The ostrich (*Struthio camelus*) is a non-flying bird from which several POMC-derived peptides have been isolated, including ACTH (19), β-LPH (20), β-END (21), γ-LPH (22), and pro-γ-MSH(23), which lacks the C-terminal segment of $γ_3$-MSH, and thus is shorter than the pro-γ-MSH as shown in **Figure 1**. The occurrence of ACTH, γ-LPH, and β-END was further confirmed in a single frozen ostrich pituitary slice through matrix-assisted laser desorption/ionization time-of flight mass spectrometry (MALDI-TOF MS) (11). Based on the results of peptide identification, we cloned the POMC cDNA from ostrich pituitary and determined its sequence. Sequence comparison of these isolated peptides with the POMC cDNA sequence suggests that all the dibasic sequences are cleaved to produce the peptides. Therefore, the major products in ostrich corticotrophs are pro-γ-MSH, ACTH, and β-LPH, although a substantial amount of β-LPH is further cleaved into γ-LPH and β-END. The generation of a substantial amount of β-END in the ostrich pituitary gland is different from what was observed in the human pituitary, in which β-LPH is a predominant form (15).

REPTILES

Similar to other tetrapods, snake and alligator POMCs contain α-MSH, β-MSH, γ-MSH, and β-END (12). These data together with those for gecko (25) and turtle POMC (26) indicate that reptile POMCs are consistently the 3MSH/1END type. Interestingly, the γ-MSH segment in snake POMC has a mutation in the essential His-Phe-Arg-Trp sequence, and the Phe and Arg residues are deleted (**Figure 2**). It is conceivable that an ancestor of snake γ-MSH had weak functional constraints and lacked

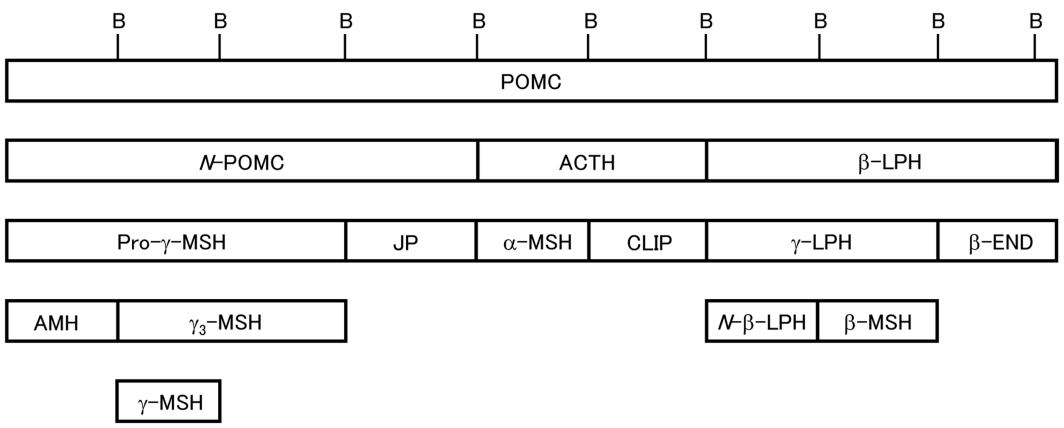

FIGURE 1 | Schematic of 3MSH/1END type POMC [modified from Ref. (24)]. Relative positions of the peptide segments are shown. Peptide terminology modified from Eberle (4). B, dibasic sequences that partition the peptide segments. In teleost POMC, *N*-POMC is not divided into subsegments due to the absence of a γ-MSH segment and pairs of basic amino acids.

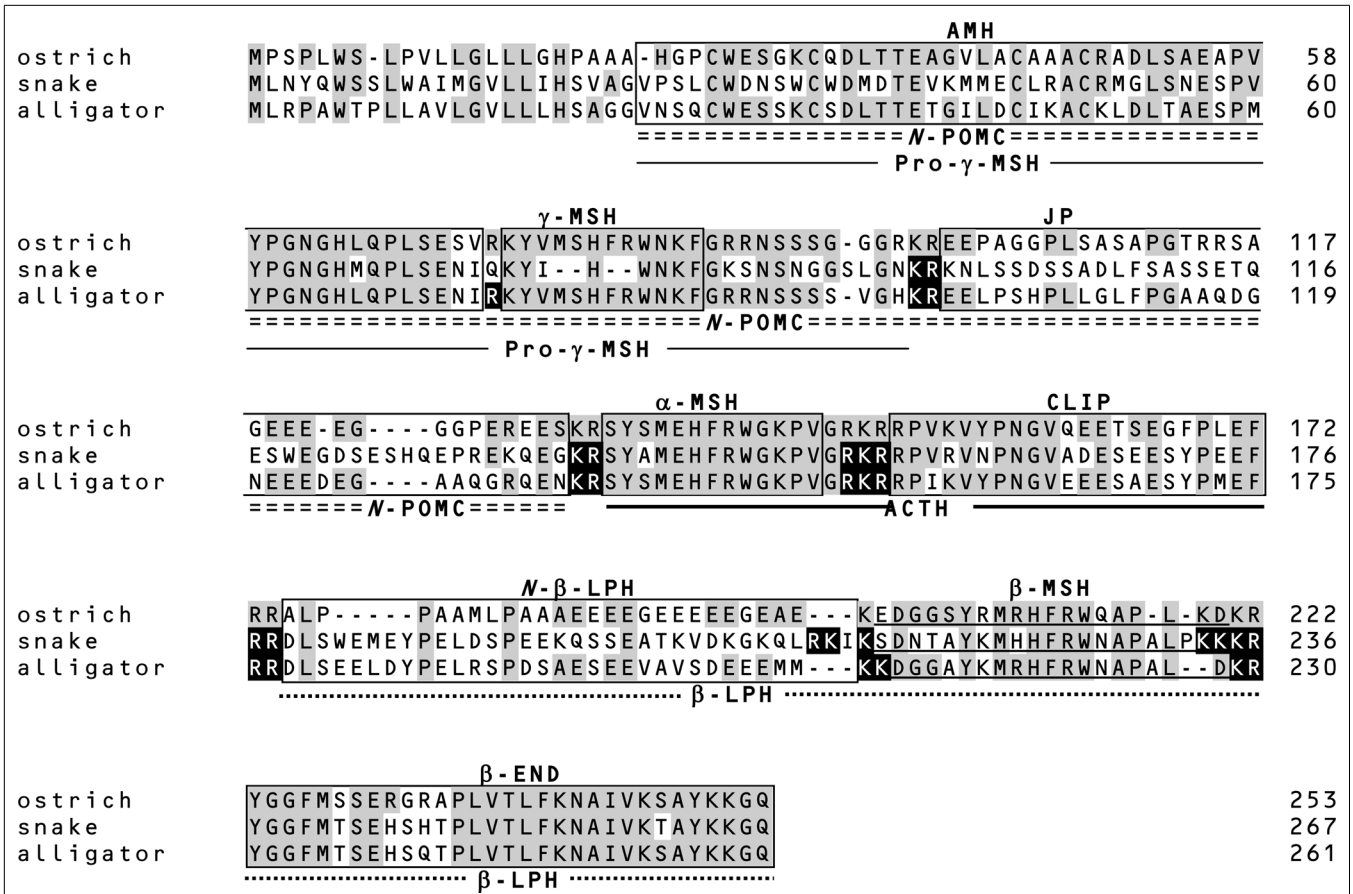

FIGURE 2 | Amino acid sequences of prePOMC from birds and reptiles. Amino acid residues in reptile POMC that are identical to those in ostrich POMC are shaded. Filled amino acid residues indicate the processing sites of snake and alligator POMCs determined based on the peptides identified by mass spectrometry and peptide analysis (11, 12). Positions of the amino acid are indicated on the right side.

biological significance during evolution. In contrast, analyses of whole snake and alligator pituitary glands by MALDI-TOF MS revealed several peptides, such as desacetyl (Des-Ac)-α-MSH, β-MSH, β-END, etc., are generated by posttranslational processing as predicted by the locations of the dibasic sequence processing sites. These results revealed interesting features of the posttranslational processing that generates γ-MSH and β-MSH with reference to the snake POMC as described below.

The γ-MSH segment of snake POMC is characterized by the change in the essential sequence from His-Phe-Arg-Trp to His-Trp (12). Based on this, the term γ-MSH-like sequence was assigned. Moreover, the amino acid residues flanking this segment are Gln-Lys and Lys-Ser at N-terminal and C-terminal sides, respectively. These characteristics suggest that the γ-MSH-like sequence is non-functional and is not liberated from the precursor protein by proteolytic cleavage. This hypothesis was supported by the identification of an *N*-POMC peptide consisting of AMH and γ-MSH-like sequences. The γ-MSH-like sequence seems to be a so-called vestige. The snake POMC is assigned as a 3MSH/1END type on the basis of its overall molecular organization. However, taking its probable lack of a functional γ-MSH into consideration, its direction in evolution is perhaps toward a 2MSH/1END type.

The amino acid sequence of the alligator γ-MSH is identical to the γ-MSH sequences of the leopard gecko, mud turtle, and birds (12). The detection of AMH and JP indicates that alligator POMC is cleaved at Arg^{75} and Arg^{89}–Arg^{90} by posttranslational processing; therefore, γ-MSH or γ_3-MSH must also be liberated. However, these peptides were not detected. Non-detection of γ_3-MSH suggests that a carbohydrate side chain is probably linked to the C-terminal region of γ_3-MSH via an N-glycosylation site at alligator $prePOMC_{91–93}$. In contrast, γ-MSH seems not to be liberated from POMC, or in other words, Arg^{89}–Arg^{90} are not functional processing signals in alligator POMC.

Despite the consistent presence of the β-MSH sequence in all vertebrate POMCs, β-MSH is not always liberated. In ostriches, β-LPH and γ-LPH peptides, both containing β-MSH, have been detected, whereas the β-MSH peptide has not been detected (11, 27). This is probably caused by the presence of just a single basic residue on the N-terminal side of β-MSH, which constitutes an incomplete processing site. A similar mutation is also observed in rodents (28, 29). In snakes, the processing signal on the N-terminal side of β-MSH is Lys^{213}-Ser^{214}, while Lys–Lys is observed in other reptiles, whereas its C-terminal side is flanked by four basic residues, Lys^{233}-Lys^{234}-Lys^{235}-Arg^{236} (**Figure 2**). The detection of

β-MSH originating from snake prePOMC$_{214–232}$ indicates that the single N-terminal basic residue and C-terminal four-basic-residue sequence function as cleavage sites. The sequence Arg^{210}-Lys^{211}-Ile^{212}-Lys^{213} on the N-terminal side of the snake β-MSH is similar to a consensus sequence for a monobasic processing site, in which Arg^{210} is especially important (30). Perhaps a synchronous mutation, a changing Lys to Ser at position 214 and substituting Arg for a non-basic residue at position 210, contributes to the liberation of β-MSH in snakes.

AMPHIBIANS

The processing of POMC in African clawed frog (*Xenopus laevis*) has been well investigated. Molecular cloning studies have shown the presence of two forms of 3MSH/1END type POMC (31). POMC-derived peptides have been detected in isolated melanotropic cells from the pituitary NIL consisting of PI and pars nervosa (32–34). The generation of almost all the peptides could be predicted by the presence of mono and dibasic amino acid residues. Further, acetylated forms, such as α-MSH and *N*-Ac-β-END, have also been detected. Therefore, it is probable that *Xenopus* melanotropic cells possess functions similar to those observed in the PI of mammals and reptiles based on the similar posttranslational modifications of their respective POMC-derived peptides

FISH

Lobe-finned fish

The lobe-finned fish include lungfish and coelacanth, and are considered to be the basal members of the lineage that led to the tetrapods (35–37). We demonstrated, for the first time in lobe-finned fish, that African lungfish POMC is the 3MSH/1END type by molecular cloning studies (38). An outline of the posttranslational processing of lungfish POMC has yet to be depicted except for α-MSH. α-MSH was shown to possess an amino acid sequence (based on its cDNA sequence) that is identical to that observed in mammals. Prior to our molecular studies, African lungfish α-MSH was characterized by high-performance liquid chromatography (HPLC) and radioimmunological detection (39). In this experiment, HPLC analysis of African lungfish pituitary extracts showed that the immunological peaks co-eluted with synthetic Des-Ac-α-MSH, α-MSH, and diacetyl (Di-Ac)-α-MSH. This indicated that at least these α-MSH-related peptides are processed and modified in lungfish, probably in the PI, as they are in tetrapod species. Similar experiments have been performed for the Australian lungfish *Neoceratodus forsteri* (40, 41).

No POMC sequence is available for the coelacanth *Latimeria chalumnae*, the other representative lobe-finned fish. However, it is possible to infer a portion of the processing system using the peptide information we obtained. We identified α-MSH, Des-Ac-α-MSH, β-MSH, CLIP, pro-γ-MSH, and *N*-Ac-β-END$_{1–30}$ in an extract from the rostral PD of the pituitary by HPLC, amino acid sequence analysis, and mass spectrometry (42). The occurrence of three different MSHs and one β-END indicates that the structural organization of coelacanth POMC is identical to that of lungfish and tetrapods (3MSH/1END type).

Among these peptides, α-MSH, Des-Ac-α-MSH, and *N*-Ac-β-END$_{1–30}$ are modified by acetylation at the N-terminus or by amidation at the C-terminus. The posttranslational processing of POMC includes cleavage of the precursor into several peptide hormones, modifications of N- and C-terminal residues, and the addition of a carbohydrate moiety (2, 3). Identification of the modified peptides indicated that the coelacanth POMC-related peptides are not produced by autolysis during-transportation or storage after capture of the specimen. Although the major POMC products in the anterior lobe of the pituitary in mammals are *N*-POMC, ACTH, β-LPH, and β-END, small amounts of so-called PI peptides have also been detected in ox, pig, and rat, and significant amounts of PI peptides have been detected in sheep pituitary anterior lobe (2). Therefore, the properties of the coelacanth pituitary rostral PD are similar to those of the anterior lobe of the sheep pituitary.

Ray-finned fish

The ray-finned fish include the chondrosteans and neopterygians. Chondrosteans include bichirs and sturgeons, and the neopterygians are divided into teleosts and another group consisting of gars and bowfin (43). POMC in all ray-finned fish, except for teleosts, is the 3MSH/1END type. Indeed, the structures of POMCs from bichir, sturgeon, and gar are similar to those of the lobe-finned fish and tetrapods. However, teleost POMC has distinct features due to the lack γ-MSH in *N*-POMC; therefore, teleost POMC is the 2MSH/1END type [see a review of Ref. (13)]. Based on the POMC-derived peptides identified in several ray-finned fish, including tuna (*Thunnus obesus*), carp (*Cyprinus carpio*), and flounder (*Verasper moseri*), we can infer the posttranslational processing system in teleosts.

Initially, extracts from whole pituitary consisting of both PD and NIL were used to identify POMC-derived peptides. These extracts were separated by chromatography, and then the mass value of each peptide was measured by mass spectrometry, and finally the mass value was assigned to an amino acid sequence deduced from the POMC cDNA sequence. Using these methods for carp (44), tuna (45), and flounder POMC (46), most of the peptides predicted from the location of processing signals in the cDNA sequences were identified. However, no PD-specific peptides, such as ACTH and β-END, were detected. These extracts were mixtures of PD and NIL. Morphologically, it is evident that there are relatively few POMC-producing cells in the PD (corticotrophs) compared to the number in the PI (melanotrophs) (47–49). Therefore, it is reasonable to suppose that a lower amount of PD-specific POMC-derived peptides than PI-specific peptides are present in the whole-pituitary extracts, and that analyses of whole pituitaries may better represent the peptide profiles in the PI.

To identify PD- and PI-specific POMC-derived peptides, pituitaries were taken from relatively large individual flounder, and the pituitaries were divided into the PD and NIL. The tissues were used for direct profiling of the pituitary slice by MALDI-TOF MS (50). A mass value identical to the estimated value from the cDNA sequence was detected in the PD, indicating that ACTH is generated in the corticotrophs of the flounder pituitary. Moreover, Des-Ac-α-MSH and CLIP were also identified in the PD. These findings indicate that in flounder, a substantial amount of ACTH is further processed to generate these two peptides in corticotrophs. Although β-END was not detected in the PD, the presence of

β-MSH indicates that the dibasic sequence Lys-Arg between β-MSH and β-END is part of the processing signal for cleavage in the flounder pituitary PD. Cleavage at this signal sequence should also generate β-END, which is located at the C-terminal end of POMC.

In contrast, ACTH-derived peptides, such as Des-Ac-α-MSH, α-MSH, and CLIP, but not ACTH itself, were identified in the flounder PI. In melanophores, most of the ACTH seems to be cleaved into Des-Ac-α-MSH and CLIP, then an acetyl group is added to the N-terminus of Des-Ac-α-MSH to form α-MSH.

Cartilaginous fish

Cartilaginous fish (chondrichthians) are composed of elasmobranchs, including sharks and rays, and holocephalans, including ratfish (43). The amino acid sequence of POMC from cartilaginous fish was first reported for the elasmobranch dogfish (*Squalus acanthias*), which was determined by molecular cloning studies (51). Subsequently, sequence information has been obtained in rays (52), ratfish (53), and other sharks (54, 55). The presence of δ-MSH in the *N*-β-LPH segment is a distinctive feature of cartilaginous fish POMC. Therefore, cartilaginous fish POMCs are the 4MSH/1END type.

The occurrence of the δ-MSH peptide as well as other types of MSH was initially shown through peptide chemical analyses using whole pituitaries (56). Tissue-specific cleavage of POMC was demonstrated in the banded houndshark (*Triakis scyllium*) using PD and NIL extracts (55). In the *Triakis* POMC, predicted segments including δ-MSH were flanked by dibasic sequences, as has been observed for POMCs from other fish and animals. Mass spectrometry was performed on PD (including most parts of the rostral and proximal PD) and NIL extracts to detect mass values corresponding to POMC-derived peptides. Consequently, ACTH, β-END, and JP were detected in the PD extract, whereas MSHs, such as α-, β-, γ-, and δ-MSH, truncated β-ENDs, such as β-$END_{1–30}$, and other POMC-derived peptides, such as JP and CLIP, were identified in the NIL extract. It is apparent that larger peptides than those found in the NIL are generated in the PD.

Based on the *Triakis* POMC sequence, pro-γ-MSH and γ-LPH should also be liberated in the pituitary PD, although these were not detected (55). Detecting these relatively large peptides might be more difficult than detecting the other small POMC-derived peptides. In contrast, in the NIL, the only two peptides whose peaks could not be identified by mass spectrometry were the C-terminal peptides of $γ_3$-MSH and *N*-β-LPH. The former peptide probably contains a carbohydrate side chain, as suggested by the presence of an N-glycosylation site at $POMC_{93–95}$. The latter peptide is highly acidic. These physicochemical characteristics might have interfered with the mass spectrometric detection of these peptides.

Agnathans

Although an identical POMC gene is expressed in the both the PD and PI of the pituitary gland in jawed vertebrates, two distinct POMC genes are expressed in jawless fish, the most primitive vertebrates (14, 57). In lampreys, an mRNA encoding proopiocortin (POC), the precursor of ACTH and β-END, is synthesized in the corticotrophs of the PD, while an mRNA encoding proopiomelanotropin (POM), the precursor of MSH and the other β-END, is synthesized in the melanotrophs of the PI (14, 57, 58). POC is a 1MSH/1END type and POM is a 2MSH/1END type.

Initially, ACTH and the two types of MSH were isolated from whole-pituitary extract of lamprey (59). Subsequently, mass spectrometric analyses demonstrated the tissue sources for each peptide, including β-END (60). In brief, the peptides that originated from POC, such as ACTH and β-END, were shown to be produced in the PD, and those that were from POM, such as MSH-A, MSH-B, and β-$END_{8–35}$ lacking the N-terminal Met-enkephalin (Met-ENK) region, were shown to be produced in the PI. The occurrence of β-$END_{8–35}$ indicates that the dibasic Arg-Lys sequence at β-$END_{6,7}$ functions as the processing signal for cleavage in lamprey. Cleavage at β-$END_{6,7}$ should also generate β-$END_{1–5}$, namely Met-ENK. The occurrence of Met-ENK in the PI of the lamprey pituitary was first proposed by Dores and McDonald (61) who fractionated a PI extract by HPLC. In this study, immunoreactive Met-ENK had a retention time that was identical to synthetic Met-ENK. Taken together, it is indicated that the major products generated through posttranslational processing are ACTH and β-END in the PD, and MSHs and Met-ENK in the PI (**Figure 3**).

Despite the expression of different genes, the roles of the POMC-producing cells in the each lobe of the lamprey are basically the same as those observed in jawed vertebrates; ACTH is a PD peptide and MSH is a PI peptide (14, 57, 58, 60). However, the generation of Met-ENK is an obvious difference between lampreys and jawed vertebrates. It is conceivable that the dibasic sequence

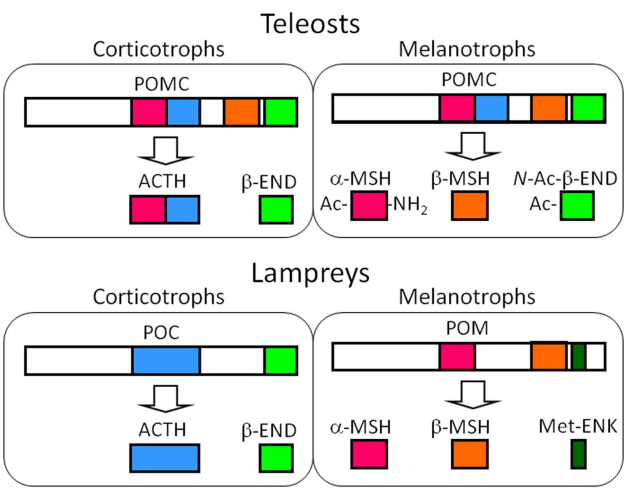

FIGURE 3 | Major POMC-derived peptides in the corticotrophs of the PD and the melanotrophs of the PI in teleost and lamprey pituitary glands based on the results from the barfin flounder (*Verasper moseri*) (14, 46, 50) and sea lamprey (*Petromyzon marinus*) (14, 57–59). In the original paper on the sea lamprey POMC, α-MSH, and β-MSH are termed MSH-B and MSH-A, respectively (59). The major products in these cells are common between teleosts and lampreys – ACTH and END in the melanotrophs, and MSHs and opioid peptides, i.e., *N*-Ac-β-END or Met-ENK. The differences between teleosts and lampreys lie in the genes expressed; identical POMCs are generated in the corticotrophs and melanotrophs of teleosts, as is the case for tetrapods. In contrast, different precursors are generated in lampreys.

located between Met-ENK and the rest of the β-END sequence undergo enzymatic cleavage. Therefore, the melanotrophs of lamprey pituitaries are a source of MSH and Met-ENK, which is different from their roles in jawed vertebrates. Based on the final products, POM should be the precursor of MSHs and Met-ENK, but not of β-END.

ACETYLATION: EVOLUTIONARY IMPLICATIONS

Acetylation of the N-termini of Des-Ac-α-MSH and β-END, phosphorylation of ACTH, and glycosylation of *N*-POMC are the representative posttranslational modifications of POMC or POMC-derived peptides (2–4). Acetylation is known to affect the biological function of POMC-derived peptides (10). Between the two lobes in which POMC is generated, acetylation frequently occur in the PI.

Desacetyl-α-MSH is an N-terminal fragment of ACTH with an amide at the C-terminus that is identical to $ACTH_{1\text{-}13}\text{-}NH_2$ (4). α-MSH has one acetyl group at the N-position of the N-terminal Ser residue, whereas Di-Ac-α-MSH has an additional acetyl group at the O-position of the N-terminal residue. In *Xenopus* α-MSH, the N-terminal residue, Ala, is the residue to which the acetyl group is added (34). In the case of β-END, the N-terminal Tyr residue is acetylated at the N-position (2, 3). The acetylated peptide is termed *N*-Ac-β-END.

Proopiomelanocortin-derived peptides containing acetyl groups, such as α-MSH, Di-Ac-α-MSH, and *N*-Ac-β-END, have been detected in fish, including teleosts (44, 45, 50, 62–65) and lobe-finned fish (39, 40, 42), and tetrapods, including amphibians (34), reptiles (12), and mammals, such as rodents and artiodactyls (2, 3). No acetylated forms of POMC-derived peptides have been detected in agnathans (59), cartilaginous fish (55), and birds (11). Considering the phylogenetic relationships of vertebrates, the ability of acetylation or the presence of a functional *N*-acetyltransferase in the melanotrophs of the PI may have been established in a common ancestor of fish and tetrapods. According to this assumption, cartilaginous fish may have secondarily lacked these acetylation systems. In contrast, the presence of a few acetylated POMC-derived peptides in the pituitary glands in birds and human corresponds to the lack of the PI in the pituitary gland.

ACETYLATION IN RELATION TO BIOLOGICAL ACTIVITIES

The presence or absence of acetyl groups modifies the biological activities of POMC-derived peptides (10). α-MSH-related peptides, such as Des-Ac-α-MSH, α-MSH, and Di-Ac-α-MSH, differentially affect melanogenesis, pigment migration in chromatophores, neural development and regeneration, melanocortinergic regulation of food intake and other behaviors, corticosteroid genesis, lipolysis, cell proliferation in bones, and lactotrope-recruiting activity. These differences may result from an altered interaction between the ligand and receptor. For instance, α-MSH showed significantly higher activities than Des-Ac-α-MSH, and Di-Ac-α-MSH is as potent as α-MSH (66–68). In contrast, *N*-Ac-β-END has no opiate activity because acetylation of β-END significantly decreased its interaction with opioid receptors (69). In this chapter, we summarize the new concept of ligand-receptor interaction based on the results of studies on pigment migration in flounder (*Verasper moseri*).

In *Verasper* skins two types of chromatophores – melanophores and xanthophores – are predominantly observed. α-MSH and Des-Ac-α-MSH exhibit pigment-dispersing activities in both melanophores and xanthophores. However, N-terminal acetylation differentially modulates the pigment-dispersing activities of these cells (70). Surprisingly, acetylation significantly decreased the pigment-dispersing activity of α-MSH in melanophores, while it stimulated the pigment-dispersing activity in xanthophores. Similar results were also obtained for another flounder species, *Paralichthys olivaceus* (**Figure 4**) (71). At first, it was thought that α-MSH has a low affinity for the MCR expressed in melanophores (70).

There are at least five subtypes of MCR (MC1R–MC5R) in fish, as in tetrapods (72–75), while *Fugu* lack MC3R (74, 76) and possess only four MCRs. We also identified the four subtypes of MCRs in *Verasper* (77–79). Among the subtypes, *Mc5r* transcript was detected in xanthophores, whereas *mc1r* and *mc5r* transcripts were detected in melanophores (78). It was reasonable to conclude that both Des-Ac-α-MSH and α-MSH stimulated pigment dispersion via MC5R on xanthophores. However, roles of two MCRs in the melanophores is still unclear.

Although the pharmacological properties of the *Verasper* MCRs have not yet been determined, they may have properties similar to those of the sea bass (*Dicentrarchus labrax*) MCRs because *Verasper* MC1R and MC5R share approximately 90% amino acid sequence identity with sea bass MC1R and MC5R. Interestingly, pharmacological studies of sea bass MC1R and MC5R have revealed that α-MSH has a much higher efficacy than Des-Ac-α-MSH in stimulating cAMP production in human embryonic kidney (HEK) 293 cells, which stably expressing either *mc1r* or *mc5r* (66, 68). If the properties of *Verasper* MCRs in HEK293 cells are similar to those of the sea bass MCRs, the negligible effects of α-MSH

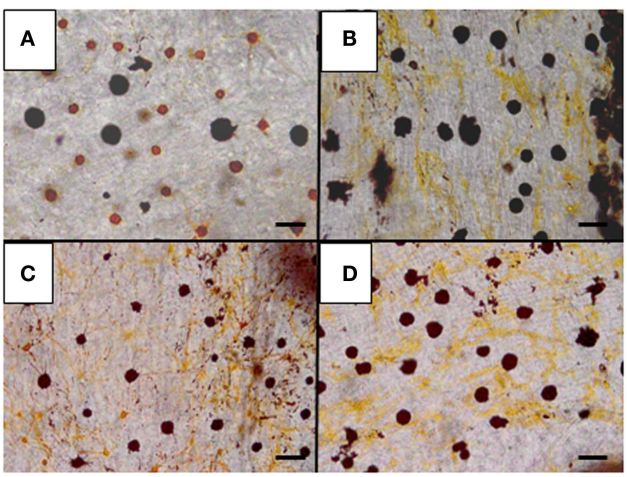

FIGURE 4 | Effects of α-MSH on pigment dispersion in chromatophores in the skin of barfin flounder. A control skin specimen was incubated in medium containing no α-MSH **(A)**. Skin specimens were treated with 10 nM **(B)**, 100 nM **(C)**, and 1 μM α-MSH **(D)** at 16°C for 1 h. Pigments in melanophores did not migrate, whereas those in xanthophores diffused. See Kobayashi et al. (71) for details. The bar equals 100 μm.

in melanophores is inconsistent with the presence of the MC1R and MC5R because these receptors can mediate the α-MSH signal. To resolve these discrepancies, we postulated the formation of a heteromer consisting of MC1R and MC5R based on increasing evidence which suggests that heterodimerization of GPCRs results in functional consequence that are different from the well-established functional characteristics of monomeric receptors (80–82). The keys to this assumption are that this putative heteromer mediates signals of Des-Ac-α-MSH, but not those of α-MSH, which would differ from the properties of each monomeric MCR (**Figure 5**). α-MSH seems to have a low binding affinity for the putative heteromer consisting of MC1R and MC5R in melanophores, or this peptide cannot stimulate intracellular signal transduction through these heteromers even though interaction would occur between the peptide and receptor. Our findings seem to suggest the presence of naturally occurring heteromeric GPCRs.

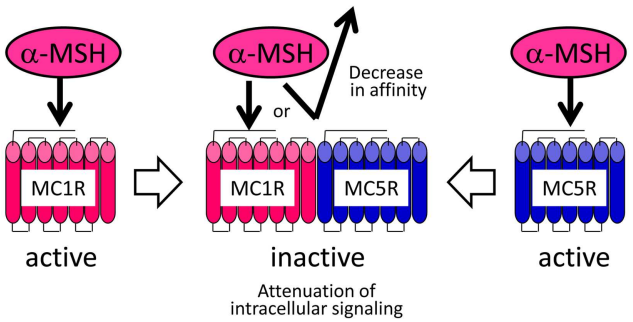

FIGURE 5 | Heteromer hypothesis explaining the negligible activities of α-MSH in flounder melanophores.

CONCLUSION

Examination of the POMC-derived peptides in a variety of vertebrates demonstrated that the posttranslational modification (or final products) of POMC in the corticotrophs is different from those in the melanotrophs. Relatively larger peptides are generated in the corticotrophs, while smaller peptides are generated in the melanotrophs. Moreover, some peptides in the melanotrophs undergo acetylation. These can be considered common processes that generate tissue-specific POMC-derived peptides in vertebrates; however, deviations in the proteolytic cleavage and acetylation are sometimes observed. Nevertheless, we can summarize that the common function of corticotrophs throughout the vertebrates is the production of ACTH and the opioid peptide β-END, and that the common function of melanotrophs is the production of MSH and the opioid peptides β-END and Met-ENK. This functional differentiation may have been established in the evolutionary antecedent of lampreys. α-MSH and β-END are frequently acetylated, and the presence or absence of an acetyl group modifies the biological activities in many vertebrate classes. The lack of acetylated peptides in the PI of lamprey and cartilaginous fish pituitaries suggests that acetylation is not a commonly occurring modification in vertebrates. However, the presence of an acetylation system in tetrapods and teleosts suggests the establishment of this system in their common ancestor. Acetylation may be associated with the interaction of the receptor molecules to regulate the roles of POMC-derived peptides. In this context, lampreys and cartilaginous fish lacking acetylation systems may have different regulating systems for the peptide generation in the melanotrophs from teleosts and tetrapods.

REFERENCES

1. Nakanishi S, Inoue A, Kita T, Nakamura M, Chang ACY, Cohen SN, et al. Nucleotide sequence of cloned cDNA for bovine corticotropin-β-lipotropin precursor. *Nature* (1979) **278**:423–7. doi:10.1038/278423a0
2. Smith AI, Funder JW. Proopiomelanocortin processing in the pituitary, central nervous system, and peripheral tissues. *Endocr Rev* (1988) **9**:159–79. doi:10.1210/edrv-9-1-159
3. Castro MG, Morrison E. Post-translational processing of proopiomelanocortin in the pituitary and in the brain. *Crit Rev Neurobiol* (1997) **11**:35–57. doi:10.1615/CritRevNeurobiol.v11.i1.30
4. Eberle AE. Proopiomelanocortin and the melanocortin peptides. In: Cone RD editor. *The Melanocortin Receptors*. Totowa, NJ: Human Press (2000). p. 3–67.
5. Mountjoy KG. Cloning of the melanocortin receptors. In: Cone RD editor. *The Melanocortin Receptors*. Totowa, NJ: Human Press (2000). p. 209–35.
6. Li CH. β-Endorphin: synthetic analogs and structure-activity relationships. In: Li CH editor. *Hormonal Proteins and Peptides*. New York, NY: Academic Press (1981). p. 2–34.
7. Stevens CW. The evolution of opioid receptors. *Front Biosci* (2011) **14**:1247–69.
8. Wittert G, Hope P, Pyle D. Tissue distribution of opioid receptor gene expression in the rat. *Biochem Biophys Res Commun* (1996) **218**:877–81. doi:10.1006/bbrc.1996.0156
9. Boston BA. Peripheral effects of melanocortins. In: Cone RD editor. *The Melanocortin Receptors*. Totowa, NJ: Human Press (2000). p. 143–69.
10. Wilkinson CW. Roles of acetylation and other post-translational modifications in melanocortin function and interaction with endorphins. *Peptides* (2006) **27**:453–71. doi:10.1016/j.peptides.2005.05.029
11. Naudé R, Oelofsen W, Takahashi A, Amano M, Kawauchi H. Molecular cloning and characterization of pre-proopiomelanocortin (prePOMC) cDNA from the ostrich (*Struthio camelus*). *Gen Comp Endocrinol* (2006) **146**:310–7.
12. Kobayashi Y, Sakamoto T, Iguchi K, Imai Y, Hoshino M, Lance VA, et al. cDNA cloning of proopiomelanocortin (POMC) and mass spectrometric identification of POMC-derived peptides from snake and alligator pituitaries. *Gen Comp Endocrinol* (2007) **152**:73–81. doi:10.1016/j.ygcen.2007.02.026
13. Takahashi A, Kawauchi H. Evolution of melanocortin systems in fish. *Gen Comp Endocrinol* (2006) **148**:85–94. doi:10.1016/j.ygcen.2005.09.020
14. Takahashi A, Amemiya Y, Sarashi M, Sower SA, Kawauchi H. Melanotropin and corticotropin are encoded on two distinct genes in the lamprey, the earliest evolved extant vertebrate. *Biochem Biophys Res Commun* (1995) **213**:490–8. doi:10.1006/bbrc.1995.2158
15. Holm IA, Majzoub JA. Adrenocorticotropin. In: Melmed S editor. *The Pituitary*. Cambridge, MA: Blackwell Science (1995). 45 p.
16. Raffin-Sanson ML, de Keyzer Y, Bertagna X. Proopiomelanocortin, a polypeptide precursor with multiple functions: from physiology to pathological conditions. *Eur J Endocrinol* (2003) **149**:79–90. doi:10.1530/eje.0.1490079
17. Asa S, Kovacs K, Melmed S. The hypothalamic-pituitary function. In: Melmed S editor. *The Pituitary*. Cambridge, MA: Blackwell Science (1995). 3 p.
18. Gorbman A, Dickhoff WW, Vigna SR, Clark NB, Ralph CL. *Comparative Endocrinology*. New York: John Wiley and Sons (1983).
19. Li CH, Chung D, Oelofsen W, Naudé RJ. Adrenocorticotropin 53. The amino acid sequence of the hormone from the ostrich pituitary gland. *Biochem Biophys Res Commun* (1978) **81**:900–6. doi:10.1016/0006-291X(78)91436-5
20. Naudé RJ, Chung D, Li CH, Oelofsen W. β-Lipotropin: primary structure of the hormone from the ostrich pituitary gland. *Int J Pept Protein Res* (1981) **18**:138–47. doi:10.1111/j.1399-3011.1981.tb02051.x

21. Naudé RJ, Chung D, Li CH, Oelofsen W. β-Endorphin: primary structure of the hormone from the ostrich pituitary gland. *Biochem Biophys Res Commun* (1981) **98**:108–14. doi:10.1016/0006-291X(81)91876-3
22. Litthauer D, Naudé RJ, Oelofsen W. Isolation, characterization and primary structure of two β-LPH variants from ostrich pituitary glands. *Int J Pept Protein Res* (1984) **24**:309–15. doi:10.1111/j.1399-3011.1984.tb00958.x
23. Naudé RJ, Litthauer D, Oelofsen W, Chrétien M, Lazure C. The production of the ostrich NH_2-terminal POMC fragment requires cleavage at a unique signal peptidase site. *Peptides* (1993) **14**:519–29. doi:10.1016/0196-9781(93)90141-3
24. Takahashi A, Kawauchi H. Diverse structures and functions of melanocortin, endorphin and melanin-concentrating hormone in fish. In: Zaccone G, Reinecke M, Kapoor BG editors. *Fish Endocrinology*. Enfield, NH: Science Publishers (2006). p. 325–92.
25. Endo D, Park MK. Molecular characterization of the leopard gecko POMC gene and expressional change in the testis by acclimation to low temperature and with a short photoperiod. *Gen Comp Endocrinol* (2004) **138**:70–7. doi:10.1016/j.ygcen.2004.04.009
26. Shen ST, Lu LM, Chen JR, Chien JT, Yu JY. Molecular cloning of proopiomelanocortin (POMC) cDNA from mud turtle, *Pelodiscus sinensis*. *Gen Comp Endocrinol* (2003) **131**:192–201. doi:10.1016/S0016-6480(03)00028-5
27. Naudé R, Oelofsen W. Isolation and characterization of β-lipotropin from the pituitary gland of the ostrich, *Struthio camelus*. *Int J Pept Protein Res* (1981) **18**:135–7. doi:10.1111/j.1399-3011.1981.tb02050.x
28. Drouin J, Goodman HM. Most of the coding region of rat ACTH and α-LPH precursor gene lacks intervening sequences. *Nature* (1980) **228**:610–3. doi:10.1038/288610a0
29. Uhler M, Herbert E. Complete amino acid sequence of mouse proopiomelanocortin derived from the nucleotide sequence of proopiomelanocortin cDNA. *J Biol Chem* (1983) **258**:257–61.
30. Devi L. Consensus sequence for processing of peptide precursors at monobasic sites. *FEBS Lett* (1991) **280**:189–94. doi:10.1016/0014-5793(91)80290-J
31. Martens GJM. Expression of two proopiomelanocortin genes in the pituitary gland of *Xenopus laevis*: complete structures of the two preprohormones. *Nucleic Acids Res* (1986) **14**:3791–8. doi:10.1093/nar/14.9.3791
32. van Strien FJC, Jenks BG, Heerma W, Versluis C, Kawauchi H, Roubos EW. α,*N*-acetyl β-endorphin (1-8) is the terminal product of processing of endorphins in the melanotrope cells of *Xenopus laevis*, as demonstrated by FAB tandem mass spectrometry. *Biochem Biophys Res Commun* (1993) **191**:262–8.
33. van Strien FJC, Devreese B, Beeumen JV, Roubos EW, Jenks BG. Biosynthesis and processing of the N-terminal part of proopiomelanocortin in *Xenopus laevis*: characterization of γ-MSH peptides. *J Neuroendocrinol* (1995) **7**:807–15.
34. van Strien FJC, Jespersen S, van der Greef J, Jenks BG, Roubos EW. Identification of POMC processing products in single melanotrope cells by matrix-assisted laser desorption/ionization mass spectrometry. *FEBS Lett* (1996) **379**:165–70.
35. Meyer A. Molecular evidence on the origin of tetrapods and the relationships of the coelacanth. *Trends Ecol Evol* (1995) **10**:111–6.
36. Venkatesh B, Erdmann MV, Brenner S. Molecular synapomorphies resolve evolutionary relationships of extant jawed vertebrates. *Proc Natl Acad Sci U S A* (2001) **98**:11382–7. doi:10.1073/pnas.201415598
37. Shan Y, Gras R. 43 Genes support the lungfish-coelacanth grouping related to the closest living relative of tetrapods with the Bayesian method under the coalescence model. *BMC Res Notes* (2011) **4**:49. doi:10.1186/1756-0500-4-49
38. Amemiya Y, Takahashi A, Meguro H, Kawauchi H. Molecular cloning of lungfish proopiomelanocortin cDNA. *Gen Comp Endocrinol* (1999) **115**:415–21. doi:10.1006/gcen.1999.7327
39. Vallarino M, Bunel DT, Vaudry H. Alpha-melanocyte-stimulating hormone (α-MSH) in the brain of the African lungfish, *Protopterus annectens*: immunohistochemical localization and biochemical characterization. *J Comp Neurol* (1992) **322**:266–74. doi:10.1002/cne.903220212
40. Dores RM, Joss JMP. Immunological evidence of multiple forms of α-melanotropin (α-MSH) in the pars intermedia of the Australian lungfish, *Neoceratodus forsteri*. *Gen Comp Endocrinol* (1988) **71**:468–74. doi:10.1016/0016-6480(88)90276-6
41. Dores RM, Sollars C, Danielson P, Lee J, Alubaian J, Joss JMP. Cloning of a proopiomelanocortin cDNA from the pituitary of the Australian lungfish, *Neoceratodus forsteri*: analyzing trends in the organization of this prohormone precursor. *Gen Comp Endocrinol* (1999) **116**:433–44. doi:10.1006/gcen.1999.7382
42. Takahashi A, Yasuda A, Sullivan CV, Kawauchi H. Identification of proopiomelanocortin-related peptides in the rostral pars distalis of the pituitary in coelacanth: evolutional implications. *Gen Comp Endocrinol* (2003) **130**:340–9. doi:10.1016/S0016-6480(02)00632-9
43. Nelson JS. *Fishes of the World*. New York: John Wiley and Sons (2006).
44. Takahashi A, Takasaka T, Yasuda A, Amemiya Y, Sakai M, Kawauchi H. Identification of carp proopiomelanocortin-related peptides and their effects on phagocytes. *Fish Shellfish Immunol* (2000) **10**:273–84. doi:10.1006/fsim.1999.0256
45. Takahashi A, Amemiya Y, Yasuda A, Meguro H, Kawauchi H. Mass spectrometric detection of proopiomelanocortin (POMC)-related peptides following molecular cloning of POMC cDNA in bigeye tuna, *Thunnus obesus*. *Fish Sci* (2002) **68**:1071–8. doi:10.1046/j.1444-2906.2002.00534.x
46. Takahashi A, Amano M, Itoh T, Yasuda A, Yamanome T, Amemiya Y, et al. Nucleotide sequence and expression of three subtypes of proopiomelanocortin mRNA in barfin flounder. *Gen Comp Endocrinol* (2005) **141**:291–303. doi:10.1016/j.ygcen.2005.01.010
47. Naito N, Takahashi A, Nakai Y, Kawauchi H. Immunocytochemical identification of the proopiocortin-producing cells in the chum salmon pituitary with antisera to endorphin and NH_2-terminal peptide of salmon proopiocortin. *Gen Comp Endocrinol* (1984) **56**:185–92. doi:10.1016/0016-6480(84)90029-7
48. Olivereau M, Olivereau JM. Corticotropin-like immunoreactivity in the brain and pituitary of three teleost species (goldfish, trout and eel). *Cell Tissue Res* (1990) **262**:115–23. doi:10.1007/BF00327752
49. Amano M, Takahashi A, Yamanome T, Oka K, Amiya N, Kawauchi H, et al. Immunocytochemical localization and ontogenic development of α-melanocyte-stimulating hormone (α-MSH) in the brain of a pleuronectiform fish, barfin flounder. *Cell Tissue Res* (2005) **320**:127–34. doi:10.1007/s00441-004-1058-4
50. Takahashi A, Amano M, Amiya N, Yamanome T, Yamamori K, Kawauchi H. Expression of three proopiomelanocortin subtype genes and mass spectrometric identification of POMC-derived peptides in pars distalis and pars intermedia of barfin flounder pituitary. *Gen Comp Endocrinol* (2006) **145**:280–6. doi:10.1016/j.ygcen.2005.09.005
51. Amemiya Y, Takahashi A, Suzuki N, Sasayama Y, Kawauchi H. A newly characterized melanotropin in proopiomelanocortin in pituitaries of an elasmobranch, *Squalus acanthias*. *Gen Comp Endocrinol* (1999) **114**:387–95. doi:10.1006/gcen.1999.7256
52. Amemiya Y, Takahashi A, Suzuki N, Sasayama Y, Kawauchi H. Molecular cloning of proopiomelanocortin cDNA from an elasmobranch, the stingray, *Dasyatis akajei*. *Gen Comp Endocrinol* (2000) **118**:105–12. doi:10.1006/gcen.1999.7444
53. Takahashi A, Itoh T, Nakanishi A, Amemiya Y, Ida H, Meguro H, et al. Molecular cloning of proopiomelanocortin cDNA in the ratfish, a holocephalan. *Gen Comp Endocrinol* (2004) **135**:159–65. doi:10.1016/j.ygcen.2003.08.007
54. Dores RM, Cameron E, Lecaude S, Danielson PB. Presence of the δ-MSH sequence in a proopiomelanocortin cDNA cloned from the pituitary of the galeoid shark, *Heterodontus portusjacksoni*. *Gen Comp Endocrinol* (2003) **133**:71–9. doi:10.1016/S0016-6480(03)00151-5
55. Takahashi A, Kobayashi Y, Moriyama S, Hyodo S. Evaluation of posttranslational processing of proopiomelanocortin in the banded houndshark pituitary by combined cDNA cloning and mass spectrometry. *Gen Comp Endocrinol* (2008) **157**:41–8. doi:10.1016/j.ygcen.2008.03.006
56. Takahashi A, Amemiya Y, Sakai M, Yasuda A, Suzuki N, Sasayama Y, et al. Occurrence of four MSHs in dogfish POMC and their immunomodulating effects. *Ann N Y Acad Sci* (1999) **885**:459–63.
57. Takahashi A, Nakata O, Moriyama S, Nozaki M, Joss JMP, Sower S, et al. Occurrence of two functionally distinct proopiomelanocortin genes in all modern lampreys. *Gen Comp Endocrinol* (2006) **148**:72–8. doi:10.1016/j.ygcen.2005.09.003
58. Nozaki M, Takahashi A, Amemiya Y, Kawauchi H, Sower SA.

Distribution of lamprey adrenocorticotropin and melanotropins in the pituitary of the adult sea lamprey, *Petromyzon marinus*. *Gen Comp Endocrinol* (1995) **98**:147–56. doi:10.1006/gcen.1995.1055
59. Takahashi A, Amemiya Y, Nozaki M, Sower SA, Joss J, Gorbman A, et al. Isolation and characterization of melanotropins from lamprey pituitary glands. *Int J Pept Protein Res* (1995) **46**:197–204. doi:10.1111/j.1399-3011.1995.tb00589.x
60. Takahashi A, Yasuda A, Sower SA, Kawauchi H. Posttranslational processing of proopiomelanocortin family molecules in sea lamprey based on mass spectrometric and chemical analyses. *Gen Comp Endocrinol* (2006) **148**:79–84. doi:10.1016/j.ygcen.2005.09.022
61. Dores RM, McDonald LK. Detection of Met-enkephalin in the pars intermedia of the lampreys, *Ichthyomyzon castaneus* and *Petromyzon marinus*. *Gen Comp Endocrinol* (1992) **88**:292–7. doi:10.1016/0016-6480(92)90262-I
62. Kawauchi H. Chemistry of proopicortin-related peptides in the salmon pituitary. *Arch Biochem Biophys* (1983) **227**:343–50. doi:10.1016/0003-9861(83)90462-9
63. Tran TN, Fryer JN, Bennett HPJ, Tonon MC, Vaudry H. TRH stimulates the release of POMC-derived peptides from goldfish melanotropes. *Peptides* (1989) **10**:835–41. doi:10.1016/0196-9781(89)90122-8
64. Lamers AE, Flik G, Atsma W, Wendelaar Bonga SE. A role for di-acetyl α-melanocyte-stimulating hormone in the control of cortisol release in the teleost *Oreochromis mossambicus*. *J Endocrinol* (1992) **135**:285–92. doi:10.1677/joe.0.1350285
65. van den Burg EH, Metz JR, Ross HA, Darras VM, Wendelaar Bonga SE, Flik G. Temperature-induced changes in thyrotropin-releasing hormone sensitivity in carp melanotropes. *Neuroendocrinology* (2003) **77**:15–23. doi:10.1159/000068331
66. Sánchez E, Rubio VC, Cerdá-Reverter JM. Characterization of the sea bass melanocortin 5 receptor: a putative role in hepatic lipid metabolism. *J Exp Biol* (2009) **212**:3901–10. doi:10.1242/jeb.035121
67. Sánchez E, Rubio VC, Thompson D, Met J, Flik G, Millhauser GL, et al. Phosphodiesterase inhibitor-dependent inverse agonism of agouti-related protein on melanocortin 4 receptor in sea bass (*Dicentrarchus labrax*). *Am J Physiol Regul Integr Comp Physiol* (2009) **296**:R1293–306. doi:10.1152/ajpregu.90948.2008
68. Sánchez E, Rubio VC, Cerdá-Reverter JM. Molecular and pharmacological characterization of the melanocortin type 1 receptor in sea bass. *Gen Comp Endocrinol* (2010) **165**:163–9. doi:10.1016/j.ygcen.2009.06.008
69. Smyth DG, Massey DE, Zakarian S, Finnie MDA. Endorphins are stored in biologically active and inactive forms: isolation of α-*N*-acetyl peptides. *Nature* (1979) **279**:252–4. doi:10.1038/279252a0
70. Kobayashi Y, Mizusawa K, Yamanome T, Chiba H, Takahashi A. Possible paracrine function of α-melanocyte-stimulating hormone and inhibition of its melanin-dispersing activity by N-terminal acetylation in the skin of the barfin flounder, *Verasper moseri*. *Gen Comp Endocrinol* (2009) **161**:419–24. doi:10.1016/j.ygcen.2009.02.009
71. Kobayashi Y, Mizusawa K, Chiba Y, Tagawa M, Takahashi A. Further evidence on acetylation-induced inhibition of the pigment-dispersing activity of α-melanocyte-stimulating hormone. *Gen Comp Endocrinol* (2012) **176**:9–17. doi:10.1016/j.ygcen.2011.12.001
72. Cerdá-Reverter JM, Ling MK, Schiöth HB, Peter RE. Molecular cloning, characterization and brain mapping of the melanocortin 5 receptor in the goldfish. *J Neurochem* (2003) **87**:1354–67. doi:10.1046/j.1471-4159.2003.02107.x
73. Cerdá-Reverter JM, Ringholm A, Schiöth HB, Peter RE. Molecular cloning, pharmacological characterization, and brain mapping of the melanocortin 4 receptor in the goldfish: involvement in the control of food intake. *Endocrinology* (2003) **144**:2336–49. doi:10.1210/en.2002-0213
74. Logan DW, Bryson-Richardson RJ, Pagan KE, Taylor MS, Currie PD, Jackson IJ. The structure and evolution of the melanocortin and MCH receptors in fish and mammals. *Genomics* (2003) **81**:184–91. doi:10.1016/S0888-7543(02)00037-X
75. Kobayashi Y, Chiba H, Mizusawa K, Suzuki N, Cerdá-Reverte JM, Takahashi A. Pigment-dispersing activities and cortisol-releasing activities of melanocortins and their receptors in xanthophores and head kidneys of the goldfish *Carassius auratus*. *Gen Comp Endocrinol* (2011) **173**:438–46. doi:10.1016/j.ygcen.2011.06.019
76. Klovins J, Haitina T, Fridmanis D, Kilianova Z, Kapa I, Fredriksson R, et al. The melanocortin system in Fugu: determination of POMC/AGRP/MCR gene repertoire and synteny, as well as pharmacology and anatomical distribution of the MCRs. *Mol Biol Evol* (2004) **21**:563–79.
77. Kobayashi Y, Tsuchiya K, Yamanome T, Schiöth HB, Kawauchi H, Takahashi A. Food deprivation increases the expression of melanocortin-4 receptor in the liver of barfin flounder, *Verasper moseri*. *Gen Comp Endocrinol* (2008) **155**:280–7. doi:10.1016/j.ygcen.2007.05.010
78. Kobayashi Y, Tsuchiya K, Yamanome T, Schiöth HB, Takahashi A. Differential expressions of melanocortin receptor subtypes in melanophores and xanthophores of barfin flounder. *Gen Comp Endocrinol* (2010) **168**:133–42. doi:10.1016/j.ygcen.2010.04.017
79. Kobayashi Y, Chiba H, Yamanome T, Schiöth HB, Takahashi A. Melanocortin receptor subtypes in interrenal cells and corticotropic activity of α-melanocyte-stimulating hormones in barfin flounder, *Verasper moseri*. *Gen Comp Endocrinol* (2011) **170**:558–68. doi:10.1016/j.ygcen.2010.11.019
80. Satake H, Sakai T. Recent advances and perceptions in studies of heterodimerization between G protein-coupled receptors. *Protein Pept Lett* (2008) **15**:300–8. doi:10.2174/092986608783744207
81. Rozenfeld R, Devi LA. Exploring a role for heteromerization in GPCR signaling specificity. *Biochem J* (2011) **433**:11–8. doi:10.1042/BJ20100458
82. Tadagaki K, Jockers R, Kamal M. History and biological significance of GPCR heteromerization in the neuroendocrine system. *Neuroendocrinology* (2012) **95**:223–31. doi:10.1159/000330000

Conflict of Interest Statement: The authors declare that the research was conducted in the absence of any commercial or financial relationships that could be construed as a potential conflict of interest.

Received: 31 August 2013; paper pending published: 16 September 2013; accepted: 25 September 2013; published online: 17 October 2013.
*Citation: Takahashi A and Mizusawa K (2013) Posttranslational modifications of proopiomelanocortin in vertebrates and their biological significance. Front. Endocrinol. **4**:143. doi: 10.3389/fendo.2013.00143*
This article was submitted to Experimental Endocrinology, a section of the journal Frontiers in Endocrinology.

frontiers in
ENDOCRINOLOGY

MINI REVIEW ARTICLE
published: 16 July 2013
doi: 10.3389/fendo.2013.00087

Production of hydrogen sulfide from D-cysteine and its therapeutic potential

Norihiro Shibuya and Hideo Kimura*

Department of Molecular Pharmacology, National Institute of Neuroscience, Kodaira, Tokyo, Japan

Edited by:
Sho Kakizawa, Kyoto University, Japan

Reviewed by:
Martin Diener, University Giessen, Germany
Sho Kakizawa, Kyoto University, Japan

****Correspondence:***
Hideo Kimura, Department of Molecular Pharmacology, National Institute of Neuroscience, 4-1-1 Ogawahigashi, Kodaira, Tokyo 187-8502, Japan
e-mail: kimura@ncnp.go.jp

Accumulating evidence shows that H_2S has physiological functions in various tissues and organs. It includes regulation of neuronal activity, vascular tension, a release of insulin, and protection of the heart, kidney, and brain from ischemic insult. H_2S is produced by enzymes from L-cysteine; cystathionine β-synthase, cystathionine γ-lyase, and 3-mercaptopyruvate sulfurtransferase (3MST) along with cysteine aminotransferase. We recently discovered an additional pathway for the production of H_2S from D-cysteine. D-Amino acid oxidase provides 3-mercaptopyruvate for 3MST to produce H_2S. D-Cysteine protects cerebellar neurons from oxidative stress and attenuates ischemia-reperfusion injury caused in the kidney more effectively than L-cysteine. This review focuses on a novel pathway for the production of H_2S and its therapeutic application especially to the renal diseases.

Keywords: hydrogen sulfide, bound sulfane sulfur, L-cysteine, D-cysteine, 3MST, DAO, ischemia-reperfusion injury

INTRODUCTION

The discovery of endogenous sulfide in the brain urged us to study the function of hydrogen sulfide (H_2S) in the brain (1–3). The recent re-evaluation showed that the endogenous levels of H_2S are much lower than those initially evaluated, but this finding confirmed the existence of sulfide in tissues (4–6).

H_2S facilitates the induction of hippocampal long-term potentiation, a synaptic model of learning and memory, by enhancing the activity of N-methyl-D-aspartate (NMDA) receptors in neurons, and it induces Ca^{2+} waves in astrocytes (7, 8). It relaxes vascular smooth muscle by activating K^+ channels, regulates the release of insulin and induces angiogenesis (9–14). It protects neurons from oxidative stress by enhancing the activity of glutathione synthesis, scavenging reactive oxygen species, and suppressing the excessive increase in the intracellular Ca^{2+} (15–17). In cardiovascular system, H_2S protects cardiomyocytes from ischemia-reperfusion injury by preserving mitochondrial function (18). A similar protective effect was also observed in the kidney (19). H_2S is produced from L-cysteine by two pyridoxal 5′-phosphate (PLP)-dependent enzymes, cystathionine β-synthase (CBS), and cystathionine γ-lyase (CSE) and PLP-independent 3-mercaptopyruvate sulfurtransferase (3MST) (**Figure 1**) (7, 9, 20–23). 3MST produces H_2S from 3-mercaptopyruvate (3MP), an achiral α-keto acid, which is generated by PLP-dependent cysteine aminotransferase (CAT) from L-cysteine and α-ketoglutarate (α-KG) (24–26). Thioredoxin (Trx) and dihydrolipoic acid (DHLA) are endogenous reducing cofactors that facilitate H_2S release from 3MST (23). We recently discovered a novel pathway with D-cysteine as a substrate (27).

PRODUCTION OF H_2S FROM D-CYSTEINE

When we examined the production of H_2S from brain homogenates, we found that H_2S was produced from D-cysteine, originally used as a negative control for L-cysteine (27). H_2S-producing pathway from D-cysteine is distinct from the pathways involving L-cysteine. There are critical differences between the two pathways; (i) the optimal pH, (ii) the dependency on PLP, and (iii) the stability against the freeze and thaw procedure. The production of H_2S from D-cysteine is optimal at pH 7.4, whereas production from L-cysteine is maximal under the alkaline condition. H_2S production from D-cysteine is PLP-independent, while that from L-cysteine is PLP-dependent. A single freeze-thaw cycle greatly increases the H_2S production from D-cysteine. D-Amino acid oxidase (DAO) that produces 3MP from D-cysteine is localized to peroxisomes, while 3MST is mainly found in mitochondria (21, 28). Mitochondria and peroxisomes exchange various metabolites via a specific form of vesicular trafficking, and are usually in close proximity to each other or have physical contact (29). 3MST and DAO can produce H_2S by the interaction of both organelles.

LOCALIZATION OF H_2S-PRODUCING ENZYMES

Enzymes producing H_2S from L-cysteine are expressed in many tissues (7, 9, 17, 20, 21, 23, 30, 31). 3MST is found in neurons in the cerebral cortex, cerebellum, olfactory bulb, pons, and retina, while CBS is preferentially expressed in cerebellar Bergmann glia and in astrocytes throughout the brain (21, 32). CSE activity in the brain is only 1% of the hepatic activity (33). CBS, CSE and 3MST, and CAT are expressed in the liver and kidney (20). Vascular endothelium co-expresses 3MST and CAT (31). The localization of CSE in vascular endothelium is controversial (31, 34). Unlike the L-cysteine pathways, the D-cysteine pathway operates predominantly in the cerebellum and the kidney (27, 35). In the cerebellum, DAO is expressed in astrocytes, Bergmann glia, and several types of neurons including the Golgi and Purkinje cells (35, 36). In the kidney, DAO and 3MST are expressed in the proximal convoluted tubules of the cortex similarly to CBS and CSE (30, 37–39).

REGULATION OF H_2S-PRODUCING ENZYMES BY CA^{2+}

3MST/CAT is regulated by Ca^{2+}; the activity is maximal in the absence of Ca^{2+} and is completely suppressed at 2.9 μM

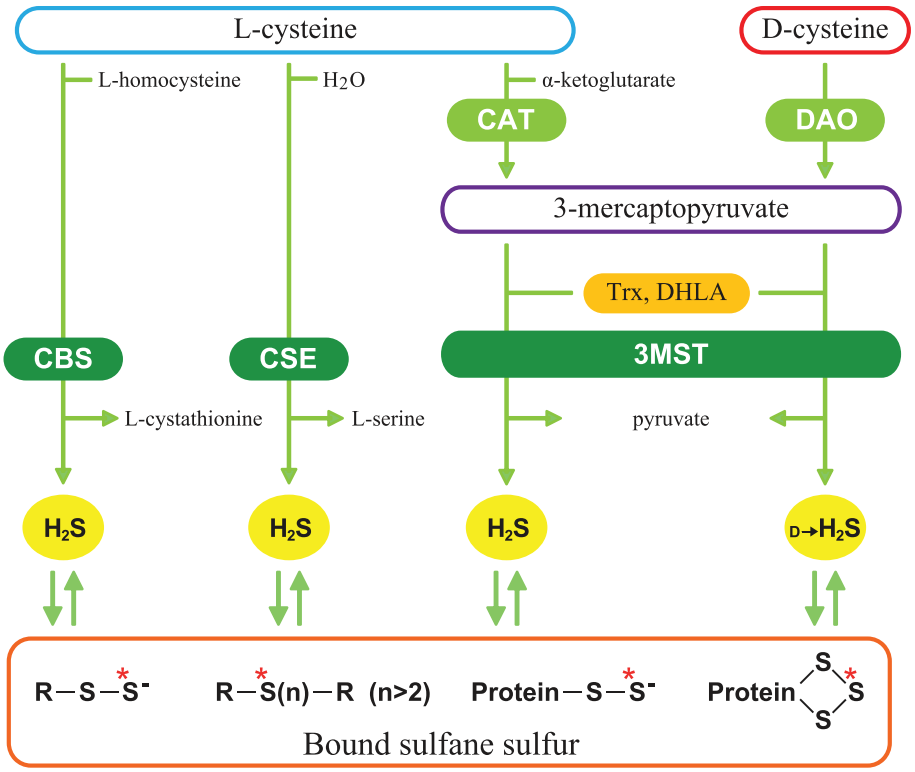

FIGURE 1 | Schematic representation of H_2S-producing pathways. Cystathionine β-synthase (CBS) catalyzes β-replacement of L-cysteine to produce H_2S and L-cystathionine. Cystathionine γ-lyase (CSE) catalyzes the hydrolysis of L-cysteine. 3-Mercaptopyruvate sulfurtransferase (3MST) produces H_2S from 3-mercaptopyruvate (3MP), which is generated by cysteine aminotransferase (CAT) and D-amino acid oxidase (DAO) from L-cysteine and D-cysteine, respectively. Thioredoxin (Trx) and dihydrolipoic acid (DHLA) are endogenous reducing cofactors that facilitate the release of H_2S from 3MST. H_2S is stored as bound sulfane sulfur, which is divalent sulfur bound only to other sulfur, such as outer sulfur atoms of persulfides and innerchain atoms of polysulfides. Red asterisks show bound sulfane sulfur.

Ca^{2+} (17). A similar regulation by Ca^{2+} is observed in CSE activity (40). H_2S is produced by CSE at the steady-state low Ca^{2+} concentrations and that the production is suppressed by increased Ca^{2+} (40). Calmodulin is not involved in the regulation of CSE activity. It was previously reported that CSE activity is regulated by Ca^{2+}/calmodulin in the presence of 1–2 mM Ca^{2+} (34). Because the intracellular Ca^{2+} concentrations are between 100 nM and 3 μM in endothelium, Ca^{2+} concentrations used in the previous study are not in the physiological range (41).

SOURCE OF D-CYSTEINE

Relatively large amounts of D-serine are found in mammalian tissues, and the content of D-serine is up to 15∼30% of the L-form in the brain (42, 43). D-Serine is thought to be produced by PLP-dependent serine racemase, but the Michaelis-constant value of serine racemase is higher than the endogenous levels of L-serine (42, 44–46). Although cysteine is structurally similar to serine with an OH replaced by an SH, serine racemase does not change L-cysteine to D-cysteine (27). Aspartate racemase is homologous to CAT and has an affinity for both aspartate and cysteine (24, 47), but does not produce D-cysteine.

A possible source of D-cysteine is absorption from food. L-Amino acids are non-enzymatically racemized by heat and alkaline treatment applied during food processing. L-Cysteine is one of the fastest racemizing amino acid, and 21–44% of L-cysteine is changed to D-cysteine by alkaline treatment (48, 49). Although D-cysteine is easily absorbed through the gastrointestinal tract and enters the blood stream (50), D-cysteine is not detected either in the cerebellum or the kidney after the oral administration. Considering the fact that the levels of bound sulfane sulfur, a storage form of H_2S (**Figure 1**), are increased after oral administration of D-cysteine (5, 27), D-cysteine may be immediately metabolized to produce bound sulfane sulfur in tissues.

CYTOPROTECTIVE EFFECT OF D-CYSTEINE

The most characteristic feature of the D-cysteine pathway is the greater H_2S-producing activity in the cerebellum and the kidney compared to the L-cysteine pathway; 7- and 80-fold greater in the cerebellum and the kidney, respectively. Although both D-cysteine and L-cysteine protect cerebellar neurons from hydrogen peroxide-induced oxidative stress (27), D-cysteine protected neurons more greatly than L-cysteine, probably because the transport activity for D-cysteine is greater than that for L-cysteine (51). D-Cysteine may have a potential to improve the developmental

neuronal diseases in the cerebellum like autism in which oxidative stress may be involved (52, 53).

Ischemia-reperfusion injury is observed after cardiovascular surgery, transplantation, or septic as well as hemorrhagic shock. Renal ischemia-reperfusion injury reduces the filtering capacity of the glomerulus and causes acute renal failure (54). Endothelin antagonists, atrial natriuretic peptides, prostaglandins, nitric oxide inhibitors, thyroxine, and human insulin-like growth factor 1 have been studied for the prophylaxis and treatment of acute tubular necrosis without clinical benefit (55–58). We found that the oral administration of D-cysteine attenuates renal ischemia-reperfusion injury (27). The structure of glomeruli, which is disintegrated after ischemia-reperfusion, is well preserved by D-cysteine. In contrast, the glomeruli are shrunk and a wide space is observed between glomerulus and the surrounding capsule after ischemia-reperfusion when L-cysteine is applied. D-Cysteine increases the levels of bound sulfane sulfur and protects the renal cortex from the ischemia-reperfusion injury more efficiently than L-cysteine.

D-CYSTEINE: ITS THERAPEUTIC POTENTIAL

L-Cysteine is metabolized to produce (i) cysteinyl-tRNA by cysteinyl-tRNA synthetase (59), (ii) γ-glutamylcysteine, a precursor of glutathione, by γ-glutamylcysteine synthetase, (iii) taurine or pyruvate by cysteine dioxygenase (60), and (iv) propionyl CoA by α-keto acid dehydrogenase. Because D-cysteine is not metabolized by these enzymes, D-cysteine must efficiently be utilized to produce H_2S in the cerebellum and the kidney.

L-Cysteine is an excitotoxin comparable in potency to other excitatory amino acids and increases the blood pressure and heart rate (61, 62). In contrast, D-cysteine neither causes excitotoxic damage to the brain nor disturbs heart function (63, 64). Therefore, D-cysteine can be systemically and repeatedly applied with less toxicity compared to L-cysteine. The administration of D-cysteine may provide a new therapeutic approach to protect specific tissues from oxidative stress or ischemia-reperfusion injury through its conversion to H_2S via a novel pathway with 3MST and DAO.

ACKNOWLEDGMENTS

This work was supported by a grant from the National Institute of Neuroscience, a KAKENHI (23659089) Grant-in-Aid for Challenging Exploratory Research to Hideo Kimura, a KAKENHI (23700434) Grant-in-Aid for Young Scientists (B), a Health Labour Sciences Research Grant from the Ministry of Health Labour and Welfare to Norihiro Shibuya.

REFERENCES

1. Goodwin LR, Francom D, Dieken FP, Taylor JD, Warenycia MW, Reiffenstein RJ, et al. Determination of sulfide in brain tissue by gas dialysis/ion chromatography: postmortem studies and two case reports. *J Anal Toxicol* (1989) **13**:105–9. doi:10.1093/jat/13.2.105
2. Warenycia MW, Goodwin LR, Benishin CG, Reiffenstein RJ, Francom DM, Taylor JD, et al. Acute hydrogen sulfide poisoning. Demonstration of selective uptake of sulfide by the brainstem by measurement of brain sulfide levels. *Biochem Pharmacol* (1989) **38**:973–81. doi:10.1016/0006-2952(89)90288-8
3. Savage JC, Gould DH. Determination of sulfide in brain tissue and rumen fluid by ion-interaction reversed-phase high-performance liquid chromatography. *J Chromatogr* (1990) **526**:540–5.
4. Furne J, Saeed A, Levitt MD. Whole tissue hydrogen sulfide concentrations are orders of magnitude lower than presently accepted values. *Am J Physiol Regul Integr Comp Physiol* (2008) **295**:R1479–85. doi:10.1152/ajpregu.90566.2008
5. Ishigami M, Hiraki K, Umemura K, Ogasawara Y, Ishii K, Kimura H. A source of hydrogen sulfide and a mechanism of its release in the brain. *Antioxid Redox Signal* (2009) **11**:205–14. doi:10.1089/ARS.2008.2132
6. Wintner EA, Deckwerth TL, Langston W, Bengtsson A, Leviten D, Hill P, et al. A monobromobimane-based assay to measure the pharmacokinetic profile of reactive sulphide species in blood. *Br J Pharmacol* (2010) **160**:941–57. doi:10.1111/j.1476-5381.2010.00704.x
7. Abe K, Kimura H. The possible role of hydrogen sulfide as an endogenous neuromodulator. *J Neurosci* (1996) **16**:1066–71.
8. Nagai Y, Tsugane M, Oka J, Kimura H. Hydrogen sulfide induces calcium waves in astrocytes. *FASEB J* (2004) **18**:557–9.
9. Hosoki R, Matsuki N, Kimura H. The possible role of hydrogen sulfide as an endogenous smooth muscle relaxant in synergy with nitric oxide. *Biochem Biophys Res Commun* (1997) **237**:527–31. doi:10.1006/bbrc.1997.6878
10. Zhao W, Zhang J, Lu Y, Wang R. The vasorelaxant effect of H_2S as a novel endogenous gaseous K_{ATP} channel opener. *EMBO J* (2001) **20**:6008–16. doi:10.1093/emboj/20.21.6008
11. Yang W, Yang G, Jia X, Wu L, Wang R. Activation of K_{ATP} channels by H_2S in rat insulin-secreting cells and the underlying mechanisms. *J Physiol* (2005) **569**:519–31. doi:10.1113/jphysiol.2005.097642
12. Kaneko Y, Kimura Y, Kimura H, Niki I. L-Cysteine inhibits insulin release from the pancreatic beta-cell: possible involvement of metabolic production of hydrogen sulfide, a novel gasotransmitter. *Diabetes* (2006) **55**:1391–7. doi:10.2337/db05-1082
13. Papapetropoulos A, Pyriochou A, Altaany Z, Yang G, Marazioti A, Zhou Z, et al. Hydrogen sulfide is an endogenous stimulator of angiogenesis. *Proc Natl Acad Sci U S A* (2009) **106**:21972–7. doi:10.1073/pnas.0908047106
14. Mustafa AK, Sikka G, Gazi SK, Steppan J, Jung SM, Bhunia AK, et al. Hydrogen sulfide as endothelium-derived hyperpolarizing factor sulfhydrates potassium channels. *Circ Res* (2011) **109**:1259–68. doi:10.1161/CIRCRESAHA.111.240242
15. Kimura Y, Kimura H. Hydrogen sulfide protects neurons from oxidative stress. *FASEB J* (2004) **18**:1165–7.
16. Kimura Y, Goto Y, Kimura H. Hydrogen sulfide increases glutathione production and suppresses oxidative stress in mitochondria. *Antioxid Redox Signal* (2010) **12**:1–13. doi:10.1089/ars.2008.2282
17. Mikami Y, Shibuya N, Kimura Y, Nagahara N, Yamada M, Kimura H. Hydrogen sulfide protects the retina from light-induced degeneration by the modulation of Ca^{2+} influx. *J Biol Chem* (2011) **286**:39379–86. doi:10.1074/jbc.M111.298208
18. Elrod JW, Calvert JW, Morrison J, Doeller JE, Kraus DW, Tao L, et al. Hydrogen sulfide attenuates myocardial ischemia-reperfusion injury by preservation of mitochondrial function. *Proc Natl Acad Sci U S A* (2007) **104**:15560–5. doi:10.1073/pnas.0705891104
19. Tripatara P, Patel NS, Collino M, Gallicchio M, Kieswich J, Castiglia S, et al. Generation of endogenous hydrogen sulfide by cystathionine gamma-lyase limits renal ischemia/reperfusion injury and dysfunction. *Lab Invest* (2008) **88**:1038–48. doi:10.1038/labinvest.2008.73
20. Stipanuk MH, Beck PW. Characterization of the enzymic capacity for cysteine desulphhydration in liver and kidney of the rat. *Biochem J* (1982) **206**:267–77.
21. Shibuya N, Tanaka M, Yoshida M, Ogasawara Y, Togawa T, Ishii K, et al. 3-Mercaptopyruvate sulfurtransferase produces hydrogen sulfide and bound sulfane sulfur in the brain. *Antioxid Redox Signal* (2009) **11**:703–14. doi:10.1089/ARS.2008.2253
22. Singh S, Padovani D, Leslie RA, Chiku T, Banerjee R. Relative contributions of cystathionine beta-synthase and gamma-cystathionase to H_2S biogenesis via alternative transsulfuration reactions. *J Biol Chem* (2009) **284**:22457–66. doi:10.1074/jbc.M109.010868

23. Mikami Y, Shibuya N, Kimura Y, Nagahara N, Ogasawara Y, Kimura H. Thioredoxin and dihydrolipoic acid are required for 3-mercaptopyruvate sulfurtransferase to produce hydrogen sulfide. *Biochem J* (2011) **439**:479–85. doi:10.1042/BJ20110841
24. Ubuka T, Umemura S, Yuasa S, Kinuta M, Watanabe K. Purification and characterization of mitochondrial cysteine aminotransferase from rat liver. *Physiol Chem Phys* (1978) **10**:483–500.
25. Akagi R. Purification and characterization of cysteine aminotransferase from rat liver cytosol. *Acta Med Okayama* (1982) **36**:187–97.
26. Cooper AJ. Biochemistry of sulfur-containing amino acids. *Annu Rev Biochem* (1983) **52**:187–222. doi:10.1146/annurev.bi.52.070183.001155
27. Shibuya N, Koike S, Tanaka M, Ishigami-Yuasa M, Kimura Y, Ogasawara Y, et al. A novel pathway for the production of hydrogen sulfide from D-cysteine in mammalian cells. *Nat Commun* (2013) **4**:1366. doi:10.1038/ncomms2371
28. Gould SJ, Keller GA, Subramani S. Identification of peroxisomal targeting signals located at the carboxy terminus of four peroxisomal proteins. *J Cell Biol* (1988) **107**:897–905. doi:10.1083/jcb.107.3.897
29. Schumann U, Subramani S. Special delivery from mitochondria to peroxisomes. *Trends Cell Biol* (2008) **18**:253–6. doi:10.1016/j.tcb.2008.04.002
30. Ishii I, Akahoshi N, Yu XN, Kobayashi Y, Namekata K, Komaki G, et al. Murine cystathionine gamma-lyase: complete cDNA and genomic sequences, promoter activity, tissue distribution and developmental expression. *Biochem J* (2004) **381**:113–23. doi:10.1042/BJ20040243
31. Shibuya N, Mikami Y, Kimura Y, Nagahara N, Kimura H. Vascular endothelium expresses 3-mercaptopyruvate sulfurtransferase and produces hydrogen sulfide. *J Biochem* (2009) **146**:623–6. doi:10.1093/jb/mvp111
32. Enokido Y, Suzuki E, Iwasawa K, Namekata K, Okazawa H, Kimura H. Cystathionine beta-synthase, a key enzyme for homocysteine metabolism, is preferentially expressed in the radial glia/astrocyte lineage of developing mouse CNS. *FASEB J* (2005) **19**:1854–6.
33. Diwakar L, Ravindranath V. Inhibition of cystathionine-gamma-lyase leads to loss of glutathione and aggravation of mitochondrial dysfunction mediated by excitatory amino acid in the CNS. *Neurochem Int* (2007) **50**:418–26. doi:10.1016/j.neuint.2006.09.014
34. Yang G, Wu L, Jiang B, Yang W, Qi J, Cao K, et al. H_2S as a physiologic vasorelaxant: hypertension in mice with deletion of cystathionine gamma-lyase. *Science* (2008) **322**:587–90. doi:10.1126/science.1162667
35. Mitchell J, Paul P, Chen HJ, Morris A, Payling M, Falchi M, et al. Familial amyotrophic lateral sclerosis is associated with a mutation in D-amino acid oxidase. *Proc Natl Acad Sci U S A* (2010) **107**:7556–61. doi:10.1073/pnas.0914128107
36. Moreno S, Nardacci R, Cimini A, Cerù MP. Immunocytochemical localization of D-amino acid oxidase in rat brain. *J Neurocytol* (1999) **28**:169–85. doi:10.1023/A:1007064504007
37. Perotti ME, Gavazzi E, Trussardo L, Malgaretti N, Curti B. Immunoelectron microscopic localization of D-amino acid oxidase in rat kidney and liver. *Histochem J* (1987) **19**:157–69. doi:10.1007/BF01695140
38. House JD, Brosnan ME, Brosnan JT. Characterization of homocysteine metabolism in the rat kidney. *Biochem J* (1997) **328**:287–92.
39. Nagahara N, Ito T, Kitamura H, Nishino T. Tissue and subcellular distribution of mercaptopyruvate sulfurtransferase in the rat: confocal laser fluorescence and immunoelectron microscopic studies combined with biochemical analysis. *Histochem Cell Biol* (1998) **110**:243–50. doi:10.1007/s004180050286
40. Mikami Y, Shibuya N, Ogasawara Y, Kimura H. Hydrogen sulfide is produced by cystathionine γ-lyase at the steady-state low intracellular Ca^{2+} concentrations. *Biochem Biophys Res Commun* (2013) **431**:131–5. doi:10.1016/j.bbrc.2013.01.010
41. Rutter GA, Rizzuto R. Regulation of mitochondrial metabolism by ER Ca2+ release: an intimate connection. *Trends Biochem Sci* (2000) **25**:215–21. doi:10.1016/S0968-0004(00)01585-1
42. Mothet JP, Parent AT, Wolosker H, Brady RO Jr, Linden DJ, Ferris CD, et al. D-serine is an endogenous ligand for the glycine site of the N-methyl-D-aspartate receptor. *Proc Natl Acad Sci U S A* (2000) **97**:4926–31. doi:10.1073/pnas.97.9.4926
43. Hamase K, Konno R, Morikawa A, Zaitsu K. Sensitive determination of D-amino acids in mammals and the effect of D-amino-acid oxidase activity on their amounts. *Biol Pharm Bull* (2005) **28**:1578–84. doi:10.1248/bpb.28.1578
44. Wolosker H, Sheth KN, Takahashi M, Mothet JP, Brady RO Jr, Ferris CD, et al. Purification of serine racemase: biosynthesis of the neuromodulator D-serine. *Proc Natl Acad Sci U S A* (1999) **96**:721–5. doi:10.1073/pnas.96.2.721
45. Strísovský K, Jirásková J, Barinka C, Majer P, Rojas C, Slusher BS, et al. Mouse brain serine racemase catalyzes specific elimination of L-serine to pyruvate. *FEBS Lett* (2003) **535**:44–8. doi:10.1016/S0014-5793(02)03855-3
46. Miyoshi Y, Konno R, Sasabe J, Ueno K, Tojo Y, Mita M, et al. Alteration of intrinsic amounts of D-serine in the mice lacking serine racemase and D-amino acid oxidase. *Amino Acids* (2012) **43**:1919–31. doi:10.1007/s00726-012-1398-4
47. Kim PM, Duan X, Huang AS, Liu CY, Ming GL, Song H, et al. Aspartate racemase, generating neuronal D-aspartate, regulates adult neurogenesis. *Proc Natl Acad Sci U S A* (2010) **107**:3175–9. doi:10.1073/pnas.0914706107
48. Liardon R, Ledermann S. Racemization kinetics of free and protein-bound amino acids under moderate alkaline treatment. *J Agric Food Chem* (1986) **34**:557–65. doi:10.1021/jf00069a047
49. Friedman M. Origin, microbiology, nutrition, and pharmacology of D-amino acids. *Chem Biodivers* (2010) **7**:1491–530. doi:10.1002/cbdv.200900225
50. Krijgsheld KR, Glazenburg EJ, Scholtens E, Mulder GJ. The oxidation of L- and D-cysteine to inorganic sulfate and taurine in the rat. *Biochim Biophys Acta* (1981) **677**:7–12. doi:10.1016/0304-4165(81)90139-2
51. Fukasawa Y, Segawa H, Kim JY, Chairoungdua A, Kim DK, Matsuo H, et al. Identification and characterization of a Na^+-independent neutral amino acid transporter that associates with the 4F2 heavy chain and exhibits substrate selectivity for small neutral D- and L-amino acids. *J Biol Chem* (2000) **275**:9690–8. doi:10.1074/jbc.275.13.9690
52. Fonnum F, Lock EA. Cerebellum as a target for toxic substances. *Toxicol Lett* (2000) **112–113**:9–16. doi:10.1016/S0378-4274(99)00246-5
53. Sajdel-Sulkowska EM, Xu M, Koibuchi N. Increase in cerebellar neurotrophin-3 and oxidative stress markers in autism. *Cerebellum* (2009) **8**:366–72. doi:10.1007/s12311-009-0105-9
54. Thadhani R, Pascual M, Bonventre JV. Acute renal failure. *N Engl J Med* (1996) **334**:1448–60. doi:10.1056/NEJM199605303342207
55. Allgren RL, Marbury TC, Rahman SN, Weisberg LS, Fenves AZ, Lafayette RA, et al. Anaritide in acute tubular necrosis. Auriculin Anaritide Acute Renal Failure Study Group. *N Engl J Med* (1997) **336**:828–34. doi:10.1056/NEJM199703203361203
56. Hirschberg R, Kopple J, Lipsett P, Benjamin E, Minei J, Albertson T, et al. Multicenter clinical trial of recombinant human insulin-like growth factor I in patients with acute renal failure. *Kidney Int* (1999) **55**:2423–32. doi:10.1046/j.1523-1755.1999.00463.x
57. Acker CG, Singh AR, Flick RP, Bernardini J, Greenberg A, Johnson JP. A trial of thyroxine in acute renal failure. *Kidney Int* (2000) **57**:293–8. doi:10.1046/j.1523-1755.2000.00827.x
58. Wang A, Holcslaw T, Bashore TM, Freed MI, Miller D, Rudnick MR, et al. Exacerbation of radiocontrast nephrotoxicity by endothelin receptor antagonism. *Kidney Int* (2000) **57**:1675–80. doi:10.1046/j.1523-1755.2000.00012.x
59. Ibba M, Söll D. Quality control mechanisms during translation. *Science* (1999) **286**:1893–7. doi:10.1126/science.286.5446.1893
60. Yamaguchi K, Hosokawa Y, Kohashi N, Kori Y, Sakakibara S, Ueda I. Rat liver cysteine dioxygenase (cysteine oxidase). Further purification, characterization, and analysis of the activation and inactivation. *J Biochem* (1978) **83**:479–91.
61. Olney JW, Zorumski C, Price MT, Labruyere J. L-cysteine, a bicarbonate-sensitive endogenous excitotoxin. *Science* (1990)

248:596–9. doi:10.1126/science.2185543
62. Janáky R, Varga V, Hermann A, Saransaari P, Oja SS. Mechanisms of L-cysteine neurotoxicity. *Neurochem Res* (2000) **25**:1397–405. doi:10.1023/A:1007616817499
63. Misra CH. Is a certain amount of cysteine prerequisite to produce brain damage in neonatal rats? *Neurochem Res* (1989) **14**:253–7. doi:10.1007/BF00971320
64. Takemoto Y. Pressor response to L-cysteine injected into the cisterna magna of conscious rats involves recruitment of hypothalamic vasopressinergic neurons. *Amino Acids* (2012) **44**:1053–60. doi:10.1007/s00726-012-1440-6

Conflict of Interest Statement: The authors declare that the research was conducted in the absence of any commercial or financial relationships that could be construed as a potential conflict of interest.

Received: 28 May 2013; paper pending published: 26 June 2013; accepted: 01 July 2013; published online: 16 July 2013.
*Citation: Shibuya N and Kimura H (2013) Production of hydrogen sulfide from D-cysteine and its therapeutic potential. Front. Endocrinol. **4**:87. doi:10.3389/fendo.2013.00087*
This article was submitted to Frontiers in Experimental Endocrinology, a specialty of Frontiers in Endocrinology.

frontiers in
ENDOCRINOLOGY

MINI REVIEW ARTICLE
published: 03 September 2013
doi: 10.3389/fendo.2013.00118

Different forms of ghrelin exhibit distinct biological roles in tilapia

Larry G. Riley*

Department of Biology, California State University Fresno, Fresno, CA, USA

Edited by:
Hiroyuki Kaiya, National Cerebral and Cardiovascular Center Research Institute, Japan

Reviewed by:
Kouhei Matsuda, University of Toyama, Japan
Yoshihiro Nishi, Kurume University, Japan

****Correspondence:***
Larry G. Riley, Department of Biology, California State University Fresno, 2555 East San Ramon, Fresno, CA 93740, USA
e-mail: lriley@csufresno.edu

Ghrelin has been identified in all vertebrate classes, including sharks. Each species possesses multiple forms of ghrelin that vary in peptide length and acyl modifications (e.g., *n*-hexanoic, *n*-non-anoic, *n*-octanoic, and *n*-decanoic acids) including des-acyl ghrelin. Octanoylated ghrelin has been shown to be a potent GH secretagogue, orexigenic factor, and plays a role in overall metabolism in vertebrates. In the tilapia model, octanoylated ghrelin (ghrelin-C8) and decanoylated ghrelin (ghrelin-C10) exhibit different biological actions. This mini review highlights the current knowledge of the differential actions of ghrelin-C8 and ghrelin-C10 from studies in the tilapia model. These findings suggest that the multiple forms of ghrelin may exhibit distinct yet complimentary actions directed toward maintaining overall energy balance in other vertebrates.

Keywords: ghrelin, GHS-R, tilapia, metabolism, appetite, homeostasis

INTRODUCTION

Ghrelin was first identified in rat stomach as an endogenous ligand for the growth hormone secretagogue receptor (GHS-R) (1). Ghrelin has since been identified in all vertebrate classes; fish (2–4), birds (5), amphibians (6), reptiles (7), mammals (1, 8), as well as sharks (9). All ghrelins identified thus far are uniquely and primarily acylated by octanoic or decanoic acid on the third amino acid from the N-terminus (10, 11). However, a variety of other acyl-forms of ghrelins (*n*-hexanoic and *n*-non-anoic acid) and unsaturated *n*-octanoic and *n*-decanoic isoforms of ghrelin have been identified (5, 12, 13). The acyl modification is necessary for ghrelins biological action (10). Indeed, the first seven amino acid residues on the N-terminus are highly conserved across vertebrates and are known as the "active core" (11, 14) suggesting an evolutionary conserved physiological role of ghrelin. Unlike tetrapod ghrelins, fish ghrelins possess an amide modification on the C-terminus (11). Ghrelin is predominately synthesized in the stomach and is also expressed in a variety of other tissues such as small and large intestine, pancreas, liver, hypothalamus, telencephalon, pituitary, gonads, kidneys, gills, adipose tissue, and many others (14, 15).

The biological actions of ghrelin are mediated by the GHS-R, which codes for two separate transcripts, GHS-R1a and GHS-R1b (16). GHS-R1a is a seven transmembrane domain G-protein coupled receptor. This receptor is responsive to both synthetic growth hormone secretagogues and ghrelin in regulating several neuroendocrine, metabolic, and non-endocrine actions (15). The GHS-R1b transcript is shorter than the GHS-R1a isoform due to the intron not being spliced out thus disrupting the normal reading frame and resulting in a "non-functional" receptor with five transmembrane domains (11, 17). GHS-R1b has been suggested to act as a dominant-negative mutant. The formation of GHS-R1a/GHS-R1b heterodimer facilitates the translocation of GHS-R1a to the nucleus decreasing the constitutive signaling of GHS-R1a, thus inhibiting ghrelin's actions (18). Both isoforms are found in a variety of endocrine and non-endocrine tissues such as hypothalamus and a variety of other brain regions, pituitary, liver, lung, heart, muscle, kidney, and gonads (19). Two GHS-R isoforms have been identified in the black seabream (20). We have recently identified two GHS-R isoforms in the tilapia and determined their tissue distribution (21, 22).

The existence of ghrelin, GHS-R1a and GHS-R1b in fish suggests that the fundamental biological functions of ghrelin are conserved across vertebrate species (19, 20). In spite of the fact that all vertebrates possess multiple forms of ghrelin, nearly all of our understanding about ghrelin's biological actions has come from studies using the ghrelin-C8, thus leaving a huge gap in our understanding of ghrelin biology. This mini review focuses on the differential effects of ghrelin-C8 and ghrelin-C10 in tilapia. For more general information on the structure and function of ghrelin within vertebrates the reader is referred to the following review papers (11, 14, 23, 24).

DIFFERENTIAL ROLES OF GHRELIN-C8 AND GHRELIN-C10 IN TILAPIA

We have identified two forms of ghrelin in the Mozambique tilapia (*Oreochromis mossambicus*) stomach (4). They exhibit 100% amino acid identity with each other, the difference being the acyl modification (*n*-octanoic or *n*-decanoic) on Ser^3. The major form of tilapia ghrelin possesses an *n*-decanoic (ghrelin-C10) modification (4). Multiple isoforms of ghrelin have been identified in other fish species, as observed in other vertebrates. Four isoforms of ghrelin have been identified in rainbow trout (2) and 11 isoforms of ghrelin have been identified in goldfish (25). In the chicken (5), ghrelin-C8 and ghrelin-C10 were isolated in similar amounts, whereas in goldfish (25), eel (3), bullfrog (26), and humans (27) ghrelin-C8 is the major form. Both acylated modifications are essential for receptor binding (28) and ghrelin transport across the blood-brain barrier (29).

Since its original discovery as a potent growth hormone secretagogue, ghrelin has been shown to be involved in a variety of neuroendocrine, metabolic, and non-endocrine functions that include, but not limited to, orexigenic activity, cardiovascular, gastrointestinal, pancreatic, and lipogenic and glucogenic actions (15, 16, 23, 30). In spite of the fact that all vertebrates studied to date possess multiple forms of ghrelin, nearly all of the published work has focused on the biological functions of ghrelin-C8 and des-acyl ghrelin. Hosoda et al. (27) have demonstrated that ghrelin-C8 and ghrelin-C10 exhibit the same potency to increase (Ca^{2+}) levels in CHO cells expressing rat GHS-R1a as well as stimulate GH release in rats. In goldfish des-acyl ghrelin was shown to attenuate the orexigenic actions of ghrelin-C8, but had no effect on food intake when administered alone (31). Notwithstanding, since des-acyl ghrelin has been shown to exhibit some biological functions [e.g., stimulate adipogenesis and cardioprotective actions (32, 33)], that the biological role – beyond stimulating GH release – of the other ghrelin forms have not been further investigated.

We have shown in tilapia that ghrelin-C8 and ghrelin-C10 appear to exhibit differential biological functions (30). Ghrelin-C10 was more potent than ghrelin-C8 in stimulating GH release from the tilapia pituitary, yet neither form altered pituitary GH mRNA expression levels (21). Both forms equally increased liver IGF-1 mRNA expression, but ghrelin-C8 was more potent than ghrelin-C10 in increasing liver growth hormone receptor mRNA expression in tilapia (21). Tilapia treated with ghrelin-C10 for 21 days (via osmotic pumps) exhibited a significant increase in food intake and body weight; ghrelin-C8 had no effect. The increase in body weight was likely a result of increased adiposity in liver and muscle tissue induced by ghrelin-C10 (34). Ghrelin-C8 has been shown to stimulate adiposity in rat bone marrow (33).

Brain neuropeptide Y (NPY) mRNA expression levels were significantly elevated 4 and 8 h following ghrelin-C10, not ghrelin-C8, injection in tilapia (30). In goldfish, the orexigenic actions of ghrelin have been shown to be mediated by the NPY pathway (35), thus suggesting a similar mechanism of control in tilapia. In spite of the orexigenic actions of NPY in vertebrates (36), we have not observed an acute increase in food intake following either ghrelin-C8 or ghrelin-C10 treatment (unpublished observations). In rainbow trout, ghrelin-C8 treatment has been shown to have no effect on food intake (37), increase food intake (38), and inhibit food intake (37). In goldfish, two forms of octanoylated ghrelin (12- and 17-amino acid residues) stimulated food intake, whereas des-acylated ghrelin17 had no effect (25). Ghrelin-C8 treatment has routinely been shown to stimulate food intake in mammals (24, 39). However, studies using ghrelin ($ghrl^{-/-}$) knockout models (40, 41) suggest that ghrelin's role in stimulating food intake is secondary to its maintenance of metabolic energy balance (16, 42). The use of $ghrl^{-/-}$ models provides a unique opportunity to investigate the differential roles of the multiple forms of ghrelin.

In tilapia, only ghrelin-C8 significantly elevated plasma glucose levels 4 and 8 h post intraperitoneal injection (30). In rainbow trout ghrelin-C8 stimulated glucokinase (GK) and pyruvate kinase activity, as well as increased the mRNA expression levels of glucose transporter-2 and *GK* in different regions of the brain, without altering plasma glucose levels (43). These data suggest that ghrelin-C8, in tilapia and rainbow trout, may play a role in central glucose-sensing as well as in glucose metabolism in fish as observed in mammals (44). Des-acyl ghrelin had no effect on plasma glucose or insulin levels in healthy humans, but counteracted the actions of ghrelin-C8 on glucose and insulin levels (45). This indicates that des-acyl ghrelin possesses metabolic functions in mammals (33, 45). These data lend support to the hypothesis that the other acyl-forms of ghrelin may exhibit distinct functions from that of *n*-octanoylated ghrelin. Recently, we have observed that ghrelin-C8 reversed the negative effects of cortisol on the mRNA expression levels of the glucocorticoid receptor (GR) and GHS-R1a-LR in the hypothalamus of tilapia (**Figures 1A,B**, respectively). These data suggest that ghrelin-C8 may be playing a role in counteracting the negative effects of chronic stress and/or stress recovery in tilapia. We have previously observed differential regulation of the GHS-R mRNA isoforms in tilapia (46, 47). Further studies are needed to elucidate the biological significance of the different expression patterns of the GHS-Rs. Taken

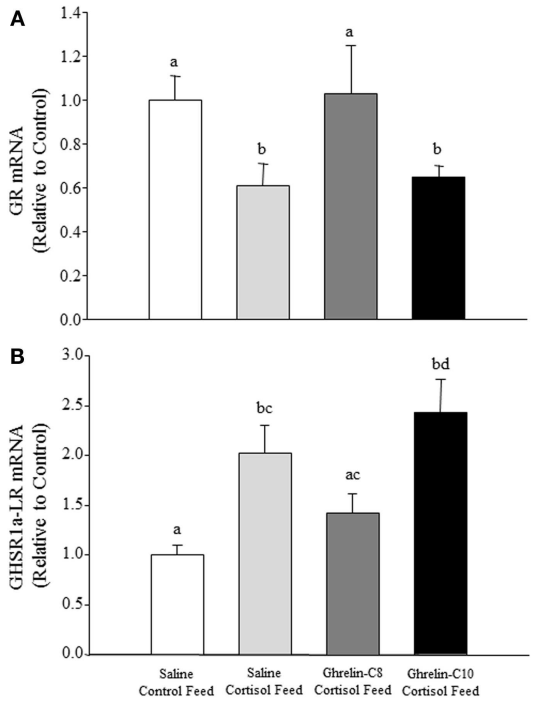

FIGURE 1 | Sexually mature male and female tilapia were surgically implanted with a micro-osmotic pump into the IP cavity containing either saline (control), 100 μg/ml of ghrelin-C8, or 100 μg/ml of ghrelin-C10 (34). The calculated rate of release at 24°C was 13 ng/h for 32 days. Twenty-four hours following the surgery fish were fed a control diet or cortisol-laden feed [500 mg/kg feed; (48)] for 21 days twice a day. Upon termination of the experiment brain sections were collected, RNA was extracted and reversed transcribed into cDNA. Relative mRNA expression levels were determined by qPCR. Ghrelin-C8 treatment significantly reversed the inhibitory effects of cortisol on GR mRNA expression levels in the hypothalamus **(A)**. Ghrelin-C8 treatment partially reversed the stimulatory effect cortisol exhibited on hypothalamic GHS-R-1a-LR mRNA expression levels **(B)**. mRNA data are presented as relative to saline control feed group. Columns with different letters are significantly different at $P < 0.05$, $n = 10–12$.

together, our data in tilapia clearly shows that ghrelin-C8 and ghrelin-C10 exhibit distinct, yet complimentary actions directed toward maintaining metabolic balance within the animal. Our laboratory is currently investigating the direct effects of ghrelin-C8 and ghrelin-C10 on neuropeptide mRNA expression patterns using brain tissue culture methods and proteomic and metabolic approaches.

CONCLUSION

To date, all vertebrates produce multiple forms of ghrelin. There are reports that des-acyl ghrelin exhibits biological functions in mammals (32, 33) and that both ghrelin-C8 and ghrelin-C10 simulate GH release in rats (27), suggesting that the other acyl-forms of ghrelin likely exhibit biological functions. In tilapia, both ghrelin-C8 and ghrelin-C10 exert distinct biological actions that appear to be directed toward maintenance of metabolic balance. It is not clear what is the mechanism underlying the different biological effects of ghrelin-C8 and ghrelin-C10. A possible hypothesis is that a third GHS-R-isoform that exhibits higher affinity toward ghrelin-C10 exists or that ghrelin-C10 binds non-specifically to a related receptor.

ACKNOWLEDGMENTS

This project was supported by Agriculture and Food Research Initiative Competitive Grant no. 2010-65206-20615 from the USDA National Institute of Food and Agriculture to Larry G. Riley.

REFERENCES

1. Kojima M, Hosoda H, Date Y, Nakazato M, Matsuo H, Kangawa K. Ghrelin is a growth-hormone-releasing acylated peptide from stomach. *Nature* (1999) **402**:656–9. doi:10.1038/45230
2. Kaiya H, Kojima M, Hosoda H, Moriyama S, Takahashi A, Kawauchi H, et al. Peptide purification, complementary deoxyribonucleic acid (DNA) and genomic DNA cloning, and functional characterization of ghrelin in rainbow trout. *Endocrinology* (2003) **144**:5215–26. doi:10.1210/en.2003-1085
3. Kaiya H, Kojima M, Hosoda H, Riley LG, Hirano T, Grau EG, et al. Amidated fish ghrelin: purification, cDNA cloning in the Japanese eel and its biological activity. *J Endocrinol* (2003) **176**:415–23. doi:10.1677/joe.0.1760415
4. Kaiya H, Kojima M, Hosoda H, Riley LG, Hirano T, Grau EG, et al. Identification of tilapia ghrelin and its effects on growth hormone and prolactin release in the tilapia, *Oreochromis mossambicus*. *Comp Biochem Physiol* (2003) **135B**:421–9.
5. Kaiya H, van der Geyten S, Kojima M, Hosoda H, Kitajima Y, Matsumoto M, et al. Chicken ghrelin: purification, cDNA cloning, and biological activity. *Endocrinology* (2002) **143**:3454–63. doi:10.1210/en.2002-220255
6. Kaiya H, Sakata I, Yamamoto K, Koda A, Sakai T, Kangawa K, et al. Identification of immunoreactive plasma and stomach ghrelin, and expression of stomach ghrelin mRNA in the bullfrog, *Rana catesbeiana*. *Gen Comp Endocrinol* (2006) **148**:236–44. doi:10.1016/j.ygcen.2006.03.008
7. Kaiya H, Sakata I, Kojima M, Hosoda H, Sakai T, Kangawa K. Structural determination and histochemical localization of ghrelin in the red-eared slider turtle, *Trachemys scripta elegans*. *Gen Comp Endocrinol* (2004) **138**:50–7. doi:10.1016/j.ygcen.2004.05.005
8. Ida T, Miyazato M, Naganobu K, Nakahara K, Sato M, Lin XZ, et al. Purification and characterization of feline ghrelin and its possible role. *Domest Anim Endocrinol* (2007) **32**:93–105. doi:10.1016/j.domaniend.2006.01.002
9. Kawakoshi A, Kaiya H, Riley LG, Hirano T, Grau EG, Miyazato M, et al. Identification of a ghrelin-like peptide in two species of shark, *Sphyrna lewini* and *Carcharhinus melanopterus*. *Gen Comp Endocrinol* (2007) **151**:259–68. doi:10.1016/j.ygcen.2006.10.012
10. Hosoda H, Kojima M, Matsuo H, Kangawa K. Ghrelin and des-acyl ghrelin: two major forms of rat ghrelin peptide in gastrointestinal tissue. *Biochem Biophys Res Commun* (2000) **279**:909–13. doi:10.1006/bbrc.2000.4039
11. Kaiya H, Miyazato M, Kangawa K, Peter RE, Unniappan S. Ghrelin: a multifunctional hormone in non-mammalian vertebrates. *Comp Biochem Physiol A Mol Integr Physiol* (2008) **149A**:109–28. doi:10.1016/j.cbpa.2007.12.004
12. Ishida Y, Sakahara S, Tsutsui C, Kaiya H, Sakata I, Oda S, et al. Identification of ghrelin in the house musk shrew (*Suncus murinus*): cDNA cloning, peptide purification and tissue distribution. *Peptides* (2009) **30**:982–90. doi:10.1016/j.peptides.2009.01.006
13. Nishi Y, Yoh J, Hiejima H, Kojima M. Structures and molecular forms of the ghrelin-family peptides. *Peptides* (2011) **32**:2175–82. doi:10.1016/j.peptides.2011.07.024
14. Unniappan S, Peter RE. Structure, distribution and physiological functions of ghrelin in fish. *Comp Biochem Physiol* (2005) **140A**:396–408.
15. Ghigo E, Broglio F, Arvat E, Maccario M, Papotti M, Muccioli G. Ghrelin: more than a natural GH secretagogue and/or an orexigenic factor. *Clin Endocrinol* (2005) **62**:1–17. doi:10.1111/j.1365-2265.2004.02160.x
16. Korbonits M, Goldstone AP, Gueorguiev M, Grossman AB. Ghrelin-a hormone with multiple functions. *Front. Neuroendocrinol.* (2004) **25**:27–68. doi:10.1016/j.yfrne.2004.03.002
17. Davenport AP, Bonner TI, Foord SM, Harmar AJ, Neubig RR, Pin JP, et al. International Union of Pharmacology. LVI. Ghrelin receptor nomenclature, distribution, and function. *Pharmacol Rev* (2005) **57**:541–6. doi:10.1124/pr.57.4.1
18. Leung PK, Chow KB, Lau PN, Chu KM, Chan CB, Cheng CH, et al. The truncated ghrelin receptor polypeptide (GHS-R1b) acts as a dominant-negative mutant of the ghrelin receptor. *Cell Signal* (2007) **19**:1011–22. doi:10.1016/j.cellsig.2006.11.011
19. van der Lely AJ, Tschop M, Heiman ML, Ghigo E. Biological, physiological, pathophysiological, and pharmacological aspects of ghrelin. *Endocr Rev* (2004) **25**:426–57. doi:10.1210/er.2002-0029
20. Chan C-B, Cheng CHK. Identification and functional characterization of two alternatively spliced growth hormone secretagogue receptor transcripts from the pituitary of black seabream, *Acanthopagrus schlegeli*. *Mol Cell Endocrinol* (2004) **214**:81–95. doi:10.1016/j.mce.2003.11.020
21. Fox BK, Riley LG, Kaiya H, Hirano T, Grau EG. Effects of homologous ghrelins on the growth hormone/insulin-like growth factor-I axis in the tilapia, *Oreochromis mossambicus*. *Zoolog Sci* (2007) **24**:391–400. doi:10.2108/zsj.24.391
22. Kaiya H, Riley LG Jr, Hirano T, Grau EG, Miyazato M, Kangawa K. Identification and genomic sequence of ghrelin receptor (GHS-R)-like receptor in the Mozambique tilapia, *Oreochromis mossambicus*. *Zoolog Sci* (2009) **26**:330–7. doi:10.2108/zsj.26.330
23. Kaiya H, Kangawa K, Miyazato M. What is the general action of ghrelin for vertebrates? – Comparisons of ghrelin's effects across vertebrates. *Gen Comp Endocrinol* (2013) **181**:187–91. doi:10.1016/j.ygcen.2012.10.015
24. Kojima M, Kangawa K. Structure and function of ghrelin. In: Civelli O, Zhou Q-Y, editors. *Results and Problems in Cell Differentiation*. Berlin: Springer Verlag (2008). p. 89–115.
25. Miura T, Maruyama K, Kaiya H, Miyazato M, Kangawa K, Uchiyama M, et al. Purification and properties of ghrelin from the intestine of the goldfish, *Carassius auratus*. *Peptides* (2009) **30**:758–65. doi:10.1016/j.peptides.2008.12.016
26. Kaiya H, Kojima M, Hosoda H, Koda A, Yamamoto K, Kitajima Y, et al. Bullfrog ghrelin is modified by n-octanoic acid at its third threonine residue. *J Biol Chem* (2001) **276**:40441–8. doi:10.1074/jbc.M105212200
27. Hosoda H, Kojima M, Mizushima T, Shimizu S, Kangawa K. Structural divergence of human ghrelin: identification of multiple ghrelin-derived molecules produced by post-translational processing. *J Biol Chem* (2003) **278**:64–70. doi:10.1074/jbc.M205366200
28. Muccioli G, Tschop M, Papotti M, Deghenghi R, Heiman ML, Ghigo E. Neuroendocrine and peripheral activities of ghrelin: implications in metabolism and obesity. *Eur J Pharmacol* (2002) **440**:235–54. doi:10.1016/S0014-2999(02)01432-2

29. Banks WA, Tschop M, Robinson SM, Heiman ML. Extent and direction of ghrelin transport across the blood-brain barrier is determined by its unique primary structure. *J Pharmacol Exp Ther* (2002) **302**:822–7. doi:10.1124/jpet.102.034827
30. Schwandt SE, Peddu SC, Riley LG. Differential roles for octanoylated and decanoylated ghrelins in regulating appetite and metabolism. *Int J Pept* (2010). doi:10.1155/2010/275804
31. Matsuda K, Miura T, Kaiya H, Maruyama K, Shimajura S-I, Uchiyama M, et al. Regulation of food intake by acyl and des-acyl ghrelins in the goldfish. *Peptides* (2006) **27**:2321–5. doi:10.1016/j.peptides.2006.03.028
32. Li L, Zhang L-K, Pang Y-Z, Pan C-S, Qi Y-F, Chen L, et al. Cardioprotective effects of ghrelin and des-octanoyl ghrelin on myocardial injury induced by isoproterenol in rats. *Acta Pharmacol Sin* (2006) **27**:527–35. doi:10.1111/j.1745-7254.2006.00319.x
33. Thompson NM, Gill DA, Davies R, Loveridge N, Houston PA, Robinson IC, et al. Ghrelin and des-octanoyl ghrelin promote adipogenesis directly in vivo by a mechanism independent of the type 1a growth hormone secretagogue receptor. *Endocrinology* (2004) **145**:234–42. doi:10.1210/en.2003-0899
34. Riley LG, Fox BK, Kaiya H, Hirano T, Grau EG. Long-term treatment of ghrelin stimulates feeding, fat deposition, and alters the GH/IGF-I axis in the tilapia, *Oreochromis mossambicus*. *Gen Comp Endocrinol* (2005) **142**:234–40. doi:10.1016/j.ygcen.2005.01.009
35. Miura T, Maruyama K, Shimajura S-I, Kaiya H, Uchiyama M, Kangawa K, et al. Neuropeptide Y mediates ghrelin-induced feeding in the goldfish, *Carassius auratus*. *Neurosci Lett* (2006) **407**:279–83. doi:10.1016/j.neulet.2006.08.071
36. Volkoff H, Canosa LF, Unniappan S, Cerda-Reverter JM, Bernier NJ, Kelly SP, et al. Neuropeptides and the control of food intake in fish. *Gen Comp Endocrinol* (2005) **142**:3–19. doi:10.1016/j.ygcen.2004.11.001
37. Jonsson E, Forsman A, Einarsdottir IE, Kaiya H, Ruohonen K, Bjornsson BT. Plasma ghrelin levels in rainbow trout in response to fasting, feeding and food composition, and effects of ghrelin on voluntary food intake. *Comp Biochem Physiol A Mol Integr Physiol* (2007) **147A**:1116–24. doi:10.1016/j.cbpa.2007.03.024
38. Shepherd BS, Johnson JK, Silverstein JT, Parhar IS, Vijayan MM, McGuire A, et al. Endocrine and orexigenic actions of growth hormone secretagogues in rainbow trout (*Oncorhynchus mykiss*). *Comp Biochem Physiol A Mol Integr Physiol* (2007) **146**:390–9. doi:10.1016/j.cbpa.2006.11.004
39. Hosoda H, Kojima M, Kangawa K. Biological, physiological, and pharamacological aspects of ghrelin. *J Pharm Sci* (2006) **100**:398–410. doi:10.1254/jphs.CRJ06002X
40. Sun Y, Butte NF, Garcia JM, Smith RG. Characterization of adult ghrelin and ghrelin receptor knockout mice under positive and negative energy balance. *Endocrinology* (2008) **149**:843–50. doi:10.1210/en.2007-0271
41. Wortley KE, Anderson KD, Garcia K, Murray JD, Malinova L, Liu R, et al. Genetic deletion of ghrelin does not decrease food intake but influences metabolic fuel preference. *Proc Natl Acad Sci U S A* (2004) **101**:8227–32. doi:10.1073/pnas.0402763101
42. Sato T, Kurokawa M, Nakashima Y, Ida T, Takahashi T, Fukue Y, et al. Ghrelin deficiency does not influence feeding performance. *Regul Pept* (2008) **145**:7–11. doi:10.1016/j.regpep.2007.09.010
43. Polakof S, Miguez JM, Soengas JL. Ghrelin effects on central glucosensing and energy homeostasis-related peptides in rainbow trout. *Domest Anim Endocrinol* (2011) **41**:126–36. doi:10.1016/j.domaniend.2011.05.006
44. Sangiao-Alvarellos S, Cordido F. Effect of ghrelin on glucose-insulin homeostasis: therapeutic implications. *Int J Pept* (2010) **2010**:doi:10.1155/2010/234709
45. Broglio F, Gottero C, Prodam F, Gauna C, Muccioli G, Papotti M, et al. Non-acylated ghrelin counteracts the metabolic but not the neuroendocrine response to acylated ghrelin in humans. *J Clin Endocrinol Metab* (2004) **89**:3062–5. doi:10.1210/jc.2003-031964
46. Janzen WJ, Duncan CA, Riley LG. Cortisol treatment reduces ghrelin signaling and food intake in tilapia, *Oreochromis mossambicus*. *Domest Anim Endocrinol* (2012) **43**:251–9. doi:10.1016/j.domaniend.2012.04.003
47. Upton KR, Riley LG. Acute stress inhibits food intake and alters ghrelin signaling in the brain of tilapia (*Oreochromis mossambicus*). *Domest Anim Endocrinol* (2013) **44**:157–64. doi:10.1016/j.domaniend.2012.10.001
48. Bernier NJ, Bedard N, Peter RE. Effects of cortisol on food intake, growth, and forebrain neuropeptide Y and corticotropin-releasing factor gene expression in goldfish. *Gen Comp Endocrinol* (2004) **135**:230–40. doi:10.1016/j.ygcen.2003.09.016

Conflict of Interest Statement: The author declares that the research was conducted in the absence of any commercial or financial relationships that could be construed as a potential conflict of interest.

Received: 01 August 2013; accepted: 21 August 2013; published online: 03 September 2013.
*Citation: Riley LG (2013) Different forms of ghrelin exhibit distinct biological roles in tilapia. Front. Endocrinol. **4**:118. doi: 10.3389/fendo.2013.00118*
This article was submitted to Experimental Endocrinology, a section of the journal Frontiers in Endocrinology.

frontiers in
ENDOCRINOLOGY

MINI REVIEW ARTICLE
published: 11 October 2013
doi: 10.3389/fendo.2013.00142

Nitric oxide-induced calcium release: activation of type 1 ryanodine receptor, a calcium release channel, through non-enzymatic post-translational modification by nitric oxide

Sho Kakizawa*

Department of Biological Chemistry, Graduate School of Pharmaceutical Sciences, Kyoto University, Kyoto, Japan

Edited by:
Hiroyuki Kaiya, National Cerebral and Cardiovascular Center Research Institute, Japan

Reviewed by:
Nilkantha Sen, Georgia Regents University, USA
Shigeki Moriguchi, Tohoku University, Japan

****Correspondence:***
Sho Kakizawa, Department of Biological Chemistry, Graduate School of Pharmaceutical Sciences, Kyoto University, 46-29 Yoshida-Shimoadachi-cho, Sakyo-ku, Kyoto 606-8501, Japan
e-mail: sho-kaki@pharm.kyoto-u.ac.jp

Nitric oxide (NO) is a typical gaseous messenger involved in a wide range of biological processes. In our classical knowledge, effects of NO are largely achieved by activation of soluble guanylyl cyclase to form cyclic guanosine-3′, 5′-monophosphate. However, emerging evidences have suggested another signaling mechanism mediated by NO: "S-nitrosylation" of target proteins. S-nitrosylation is a covalent addition of an NO group to a cysteine thiol/sulfhydryl (RSH), and categorized into non-enzymatic post-translational modification (PTM) of proteins, contrasted to enzymatic PTM of proteins, such as phosphorylation mediated by various protein kinases. Very recently, we found novel intracellular calcium (Ca^{2+}) mobilizing mechanism, NO-induced Ca^{2+} release (NICR) in cerebellar Purkinje cells. NICR is mediated by type 1 ryanodine receptor (RyR1), a Ca^{2+} release channel expressed in endoplasmic-reticular membrane. Furthermore, NICR is indicated to be dependent on S-nitrosylation of RyR1, and involved in synaptic plasticity in the cerebellum. In this review, molecular mechanisms and functional significance of NICR, as well as non-enzymatic PTM of proteins by gaseous signals, are described.

Keywords: gaseous messenger, post-translational modification, nitric oxide, ryanodine receptor, S-nitrosylation, calcium release, synaptic plasticity, Purkinje cell

INTRODUCTION

Primary structure of proteins obtained from genome analysis is not sufficient to explain their various biological functions: while it is estimated that the human genome, for example, comprises ∼27,000 genes, the total number of proteins in the human proteome is estimated at over one million. In addition to changes at the transcriptional and mRNA levels, it is now increasingly recognized that "post-translational modification (PTM) of proteins" provide important roles in a wide range of signaling pathways, including intercellular signaling pathways such as endocrine systems as well as intracellular pathways. PTMs are covalent processing events that change the properties of a protein by proteolytic cleavage or by addition of a modifying group to one or more amino acids. PTMs of proteins are indicated to be involved in various biological events through changes in protein activity, their cellular locations and dynamic interactions with other proteins (1, 2).

More than 300 different types of PTMs are currently known, and new ones are regularly discovered (3). In general, PTMs are categorized into two groups: enzymatic modification and non-enzymatic modification. Enzymatic PTM, including phosphorylation, acetylation, glycosylation, and lipidation, are demonstrated to be involved in a wide range of physiological and pathophysiological events in eukaryotic cellular systems. On the other hand, accumulation of products derived from non-enzymatic PTM is seen in various tissues of metabolic and age-related diseases such as Alzheimer's disease, Parkinson's disease, cataractogenesis, atherosclerosis, diabetic secondary complications, etc. (4–7). Consequently, it is thought that these accumulations are possibly causative to age-related pathology, and non-enzymatically modified proteins are considered to be useful biomarkers for these diseases (8, 9).

However, recent studies indicate that non-enzymatic PTM of proteins is also associated with physiological events. For example, S-nitrosylation by nitric oxide (NO) is now well established as a major source of NO bioactivity (10–12), and proteins shown to be modified *in situ* by S-nitrosylation (SNO-proteins) participate in a wide range of biological process including those involved in cellular trafficking (13), muscle contractility (14), apoptosis (15, 16), and circulation (17). In addition to non-enzymatic PTMs by reducing molecules, such as glycation by glucose, non-enzymatic modification by gaseous messengers is now attracting much attention.

POST-TRANSLATIONAL MODIFICATION BY GASEOUS MESSENGERS

A gas is a state of matter different from either the liquid or solid states. Gases possess the ability to diffuse readily in different materials and distribute uniformly within a defined space. Biological gases are assumed to diffuse freely across biologic membranes (18). Thus, gases do not bind to cell surface receptors, and do not require the intermediation of conventional membrane receptors and second messenger machinery such as G-proteins and adenylyl cyclase

(19). Instead, the gases directly interact with targets, such as guanylyl cyclase (20). In addition to the reactions with metal centers of metalloproteins (e.g., hemoglobin), significant proportion of the direct action of gaseous messengers is mediated through non-enzymatic PTM of proteins, such as S-nitrosylation by NO and sulfhydration of hydrogen sulfide (H_2S) (21–23).

Probably most prevalent is the "S-nitrosylation" by NO. NO is produced enzymatically in cells expressing NO synthase (NOS) (19). Addition of NO group to the thiol side chain of cysteine residues within proteins and peptides is termed S-nitrosylation. Furthermore, peroxynitrite, produced by the reaction of NO with superoxide, is demonstrated to regulate cellular signaling (24). Peroxynitrite reacts with several amino acids. Cysteine, methionine, and tryptophan react directly, whereas tyrosine, phenylalanine, and histidine are modified through intermediary secondary species (25). Therefore, emerging evidence have indicated that non-enzymatic PTM of proteins by gaseous messengers is involved in physiological and pathological events in various biological systems (26).

FUNCTIONAL MODIFICATION OF RYANODINE RECEPTORS BY S-NITROSYLATION

Skeletal and cardiac muscles mainly express neuronal NOS (nNOS) and endothelial NOS (eNOS), respectively (27, 28), and endogenously produced NO can promote two physiological functions of these muscles. The first is to induce relaxation through the cGMP signaling pathway (29, 30). The second is to modulate increases in contraction that are dependent on reactive oxygen intermediates and independent on cGMP (27). Stoyanovsky et al. (31) thus examined effects of NO-related compounds on Ca^{2+} release from sarcoplasmic reticulum (SR) isolated from skeletal and cardiac muscles (31). The compounds, such as *S*-nitrosocysteine (cysNO), *S*-nitroso-*N*-acetylpenicillamine (SNAP), and S-nitrosylated glutathione (GSNO), induced Ca^{2+} release from the isolated SR vesicles. Correspondingly, application of SNAP increased open probability of SR channels in lipid bilayer (31). The effects of NO-related compounds on the activity of Ca^{2+} release channels were observed in subsequent study: Xu et al. (14) showed that GSNO and cysNO increased open probability of cardiac Ca^{2+} release channel in lipid bilayer (14). In this study, the rise in open probability of cardiac Ca^{2+} release channel was accompanied with the increased amount of *S*-nitrosothiol group per channel protein, the result suggesting the activation of cardiac Ca^{2+} release channels by S-nitrosylation (14). However, as is demonstrated later, NO or 1-hydroxy-2-oxo-3-(*N*-ethyl-2-aminoethyl)-3-ethyl-1-triazene (NOC12) (an NO donor) do not activate or *S*-nitrosylate RyR2 while GSNO induce activation and S-nitrosylation of RyR2 (32). Thus, at that time, cardiac Ca^{2+} release channels, possibly RyR2, was suggested to be activated by GSNO-induced S-nitrosylation of the channel (14).

Subsequently, NO-induced S-nitrosylation of skeletal Ca^{2+} release channel was demonstrated. In these studies, NO-sensitivity of the channels had been studied extensively in ambient O_2 tension (pO_2 ∼150 mmHg), whereas tissue pO_2 is ∼10–20 mmHg and even lower in exercising muscle (33, 34). Eu et al. (35) showed that Ca^{2+} release channel in SR isolated from skeletal muscle, possibly type 1 ryanodine receptor (RyR1), was activated and S-nitrosylated by submicromolar concentration of NO (35). This modification of the channel was induced restrictedly in the case that pO_2 was at tissue level (∼10 mmHg) but not at ambient level (∼150 mmHg). However, when the concentration of NO was increased to micromolar ranges, the channels were activated by NO even in the ambient O_2 levels (35). Moreover, unlike the case in NO, activation of the channels by NOC12 or GSNO was indicated to be insensitive to pO_2 levels: NOC12 and GSNO activated skeletal Ca^{2+} channels in SR at ambient O_2 levels even when the concentration of these compounds were low enough and the estimated levels of NO produced from these compounds were submicromolar ranges (36).

Eu et al. (35) also estimated that only one cysteine in RyR1 was S-nitrosylated by submicromolar concentrations of NO at tissue O_2 level (35). Subsequently, the target of S-nitrosylation was identified as Cys3635: single-cite C3635A-mutaion in RyR1 abolished NO-induced S-nitrosylation of the mutated channels expressed in HEK 293 cells (37). In addition, the NO-induced rise in open probability was abolished in the C3635A-mutant channels in lipid bilayer (36). C3635 is intercalated within the hydrophobic calmodulin (CaM)-binding domain of RyR1, and thereby S-nitrosylation of C3635 is thought to reverse channel inhibition by CaM (38–40). Furthermore, C3635 was indicated to be not required for the activation of the channel by GSNO (36). Taken together, these observations suggest that NO, NOC12, and GSNO activate the redox-sensitive RyR1 channel by different mechanisms, and the effect of O_2 tension on S-nitrosylation by NO is best rationalized by an allosteric mechanism (36).

It is also demonstrated that RyR2 is not activated by NO and the response of RyR3 to NO is much smaller than that of RyR1 (32, 41). Because the important cysteine (i.e., C3635 of rabbit RyR1) is conserved among all RyR subtypes, the three-dimensional structure around the critical cysteine residue may be important for the subtype specificity of S-nitrosylation or channel gating. However, this mechanism requires further clarification.

BIOLOGICAL FUNCTION OF RyR1

Type 1 ryanodine receptor is an intracellular calcium release channel involved in regulation of cytosolic calcium levels. The highest levels of RyR1 expression are observed in skeletal muscle, and significantly higher levels of RyR1 mRNA are seen in the esophagus and testis, when compared to other tissues (42). In addition, lower amount are found in the spleen, gut kidney, stomach, submaxillary gland, thymus, adrenal gland, and ovary. In mammalian brain, RyR1 mRNA is prominent in the cerebellar Purkinje cell (PC) layer and dentate dyrus in the hippocampal region (43). It is well known that RyR1 is essential for contraction of skeletal muscles. However, the function of RyR1 has yet to be clarified in the other tissues, because the mutant deficient in RyR1 gene shows postnatal lethality (44). Furthermore, RyR1 is demonstrated to be physiologically regulated by protein–protein interaction to voltage-gated calcium channels in skeletal muscle cells (45). Although RyR1 is also expressed in the brain, as is described above, such tight Ca^{2+} channel-mediated regulation of intracellular Ca^{2+} release through RyR1, as seen in skeletal muscle cells, is absent in central neurons (46). Therefore, further study into the regulatory mechanisms and functions of RyR1 in the brain is warranted.

NO-INDUCED Ca^{2+} RELEASE INDUCED BY NEURONAL ACTIVITY

As is described so far, the redox regulation of RyRs were extensively studied using *in vitro* experimental systems, especially in lipid bilayer and SR isolated from skeletal and cardiac muscles. On the other hand, involvement of S-nitrosylation of RyR in Ca^{2+} release in living cells and physiological function of the channel modulation by endogenous NO have yet to be demonstrated, although increased open probability of RyR1 by S-nitrosylation was suggested to enhance Ca^{2+} leakage from skeletal muscle Ca^{2+} stores (SR) under pathological conditions (47, 48).

Involvement of S-nitrosylation in neuronal function has been suggested in the cerebellar cortex. PCs, the principal and solely output neurons in the cerebellar cortex, receive two types of excitatory (glutamatergic) inputs: climbing fiber, originate from inferior olive, and parallel fiber (PF), axon of cerebellar granule cells (49). The PF-to-PC synapse (PF synapse) is extensively studied, because many studies indicate that long-term depression (LTD), a kind of synaptic plasticity, of PF synapse is a cellular basis for the cerebellar-dependent learning such as eyeblink conditioning (49–51). In addition to LTD, long-term potentiation (LTP) is observed in PF synapse (PF-LTP). When PF are repeatedly stimulated, the current response of PF synapse is potentiated for 30 min, at least. Three groups demonstrated that the PF-LTP is dependent on NO signals (52–54). Furthermore, although the protocol (the stimulus pattern) for the LTP induction are slightly different between Lev-Ram et al. (53) and Namiki et al. (54), both groups demonstrated that this NO-dependent LTP is insensitive to 1H-[1,2,4]oxadiazolo[4,3-a]quinoxalin-1-one (ODQ), a selective inhibitor of sGC activation by NO (53, 54). Thus, PF-LTP is indicated to be dependent on signaling pathways mediated by S-nitrosylation. Furthermore, in their preliminary experiments, Kakizawa et al. observed that PF-LTP was dependent also on intracellular Ca^{2+} signals. Taken together, PF-LTP was indicated to be dependent on S-nitrosylation and Ca^{2+} signals, and these results lead to our hypothesis: S-nitrosylation-mediated Ca^{2+} release is induced by PF activity and involved in the induction of PF-LTP.

First, Kakizawa et al. (41) demonstrated that bath application of 1-hydroxy-2-oxo-3-(*N*-methyl-3-aminopropyl)-3-methyl-1-triazene (NOC7), an NO donor, induced Ca^{2+} elevation in cerebellar PC in acute slice preparation from young-adult (1- to 2-month-old) mice (41). Subsequently, this NO-induced Ca^{2+} elevation was revealed to be Ca^{2+} release mediated by RyR1: the NO-induced Ca^{2+} increase was abolished by thapsigargin, cyclopiazonic acid (CPA) [inhibitors of sarco/endoplasmic-reticulum Ca^{2+} ATPase (SERCA)], and dantrolene (a specific inhibitor for RyR1), but insensitive to chelating the extracellular Ca^{2+} and heparin (a specific inhibitor for IP_3Rs) (**Figure 1**). Involvement of RyR1 was further confirmed by impaired NO-induced Ca^{2+} elevation in PCs in RyR1-knockout mice (44). Moreover, RyR1 was indicated to be necessary and sufficient for NO-induced Ca^{2+} increase by the experiment using HEK 293 cells, expressing little endogenous RyRs: NO-induced Ca^{2+} elevation was observed only in the cells expressing exogenous RyR1, identified by Ca^{2+} response to caffeine, a well-known agonist of RyRs. Furthermore, NO-induced Ca^{2+} increase was indicated to be insensitive to ODQ, a sGC inhibitor. The result suggested that the Ca^{2+} increase is independent on sGC-mediated pathways, including activation of RyRs by cyclic ADP ribose, whose formation is induced by cGMP (55). Instead, the result indirectly suggested that NO-induced Ca^{2+} increase is dependent on S-nitrosylation of proteins (**Figure 1**). Correspondingly, biochemical analysis indicated that NO-induced Ca^{2+} elevation was accompanied with the transient increase in S-nitrosylation levels of endogenous RyR1 in cerebellar slices. NO-induced increase in S-nitrosylation level was also observed in exogenous RyR1 expressed in HEK cells. Thus, NO-induced Ca^{2+} elevation was revealed to be Ca^{2+} release mediated by RyR1 (**Figure 1**), and was named "NO-induced Ca^{2+} release (NICR)" (41).

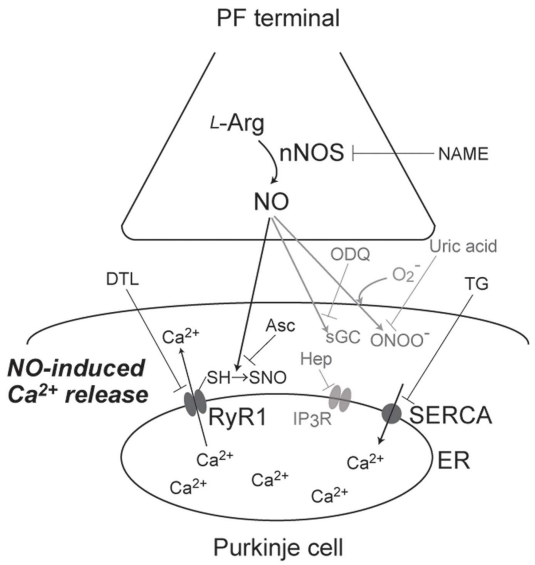

FIGURE 1 | A schematic diagram of signaling pathways for NO-induced Ca^{2+} release. NO, produced at PF terminal, diffuse and induce Ca^{2+} increase in Purkinje cell. This NO-induced Ca^{2+} increase is sensitive to NAME (broad NOS inhibitor), Asc (reducing reagent), DTL (RyR1 antagonist), and TG (SERCA inhibitor), but not affected by ODQ (sGC inhibitor), heparin (IP_3R antagonist), and uric acid (peroxynitrite scavenger). Thus, the Ca^{2+} increase is revealed to be Ca^{2+} release mediated by S-nitrosylation of RyR1 by endogenous NO.

Subsequently, Kakizawa et al. (41) examined induction of NICR by physiological patterns of neuronal activity. When the burst stimulus (BS) inducing PF-LTP was applied to PF, Ca^{2+} levels in PCs were transiently but clearly elevated. This BS-induced Ca^{2+} increase was indicated to be Ca^{2+} release mediated by RyR1, because the Ca^{2+} increase was abolished by bath application of thapsigargin, CPA, and dantrolene. Furthermore, BS-induced Ca^{2+} elevation was inhibited by NG-nitro-L-arginine methyl ester (L-NAME), a broad antagonist of NOSs, and abolished also in nNOS-knockout mice (56). Taken together, BS-induced Ca^{2+} elevation was revealed to be dependent on both NO signals and Ca^{2+} release through RyR1 (**Figure 1**). Thus, BS-induced Ca^{2+} increase is indicated to be NICR, and NICR is demonstrated to be induced by physiological patterns of neuronal activity.

Neuronal activity in conjunction with certain forms of synaptic plasticity may be associated with superoxide generation, and NO

generation leads to peroxynitrite formation when superoxide is simultaneously generated (57, 58). Because peroxynitrite is known to regulate cell signaling via molecular modifications, including protein nitration (57, 58), it seems possible that NICR is affected by peroxynitrite produced from endogenous NO in the presence of superoxide. Therefore, Kakizawa et al. (59) examined the potential role of peroxynitrite in the BS-induced Ca^{2+} release and LTP (59). Bath application of the peroxynitrite scavenger, uric acid, and the peroxynitrite decomposition catalyst, 5,10,15,20-tetrakis(4-sulfonatophenyl)porphyrinato iron(III) (FeTPPS), had no effect on BS-induced Ca^{2+} increase), although the concentration of uric acid (100 μM) and FeTPPS (10 μM) were thought to be high enough. In accordance with the insensitivity of NICR to these reagents, neither uric acid nor FeTPPs impaired the induction of PF-LTP induced by BS. These results do not support the involvement of peroxynitrite in NICR and PF-LTP induction, and NICR is indicated to by induced directly by endogenous NO (**Figure 1**).

PHYSIOLOGICAL FUNCTION OF NICR

Because the BS, which induces NICR, has been already indicated to induce PF-LTP (54), it is strongly suggested that NICR is involved in the induction of PF-LTP. Actually, all manipulations that inhibit NICR (application of L-NAME, thapsigargin, and dantrolene; see also **Figure 1**) abolished PF-LTP in PCs. In addition, neither PF-LTP nor NICR was induced in the cerebellum of nNOS-knockout mice. Furthermore, both PF-LTP and NICR were inhibited by intracellular application of ascorbic acid from patch pipette (**Figure 1**). Because ascorbic acid is a reducing agent, the results also support the idea that S-nitrosylation is required for the induction of NICR as well as PF-LTP. On the other hand, bath application of uric acid, a scavenger of peroxynitrite ($ONOO^-$, produced by reaction of NO with superoxide), or pipette application of heparin inhibited neither NICR nor PF-LTP. Taken together, NICR is revealed to be induced by physiological activity of PF and essential for the induction of PF-LTP, and these observations strongly indicate that Ca^{2+} release mediated by S-nitrosylation of RyR1 is induced in living cells and has physiological function(s) (41) (**Figure 1**).

PERSPECTIVES: POSSIBLE INDUCTION AND PHYSIOLOGICAL FUNCTION OF NICR *IN VIVO*

In the study by Kakizawa et al. (41), NICR was induced by physiological patterns of neuronal activity (BS to PF) in artificial cerebrospinal fluid (ACSF) bubbled with 95% O_2/5% CO_2. In the component of PF-PC synapse, expression of nNOS is observed in PFs and NO is thought to be released from PF terminal (60, 61). Thus, NO, produced at PF in response to the neuronal activity, is thought to diffuse and induce S-nitrosylation of RyR1 in PCs. As is already demonstrated by Eu et al. (35), RyR1 is S-nitrosylated in the ambient pO_2 levels only when the concentration of NO is micromolar level (35). Is the level of NO produced by the BS inducing NICR and PF-LTP micromolar range? Using the NO-sensitive fluorescent probe, Namiki et al. (54) estimated the BS-induced NO level in PCs in the cerebellar slice (54). The NO concentration induced by the BS was estimated to the order of ∼5 μM. Correspondingly, in the cerebellar PCs, NICR was induced when NOC7 was higher than 10 μM (Kakizawa et al., unpublished data), and 10 μM NOC7 is estimated to yield ∼1 μM NO (54). Thus, NICR is suggested to be induced by physiological patterns of neuronal activity, which induces PF-LTP, through the micromolar levels of NO in the ambient pO_2 condition. On the other hand, it is still possible that the level of NO required for the induction of NICR and PF-LTP is overestimated. because pO_2 at tissue level (∼10 mmHg) is much lower than the ambient level (∼150 mmHg), and the submicromolar levels of NO is indicated to induce S-nitrosylation and activation of RyR1 at the tissue pO_2 levels (35).

Expressions of RyR1 as well as NOS (especially nNOS) are observed in various regions of the brain (43, 60). Furthermore, expression of RyR1 is demonstrated in various tissues other than brain and skeletal muscles, such as digestive tissues and reproductive tissues (42). Therefore, NICR may have a wide range of physiological functions in these tissues.

ACKNOWLEDGMENTS

This work was supported by JSPS KAKENHI [Grant-in-Aid for Scientific Research on Innovative Areas (Brain Environment), Grant-in-Aid for Challenging Exploratory Research and Grants-in-Aid for Scientific Research (C)], and Grants from Narishige Neuroscience Foundation, Takeda Science Foundation, Mochida Memorial Foundation, Suzuken Memorial Foundation, and Brain Science Foundation. I also appreciate Prof. Masamitsu Iino (University of Tokyo), Prof. Nozomu Mori (Nagasaki University), and Prof. Hiroshi Takeshima (Kyoto University) for their continuous encouragements.

REFERENCES

1. Mann M, Jensen ON. Proteomic analysis of post-translational modifications. *Nat Biotechnol* (2003) **21**:255–61. doi:10.1038/nbt0303-255
2. Seo J, Lee KJ. Post-translational modifications and their biological functions: proteomic analysis and systematic approaches. *J Biochem Mol Biol* (2004) **37**: 35–44. doi:10.5483/BMBRep.2004.37.1.035
3. Jensen ON. Modification-specific proteomics: characterization of post-translational modifications by mass spectrometry. *Curr Opin Chem Biol* (2004) **8**: 33–41. doi:10.1016/j.cbpa.2003.12.009
4. Grune T, Jung T, Merker K, Davies KJA. Decreased proteolysis caused by protein aggregates, inclusion bodies, plaques, lipofuscin, ceroid, and "aggresomes" during oxidative stress, aging, and disease. *Int J Biochem Cell Biol* (2004) **36**:2519–30. doi:10.1016/j.biocel.2004.04.020
5. Hipkiss AR. Accumulation of altered proteins and ageing: causes and effects. *Exp Gerontol* (2006) **41**:464–73. doi:10.1016/j.exger.2006.03.004
6. Jaisson S, Gillery P. Evaluation of nonenzymatic posttranslational modification-derived products as biomarkers of molecular aging of proteins. *Clin Chem* (2010) **56**:1401–12. doi:10.1373/clinchem.2010.145201
7. Jay D, Hitomi H, Griendling KK. Oxidative stress and diabetic cardiovascular complications. *Free Radic Biol Med* (2006) **40**:183–92. doi:10.1016/j.freeradbiomed.2005.06.018
8. Baynes JW. The clinical chemome: a tool for the diagnosis and management of chronic disease. *Clin Chem* (2004) **50**: 1116–7. doi:10.1373/clinchem.2004.034645
9. Meerwaldt R, Links T, Zeebregts C, Tio R, Hillebrands JL, Smit A. The clinical relevance of assessing advanced glycation endproducts accumulation in diabetes. *Cardiovasc Diabetol* (2008) **7**:29. doi:10.1186/1475-2840-7-29
10. Hess DT, Matsumoto A, Kim SO, Marshall HE, Stamler JS. Protein S-nitrosylation: purview and parameters. *Nat Rev Mol Cell Biol* (2005) **6**:150–66. doi:10.1038/nrm1569

11. Seth D, Stamler JS. The SNO-proteome: causation and classifications. *Curr Opin Chem Biol* (2011) **15**:129–36. doi:10.1016/j.cbpa.2010.10.012
12. Shahani N, Sawa A. Nitric oxide signaling and nitrosative stress in neurons: role for S-nitrosylation. *Antioxid Redox Signal* (2011) **14**:1493–504. doi:10.1089/ars.2010.3580
13. Ozawa K, Whalen EJ, Nelson CD, Mu Y, Hess DT, Lefkowitz RJ, et al. S-nitrosylation of beta-arrestin regulates beta-adrenergic receptor trafficking. *Mol Cell* (2008) **31**: 395–405. doi:10.1016/j.molcel.2008.05.024
14. Xu L, Eu JP, Meissner G, Stamler JS. Activation of the cardiac calcium release channel (ryanodine receptor) by poly-S-nitrosylation. *Science* (1998) **279**:234–7. doi:10.1126/science.279.5348.234
15. Benhar M, Forrester MT, Hess DT, Stamler JS. Regulated protein denitrosylation by cytosolic and mitochondrial thioredoxins. *Science* (2008) **320**:1050–4. doi:10.1126/science.1158265
16. Cho DH, Nakamura T, Fang J, Cieplak P, Godzik A, Gu Z, et al. S-nitrosylation of Drp1 mediates beta-amyloid-related mitochondrial fission and neuronal injury. *Science* (2009) **324**:102–5. doi:10.1126/science.1171091
17. Singel DJ, Stamler JS. Chemical physiology of blood flow regulation by red blood cells: the role of nitric oxide and S-nitrosohemoglobin. *Annu Rev Physiol* (2005) **67**:99–145. doi:10.1146/annurev.physiol.67.060603.090918
18. Kajimura M, Fukuda R, Bateman RM, Yamamoto T, Suematsu M. Interactions of multiple gas-transducing systems: hallmarks and uncertainties of CO, NO, and H2S gas biology. *Antioxid Redox Signal* (2010) **13**:157–92. doi:10.1089/ars.2009.2657
19. Sen N, Snyder SH. Protein modifications involved in neurotransmitter and gasotransmitter signaling. *Trends Neurosci* (2010) **33**: 493–502. doi:10.1016/j.tins.2010.07.004
20. Garthwaite J. New insight into the functioning of nitric oxide-receptive guanylyl cyclase: physiological and pharmacological implications. *Mol Cell Biochem* (2010) **334**:221–32. doi:10.1007/s11010-009-0318-8
21. Kimura H. Hydrogen sulfide: from brain to gut. *Antioxid Redox Signal* (2010) **12**:1111–23.
22. Mustafa AK, Gadalla MM, Sen N, Kim S, Mu W, Gazi SK, et al. H2S signals through protein S-sulfhydration. *Sci Signal* (2009) **2**(96):ra72. doi:10.1126/scisignal.2000464
23. Paul BD, Snyder SH. H2S signalling through protein sulfhydration and beyond. *Nat Rev Mol Cell Biol* (2012) **13**:499–507. doi:10.1038/nrm3391
24. Szabo C, Ischiropoulos H, Radi R. Peroxynitrite: biochemistry, pathophysiology and development of therapeutics. *Nat Rev Drug Discov* (2007) **6**:662–80. doi:10.1038/nrd2222
25. Abello N, Kerstjens HAM, Postma DS, Bischoff R. Protein tyrosine nitration: selectivity, physicochemical and biological consequences, denitration, and proteomics methods for the identification of tyrosine-nitrated proteins. *J Proteome Res* (2009) **8**:3222–38. doi:10.1021/pr900039c
26. Kajimura M, Nakanishi T, Takenouchi T, Morikawa T, Hishiki T, Yukutake Y, et al. Gas biology: tiny molecules controlling metabolic systems. *Respir Physiol Neurobiol* (2012) **184**:139–48. doi:10.1016/j.resp.2012.03.016
27. Kobzik L, Reid MB, Bredt DS, Stamler JS. Nitric-oxide in skeletal-muscle. *Nature* (1994) **372**:546–8. doi:10.1038/372546a0
28. Sartoretto JL, Kalwa H, Pluth MD, Lippard SJ, Michel T. Hydrogen peroxide differentially modulates cardiac myocyte nitric oxide synthesis. *Proc Natl Acad Sci U S A* (2011) **108**:15792–7. doi:10.1073/pnas.1111331108
29. Balligand JL, Kelly RA, Marsden PA, Smith TW, Michel T. Control of cardiac-muscle cell-function by an endogenous nitric-oxide signaling system. *Proc Natl Acad Sci U S A* (1993) **90**:347–51. doi:10.1073/pnas.90.1.347
30. Mohan P, Brutsaert DL, Paulus WJ, Sys SU. Myocardial contractile response to nitric oxide and cGMP. *Circulation* (1996) **93**: 1223–9. doi:10.1161/01.CIR.93.6.1223
31. Stoyanovsky D, Murphy T, Anno PR, Kim YM, Salama G. Nitric oxide activates skeletal and cardiac ryanodine receptors. *Cell Calcium* (1997) **21**:19–29. doi:10.1016/S0143-4160(97)90093-2
32. Sun J, Yamaguchi N, Xu L, Eu JP, Stamler JS, Meissner G. Regulation of the cardiac muscle ryanodine receptor by O(2) tension and S-nitrosoglutathione. *Biochemistry* (2008) **47**:13985–90. doi:10.1021/bi8012627
33. Gorczynski RJ, Duling BR. Role of oxygen in arteriolar functional vasodilation in hamster striated-muscle. *Am J Physiol* (1978) **235**:H505–15.
34. Honig CR, Gayeski TEJ. Resistance to O2 diffusion in anemic red muscle: roles of flux-density and cell PO2. *Am J Physiol* (1993) **265**:H868–75.
35. Eu JP, Sun JH, Xu L, Stamler JS, Meissner G. The skeletal muscle calcium release channel: coupled O2 sensor and NO signaling functions. *Cell* (2000) **102**:499–509. doi:10.1016/S0092-8674(00)00054-4
36. Sun JH, Xu L, Eu JP, Stamler JS, Meissner G. Nitric oxide, NOC-12, and S-nitrosoglutathione modulate the skeletal muscle calcium release channel/ryanodine receptor by different mechanisms – an allosteric function for O2 in S-nitrosylation of the channel. *J Biol Chem* (2003) **278**:8184–9. doi:10.1074/jbc.M211940200
37. Sun JH, Xin CL, Eu JP, Stamler JS, Meissner G. Cysteine-3635 is responsible for skeletal muscle ryanodine receptor modulation by NO. *Proc Natl Acad Sci U S A* (2001) **98**:11158–62. doi:10.1073/pnas.201289098
38. Hess DT, Matsumoto A, Nudelman R, Stamler JS. S-nitrosylation: spectrum and specificity. *Nat Cell Biol* (2001) **3**:E46–9. doi:10.1038/35055152
39. Lanner JT, Georgiou DK, Joshi AD, Hamilton SL. Ryanodine receptors: structure, expression, molecular details, and function in calcium release. *Cold Spring Harb Perspect Biol* (2010) **2**(11):a003996. doi:10.1101/cshperspect.a003996
40. Moore CP, Zhang JZ, Hamilton SL. A role for cysteine 3635 for RYR1 in redox modulation and calmodulin binding. *J Biol Chem* (1999) **274**:36831–4. doi:10.1074/jbc.274.52.36831
41. Kakizawa S, Yamazawa T, Chen Y, Ito A, Murayama T, Oyamada H, et al. Nitric oxide-induced calcium release via ryanodine receptors regulates neuronal function. *EMBO J* (2012) **31**:417–28. doi:10.1038/emboj.2011.386
42. Giannini G, Conti A, Mammarella S, Scrobogna M, Sorrentino V. The ryanodine receptor calcium-channel genes are widely and differentially expressed in murine brain and peripheral-tissues. *J Cell Biol* (1995) **128**:893–904. doi:10.1083/jcb.128.5.893
43. Mori F, Fukaya M, Abe H, Wakabayashi K, Watanabe M. Developmental changes in expression of the three ryanodine receptor mRNAs in the mouse brain. *Neurosci Lett* (2000) **285**: 57–60. doi:10.1016/S0304-3940(00)01046-6
44. Takeshima H, Iino M, Takekura H, Nishi M, Kuno J, Minowa O, et al. Excitation-contraction uncoupling and muscular degeneration in mice lacking functional skeletal-muscle ryanodine-receptor gene. *Nature* (1994) **369**:556–9. doi:10.1038/369556a0
45. Endo M. Calcium-induced calcium release in skeletal muscle. *Physiol Rev* (2009) **89**:1153–76. doi:10.1152/physrev.00040.2008
46. Kano M, Garaschuk O, Verkhratsky A, Konnerth A. Ryanodine receptor-mediated intracellular calcium-release in rat cerebellar Purkinje neurons. *J Physiol* (1995) **487**: 1–16.
47. Bellinger AM, Reiken S, Carlson C, Mongillo M, Liu X, Rothman L, et al. Hypernitrosylated ryanodine receptor calcium release channels are leaky in dystrophic muscle. *Nat Med* (2009) **15**:325–30. doi:10.1038/nm.1916
48. Durham WJ, Aracena-Parks P, Long C, Rossi AE, Goonasekera SA, Boncompagni S, et al. RyR1 S-nitrosylation underlies environmental heat stroke and sudden death in Y522S RyR1 knockin mice. *Cell* (2008) **133**:53–65. doi:10.1016/j.cell.2008.02.042
49. Ito M. Cerebellar circuitry as a neuronal machine. *Prog Neurobiol* (2006) **78**:272–303. doi:10.1016/j.pneurobio.2006.02.006
50. Ito M. Cerebellar long-term depression: characterization, signal transduction, and functional roles. *Physiol Rev* (2001) **81**: 1143–95.
51. Ito M. The molecular organization of cerebellar long-term depression. *Nat Rev Neurosci* (2002) **3**:896–902. doi:10.1038/nrn962
52. Kakegawa W, Yuzaki M. A mechanism underlying AMPA receptor trafficking during cerebellar long-term potentiation. *Proc Natl Acad Sci U S A* (2005) **102**: 17846–51. doi:10.1073/pnas.0508910102
53. Lev-Ram V, Wong ST, Storm DR, Tsien RY. A new form of cerebellar long-term potentiation is postsynaptic and depends on nitric oxide but not cAMP. *Proc Natl Acad Sci U S A* (2002) **99**:8389–93. doi:10.1073/pnas.122206399

54. Namiki S, Kakizawa S, Hirose K, Iino M. NO signalling decodes frequency of neuronal activity and generates synapse-specific plasticity in mouse cerebellum. *J Physiol* (2005) **566**:849–63. doi:10.1113/jphysiol.2005.088799
55. Galione A. Cyclic ADP-ribose, the ADP-ribosyl cyclase pathway and calcium signaling. *Mol Cell Endocrinol* (1994) **98**: 125–31. doi:10.1016/0303-7207(94)90130-9
56. Huang PL, Dawson TM, Bredt DS, Snyder SH, Fishman MC. Targeted disruption of the neuronal nitric-oxide synthase gene. *Cell* (1993) **75**: 1273–86. doi:10.1016/0092-8674(93)90615-W
57. Kishida KT, Klann E. Sources and targets of reactive oxygen species in synaptic plasticity and memory. *Antioxid Redox Signal* (2007) **9**:233–44.
58. Pacher P, Beckman JS, Liaudet L. Nitric oxide and peroxynitrite in health and disease. *Physiol Rev* (2007) **87**:315–424. doi:10.1152/physrev.00029.2006
59. Kakizawa S, Yamazawa T, Iino M. Nitric oxide-induced calcium release activation of type 1 ryanodine receptor by endogenous nitric oxide. *Channels* (2013) **7**:1–5. doi:10.4161/chan.22555
60. Bredt DS, Hwang PM, Snyder SH. Localization of nitric-oxide synthase indicating a neural role for nitric-oxide. *Nature* (1990) **347**:768–70. doi:10.1038/347768a0
61. Shibuki K, Kimura S. Dynamic properties of nitric oxide release from parallel fibres in rat cerebellar slices. *J Physiol* (1997) **498**: 443–52.

Conflict of Interest Statement: The author declares that the research was conducted in the absence of any commercial or financial relationships that could be construed as a potential conflict of interest.

Received: 03 September 2013; accepted: 25 September 2013; published online: 11 October 2013.
*Citation: Kakizawa S (2013) Nitric oxide-induced calcium release: activation of type 1 ryanodine receptor, a calcium release channel, through non-enzymatic post-translational modification by nitric oxide. Front. Endocrinol. **4**:142. doi: 10.3389/fendo.2013.00142*
This article was submitted to Experimental Endocrinology, a section of the journal Frontiers in Endocrinology.

frontiers in
ENDOCRINOLOGY

MINI REVIEW ARTICLE
published: 21 October 2013
doi: 10.3389/fendo.2013.00154

Regulated control of melanin-concentrating hormone receptor 1 through posttranslational modifications

Yumiko Saito*, Akie Hamamoto and Yuki Kobayashi

Graduate School of Integrated Arts and Sciences, Hiroshima University, Hiroshima, Japan

Edited by:
Sho Kakizawa, Kyoto University, Japan

Reviewed by:
Shigeki Takeda, Gunma University, Japan
Qun Yong Zhou, University of California, USA

****Correspondence:***
Yumiko Saito, Graduate School of Integrated Arts and Sciences, Hiroshima University, 1-7-1 Kagamiyama, Higashi-Hiroshima, Hiroshima 739-8521, Japan
e-mail: yumist@hiroshima-u.ac.jp

Melanin-concentrating hormone (MCH) is a hypothalamic neuropeptide that plays an important role in feeding behavior. It activates two G-protein-coupled receptors, MCHR1 and MCHR2, of which MCHR1 is the primary regulator of food intake and energy homeostasis in rodents. In mammalian cells transfected with MCHR1, MCH is able to activate multiple signaling pathways including calcium mobilization, extracellular signal-regulated kinase activation, and inhibition of cyclic AMP generation through Gi/o- and Gq-coupled pathways. Further evidence suggests that MCHR1 is regulated through posttranslational modifications, which control its intracellular localization and provide appropriate cellular responses involving G-protein signaling. This review summarizes the current data on the control of MCHR1 function through glycosylation and phosphorylation, as related to cell function. Especially, a series of mutagenesis study highlights the importance of complete glycosylation of MCHR1 for efficient trafficking to the plasma membrane.

Keywords: melanin-concentrating hormone, structure-function relationship, glycosylation, phosphorylation, G-protein

INTRODUCTION

The G-protein-coupled receptor (GPCR) gene family is one of the largest families in the mammalian genome. GPCRs are typical heptahelical receptors composed of an extracellular N-terminus, an intracellular C-terminus, and seven transmembrane bundles connected by three intracellular loops and three extracellular loops. Activation of GPCRs induces second messenger responses that change the biochemical properties of the recipient cell and can modulate not only its electrophysiological responsiveness, but also its transcriptional activity. Thus, the diverse signaling and wide array of functions have allowed GPCRs to be employed in the physiological regulation of nearly all biological functions. These features coupled with ligands that are chemically highly specific for the receptors have resulted in the extensive utilization of GPCR-targeted drug design. Furthermore, the dynamic posttranslational modifications may provide tissue-specific functions, since distinct cellular environments or agonists can mediate different effects on receptor signaling or regulation of a number of GPCRs (1–5). Consequently, these regulatory processes may hold the keys to alternative targets for GPCR research. In this article, we focus solely on the posttranslational modification of one GPCR, melanin-concentrating hormone (MCH) receptor, which is one of the potential targets for obesity research.

ROLE OF MCH IN FOOD INTAKE

Melanin-concentrating hormone was originally discovered as a 17-amino-acid neuropeptide in the chum salmon pituitary (6). MCH is secreted from the pituitary into the circulation, and induces paling of the skin in teleost fish. Mammalian MCH was subsequently identified as a 19-amino-acid peptide in the rat hypothalamus (7). Although the peptide structures are highly conserved between fish and mammals, no direct effects of MCH on skin pigmentation in mammals are demonstrable. Mammalian MCH is predominantly synthesized in the brain, especially in the lateral hypothalamus (LH) and zona incerta with projections to numerous areas in the brain (8). The LH is classically known as the "hunger center," since lesions in this area produce anorexia and stimulation of the area leads to overeating. The important role of MCH in feeding was supported by a study showing that the *MCH* gene is overexpressed upon fasting and in *ob*/*ob* leptin-deficient mice (9). Moreover, direct intracerebroventricular administration of MCH increases food intake in rats, suggesting that MCH is an orexigenic peptide (9), while chronic infusion of MCH or MCH analogs significantly increases food intake, body weight, white adipose tissue mass, and liver mass in mice fed a moderately high-fat diet *ad libitum* (10, 11). Further evidence of the significance of MCH in feeding came from studying the effects of altering the MCH levels using knockout and overexpression techniques (12–14). It has shown that ablation of functional MCH results in a lean phenotype, increased energy expenditure, and resistance to diet-induced obesity. Such phenotypes are not observed for many other neuropeptides, suggesting a crucial role for MCH in feeding behavior. On the basis of these data, MCH appears to be a critical effector of feeding behavior and energy balance.

MCH ACTS THROUGH GPCRs

Despite the discovery of the MCH peptide, the site of its biological action remained obscure until 1999. At that time, five independent groups, including us, identified that the MCH receptor (MCHR1) was SLC-1/GPR24, an orphan GPCR, by applying orphan receptor strategies and reverse pharmacology (15–19). MCHR1 belongs to the γ-group of rhodopsin family class A GPCRs (20), and shows 40% homology with the somatostatin receptor as its closest neighbor. High expression of MCHR1 mRNA in rats is detected

in most anatomical areas implicated in the control of olfaction, such as the olfactory nerve layer, olfactory nucleus, and tubercle (21). Strong labeling is also detected in several limbic structures, such as the hippocampal formation, septum, and amygdala, all of which are implicated in the regulation of stress and emotional processes. Furthermore, MCHR1 is abundantly expressed in the nucleus accumbens shell, where it may play roles in the regulation of motivation and reward. In recombinant cell lines, MCH binds to MCHR1 with affinities of ∼1 nM, and couples to Gi, Go, and Gq proteins (15, 16, 22). Thus, activation of MCHR1 leads to increases in intracellular calcium mobilization via both Gi/o- and Gq-coupled pathways and to decreased cyclic AMP (cAMP) levels via the Gi/o-coupled pathway. Further analyses of MCHR1 signaling in recombinant cell lines and hippocampal brain slices demonstrated that activation of MCHR1 also leads to extracellular signal-regulated kinase (ERK) phosphorylation (22, 23). Recently, accumulating evidence has supported the notion that receptor-binding partners regulate the magnitude, duration, and spatial components of GPCR signaling. MCHR1-binding proteins have also been detected and described. Periplakin and neurochondrin, which interact with the proximal C-terminus of MCHR1, reduce the capacity to initiate calcium mobilization (24, 25). Furthermore, RGS8, one of the GTPase-activating proteins for Gα subunits, was identified as a negative regulator. Arg253 and Arg256 at the distal end of the third cytoplasmic loop were found to comprise a structurally important site for the functional interaction with RGS8 (26). Clarification of the physiological consequences of these proteins that interact with the MCHR1 system will be achieved by assessing their coexpressions in the nervous system.

A second MCH receptor (MCHR2) was subsequently identified by six groups using human genomic sequence searches (27). It shares 38% amino acid identity with MCHR1 and binds to MCH with high affinity (28). The distribution of MCHR2 in humans is relatively limited, in that it is expressed in the cerebral cortex, amygdala, and hippocampus, but not in the hypothalamus (29). In contrast to human MCHR1, human MCHR2 only couples to Gq protein, and the signaling is not sensitive to pertussis toxin. Of note, MCHR2 was found to be a pseudogene in rodent species, but is functional in dogs, ferrets, rhesus monkeys, and humans (30). The physiological importance of MCHR2 remains unknown owing to the lack of available animal models. Later studies identified three MCH receptor sequences in zebrafish and two receptor sequences from fugu, barfin flounder, and goldfish in whole-genome datasets (31–33). Moreover, based on predictions from a preliminary genome assembly of *Xenopus tropicalis*, information for four MCH receptors has been obtained (34). Phylogenetic analyses of these receptors suggest that an initial duplication of the MCH receptor occurred early in evolution, giving rise to MCHR1 and MCHR2. MCH receptors are only found in vertebrates (35). Therefore, the characterization of MCH receptors from birds and reptiles may serve as a valuable reference to elucidate the role of the MCH system during evolution.

The gene for prepro MCH encodes two additional peptides, NEI and NGE of unknown function. MCHR1 is the sole receptor expressed in rodents, MCHR1 knockout mice may provide confirmation of the role of MCH in energy homeostasis. To date, MCHR1 knockout mice have been reported to exhibit an obesity-prone phenotype (36, 37). In contrast to MCH knockout mice, MCHR1 knockout mice remained lean on a regular chow diet. On a high-fat diet, the mice gained less weight, characterized by hyperphagia, hyperactivity, and hypermetabolism. To better understand the role of MCH-MCHR1 system in energy homeostasis, several structurally distinct small molecule antagonists for the MCHR1 have been synthesized and tested in cell-based assays for their selectivity and for *in vivo* potency in the rodent. Comprehensive review of desired selectivity and efficacy of MCHR1 antagonist *in vivo* should consult some recent reviews (38, 39). The majority of studies indicated that the MCHR1 antagonists are effective in different models of obesity in a variety of different rodent strains, due to inhibition of food intake and/or energy expenditure (40, 41). Overall, both rodent genetic studies and rodent pharmacologic studies on MCHR1 have confirmed the importance of the MCH-MCHR1 system for modulating energy homeostasis. With the broad distribution of MCH fibers and MCHR1 in the rodent brain, the physiological function of the MCH system is not only restricted to feeding behavior. In accordance with these observations, multiple rodent models have suggested functional implications of the MCH-MCHR1 system in sleep, emotion, and reward effects of psychostimulants (42–45). In peripheral tissues, the MCH-MCHR1 system has been shown to play important roles in pancreatic islet function and intestinal inflammation (46, 47).

POSTTRANSLATIONAL CONTROL OF MCH RECEPTORS

Posttranslational modifications are considered to be the primary regulatory mechanisms of virtually all GPCRs. Since most GPCRs are naturally expressed at low levels, except for rhodopsin, *in vitro* eukaryotic heterologous expression systems are often employed for their biochemical characterization, including the complex posttranslational modifications.

The most well-understood posttranslational modifications include palmitoylation, glycosylation, and phosphorylation. Most GPCRs are posttranslationally modified with one or more palmitic acids, a 16-carbon saturated fatty acid, covalently bound to cysteine(s) localized in the C-terminal cytoplasmic tail. The insertion of palmitate into the cytoplasmic leaflet of the plasma membrane can create a fourth loop named helix 8, thereby profoundly affecting the GPCR structure and consequently the interactions with intracellular partner proteins. Although a putative palmitoylation site has not been identified in mammalian MCHR1 (48), the existence of helix 8 was predicted by a computational analysis and its functional importance in the signaling pathway has been experimentally confirmed in HEK293T cells (49, 50).

N-linked glycosylation is one of the most common forms of posttranslational modification. The consensus sequences for N-linked glycosylation, Asn-X-Thr and Asn-X-Ser, in which oligosaccharides can bind to the asparagine residues, are found in many GPCRs and are shared by almost all eukaryotic cells, including yeast cells. The significance of these asparagine residues has been demonstrated in various receptors, and they seem to play several important roles including receptor folding, trafficking, and stability, thereby allowing fine-tuning of the receptor function. When Flag-tagged rat MCHR1 is expressed in HEK293 cells, several characteristic immunoreactive bands of ∼35–65 kDa are detected by western blotting (51). These molecular weights are

higher than those predicted from MCHR1 cDNA sequences, suggesting glycosylated forms of MCHR1. This notion is supported by the fact that the N-terminal domain of rat MCHR1 includes three N-glycosylation sites at Asn13, Asn16, and Asn23 (48), all of which are conserved among the goldfish, *Xenopus*, mouse, and human orthologs (**Figure 1**). We proved the presence of

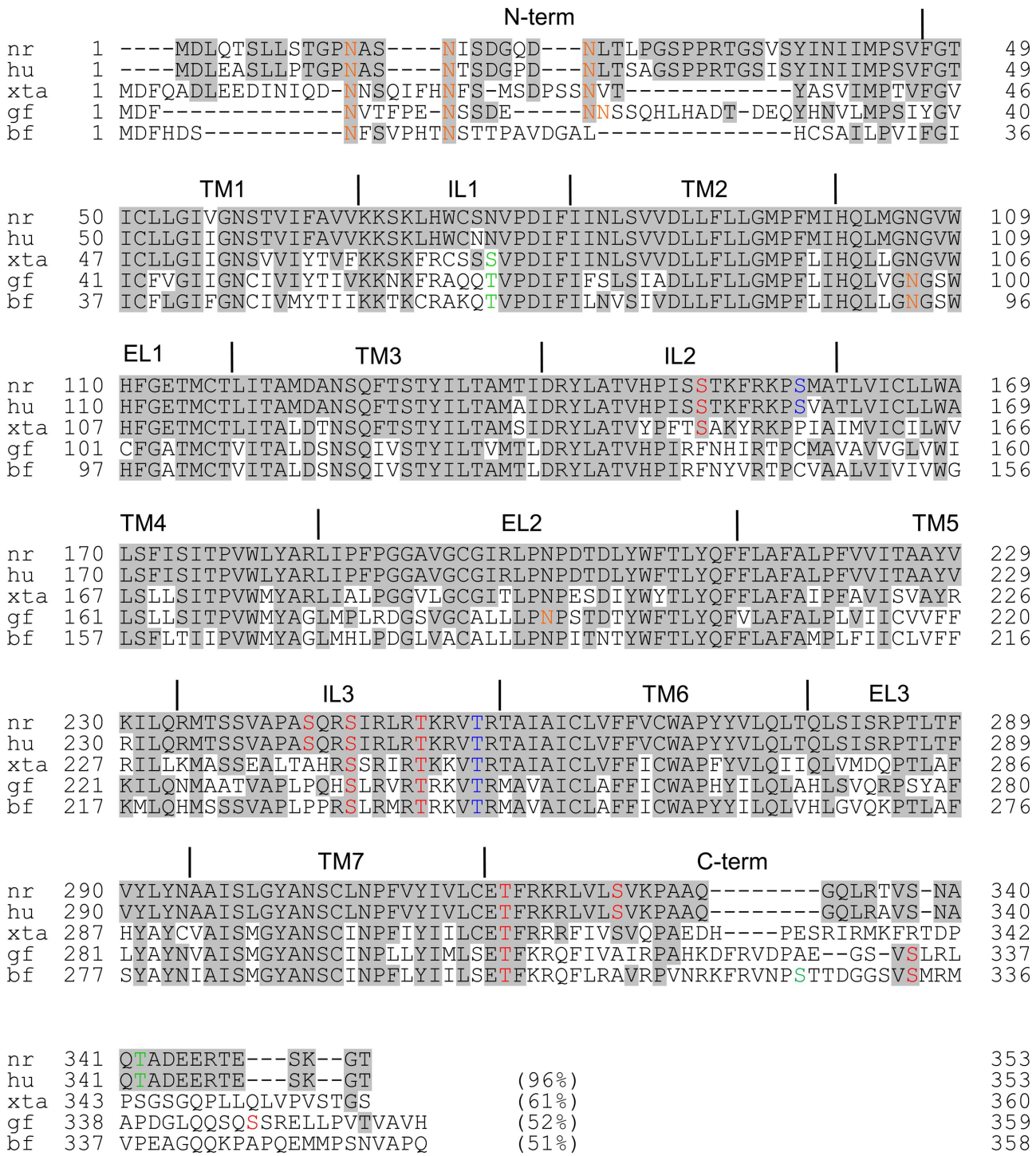

FIGURE 1 | Amino acid comparisons of Norway rat MCHR1 and its mammalian, amphibian, and fish orthologs. The accession numbers are as follows: Norway rat (nr), NP_113946; human (hu), NP_005288; *Xenopus tropicalis* 1a (xta), NP_001072243; goldfish (gf), BAH70338; barfin flounder (bf), BAF49517. Common amino acids with rat MCHR1 are shaded. Colored amino acids show individual motifs: orange, N-glycosylation site; green, casein kinase 2 phosphorylation site; red, protein kinase C phosphorylation site; blue, cAMP-dependent protein kinase phosphorylation site. The numbers in parentheses show the sequence identities with the rat sequence.

oligosaccharides in MCHR1 by enzymatic treatment. Furthermore, single or multiple mutations of Asn13, Asn16, and Asn23 to Gln (N23Q, N13Q/N16Q, N13Q/N23Q, N16Q/N23Q, and N13Q/N16Q/N23Q) caused pronounced reductions in the levels of glycosylation of the receptor protein, and impaired the receptor expression at the cell surface. In particular, the N-linked glycosylation at Asn23 is necessary for the cell surface expression and signal transduction (51, 52). Mutation of residues other than the N-glycosylation sites also caused incomplete glycosylation of MCHR1, and impaired receptor trafficking and signaling. MCHR1 belongs to the rhodopsin family of GPCRs, and the Glu/Asp3.49-Arg3.50-Tyr3.51 (E/DRY) sequence is a highly conserved motif in this family. It was found that substitution of Asp140 or Tyr142 to Ala (D140A and Y142A, respectively) resulted in non-functional receptors without changing the high affinity constant values in HEK293 cells (53). The cell surface expression levels of both mutants were about 40% of the wild-type MCHR1 level, with pronounced decreases in the 65-kDa immunoreactive band (highly glycosylated form). Different types of site-directed mutants that exhibited much less glycosylation were found for highly conserved Pro residues at transmembrane regions 2, 4, 5, 6, and 7 (P97A, P177A, P220A, P271A, and P308A, respectively) (**Figure 1**). These mutations all produced complete loss of signaling with lack of the 65-kDa immunoreactive band in HEK293 cells (50). The importance of proper glycosylation for receptor trafficking and signaling was extensively analyzed using substitution of Thr255 to Ala (T255A), which is located at the junction of intracellular loop 3 and transmembrane region 6 (52). T255A was largely retained in the endoplasmic reticulum (ER) and associated with the chaperon protein calnexin in HEK293 cells. This arose through receptor misfolding, which prevented some N-glycosylation. Interestingly, addition of a small molecule MCHR1 antagonist to T255A- and N13Q/N16Q/N23Q-expressing cells led to functional receptors becoming fully glycosylated at similar extents to wild-type MCHR1. Thus, complete glycosylation of MCHR1 is necessary to allow its efficient trafficking through the ER and Golgi to the plasma membrane.

Ligand-stimulated GPCR activation, desensitization, internalization, and recycling occur in a controlled cyclical process. Since the magnitude and duration of ligand-induced GPCR responses are linked to the balance between signal generation and signal termination, the endocytic pathway that starts with internalization tightly controls the activity of GPCRs. The process of endocytosis is promoted by agonist-induced phosphorylation of receptors. Upon GPCR activation, several sites in GPCRs are immediately phosphorylated by G-protein receptor kinases and other protein kinases. The receptor phosphorylation and subsequent binding of β-arrestin prevent consequent interactions of the receptors with G-proteins, thereby effectively terminating the G-protein-mediated signaling and initiating the endocytic process. The endocytic activity of arrestin is also subject to dynamic regulation by dephosphorylation and ubiquitination. GPCR phosphorylation usually occurs predominantly on Ser and Thr residues within the C-terminal receptor tail and third intracellular loop. In the intracellular loop of rat MCHR1, there are nine predicted phosphorylation sites, comprising two for protein kinase A (Arg/Lys–Arg/Lys–X–Ser/Thr: S158 and T255), six for protein kinase C (Ser/Thr–X–Arg/Lys: S151, S243, S246, T251, T317, and S325), and one for protein kinase casein kinase 2 (Ser/Thr–X–X–Asp/Glu: T342) (**Figure 1**). It has been described that the Ser and Thr residues are phosphorylated in agonist-independent manners in some GPCRs (54). However, to our knowledge, no previous studies have identified whether MCHR1 is phosphorylated under basal conditions or in response to MCH using a [^{32}P]orthophosphate metabolic pre-labeling approach. On the other hand, the results of a mutational study suggested the importance of several predicted phosphorylation sites in MCHR1 for the receptor function. A triple substituted mutant in the C-terminus, T317A/S325A/T342A, has no effects on the signal transduction in calcium mobilization, but significantly prevents MCH-induced receptor internalization through protein kinase C and β-arrestin 2-dependent processes (55). Since S246, T251, and T255 in the third intracellular loop are all conserved in MCHR1 derived from goldfish, *Xenopus*, mice, and humans (**Figure 1**), they may play a critical role in receptor function via phosphorylation. The T255A mutation produces a non-functional receptor as described above (52), while the importance of S245 and T251 remains unclear. Thus far, we have preliminary data that point mutations at these residues produce no significant changes in either the cellular localization or calcium mobilization (Honda and Hamamoto, unpublished data). It has been reported that the generation of phosphosite-specific antibodies accompanied by site-directed mutagenesis and chemical kinase inhibitors can provide more direct evidence for phosphorylation in GPCR-expressing cells (2, 3). Since rat MCHR1 possesses nine potential phosphorylation sites, a series of phosphate acceptor site-specific antibodies are potentially obtainable to reveal the coordinated biochemical mechanism involving sequential and hierarchical multisite phosphorylation of the receptor, similar to somatostatin or μ opioid receptors (4, 56).

FUTURE DIRECTIONS

The MCH-MCHR1 system has integral roles in many cellular events, and represents an important therapeutic target. For example, it may be targeted in strategies for developing treatments against obesity and mood disorders, and possibly also for inflammatory diseases. Therefore, the regulation of the MCH system by posttranslational modifications remains an emerging area at the nexus of endocrinology with important implications for drug development. However, our understanding of the regulation of MCHR1 signaling by glycosylation and phosphorylation is limited (**Table 1**). At present, several methodological advances could facilitate analyses of GPCR posttranslational modifications. In particular, significant improvements have been achieved in mass spectrometry (MS) and related procedures such as tandem MS or chemical microsequencing, such that MS is becoming a major tool for analyzing posttranslational modifications. Since purification of hydrophobic membrane proteins has been enhanced by the utilization of specific detergents and several enrichment procedures, MS analyses could have broad utility, such as direct identification of glycosylated or phosphorylated residues, even for low amounts in GPCRs (1, 5, 57, 58). Moreover, it has been shown that distinct cellular environments can mediate different glycosylation patterns in rhodopsin and serotonin receptor type 4 (5). For example, rhodopsin is heavily and heterogeneously glycosylated

Table 1 | Posttranslational modifications with cellular function in mammal MCHR1.

Region		Mutant receptor	Impact on MCHR1 in HEK293 cells	Reference
Extracellular N-terminus		N23Q[a] N13Q/N16Q[a] N13Q/N23Q[a] N16Q/N23Q[a] N13Q/N16Q/N23Q[a]	⇓ Mature glycosylation ⇓ Cell surface expression ⇓ Ca^{2+} mobilization	(51, 52)
Intracellular loop 2		D140A Y142A	⇓ Mature glycosylation ⇓ Cell surface expression Loss of function (Ca^{2+} mobilization, cAMP inhibition, ERK activation)	(53)
Transmembrane region	2	P97A	⇓ Mature glycosylation Loss of function (Ca^{2+} mobilization)	
	4	P177A		
	5	P220A		
	6	P271A		
	7	P308A		(50)
Junction of intracellular loop 3 and transmembrane region 6		T255A[b]	⇓ Mature glycosylation ⇓ Cell surface expression (retained in the ER) Loss of function (Ca^{2+} mobilization)	(52)
Intracellular C-terminus		T317A/S325A/T342A[b]	→ Ca^{2+} mobilization ⇓ Receptor internalization (protein kinase C and β-arrestin 2-dependent)	(55)

[a]*The consensus sequences for N-linked glycosylation.*

[b]*Predicted phosphorylation sites.*

when expressed in HEK293 and COS-1 cells, but shows a sparser and more homogeneous glycosylation pattern in its native retinal tissue. Thus, these features remind us of the significant importance of studying both heterologous and natural expression systems, and offer a comprehensive view of the posttranslational modifications in MCHR1.

REFERENCES

1. Trester-Zedlitz M, Burlingame A, Kobilka B, von Zastrow M. Mass spectrometric analysis of agonist effects on posttranslational modifications of the beta-2 adrenoceptor in mammalian cells. *Biochemistry* (2005) **44**:6133–43. doi:10.1021/bi0475469
2. Nagel F, Doll C, Pöll F, Kliewer A, Schröder H, Schulz S. Structural determinants of agonist-selective signaling at the sst(2A) somatostatin receptor. *Mol Endocrinol* (2011) **25**:859–66. doi:10.1210/me.2010-0407
3. Petrich A, Mann A, Kliewer A, Nagel F, Strigli A, Märtens JC, et al. Phosphorylation of threonine 333 regulates trafficking of the human sst5 somatostatin receptor. *Mol Endocrinol* (2013) **27**:671–82. doi:10.1210/me.2012-1329
4. Just S, Illing S, Trester-Zedlitz M, Lau EK, Kotowski SJ, Miess E, et al. Differentiation of opioid drug effects by hierarchical multi-site phosphorylation. *Mol Pharmacol* (2013) **83**:633–9. doi:10.1124/mol.112.082875
5. Salom D, Wang B, Dong Z, Sun W, Padayatti P, Jordan S, et al. Posttranslational modifications of the serotonin type 4 receptor heterologously expressed in mouse rod cells. *Biochemistry* (2012) **51**:214–24. doi:10.1021/bi201707v
6. Kawauchi H, Kawazoe I, Tsubokawa M, Kishida M, Baker BI. Characterization of melanin-concentrating hormone in chum salmon pituitaries. *Nature* (1983) **305**:321–3. doi:10.1038/305321a0
7. Vaughan JM, Fischer WH, Hoeger C, Rivier J, Vale W. Characterization of melanin-concentrating hormone from rat hypothalamus. *Endocrinology* (1989) **125**:1660–5. doi:10.1210/endo-125-3-1660
8. Bittencourt JC, Presse F, Arias C, Peto C, Vaughan J, Nahon JL, et al. The melanin-concentrating hormone system of the rat brain: an immuno- and hybridization histochemical characterization. *J Comp Neurol* (1992) **319**:218–45. doi:10.1002/cne.903190204
9. Qu D, Ludwig DS, Gammeltoft S, Piper M, Pelleymounter MA, Cullen MJ, et al. A role for melanin-concentrating hormone in the central regulation of feeding behaviour. *Nature* (1996) **380**:243–7. doi:10.1038/380243a0
10. Rossi M, Choi SJ, O'Shea D, Miyoshi T, Ghatei MA, Bloom SR. Melanin-concentrating hormone acutely stimulates feeding, but chronic administration has no effect on body weight. *Endocrinology* (1997) **138**:351–5. doi:10.1210/en.138.1.351
11. Ito M, Gomori A, Ishihara A, Oda Z, Mashiko S, Matsushita H, et al. Characterization of MCH-mediated obesity in mice. *Am J Physiol Endocrinol Metab* (2003) **284**:E940–5. doi:10.1152/ajpendo.00529.2002
12. Shimada M, Tritos NA, Lowell BB, Flier JS, Maratos-Flier E. Mice lacking melanin-concentrating hormone are hypophagic and lean. *Nature* (1998) **396**:670–4. doi:10.1038/25341
13. Ludwig DS, Tritos NA, Mastaitis JW, Kulkarni R, Kokkotou E, Elmquist J, et al. Melanin-concentrating hormone overexpression in transgenic mice leads to obesity and insulin resistance. *J Clin Invest* (2001) **107**:379–86. doi:10.1172/JCI10660
14. Alon T, Friedman JM. Late-onset leanness in mice with targeted ablation of melanin concentrating hormone neurons. *J Neurosci* (2006) **26**:389–97. doi:10.1523/JNEUROSCI.1203-05.2006
15. Chambers J, Ames RS, Bergsma D, Muir A, Fitzgerald LR, Hervieu G, et al. Melanin-concentrating hormone is the cognate ligand for the orphan G-protein-coupled receptor SLC-1. *Nature* (1999) **400**:261–5. doi:10.1038/22313
16. Saito Y, Nothacker HP, Wang Z, Lin SH, Leslie F, Civelli O. Molecular characterization of the melanin-concentrating-hormone receptor. *Nature* (1999) **400**:265–9. doi:10.1038/22321
17. Shimomura Y, Mori M, Sugo T, Ishibashi Y, Abe M, Kurokawa T, et al. Isolation and identification of melanin-concentrating hormone as the endogenous ligand of the SLC-1 receptor. *Biochem Biophys Res Commun* (1999) **261**:622–6. doi:10.1006/bbrc.1999.1104

18. Bächner D, Kreienkamp H, Weise C, Buck F, Richter D. Identification of melanin concentrating hormone (MCH) as the natural ligand for the orphan somatostatin-like receptor 1 (SLC-1). *FEBS Lett* (1999) **457**:522–4. doi:10.1016/S0014-5793(99)01092-3
19. Lembo PM, Grazzini E, Cao J, Hubatsch DA, Pelletier M, Hoffert C, et al. The receptor for the orexigenic peptide melanin-concentrating hormone is a G-protein-coupled receptor. *Nat Cell Biol* (1999) **1**:267–71. doi:10.1038/12978
20. Fredriksson R, Lagerström MC, Lundin LG, Schiöth HB. The G-protein-coupled receptors in the human genome form five main families. Phylogenetic analysis, paralogon groups, and fingerprints. *Mol Pharmacol* (2003) **63**:1256–72. doi:10.1124/mol.63.6.1256
21. Saito Y, Cheng M, Leslie FM, Civelli O. Expression of the melanin-concentrating hormone (MCH) receptor mRNA in the rat brain. *J Comp Neurol* (2001) **435**:26–40. doi:10.1002/cne.1191
22. Hawes BE, Kil E, Green B, O'Neill K, Fried S, Graziano MP. The melanin-concentrating hormone couples to multiple G proteins to activate diverse intracellular signaling pathways. *Endocrinology* (2000) **141**:4524–32. doi:10.1210/en.141.12.4524
23. Pissios P, Trombly DJ, Tzameli I, Maratos-Flier E. Melanin-concentrating hormone receptor 1 activates extracellular signal-regulated kinase and synergizes with Gs-coupled pathways. *Endocrinology* (2003) **144**:3514–23. doi:10.1210/en.2002-0004
24. Murdoch H, Feng GJ, Bachner D, Ormiston L, White JH, Richter D, et al. Periplakin interferes with G protein activation by the melanin-concentrating hormone receptor-1 by binding to the proximal segment of the receptor C-terminal tail. *J Biol Chem* (2005) **280**:8208–20. doi:10.1074/jbc.M405215200
25. Francke F, Ward RJ, Jenkins L, Kellett E, Richter D, Milligan G, et al. Interaction of neurochondrin with the melanin-concentrating hormone receptor 1 interferes with G protein-coupled signal transduction but not agonist-mediated internalization. *J Biol Chem* (2006) **281**:32496–507. doi:10.1074/jbc.M602889200
26. Miyamoto-Matsubara M, Saitoh O, Maruyama K, Aizaki Y, Saito Y. Regulation of melanin-concentrating hormone receptor 1 signaling by RGS8 with the receptor third intracellular loop. *Cell Signal* (2008) **20**:2084–94. doi:10.1016/j.cellsig.2008.07.019
27. An S, Cutler G, Zhao JJ, Huang SG, Tian H, Li W, et al. Identification and characterization of a melanin-concentrating hormone receptor. *Proc Natl Acad Sci U S A* (2001) **98**:7576–81. doi:10.1073/pnas.131200698
28. Sailer AW, Sano H, Zeng Z, McDonald TP, Pan J, Pong SS, et al. Identification and characterization of a second melanin-concentrating hormone receptor, MCH-2R. *Proc Natl Acad Sci U S A* (2001) **98**:7564–9. doi:10.1073/pnas.121170598
29. Hill J, Duckworth M, Murdock P, Rennie G, Sabido-David C, Ames RS, et al. Molecular cloning and functional characterization of MCH2, a novel human MCH receptor. *J Biol Chem* (2001) **276**:20125–9. doi:10.1074/jbc.M102068200
30. Tan CP, Sano H, Iwaasa H, Pan J, Sailer AW, Hreniuk DL, et al. Melanin-concentrating hormone receptor subtypes 1 and 2: species-specific gene expression. *Genomics* (2002) **79**:785–92. doi:10.1006/geno.2002.6771
31. Logan DW, Bryson-Richardson RJ, Pagán KE, Taylor MS, Currie PD, Jackson IJ. The structure and evolution of the melanocortin and MCH receptors in fish and mammals. *Genomics* (2003) **81**:184–91. doi:10.1016/S0888-7543(02)00037-X
32. Takahashi A, Kosugi T, Kobayashi Y, Yamanome T, Schiöth HB, Kawauchi H. The melanin-concentrating hormone receptor 2 (MCH-R2) mediates the effect of MCH to control body color for background adaptation in the barfin flounder. *Gen Comp Endocrinol* (2007) **151**:210–9. doi:10.1016/j.ygcen.2007.01.011
33. Mizusawa K, Saito Y, Wang Z, Kobayashi Y, Matsuda K, Takahashi A. Molecular cloning and expression of two melanin-concentrating hormone receptors in goldfish. *Peptides* (2009) **30**:1990–6. doi:10.1016/j.peptides.2009.04.010
34. Ji Y, Zhang Z, Hu Y. The repertoire of G-protein-coupled receptors in *Xenopus tropicalis*. *BMC Genomics* (2009) **10**:263. doi:10.1186/1471-2164-10-263
35. Fredriksson R, Schiöth HB. The repertoire of G-protein-coupled receptors in fully sequenced genomes. *Mol Pharmacol* (2005) **67**:1414–25. doi:10.1124/mol.104.009001
36. Chen Y, Hu C, Hsu CK, Zhang Q, Bi C, Asnicar M, et al. Targeted disruption of the melanin-concentrating hormone receptor-1 results in hyperphagia and resistance to diet-induced obesity. *Endocrinology* (2002) **143**:2469–77. doi:10.1210/en.143.7.2469
37. Marsh DJ, Weingarth DT, Novi DE, Chen HY, Trumbauer ME, Chen AS, et al. Melanin-concentrating hormone 1 receptor-deficient mice are lean, hyperactive, and hyperphagic and have altered metabolism. *Proc Natl Acad Sci U S A* (2002) **99**:3240–5. doi:10.1073/pnas.052706899
38. Luthin DR. Anti-obesity effects of small molecule melanin-concentrating hormone receptor 1 (MCHR1) antagonists. *Life Sci* (2007) **81**:423–40. doi:10.1016/j.lfs.2007.05.029
39. MacNeil DJ. The role of melanin-concentrating hormone and its receptors in energy homeostasis. *Front Endocrinol (Lausanne)* (2013) **4**:49. doi:10.3389/fendo.2013.00049
40. Takekawa S, Asami A, Ishihara Y, Terauchi J, Kato K, Shimomura Y, et al. T-226296: a novel, orally active and selective melanin-concentrating hormone receptor antagonist. *Eur J Pharmacol* (2002) **438**:129–35. doi:10.1016/S0014-2999(02)01314-6
41. Gehlert DR, Rasmussen K, Shaw J, Li X, Ardayfio P, Craft L, et al. Preclinical evaluation of melanin-concentrating hormone receptor 1 antagonism for the treatment of obesity and depression. *J Pharmacol Exp Ther* (2009) **329**:429–38. doi:10.1124/jpet.108.143362
42. Borowsky B, Durkin MM, Ogozalek K, Marzabadi MR, DeLeon J, Lagu B, et al. Antidepressant, anxiolytic and anorectic effects of a melanin-concentrating hormone-1 receptor antagonist. *Nat Med* (2002) **8**:825–30. doi:10.1038/nm0902-1039b
43. Verret L, Goutagny R, Fort P, Cagnon L, Salvert D, Léger L, et al. A role of melanin-concentrating hormone producing neurons in the central regulation of paradoxical sleep. *BMC Neurosci* (2003) **4**:19. doi:10.1186/1471-2202-4-19
44. Antal-Zimanyi I, Khawaja X. The role of melanin-concentrating hormone in energy homeostasis and mood disorders. *J Mol Neurosci* (2009) **39**:86–98. doi:10.1007/s12031-009-9207-6
45. Chung S, Saito Y, Civelli O. MCH receptors/gene structure-in vivo expression. *Peptides* (2009) **30**:1985–9. doi:10.1016/j.peptides.2009.07.017
46. Pissios P, Ozcan U, Kokkotou E, Okada T, Liew CW, Liu S, et al. Melanin concentrating hormone is a novel regulator of islet function and growth. *Diabetes* (2007) **56**:311–9. doi:10.2337/db06-0708
47. Kokkotou E, Moss AC, Torres D, Karagiannides I, Cheifetz A, Liu S, et al. Melanin-concentrating hormone as a mediator of intestinal inflammation. *Proc Natl Acad Sci U S A* (2008) **105**:10613–8. doi:10.1073/pnas.0804536105
48. Lakaye B, Minet A, Zorzi W, Grisar T. Cloning of the rat brain cDNA encoding for the SLC-1 G protein-coupled receptor reveals the presence of an intron in the gene. *Biochim Biophys Acta* (1998) **1401**:216–20. doi:10.1016/S0167-4889(97)00135-3
49. Tetsuka M, Saito Y, Imai K, Doi H, Maruyama K. The basic residues in the membrane-proximal C-terminal tail of the rat melanin-concentrating hormone receptor 1 are required for receptor function. *Endocrinology* (2004) **145**:3712–23. doi:10.1210/en.2003-1638
50. Hamamoto A, Horikawa M, Saho T, Saito Y. Mutation of Phe318 within the NPxxY(x)(5,6)F motif in melanin-concentrating hormone receptor 1 results in an efficient signaling activity. *Front Endocrinol (Lausanne)* (2012) **3**:147. doi:10.3389/fendo.2012.00147
51. Saito Y, Tetsuka M, Yue L, Kawamura Y, Maruyama K. Functional role of *N*-linked glycosylation on the rat melanin-concentrating hormone receptor 1. *FEBS Lett* (2003) **533**:29–34. doi:10.1016/S0014-5793(02)03744-4
52. Fan J, Perry SJ, Gao Y, Schwarz DA, Maki RA. A point mutation in the human melanin concentrating hormone receptor 1 reveals an important domain for cellular trafficking. *Mol Endocrinol* (2005) **19**:2579–90. doi:10.1210/me.2004-0301
53. Aizaki Y, Maruyama K, Nakano-Tetsuka M, Saito Y. Distinct roles of the DRY motif in rat melanin-concentrating hormone receptor 1 in signaling control. *Peptides* (2009) **30**:974–81. doi:10.1016/j.peptides.2009.01.017
54. Mokros T, Rehm A, Droese J, Oppermann M, Lipp M, Höpken UE. Surface expression and endocytosis of the human cytomegalovirus-encoded chemokine receptor

US28 is regulated by agonist-independent phosphorylation. *J Biol Chem* (2002) **277**:45122–8. doi:10.1074/jbc.M208214200

55. Saito Y, Tetsuka M, Li Y, Kurose H, Maruyama K. Properties of rat melanin-concentrating hormone receptor 1 internalization. *Peptides* (2004) **25**:1597–604. doi:10.1016/j.peptides.2004.03.026
56. Ghosh M, Schonbrunn A. Differential temporal and spatial regulation of somatostatin receptor phosphorylation and dephosphorylation. *J Biol Chem* (2011) **286**: 13561–73. doi:10.1074/jbc.M110.215723
57. Lau EK, Trester-Zedlitz M, Trinidad JC, Kotowski SJ, Krutchinsky AN, Burlingame AL, et al. Quantitative encoding of a partial agonist effect on individual opioid receptors by multi-site phosphorylation and threshold detection. *Sci Signal* (2011) **9**:ra52. doi:10.1126/scisignal.2001748
58. Heo S, Yang JW, Huber ML, Planyavsky M, Bennett KL, Lubec G. Mass spectrometric characterization of recombinant rat 5-hydroxytryptamine receptor 1A (5-HT(1A)R) expressed in tsA201 human embryonic kidney cells. *Proteomics* (2012) **12**:3338–42. doi:10.1002/pmic.201200183

Conflict of Interest Statement: The authors declare that the research was conducted in the absence of any commercial or financial relationships that could be construed as a potential conflict of interest.

Received: 22 September 2013; accepted: 07 October 2013; published online: 21 October 2013.
*Citation: Saito Y, Hamamoto A and Kobayashi Y (2013) Regulated control of melanin-concentrating hormone receptor 1 through posttranslational modifications. Front. Endocrinol. **4**:154. doi: 10.3389/fendo.2013.00154*
This article was submitted to Experimental Endocrinology, a section of the journal Frontiers in Endocrinology.

frontiers in
ENDOCRINOLOGY

MINI REVIEW ARTICLE
published: 02 December 2013
doi: 10.3389/fendo.2013.00186

The multiplicity of post-translational modifications in pro-opiomelanocortin-derived peptides

***Akikazu Yasuda*[1]*, *Leslie Sargent Jones*[2] *and Yasushi Shigeri*[1]**

[1] *Health Research Institute, National Institute of Advanced Industrial Science and Technology (AIST), Ikeda, Japan*
[2] *Department of Biology, Appalachian State University, Boone, NC, USA*

Edited by:
Sho Kakizawa, Kyoto University, Japan

Reviewed by:
Akiyoshi Takahashi, Kitasato University, Japan
Kanta Mizusawa, Kitasato University, Japan

***Correspondence:**
Akikazu Yasuda, Health Research Institute, National Institute of Advanced Industrial Science and Technology (AIST), 1-8-31 Midorigaoka, Ikeda, Osaka 563-8577, Japan
e-mail: yasuda-a@osa.att.ne.jp

The precursor protein, pro-opiomelanocortin (POMC) undergoes extensive post-translational processing in a tissue-specific manner to yield various biologically active peptides involved in diverse cellular functions. The recently developed method of matrix-assisted laser desorption/ionization mass spectrometry (MALDI-MS) for direct tissue analysis has proved to be a powerful tool for investigating the distribution of peptides and proteins. In particular, topological mass spectrometry analysis using MALDI-MS can selectively provide a mass profile of the hormones included in cell secretory granules. An advantage of this technology is that it is possible to analyze a frozen thin slice section, avoiding an extraction procedure. Subsequently, tandem mass spectrometry (MS/MS) has a profound impact on addressing the modified residues in the hormone molecules. Based on these strategies with mass spectrometry, several interesting molecular forms of POMC-derived peptides have been found in the fish pituitary, such as novel sites of acetylation in α-melanocyte-stimulating hormone (MSH), hydroxylation of a proline residue in β-MSH, and the phosphorylated form of corticotropin-like intermediate lobe peptide.

Keywords: CLIP, END, MALDI-MS, MSH, POMC, post-translational modification, topological mass spectrometry analysis

INTRODUCTION

It is now recognized that pituitary hormones such as melanocyte-stimulating hormone (MSH), corticotropin-like intermediate lobe peptide (CLIP), and endorphin (END), are processing products of a common precursor protein, pro-opiomelanocortin (POMC). This knowledge was discovered through traditional endocrine research and nucleotide sequencing of the cloned cDNA for the POMC precursor. In 1916, the first demonstrations that the pituitary is involved in controlling skin color were found when hypophysectomy of tadpoles caused a skin lightening, while injection of pituitary extracts produced skin darkening (1, 2). The development of assays was then devised to test the response to the melanocyte-stimulating factors (3), for control of the adrenal cortex (4), and for opiate-like actions (5). The strategy using the bioassay is the commonly accepted approach for the purification of pituitary hormones. Nakanishi et al. (6) first reported the nucleotide sequence of a cloned cDNA encoding bovine corticotropin and β-lipotropin precursor, which consists of repetitive units of melanotropin, CLIP, and END sequences. Electron microscopy was applied to pituitary studies in 1950s. These revealed that secretory proteins are temporarily stored within special storage granules and subsequently secreted into the blood stream. In the late 1960s, there were several attempts to isolate secretory granules in an application of ultracentrifugation, and then the bioassay and granule measurement supporting the ultrastructural identification of the pituitary cell types were reported by many investigators. After 30 years of these types of studies, matrix-assisted laser desorption/ionization with time-of-flight mass spectrometry (MALDI-TOF MS) was developed to analyze the secretory granules directly in frozen sections. In this review we shall focus on recent studies of the post-translational modifications that have been found in POMC-derived peptides in fish pituitary, starting with a background on the application of mass spectrometry that has been used for these studies.

DIRECT TISSUE ANALYSIS USING MALDI-TOF MS

The origin of direct laser desorption/ionization for mass spectral analysis may be traced to the early 1960s (7). This technology evolved into the laser microprobe mass analyzer (LAMMA) as a tool for medical and biological samples that could be aimed at a region of interest in a histological microtome section (8). Interpretation of the LAMMA spectra subsequently led to the discovery of the MALDI principle in 1985 (9). Recently, MALDI imaging mass spectrometry (IMS) has emerged as a new method that allows mapping of a wide range of biomolecules within a thin tissue section [see, Ref. (10)]. Independently of, and parallel to IMS studies, we proposed "topological mass spectrometry analysis" (11) as a strategy based on an application of MALDI-TOF MS analysis that allows for the search for novel hormones and neuropeptides. A key benefit in our method of sample preparation is that, while the ion peaks generally could not be detected in the frozen slices of an endocrine gland or neuron prepared at a 30–40 μm thicknesses, significant signaling in the spectrum could be measured specifically from the secretory cells irradiated by the laser light. The resulting spectrum indicates that MALDI-TOF MS selectively provides a mass profile of the peptides and proteins derived from cell secretory granules. Our hypothesis is that selective detection

of secretory granules seems to be caused by proton capture of granules during MALDI ion formation, and not by other cellular components. Another benefit of direct tissue MALDI-TOF MS is that any enzymatic event in the sample preparation is suppressed by the matrix solution, which possesses a strong inhibitory effect. Thus, instead of a bioassay, the resulting molecular weight becomes an index of hormone purification. In contrast, IMS peak intensity and the number of observed peaks are prominently increased by the thinness of a slice decreased to $<10\,\mu m$, in which most of the ion peaks seem to be from substances of cytoplasmic origin. Topological mass spectrometry analysis comprises three steps. The first one is the site-specific molecular mass profiling of the peptides and proteins contained in the secretory granules by direct tissue analysis using MALDI-TOF MS. The identification of hormones is accomplished by matching the observed masses to the theoretical masses derived from a sequence database. Thus, the unidentified ion peaks in the spectrum may suggest the presence of a novel candidate hormone or a modified hormone in the pituitary. In the interpretation of the resulting spectrum, it is interesting that mass differences such as −1, 16, 42, and 80 Da correspond to carboxy-terminal amidation, oxidation, or hydroxylation, acetylation, and phosphorylation, respectively. This rule can be applied to predict the modified residue in a hormone. The second step is purification of a given peptide from the tissue extract by monitoring of the resulting mass number, and then sequencing the peptide using a protein sequencer or tandem mass spectrometry (MS/MS) analysis. The third step is molecular cloning to determine the precursor sequence corresponding to the isolated peptides. The liquid chromatography (LC) MS/MS analysis is also available to determine the mature molecules with post-translational modifications. Application of topological mass spectrometry analysis is widely used in the fields of endocrinology and neuroscience in fish, crustaceans, insects, and plants (12–20). Among them, the medaka pituitary provides a unique spectrum in direct MALDI-TOF MS that was the basis of the first report of the structural determination of tri-acetylated and hydroxylated POMC-related hormone in vertebrates (19).

ACETYLATION

Acetylation is a major modification in POMC-derived peptides, such as α-MSH and END. α-MSH is mainly produced in the pituitary and controls melanosome dispersion in melanocytes. The structure of α-MSH is characterized as a tri-decapeptide including an amino-terminal acetylation and a carboxy-terminal amidation that is identical in most vertebrates. Structural variations of α-MSH were first found in bovine pituitary as the diacetyl form (21), and identified from salmon pituitary as the non-acetylated form (22). Recently, based on topological mass spectrometry analysis, we have reported that four molecular forms, *N*-desacetyl-, monoacetyl-, diacetyl-, and triacetyl-α-MSH, were present in medaka pituitary as shown in **Figure 1** (19). Tandem mass spectrometry (MS/MS) analysis has shown that N,O-diacetylation of the Ser residue at position 1 was deduced from diacetyl-α-MSH, and N,O-diacetylation of that same Ser residue at position 1 and O-acetylation of the Ser residue at position 3 from triacetyl-α-MSH. In an earlier study on fish endocrinology, *N*-desacetyl-, monoacetyl-, and diacetyl-α-MSH were identified from two species of Cyprinidae: goldfish and carp (23). More recently, when we have checked pituitary further in carp and goldfish using direct MALDI-TOF MS, the existence of triacetyl-α-MSH was observed. However, in a comparison of triacetyl-α-MSH between medaka and carp/goldfish with MS/MS, the resulting spectra were different from each other. The N,O-diacetylation of the Ser residue at position 1 and O-acetylation of the Tyr residue at position 2 in the triacetyl-α-MSH molecule were deduced in carp and goldfish (20). The acetylation reaction of the α-MSH molecule starts with the amino group on the Ser residue at position 1, and then act with the hydroxyl group at the N-terminal Ser residue. A definitive O-acetylation for [*N,O*-diacetyl Ser^1]-α-MSH may vary from species to species.

We have carried out a physiological study using a MALDI-TOF MS that directly analyzes and measures those hormones. The percentages as a total of α-MSH molecules were compared for medaka and goldfish reared in a white or black tank for 5 days. Among structural variants, diacetyl-α-MSH was the predominant

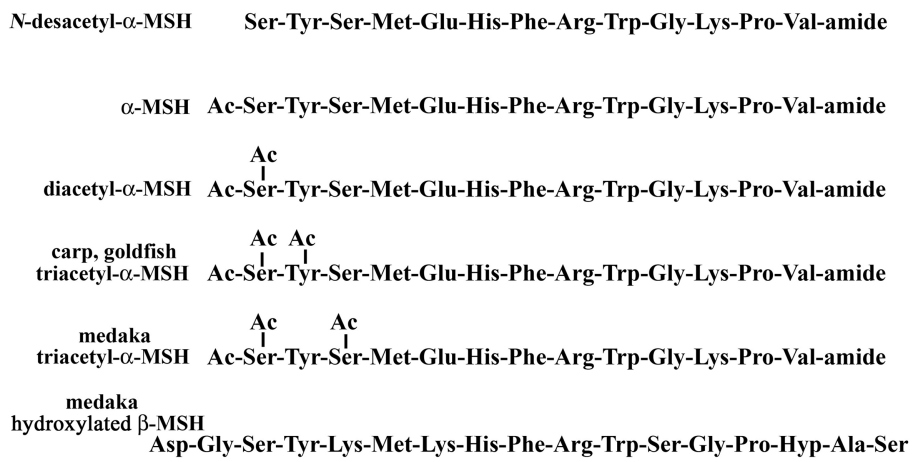

FIGURE 1 | Post-translational modifications of melanotropins in the pituitary.

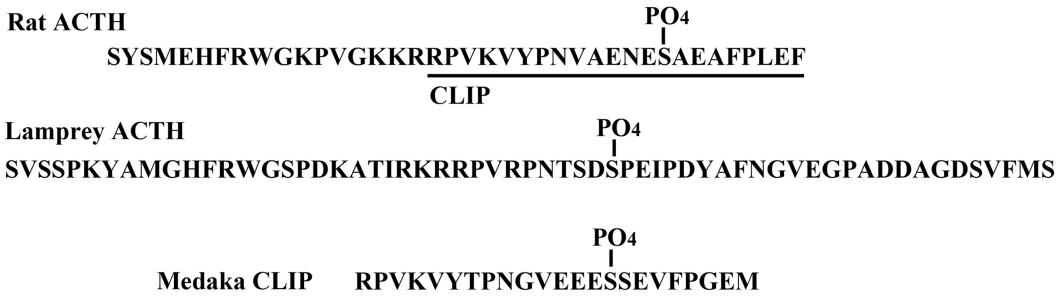

FIGURE 2 | Phosphorylation of ACTH and CLIP molecules in the pituitary.

form in goldfish and *N*-desacetyl-α-MSH in medaka, respectively. In both species, the relative level of the predominant form in the pituitary of white-adapted fish tended to be lower than that of black-adapted fish, but no significant difference was observed in the relative content of goldfish triacetyl-α-MSH in both backgrounds. Furthermore, the lowest content of triacetyl-α-MSH was found in black-adapted medaka. These preliminary data beg the question of how the physiological events regulate the variation in α-MSH levels or the different pattern of acetylation of α-MSH in the fish pituitary.

HYDROXYLATION

Hydroxylation of the proline residue in the pituitary hormones has never been found previously. Recently, we reported the existence of a hydroxyproline (Hyp) residue in the β-MSH molecule in medaka pituitary (19). β-MSH is a slightly basic peptide and there are some variations between different species. A post-translational modification of the β-MSH molecule was not previously observed in any species. In fact, direct tissue MALDI-TOF MS analysis using tissue slices from carp, goldfish, rainbow trout, etc. indicated that β-MSH containing a Hyp residue was not present. Thus, β-MSH is an enigmatic hormone with hydroxylation of melanotropin, restricted to β-MSH in the medaka species, and a physiological role of β-MSH in teleost fish has not yet been elucidated. On the other hand, in mammalian and frog hypothalamus, an endogenous, hydroxylated post-translational product of the luteinizing hormone-releasing hormone sequence [Hyp^9]-LHRH, has been isolated (24). In rodent, the [Hyp^9]-LHRH may play a specific role in development, as [Hyp^9]-LHRH is the major molecular form in the fetal rat hypothalamus, but is less potent than LHRH on gonadotropin secretion.

PHOSPHORYLATION

The structure of CLIP is known as a C-terminal fragment of the adrenocorticotropic hormone (ACTH) sequence. A phosphorylated form of CLIP has been identified in rat pituitary (25), in which a serine residue at position 14 is phosphorylated (*O*-pSer). The location of the *O*-pSer residue in medaka CLIP is in a similar position to that of the rat CLIP. In addition, similar to rat and human ACTH, the lamprey ACTH is partially phosphorylated at the Ser residue at position 35 as shown in **Figure 2** (16). In comparing mammalian ACTH and CLIP, the sequence of -Ser-Ala-Glu- is part of the signal for possible phosphorylation of the Ser residue. In fish hormones, the sequence of -Ser-Ser-Glu- in medaka CLIP and sequence of -Ser-Pro-Glu- in lamprey ACTH are observed. In contrast, in porcine ACTH, a leucine residue is found at position 31 instead of a serine residue (26). So far, a phospho-ACTH or phospho-CLIP have not been found in porcine samples. Thus, a consensus sequence of Ser-X-Glu seems to be a signal of phosphorylation in the pituitary hormone. However, the physiological role of phosphorylation in ACTH and CLIP molecules as a primary messenger remains to be elucidated in any vertebrate species including the lamprey.

CONCLUSION AND RECOMMENDATIONS

Mass spectrometry has developed into the method for identifying proteins and elucidating their post-translational modifications, by using the amino acid sequence in a public database. Most POMC-derived peptides undergo some form of modification following translation. In recent studies, multiple forms of hormones with post-translational modifications, such as acetylation, hydroxylation, and phosphorylation, can be identified in fish pituitary. These modifications result in mass changes that are detected during analysis, such as topological mass spectrometry. As a result, the mass spectrometric analysis of these post-translational modifications is particularly important in endocrine research. Furthermore, direct tissue analysis using MALDI-TOF MS is an analyzable experimentation if there is one only pituitary and if there are just several minutes. Thus, this strategy is becoming an essential tool for endocrine researchers to elucidate molecular mechanisms within cellular systems. On the other hands, the post-translational modifications of hormone seem to be involved in diverse functions. However, the physiological significance of the modified hormones remains to be elucidated. It is, therefore, necessary to clear a physiologic role about the multiplicity of pituitary hormone in the future.

REFERENCES

1. Smith PE. Experimental ablation of the hypophysis in the frog embryo. *Science* (1916) **44**:280–2. doi:10.1126/science.44.1130.280
2. Allen BM. The results of extirpation of the anterior lobe of the hypophysis and of the thyroid of *Rana pipiens* larvae. *Science* (1916) **44**:755–8. doi:10.1126/science.44.1143.755
3. Hogben L, Slome D. The pigmentary effector system: VI. The dual character of endocrine co-ordination in amphibian colour changes. *Proc R Soc Lond B Biol Sci* (1931) **108**:10–53. doi:10.1098/rspb.1931.0020

4. Sayers MA, Sayers G, Woodbury LA. The assay of adrenocorticotropic hormone by the adrenal-ascorbic acid deletion methods. *Endocrinology* (1948) **42**:379–93. doi:10.1210/endo-42-5-379
5. Simon EJ, Hiller JM, Edelman I. Steriospecific binding of the potent narcotic analgesic [^{3}H]etorphine to rat-brain homogenate. *Proc Natl Acad Sci U S A* (1973) **70**:1947–9. doi:10.1073/pnas.70.7.1947
6. Nakanishi S, Inoue A, Kita T, Inoue A, Nakamura M, Chang ACY, et al. Nucleotide sequence of cloned cDNA for bovine corticotropin-β-lipotropin precursor. *Nature* (1979) **278**:423–7. doi:10.1038/278423a0
7. Honig RE, Woolston JR. Laser-induced emission of electrons, ions, and neutral atoms from solid surfaces. *Appl Phys Lett* (1963) **2**:138–9. doi:10.1063/1.1753812
8. Kaufmann R, Hillenkamp F, Wechsung R, Heinen HJ, Schürmann M. Laser microprobe mass analysis: achievements and aspects. *Scan Electron Microsc* (1979) **2**:279–90.
9. Karas M, Bachmann D, Hillenkamp F. Influence of the wavelength in high irradiance ultraviolet laser desorption mass spectrometry of organic molecules. *Anal Chem* (1985) **57**:2935–9. doi:10.1021/ac00291a042
10. Setou M editor. *Imaging Mass Spectrometry: Protocols for Mass Microscopy*. Tokyo: Springer (2010).
11. Yasuda-Kamatani Y, Yasuda A. Identification of orcokinin gene-related peptides in the brain of the crayfish *Procambarus clarkii* by the combination of MALDI-TOF and on-line capillary HPLC/Q-Tof mass spectrometries and molecular cloning. *Gen Comp Endocrinol* (2000) **118**:161–72. doi:10.1006/gcen.1999.7453
12. Takeuchi H, Yasuda A, Yasuda-Kamatani Y, Kubo T, Nakajima T. Identification of a tachykinin-related neuropeptide from the honeybee brain using direct MALDI-TOF MS and its gene expression in worker, queen, and drone heads. *Insect Mol Biol* (2003) **12**:291–8. doi:10.1046/j.1365-2583.2003.00414.x
13. Yasuda A, Yasuda-Kamatani Y, Nozaki M, Nakajima T. Identification of GYRKPPFNGSIFamide (crustacean-SIFamide) in the crayfish *Procambarus clarkii* by topological mass spectrometry analysis. *Gen Comp Endocrinol* (2004) **135**:391–400. doi:10.1016/j.ygcen.2003.10.001
14. Yasuda-Kamatani Y, Yasuda A. APSGFLGMRamide is a unique tachykinin-related peptide in crustaceans. *Eur J Biochem* (2004) **271**:1546–56. doi:10.1111/j.1432-1033.2004.04065.x
15. Kondo T, Sawa S, Kinoshita A, Mizuno S, Kakimoto T, Fukuda H, et al. A plant peptide encoded by CLV3 identified by in situ MALDI-TOF MS analysis. *Science* (2006) **313**:845–8. doi:10.1126/science.1128439
16. Takahashi A, Yasuda A, Sower SA, Kawauchi H. Posttranslational processing of proopiomelanocortin family molecules in sea lamprey based on mass spectrometric and chemical analyses. *Gen Comp Endocrinol* (2006) **148**:79–84. doi:10.1016/j.ygcen.2005.09.022
17. Suehiro Y, Yasuda A, Okuyama T, Imada H, Kuroyanagi Y, Kubo T, et al. Mass spectrometric map of neuropeptide expression and analysis of the γ-preprotachykinin gene expression in the medaka (*Oryzias latipes*) brain. *Gen Comp Endocrinol* (2009) **161**:138–45. doi:10.1016/j.ygcen.2008.12.001
18. Inosaki A, Yasuda A, Shinada T, Ohfune Y, Numata H, Shiga S. Mass spectrometric analysis of peptides in brain neurosecretory cells and neurohemal organs in the adult blowfly, *Protophormia terraenovae*. *Comp Biochem Physiol A Mol Integr Physiol* (2010) **155**:190–9. doi:10.1016/j.cbpa.2009.10.036
19. Yasuda A, Tatsu Y, Kawata Y, Akizawa T, Shigeri Y. Post-translational modifications of pro-opiomelanocrtin related hormones in medaka pituitary based on mass spectrometric analyses. *Peptides* (2011) **32**:2127–30. doi:10.1016/j.peptides.2011.08.016
20. Yasuda A, Tatsu Y, Shigeri Y. Characterization of triacetyl-α-melanocyte-stimulating hormone in carp and goldfish. *Gen Comp Endocrinol* (2012) **175**:270–6. doi:10.1016/j.ygcen.2011.11.009
21. Rudman D, Chawla RK, Hollins BM. *N,O*-Diacetylserine α-melanocyte stimulating hormone, a naturally occurring melanotropic peptide. *J Biol Chem* (1979) **254**:10102–8.
22. Kawauchi H, Muramoto K. Isolation and primary structure of melanotropins from salmon pituitary glands. *Int J Pept Protein Res* (1979) **14**:373–4. doi:10.1111/j.1399-3011.1979.tb01946.x
23. Follenius E, van Dorsselaer A, Meunier A. Separation and partial characterization by high-performance liquid chromatography and radioimmunoassay of different forms of melanocyte-stimulating hormone from fish (Cyprinidae) neurointermediate lobes. *Gen Comp Endocrinol* (1985) **57**:198–207. doi:10.1016/0016-6480(85)90264-3
24. Gautron JP, Pattou E, Bauer K, Kordon C. (Hydroxyproline^9) luteinizing hormone-releasing hormone: a novel peptide in mammalian and frog hypothalamus. *Neurochem Int* (1991) **18**:221–35. doi:10.1016/0197-0186(91)90189-K
25. Browne CA, Bennett HPJ, Solomon S. Isolation and characterization of corticotropin- and melanotropin-related peptides from the neurointermediary lobe of the rat pituitary by reversed-phase liquid chromatography. *Biochemistry* (1981) **20**:4538–46. doi:10.1021/bi00519a005
26. Shepherd RG, Willson SD, Howard KS, Bell PH, Davies DS, Davis SB, et al. Studies with corticotropin. III. Determination of the structure of β-corticotropin1 and its active degradation products. *J Am Chem Soc* (1956) **78**:5067–76. doi:10.1021/ja01600a067

Conflict of Interest Statement: The authors declare that the research was conducted in the absence of any commercial or financial relationships that could be construed as a potential conflict of interest.

Received: 19 September 2013; accepted: 14 November 2013; published online: 02 December 2013.

*Citation: Yasuda A, Jones LS and Shigeri Y (2013) The multiplicity of post-translational modifications in pro-opiomelanocortin-derived peptides. Front. Endocrinol. **4**:186. doi: 10.3389/fendo.2013.00186*

This article was submitted to Experimental Endocrinology, a section of the journal Frontiers in Endocrinology.

frontiers in
ENDOCRINOLOGY

ORIGINAL RESEARCH ARTICLE
published: 09 July 2013
doi: 10.3389/fendo.2013.00084

Changes in subcellular distribution of *n*-octanoyl or *n*-decanoyl ghrelin in ghrelin-producing cells

***Yoshihiro Nishi*[1]*, *Hiroharu Mifune*[2]*, *Akira Yabuki*[3], *Yuji Tajiri*[4], *Rumiko Hirata*[1,5], *Eiichiro Tanaka*[1], *Hiroshi Hosoda*[6], *Kenji Kangawa*[6] and *Masayasu Kojima*[7]**

[1] *Department of Physiology, School of Medicine, Kurume University, Kurume, Japan*
[2] *Institute of Animal Experimentation, School of Medicine, Kurume University, Kurume, Fukuoka, Japan*
[3] *Laboratory of Veterinary Clinical Pathology, Joint Faculty of Veterinary Medicine, Kagoshima University, Kagoshima, Japan*
[4] *Division of Endocrinology and Metabolism, School of Medicine, Kurume University, Kurume, Fukuoka, Japan*
[5] *Department of Pediatrics and Child Health, School of Medicine, Kurume University, Kurume, Fukuoka, Japan*
[6] *Department of Biochemistry, National Cerebral and Cardiovascular Center Research Institute, Osaka, Japan*
[7] *Molecular Genetics, Institute of Life Science, Kurume University, Kurume, Fukuoka, Japan*

Edited by:
Hiroyuki Kaiya, National Cerebral and Cardiovascular Center Research Institute, Japan

Reviewed by:
Isabel Navarro, University of Barcelona, Spain
Suraj Unniappan, York University, Canada

****Correspondence:***
Yoshihiro Nishi, Department of Physiology, School of Medicine, Kurume University, 67 Asahi-machi, Kurume 830-0011, Japan
e-mail: nishiy@med.kurume-u.ac.jp;
Hiroharu Mifune, Institute of Animal Experimentation, Asahi-machi, Kurume University, 67 Asahi-machi, Kurume 830-0011, Japan
e-mail: mifune@med.kurume-u.ac.jp

Background: The enzyme ghrelin *O*-acyltransferase (GOAT) catalyzes the acylation of ghrelin. The molecular form of GOAT, together with its reaction *in vitro*, has been reported previously. However, the subcellular processes governing the acylation of ghrelin remain to be elucidated.

Methods: Double immunoelectron microscopy was used to examine changes in the relative proportions of secretory granules containing *n*-octanoyl ghrelin (C8-ghrelin) or *n*-decanoyl ghrelin (C10-ghrelin) in ghrelin-producing cells of mouse stomachs. The dynamics of C8-type (possessing C8-ghrelin exclusively), C10-type (possessing C10-ghrelin only), and mixed-type secretory granules (possessing both C8- and C10-ghrelin) were investigated after fasting for 48 h or after 2 weeks feeding with chow containing glyceryl-tri-octanoate (C8-MCT) or glyceryl-tri-decanoate (C10-MCT). The dynamics of C8- or C10-ghrelin-immunoreactivity (ir-C8- or ir-C10-ghrelin) within the mixed-type granules were also investigated.

Results: Immunoelectron microscopic analysis revealed the co-existence of C8- and C10-ghrelin within the same secretory granules (mixed-type) in ghrelin-producing cells. Compared to control mice fed standard chow, the ratio of C10-type secretory granules increased significantly after ingestion of C10-MCT, whereas that of C8-type granules declined significantly under the same treatment. After ingestion of C8-MCT, the proportion of C8-type secretory granules increased significantly. Within the mixed-type granules the ratio of ir-C10-ghrelin increased significantly and that of ir-C8-ghrelin decreased significantly upon fasting.

Conclusion: These findings confirmed that C10-ghrelin, another acyl-form of active ghrelin, is stored within the same secretory granules as C8-ghrelin, and suggested that the types of medium-chain acyl-molecules surrounding and available to the ghrelin-GOAT system may affect the physiological processes of ghrelin acylation.

Keywords: decanoyl ghrelin, fasting, ghrelin *O*-acyltransferase, immunoelectron microscopy, medium-chain triglycerides, octanoyl ghrelin, radioimmunoassay, secretory granules

INTRODUCTION

Ghrelin is an acylated peptide hormone mainly produced in the stomach (1). A main acyl-form of ghrelin in rodents and humans is an *n*-octanoyl ghrelin (C8-ghrelin), a serine 3 residue (Ser^3) of which is modified by an *n*-octanoic acid (2, 3). The acylation of ghrelin is catalyzed by an enzyme: ghrelin *O*-acyltransferase (GOAT: previously known as MBOAT4) that belongs to the superfamily of membrane-bound *O*-acyltransferase (MBOAT) (4, 5). Since the discovery of GOAT (6, 7), many *in vitro* and *in vivo* studies on the mechanism of ghrelin acylation by this enzyme have been carried out (8–11). However, several discrepancies have emerged between the *in vitro* and *in vivo* findings (5, 12). For example, as regards the stomach content of acyl-ghrelins modified by a fatty acid with a carbon-chain shorter or a longer than eight (C8), we have detected a very low content of *n*-hexanoyl ghrelin (C6-ghrelin) in stomachs of mice under physiological conditions (i.e., without the ingestion of glyceryl-tri-hexanoate: a medium-chain triglyceride (MCTs) composed of three sets of *n*-hexanoyl group, C6-MCT) (13). We have also detected a considerable amount of *n*-decanoyl ghrelin (C10-ghrelin) in stomachs of mice, rabbits, or golden hamster fed *ad libitum* a standard chow (12). Furthermore, after fasting, the content of C10-ghrelin

in mouse stomachs increased to nearly one third that of C8-ghrelin (14). These observations *in vivo* did not match the findings *in vitro* showing that GOAT has a preference for *n*-hexanoyl-CoA (C6-CoA) over *n*-octanoyl-CoA (C8-CoA), and also has greater preference for C8-CoA than *n*-decanoyl-CoA (C10-CoA) as an acyl donor (9).

Several groups have used immunoelectron microscopy to study the subcellular distribution of ghrelin (15–17) and ghrelin-related molecules (18, 19). However, there have been no reports concerning the distributional changes of acyl-ghrelins within ghrelin-producing cells (subcellular dynamics of acyl-ghrelins) under different nutritional conditions.

The present study used double immunoelectron microscopy to confirm the subcellular distribution of C8- and C10-ghrelins within ghrelin-producing cells. To shed light on the subcellular processes of ghrelin acylation, changes in the distribution of C8- or C10-ghrelin in ghrelin-producing cells were investigated after fasting or after ingestion of glyceryl-tri-octanoate (C8-MCT) or glyceryl-tri-decanoate (C10-MCT). In order to relate the present electron microscopic findings to the biochemical findings reported previously (11, 13, 14, 20), we also examined the change in stomach contents of C8- or C10-ghrelin by respective radioimmunoassay system (RIA), and studied the changes of ghrelin and GOAT mRNA levels in the mouse stomach.

MATERIALS AND METHODS

ANIMALS

Male C57BL/6J mice (Jcl: C57BL/6J, CLEA Japan, Inc., Osaka, Japan) weighing 20–25 g (10–13 weeks old) were used in this study. The animals were maintained under controlled temperature (24 ± 1°C), humidity (55 ± 5%), and light conditions (light on 07:00–19:00 h) with free access to standard laboratory chow (CE-2, CLEA Co. Ltd., Osaka, Japan) and water. Stomach and plasma samples from mice were obtained under anesthesia with sodium pentobarbital 30 mg/kg i.p. (Nembutal™, Dainippon Pharmaceutical Co., Ltd., Osaka, Japan). All experiments were undertaken in accordance with the *Guidelines for Animal Experimentation*, Kurume University.

SCHEDULE FOR THE INGESTION OF MEDIUM-CHAIN TRIGLYCERIDES

To examine the effect of dietary MCTs on the cellular distribution of stomach *n*-octanoyl ghrelin (C8-ghrelin) or *n*-decanoyl ghrelin (C10-ghrelin), mice ($n = 5$ in each ingestion group) were fed chow mixed with 3% (wt/wt) glyceryl-tri-octanoate or tri-decanoate (C8-MCT or C10-MCT; Wako Pure Chemical, Osaka, Japan) for 2 weeks as described previously (13, 21). The control animals were fed a CE-2 pellet diet and water *ad libitum*. Body weights of mice were measured before and after feeding with chow containing C8- or C10-MCT (C8-MCT-fed or C10-MCT-fed), and compared to those of control mice fed a standard laboratory chow *ad libitum* (Control). Daily food intake of the mouse (g/day/mouse) in each feeding condition (C8-MCT, C10-MCT, or Control) was also estimated by measuring the weight of chow every 24 h-period.

SCHEDULE FOR FASTING EXPERIMENT

Prior to performing the fasting experiment, the mice had free access to food and water. The fasting time was calculated from the time when food was withdrawn on the first day of the experiment. For the sampling from fasted mice ($n = 5$), food was withdrawn at 8:00 a.m. on the first day of the experiment and samples (stomach and plasma) were obtained at 8:00 a.m. on the third day (two-overnight) of the experiment. Body weights of mice before and after fasting were measured and compared.

IMMUNOHISTOCHEMISTRY FOR C8- AND C10-GHRELIN

The fundi of the stomach in the control mice (fed with free access to standard laboratory chow, $n = 5$), mice receiving chow with glyceryl-tri-octanoate (C8-MCT, $n = 5$) or tri-decanoate (C10-MCT, $n = 5$), and fasted mice ($n = 5$) were collected and fixed in Zamboni's solution and routinely embedded in paraffin. Immunohistochemical staining was performed according to the modified avidin-biotin-peroxidase complex (ABC) technique described in our previous report (17). For C8- and C10-ghrelin immunohistochemical study, rabbit antiserum against C8-ghrelin diluted 1: 100,000 or rabbit antiserum against C10-ghrelin diluted 1:2000 was used as the primary antibody. Negative control studies were performed with anti-C8- or C10-ghrelin antisera, each of which had been abolished by 10 μg of synthesized C8-ghrelin or C10-ghrelin, respectively. Negative control studies were also done by omitting antisera against C8-ghrelin or C10-ghrelin. These negative controls showed no immunoreactions. For light-microscopic morphometry, three to five sections from each mouse stomach ($n = 5$ mice in each group) were observed at random using an ocular micrometer, and the number of immunopositive cells for C8- or C10-ghrelin per unit area of glandular portions (mm^2) was counted.

DOUBLE IMMUNOFLUORESCENCE FOR C8- AND C10-GHRELIN

Immunofluorescent staining was performed according to the double immunofluorescence technique described in our previous report (17). For C8- and C10-ghrelin immunofluorescent study, mouse monoclonal antibody against the N-terminal sequence of C8-ghrelin (Mitsubishi Kagaku Iatron Inc., Tokyo, Japan) diluted 1:2000 and rabbit antiserum against C10-ghrelin diluted 1:3000 were used as the primary antibody, respectively. Three sections from each mouse in control group were observed.

IMMUNOELECTRON MICROSCOPY FOR C8- OR C10-GHRELIN

Samples for immunoelectron microscopy were prepared as described previously (17). Ultrathin sections were labeled by the post-embedding double immunogold labeling method as described previously (22) with slight modification. The double immunogold labeling was carried out using the two polyclonal antibodies against C8-ghrelin and C10-ghrelin. One face of a section was incubated in rabbit anti-C8-ghrelin antibody diluted 1:2000, and anti-rabbit IgG (British Biocell International, Cardiff, UK) conjugated with 20 nm gold particles (large particles) was used for the immunogold labeling of this face of the section. Rabbit anti-C10-ghrelin antibody (diluted 1:400) and anti-rabbit IgG (British Biocell International) conjugated with 10 nm gold

particles (small particles) were used for the immunogold labeling of the other face of the section. For morphometric analysis, at least 10 electron micrographs of ghrelin cells were taken from each animal at a primary magnification of ×20,000 and printed at a final magnification of ×50,000.

QUANTITATIVE IMMUNOELECTRON MICROSCOPIC ANALYSES FOR C8- AND C10-GHRELIN

Immunogold ultrastructural morphometric analysis was done as described in the previous reports (16, 23, 24). Approximately three to five photographs of ghrelin-producing cells per section of fundi were randomly selected from three to five sections per mouse in the stomach of each mouse (over 100 images). Based on our previous findings for the average diameter of ghrelin-positive granules in mice (277 ± 11.1 nm) (17), we randomly chose secretory granules of 250–300 nm diameter from one ghrelin-producing cell per photograph. The observed counts for immunogold-particles within a single secretory granule were used to construct numerical and percentage frequency distributions for C8- or C10-ghrelin in the control, C8-MCT-fed, C10-MCT-fed, and fasted mice ($n = 5$ mice in each group). Immunogold-labeled secretory granules containing only immunoreactivity for C8-ghrelin (large immunogold-particles) were defined as C8-type; those showing immunoreactivity only for C10-ghrelin (small immunogold particles) were defined as C10-type; and those containing immunoreactivity for both C8- and C10-ghrelin (both large and small immunogold particles) were mixed-type. The number of secretory granules (C8-, C10-, or mixed-type) in ghrelin-producing cells of C8-MCT-fed, C10-MCT-fed, or fasted mice was counted (approximately 250 secretory granules per each group of mice), and the proportion (%) of respective granule type was calculated within ghrelin-producing cells from each group of mice (C8-MCT-fed, C10-MCT-fed, fasted, or fed *ad libitum*; $n = 5$ mice in each group). Furthermore, with regard to the mixed-type secretory granules that were immunopositive for both C8- and C10-ghrelin, the number of small immunogold particles (reflecting the C8-ghrelin-immunoreactivity) and large immunogold particles (reflecting the C10-ghrelin-immunoreactivity) within a single secretory granule were counted separately, and the proportions of each type were calculated relative to the total number (small plus large particles). The average rate of immunoreactivity for C8- or C10-ghrelin within the mixed-type secretory granules was calculated from three to five photographs of double immunoelectron microscopy per mouse. Thereafter, the changes in the proportions of C8- or C10-ghrelin-immunoreactivity per mixed-type secretory granule were evaluated under fasting conditions and compared with the results in control mice fed standard chow *ad libitum* ($n = 5$ mice in each group).

RIAs FOR C8-GHRELIN, C10-GHRELIN, AND TOTAL GHRELIN

The RIA for C8- or C10-ghrelin (C8-ghrelin RIA, C10-ghrelin RIA) was performed as described previously for rat and mouse ghrelin (14, 25, 26). The anti-C8-ghrelin antiserum exhibited 100% cross-reactivity with rat, mouse, and human C8-ghrelin but does not recognize *des*-acyl-ghrelin. The anti-C10-ghrelin antiserum exhibited 100% cross-reactivity with rat, mouse, and human C10-ghrelin but does not recognize *des*-acyl-ghrelin. The cross-reactivity of anti-C10-ghrelin antiserum against C8-ghrelin was less than 2%. Cross-reactivity of both anti-C8- and anti-C10-ghrelin antisera to *n*-butyryl, *n*-hexanoyl, *n*-lauryl, and *n*-palmitoyl ghrelin was all less than 5%. The RIA for total ghrelin was also performed as described previously for rat and mouse ghrelin (14, 25). The antiserum used for the total ghrelin RIA recognized all ghrelin peptides with intact C-terminal sequences irrespective of their N-terminal acylation, and exhibited complete cross-reactivity with human, mouse, and rat forms of ghrelin. Stomach or plasma samples for C8-ghrelin, C10-ghrelin, or total ghrelin RIA from mice were prepared as described previously (14, 25, 27).

REVERSE TRANSCRIPTASE POLYMERASE CHAIN REACTION FOR mRNAs OF GHRELIN AND GOAT

The expression levels of mRNA for ghrelin and GOAT in stomachs of mice were examined using semi-quantitative reverse transcriptase polymerase chain reaction (PCR) as described previously (28, 29). The PCR was performed using a commercially available PCR kit (Go-Taq Master Mix; Promega, Madison, WI, USA) with each primer set necessary to amplify the transcripts for ghrelin (Accession No. NM_021488.4, 32 cycles, 329 bps), GOAT (Accession No. NM_001126314, 36 cycles, 141 bps), and β-actin (Accession No. XM_136101, 22 cycles, 224 bps). The sense or reverse primer for the amplification of mouse ghrelin mRNA was 5′-AGTCCTGTCAGTG GTTACTTG-3′ or 5′-AGGCCTGTCCGTGGTTACTTG-3′, respectively. The sense or reverse primer for the amplification of mouse GOAT mRNA was 5′-GGGCCAGGTACCTCTTTCTC-3′ or 5′-GCCTATGGACTTCCTGTGGA-3′, respectively. The sense or reverse primer for the amplification of mouse β-actin mRNA was 5′-CCTAGCACCATGAAGATCAA-3′ or 5′-TTTCTGCACAAGTTAGG TTTTGTCAA-3′, respectively. The NIH-Image program was used to determine the relative amount of each PCR product after gel electrophoresis, and the amount was normalized using simultaneously amplified β-actin (30).

STATISTICAL ANALYSIS

Data were presented as the means ± SD. The statistical significance was determined by ANOVA, two-tailed Student's paired *t*-test, or Chi-square test. A p-value < 0.05 was considered to be statistically significant on ANOVA and Student's *t*-test. A p-value < 0.016 was considered to be statistically significant concerning the difference among the proportion for types of secretory granules (Chi-square test followed by Bonferroni's procedure for multiple tests of significance). All tests were performed using SAS version 9.2 (SAS Institute, Cary, NC, USA).

RESULTS

BODY WEIGHTS AND DAILY FOOD INTAKE OF MICE

Body weight of mice before the treatment with MCT-containing chow was 24.5 ± 1.2 g in the control group fed a standard chow (CE-2, CREA, Japan), 24.2 ± 0.7 g in the C8-MCT-fed group, and 23.4 ± 0.6 g in the C10-MCT-fed group ($n = 5$ in each group). After 2 weeks of the respective feeding regimens, body weights of mice fed control chow, C8-MCT- and C10-MCT-containing chow were 25.2 ± 1.7, 25.2 ± 0.9, and 24.0 ± 0.2 g, respectively. Among the three groups of mice, there were no significant differences in

body weights before or after the treatment. The average daily food consumption (g/day) in each group was 3.36 ± 0.49 g for control group, 3.18 ± 0.44 g for C8-MCT-fed group, and 3.06 ± 0.40 g for C10-MCT-fed group. Again, there were no significant differences in daily food consumption among these three groups. Average body weights of mice upon fasting for 48 h (16.7 ± 1.8 g, $n = 5$) were significantly ($p < 0.05$) lower than that of control mice fed *ad libitum* a standard chow.

IMMUNOREACTIVITY FOR C8- OR C10-GHRELIN IN STOMACHS OF MICE

Immunopositive cells for C8-ghrelin (ip-C8-ghrelin) and C10-ghrelin (ip-C10-ghrelin) in stomachs of control mice given free access to standard laboratory chow, were sparsely distributed in the middle to lower part of the gastric mucosal layer, where they were moderately abundant (**Figures 1A,B**). A small amount of immunopositive cells for C8- or C10-ghrelin was also detected in the gastric submucosal layer. No immunopositive cells for C8- or C10-ghrelin were observed in the gastric superficial epithelial layer. In control mice, the density of DAB staining, reflecting the C10-ghrelin-immunoreactivity (ir-C10-ghrelin), within the ip-C10-ghrelin cells was lower than that for the C8-ghrelin-immunoreactivity (ir-C8-ghrelin) within the C8-ghrelin-immunopositive (ip-C8-ghrelin) cells (**Figures 1A,B**).

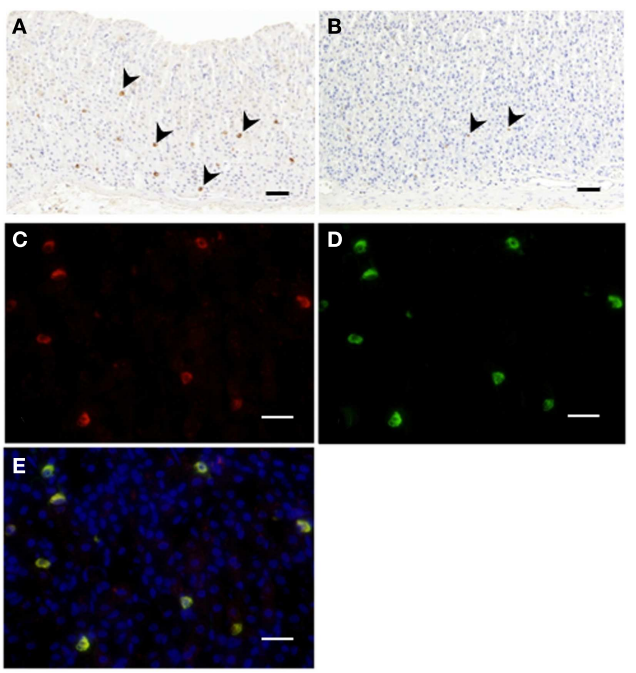

FIGURE 1 | Immunohistochemistry for C8-ghrelin (A) or C10-ghrelin (B) in fundi of stomachs in control mice. The density of DAB staining in cells reflecting C10-ghrelin-immunoreactivity (ir-C10-ghrelin) was lower than that of ir-C8-ghrelin **(A,B)**. Immunofluorescence in fundi of stomachs in control mice **(C–E)**. Ir-C8-ghrelin **(C)** labeled with Alexa 555 (red), and ir-C10-ghrelin **(D)** labeled with Alexa 488 (green) are observed in the same section. The yellow color in the merged image **(E)** indicated a co-localization of ir-C8- and ir-C10-ghrelin. Arrowheads indicate ghrelin-positive cells **(A,B)**. Scale bars represent 100 μm **(A,B)** and represent 25 μm **(C–E)**.

In the fundic mucosa of the mouse stomach, the density of ip-C10-ghrelin cells (21.3 ± 3.7 cells/mm^2 mucosa) was approximately one third that of ip-C8-ghrelin cells (57.5 ± 4.6 cells/mm^2 mucosa) in the same section (**Table 1**).

IMMUNOFLUORESCENCE OF C8- AND C10-GHRELIN IN STOMACHS OF MICE

Double immunostaining for ir-C8-ghrelin and ir-C10-ghrelin revealed a co-localization of the immunoreactivity for both C8-ghrelin (red fluorescence, **Figure 1C**) and C10-ghrelin (green fluorescence, **Figure 1D**) within the same cells (yellow fluorescence in the merged image, **Figure 1E**) in mouse stomachs fed standard laboratory chow *ad libitum*. These findings clearly indicated the co-localization of C8- and C10-ghrelin in the same cell population.

INTRACELLULAR DISTRIBUTION OF C8- OR C10-GHRELIN-IMMUNOREACTIVITY WITHIN THE GHRELIN-PRODUCING CELLS

Double immunogold labeling of C8-ghrelin and C10-ghrelin revealed that, in control mice, over 70% of the secretory granules in ghrelin-producing cells possessed both large (20 nm in diameter) and small (10 nm in diameter) particles of immunogold (**Figure 2**). Two other types of secretory granules were also observed in these cells, one containing only the large particles of immunogold (reflecting *ir*-C8-ghrelin), and the other containing only the small particles of immunogold (reflecting ir-C10-ghrelin). We defined these three types of secretory granules as C8-type (possessing only the ir-C8-ghrelin), C10-type (possessing only the ir-C10-ghrelin), or mixed-type (possessing both ir-C8 and ir-C10-ghrelin). Aside from the secretory granules in ghrelin-producing cells, we observed an extremely small population of Golgi-complexes that were immunopositive for C8- and/or C10-ghrelin (**Figure 2**).

THE PROPORTION OF C8-TYPE, C10-TYPE, OR MIXED-TYPE SECRETORY GRANULES WITHIN GHRELIN-PRODUCING CELLS

As shown in **Figure 3**, we examined the intracellular proportions of the three types (C8-, C10-, mixed-type) of immunogold-labeled

Table 1 | Numbers of immunopositive cells for C8- or C10-ghrelin in stomachs of mice.

	ip-C8-ghrelin	ip-C10-ghrelin
C8-MCT-fed	$140.6 \pm 15.5^{**,\$}$	$18.7 \pm 3.1^{\#,\$}$
C10-MCT-fed	$51.4 \pm 1.9^{*}$	$96.5 \pm 15.4^{**,\#}$
Fasted	51.3 ± 3.7	$47.7 \pm 4.1^{**}$
Control	57.5 ± 4.6	21.3 ± 3.7

Data represent mean ± SD for the number of immunopositive cells for C8-ghrelin (ip-C8-ghrelin) or C10-ghrelin (ip-C10-ghrelin) per unit area (mm^2) of the stomach mucosa (the average value obtained from three to five sections per each stomach) (n = 5 mice in each group). C8-MCT-fed, stomachs of mice fed with glyceryl-tri-octanoate containing chow for 2 weeks; C10-MCT-fed, those fed with glyceryl-tri-decanoate containing chow for 2 weeks; Fasted, those fasted for 48 h with free access to water; Control, those fed ad libitum with standard laboratory chow (CE-2). $^{*}p < 0.05$; $^{**}p < 0.01$ vs. values in Control; $^{\$}p < 0.01$ vs. values in C10-MCT-fed; $^{\#}p < 0.01$ vs. values in Fasted.

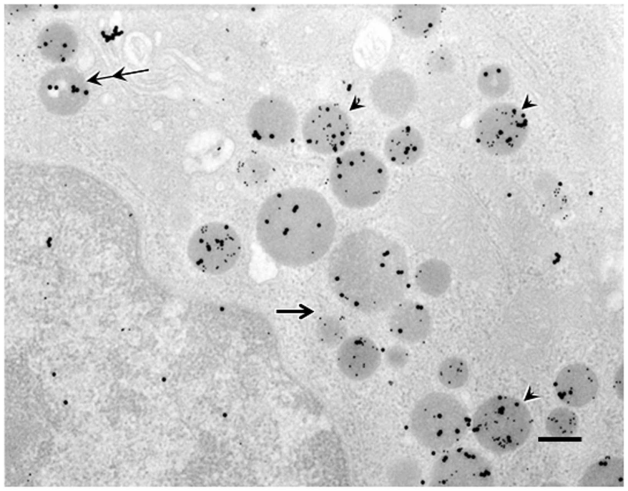

FIGURE 2 | Double immunogold labeling in ghrelin-producing cells in the stomachs of control mice. Large particles of immunogold (20 nm in diameter) or small particles of immunogold (10 nm in diameter) demonstrated immunoreactivity for C8-ghrelin (ir-C8-ghrelin) or C10-ghrelin (ir-C10-ghrelin), respectively. Over 70% of secretory granules in ghrelin-producing cells exhibited both ir-C8-ghrelin and ir-C10-ghrelin (arrowheads). Occasionally (10–20% of the secretory granules), there appeared granules stained only for ir-C8-ghrelin reflected by large particles (double arrows) or ir-C10-ghrelin reflected by small particles of immunogold (single arrow) in ghrelin-producing cells. Scale bar represents 200 nm.

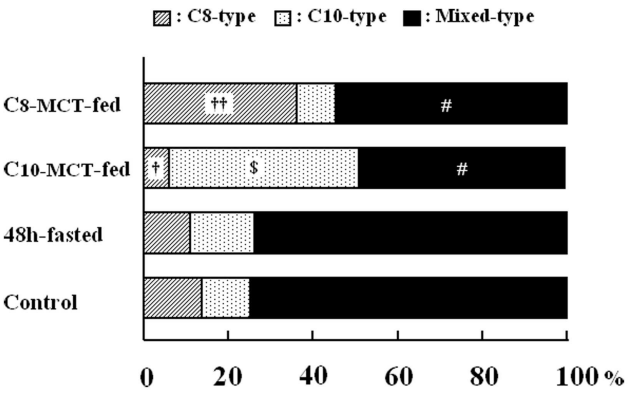

FIGURE 3 | The proportion of secretory granules that possessed immunoreactivity exclusively for C8-ghrelin (C8-type, cross-hatched column), or exclusively for C10-ghrelin (C10-type, dotted column), or for both C8- and C10-ghrelin (mixed-type, filled column) in ghrelin-producing cells of the stomach in control mice fed *ad libitum* a standard chow (Control), in mice fasted for 48 h (fasted), or in mice after 2-weeks ingestion of glyceryl-tri-octanoate (C8-MCT-fed) or glyceryl-tri-decanoate (C10-MCT-fed). Data were extracted and analyzed from approximately 250 secretory granules of ghrelin-producing cells in each group ($n = 5$ mice in each group). $^{\dagger}p < 0.01$; $^{\dagger\dagger}p < 0.001$ vs. control and fasted. $p < 0.001$ vs. control, C8-MCT-fed, and fasted. $^{\#}p < 0.001$ vs. control and fasted.

granules in ghrelin-producing cells under different nutritional conditions: fasted, C8-MCT-fed and C10-MCT-fed, and compared them with that of control mice fed *ad libitum*. Ghrelin-producing cells of control mice contained relatively small proportions of secretory granules that were exclusively immunopositive for either C8- or C10-ghrelin (C8-type; $13.8 \pm 3.3\%$, C10-type; $9.2 \pm 3.5\%$), whereas approximately 80% ($77.1 \pm 6.4\%$) of the secretory granules were mixed-type. In mice fed for 2 weeks with chow containing 3% glyceryl-tri-octanoate (C8-MCT-fed), the ratio of C8-type secretory granules ($38.8 \pm 5.4\%$) to the total number of ghrelin-secretory granules (the sum of C8-, C10-, and mixed-type) increased significantly ($p < 0.01$) compared with the control ($13.8 \pm 3.3\%$), while that of C10-type granules ($6.8 \pm 2.1\%$) in C8-MCT-fed mice slightly decreased in comparison to the control mice ($9.2 \pm 3.5\%$). The ratio of mixed-type secretory granules in ghrelin-producing cells of C8-MCT-fed mice ($54.4 \pm 5.9\%$) also decreased significantly ($p < 0.001$) compared with control mice ($77.1 \pm 6.4\%$). When we fed mice with chow containing 3% glyceryl-tri-decanoate for 2 weeks (C10-MCT-fed), the ratio of C10-type secretory granules ($47.2 \pm 6.9\%$) increased significantly ($p < 0.001$) compared with the control ($9.2 \pm 3.5\%$), while that of C8-type granules ($4.6 \pm 1.3\%$) in C10-MCT-fed mice decreased significantly ($p < 0.001$) compared with the control mice ($13.8 \pm 3.3\%$). The ratio of mixed-type secretory granules in ghrelin-producing cells of C10-MCT-fed mice ($48.1 \pm 6.3\%$) also decreased significantly ($p < 0.001$) relative to control mice ($77.1 \pm 6.4\%$). In contrast, after fasting, there were no significant changes in the proportions of these three types of secretory granules (C8-type, $10.5 \pm 2.9\%$; C10-type, $15.3 \pm 3.3\%$; mixed-type, $74.2 \pm 5.3\%$) in comparison to those in control mice.

THE EFFECT OF FASTING ON THE PROPORTION OF C8- OR C10-GHRELIN-IMMUNOREACTIVITY WITHIN THE MIXED-TYPE SECRETORY GRANULES

In control mice (fed *ad libitum* a standard chow), the proportions of C8-ghrelin-immunoreactivity (ir-C8-ghrelin) and C10-ghrelin-immunoreactivity (ir-C10-ghrelin) within the mixed-type granules (as determined by the proportion of large or small particles of immunogold within the secretory granule) were 46.5 ± 3.0 and $53.5 \pm 3.1\%$, respectively. After fasting for 48 h, the proportion of ir-C8-ghrelin within the mixed-type secretory granules (reflected by the number of large particles of immunogold) fell to $33.7 \pm 2.1\%$ of the total immunoreactivity of ghrelin (the sum of ir-C8- and ir-C10-ghrelin reflected by the number of large and small immunogold particles). Upon fasting, the proportion of ir-C10-ghrelin within the mixed-type secretory granules, which was reflected by the number of small particles of immunogold, increased to $66.2 \pm 1.9\%$ of total ghrelin immunoreactivity.

When we defined the average rate of ir-C8-ghrelin within the mixed-type secretory granules in one of the control mice as 1.0, and compared the relative value for the proportion of ir-C8-ghrelin before and after fasting, the value for the rate of ir-C8-ghrelin in fasted mice (0.76 ± 0.06) was significantly lower ($p < 0.001$) than that in control mice (1.05 ± 0.07) ($n = 5$ mice in each group). In contrast, the relative value for the proportion of ir-C10-ghrelin in fasted mice (1.19 ± 0.05) was significantly higher ($p < 0.001$) than that in control mice (0.96 ± 0.05) ($n = 5$ mice in each group).

Table 2 | Stomach contents of C8- or C10-ghrelin under different nutritional conditions.

	C8-ghrelin	C10-ghrelin	Total ghrelin
C8-MCT-fed	$3.62 \pm 0.33^{**,\#,\$}$	$0.13 \pm 0.02^{*,\#,\$}$	$6.57 \pm 0.79^{*}$
C10-MCT-fed	$2.70 \pm 0.36^{\$}$	$1.21 \pm 0.12^{**,\$}$	$6.49 \pm 0.80^{*}$
Fasted	$1.63 \pm 0.32^{*}$	$0.58 \pm 0.10^{**}$	$6.57 \pm 0.71^{*}$
Control	2.29 ± 0.23	0.27 ± 0.20	7.61 ± 0.66

Data represent mean ± SD for the stomach contents (pmol/mg-tissue) of each ghrelin molecule (C8-ghrelin, C10-ghrelin, or total ghrelin) measured by C8-ghrelin RIA, C10-ghrelin RIA, or total ghrelin RIA (n = 5 mice in each group). Control, fed ad libitum a control laboratory chow (the same group of mice used for the electron- and light-microscopic analysis); C8-MCT-fed, fed with chow containing glyceryl-tri-octanoate; C10-MCT-fed, fed with chow containing glyceryl-tri-decanoate; Fasted, fasted for 48 h with free access to water. $^{*}p < 0.05$; $^{**}p < 0.01$ vs. values in Control. $^{\#}p < 0.01$ vs. values in C10-MCT-fed. $^{\$}p < 0.01$ vs. values in Fasted.

Table 3 | Expression levels of ghrelin and GOAT mRNAs in stomachs of mice under different nutritional conditions.

	Ghrelin	GOAT
C8-MCT-fed	101.2 ± 13.6	105.4 ± 9.0
C10-MCT-fed	93.0 ± 8.7	$82.8 \pm 9.2^{*,\$}$
Fasted	$174.0 \pm 0.33^{**}$	103.6 ± 18.5
Control	100.0 ± 7.8	100.0 ± 11.4

Data represent mean ± SD for the relative expression level of mRNAs for ghrelin or ghrelin O-acyltransferase (GOAT) measured by semi-quantitative RT-PCRs (n = 5 mice in each group). C8-MCT-fed, fed with glyceryl-tri-octanoate containing chow; C10- MCT-fed, fed with glyceryl-tri-decanoate containing chow; Fasted, fasted for 48 h with free access to water; Control, fed ad libitum with standard laboratory chow (the same group of mice used for the electron- and light-microscopic analysis). $^{*}p < 0.05$; $^{**}p < 0.01$ vs. values in Control. $^{\$}p < 0.05$ vs. values in C8-MCT-fed. Expression level for the respective mRNAs for ghrelin, or GOAT in one of the control mice was defined as 100.

Table 4 | Plasma ghrelin levels under different nutritional conditions.

	C8-ghrelin	C10-ghrelin	Total ghrelin
C8-MCT-fed	$25.0 \pm 5.5^{\#}$	$11.4 \pm 2.0^{\#\#}$	298.4 ± 56.2
C10-MCT-fed	$21.0 \pm 5.7^{\#}$	$13.8 \pm 1.3^{\#\#}$	351.8 ± 66.4
Fasted	$88.3 \pm 39.8^{*}$	$45.8 \pm 23.9^{**}$	383.1 ± 231.9
Control	21.8 ± 7.0	9.7 ± 2.4	330.6 ± 132.5

Data represent mean ± SD for the plasma concentrations (fmol/ml) of each ghrelin molecule (C8-ghrelin, C10-ghrelin, or total ghrelin) measured by C8-ghrelin RIA, C10-ghrelin RIA, or total ghrelin RIA (n = 5 mice in each group). C8-MCT-fed, fed with glyceryl-tri-octanoate containing chow; C10-MCT-fed, fed with glyceryl-tri-decanoate containing chow; Fasted, plasma samples from mice upon fasting for 48 h; Control, control mice fed ad libitum a standard laboratory chow. $^{*}p < 0.05$; $^{**}p < 0.01$ vs. values in Control. $^{\#}p < 0.05$; $^{\#\#}p < 0.01$ vs. values in Fasted.

CONTENTS OF C8- OR C10-GHRELIN-IMMUNOREACTIVITY IN STOMACHS OF MICE

As shown in **Table 2**, the stomach content of C8-ghrelin, as measured by C8-ghrelin RIA, was significantly larger ($p < 0.01$) in C8-MCT-fed stomachs than that in control stomachs. The stomach content of C10-ghrelin, which was measured by C10-ghrelin RIA, was significantly smaller ($p < 0.05$) in C8-MCT-fed stomachs, and was significantly larger ($p < 0.01$) in C10-MCT-fed stomachs compared with the controls. The stomach content of total ghrelin (measured by total ghrelin RIA which recognized both acyl- and *des*-acyl-ghrelin with intact C-termini) in both C8-MCT-fed and C10-MCT-fed stomachs were slightly but significantly decreased ($p < 0.05$) compared to that of control stomachs. Upon fasting, stomach contents of both C8-ghrelin and total ghrelin declined significantly ($p < 0.05$), and that of C10-ghrelin increased significantly ($p < 0.01$) than that in stomachs of control mice.

EXPRESSION LEVELS OF mRNAs FOR GHRELIN OR GOAT IN STOMACHS OF MICE

The relative expression levels of mRNA for ghrelin, corrected by β-actin levels, in stomachs of fasted mice were significantly higher ($p < 0.01$) than in stomachs of control mice fed *ad libitum* a standard laboratory chow (**Table 3**). However, the levels of ghrelin mRNA in stomachs of C8-MCT or C10-MCT-fed mice did not differ from that in control mice. The relative expression levels of GOAT mRNA in fasted or C8-MCT-fed stomachs of mice did not differ from that in control stomachs. Whereas, the levels of GOAT mRNA in stomachs of C10-MCT-fed mice were significantly ($p < 0.05$) lower than those in control and C8-MCT-fed mice.

PLASMA CONCENTRATIONS OF C8- OR C10-GHRELIN-IMMUNOREACTIVITY IN MICE

As shown in **Table 4**, plasma levels of C8-ghrelin increased significantly after fasting for 48 h. In contrast, plasma levels of C8-ghrelin did not change after the ingestion of C8-MCT for 2 weeks. Similarly, the change in C10-ghrelin level after ingestion of C10-MCT was far smaller than that seen upon fasting.

DISCUSSION

The present study by double immunoelectron microscopy confirmed our previous findings by light microscopy concerning the co-existence of C8- and C10-ghrelin-immunoreactivity (ir-C8- and ir-C10-ghrelin) within the same ghrelin-producing cells (14). On immunoelectron microscopy, we observed both ir-C8- and ir-C10-ghrelin within round and compact dense granules of X/A-like cell type, a characteristics of ghrelin-producing cells in rats (15), mice (18), and hamster (17).

Concerning the subcellular distribution of ir-C8- or ir-C10-ghrelin outside of secretory granules, we did not detect any significant signals of immunogold within the endoplasmic reticulum or Golgi complex. However, these findings did not disprove the putative concept (31) that the acylation of ghrelin by GOAT precedes the protease cleavage of pro-ghrelin to ghrelin, because the antibodies we used in this study possessed little or no cross-reactivity to pro-ghrelin peptides irrespective of their acylation status (12, 25).

After feeding mice with chow containing C8-MCT or C10-MCT for 2 weeks, a significant increase was noted in the proportion of C8- or C10-type secretory granules, respectively, to the total number of ghrelin-secretory granules in ghrelin-producing cells,

while the proportion of mixed-type granules to the total number of ghrelin-secretory granules in ghrelin-producing cells declined significantly. These findings suggested that a certain proportion (10–20%) of the mixed-type secretory granules changed to C8-type or C10-type after a feeding regimen containing C8-MCT or C10-MCT, respectively. These findings also implied that the type of medium-chain acyl-molecules (i.e., C8-CoA or C10-CoA) surrounding the ghrelin-GOAT system has strong effect on the type of acyl-ghrelins (i.e., C8-ghrelin or C10-ghrelin) stored within the ghrelin-secretory granules.

When we evaluated the stomach contents of ir-C8- or ir-C10-ghrelin by RIA, the levels of ir-C10-ghrelin increased significantly in both C10-MCT-fed and fasted conditions, which was in line with previous reports (11–14, 21). In contrast, upon fasting, the ratios of secretory granules (C8-, C10-, or mixed-type) to the total number of ghrelin-secretory granules in ghrelin-producing cells did not differ from those in control mice fed *ad libitum*. However, in the same ghrelin-producing cells of fasted mice, we detected a significant increase in the proportion of ir-C10-ghrelin and a significant decline in the proportion of ir-C8-ghrelin within the mixed-type granules. On the other hand, we could not detect any significant change in the proportions of ir-C8- or ir-C10-ghrelin within the mixed-type granules after feeding mice with C8- or C10-MCT-containing chow for 2 weeks (data not shown here). These differences in the subcellular distribution of ir-C8- or ir-C10-ghrelin together with its kinetics under different nutritional conditions, such as fasting or constant feeding with C8- or C10-MCT, might offer important clues on the subcellular process of ghrelin acylation.

Two-weeks treatment with C8- or C10-MCT did not alter the expression levels of ghrelin mRNA in mouse stomachs, which was supported by our previous report (13). As for GOAT mRNA, no significant changes were detected except for a slight but significant decline after 2-weeks treatment with C10-MCT. Although the precise mechanism of suppression of GOAT mRNA level by C10-MCT-feeding remains to be solved, the influence of ghrelin and/or GOAT mRNA levels on the subcellular kinetics of ir-C8- or ir-C10-ghrelins appeared to be limited.

Differences in the dynamics of plasma ghrelin levels upon different nutritional conditions examined (i.e., upon fasting or 2 weeks feeding with MCT-containing chow), which may reflect the release of ghrelin from secretory granules into circulation, should also be considered to be one of the key processes governing the changes of ir-C8- or ir-C10-ghrelin within the secretory granule. In fact, changes in the level of C8- or C10-ghrelin in plasma upon fasting were far larger than those seen after feeding mice with chow containing C8-MCT or C10-MCT.

Based on the above findings, especially on those revealed by our double immunoelectron microscopy, one may speculate that the mechanism underlining ghrelin acylation is complicated, and cannot be explained simply by the enzymatic activity of GOAT within ghrelin-producing cells. However, our immunoelectron microscopic study on ghrelin acylation also has several limitations. Within the mixed-type secretory granules, relatively larger proportion of ir-C10-ghrelin was observed as compared with ir-C8-ghrelin. This finding, however, did not reflect the absolute content of ir-C8-, or ir-C10-ghrelin in the mixed-type granule, since we used different antibodies possessing different affinities to the C8- or C10-forms of acyl-ghrelin. In our study, we only compared the subcellular distribution of ir-C10- or ir-C8-ghrelin and changes in this distribution under different nutritional conditions, and did not look at the distribution or the changes of other acyl-ghrelins including *n*-hexanoyl ghrelin, an intriguing molecule whose production rate catalyzed by GOAT *in vitro* is far higher than that of C10-ghrelin (9, 10), while it's biological activity is far smaller than that of C10- or C8-ghrelin (21, 32).

In conclusion, in this study we investigated changes in the subcellular distribution of ir-C8- or C10-ghrelin under different nutritional conditions by double immunoelectron microscopy. Present findings indicated that there existed several steps for the synthesis of acyl-ghrelins within ghrelin-secretory granules, and also implied that the types of medium-chain acyl-molecules surrounding the ghrelin-GOAT system affect the acylation process of ghrelin. Further study using immunoelectron microscopy on the subcellular distribution of acyl-ghrelins will shed light on the mechanism underlining the acylation process of ghrelin.

REFERENCES

1. Kojima M, Hosoda H, Date Y, Nakazato M, Matsuo H, Kangawa K. Ghrelin is a growth-hormone-releasing acylated peptide from stomach. *Nature* (1999) **402**:656–60. doi:10.1038/45230
2. Hosoda H, Kojima M, Mizushima T, Shimizu S, Kangawa K. Structural divergence of human ghrelin. Identification of multiple ghrelin-derived molecules produced by post-translational processing. *J Biol Chem* (2003) **278**: 64–70. doi:10.1074/jbc.M205366200
3. Kojima M, Kangawa K. Ghrelin: structure and function. *Physiol Rev* (2005) **85**: 495–522. doi:10.1152/physrev.00012.2004
4. Hofmann K. A superfamily of membrane-bound O-acyltransferases with implications for wnt signaling. *Trends Biochem Sci* (2000) **25**:111–2. doi:10.1016/S0968-0004(99)01539-X
5. Al Massadi O, Tschop MH, Tong J. Ghrelin acylation and metabolic control. *Peptides* (2011) **32**:2301–8. doi:10.1016/j.peptides.2011.08.020
6. Yang J, Brown MS, Liang G, Grishin NV, Goldstein JL. Identification of the acyltransferase that octanoylates ghrelin, an appetite-stimulating peptide hormone. *Cell* (2008) **132**:387–96. doi:10.1016/j.cell.2008.01.017
7. Gutierrez JA, Solenberg PJ, Perkins DR, Willency JA, Knierman MD, Jin Z, et al. Ghrelin octanoylation mediated by an orphan lipid transferase. *Proc Natl Acad Sci U S A* (2008) **105**: 6320–5. doi:10.1073/pnas.0800708105
8. Yang J, Zhao TJ, Goldstein JL, Brown MS. Inhibition of ghrelin O-acyltransferase (GOAT) by octanoylated pentapeptides. *Proc Natl Acad Sci U S A* (2008) **105**: 10750–5. doi:10.1073/pnas.0805353105
9. Ohgusu H, Shirouzu K, Nakamura Y, Nakashima Y, Ida T, Sato T, et al. Ghrelin O-acyltransferase (GOAT) has a preference for n-hexanoyl-CoA over n-octanoyl-CoA as an acyl donor. *Biochem Biophys Res Commun* (2009) **386**: 153–8. doi:10.1016/j.bbrc.2009.06.001
10. Ohgusu H, Takahashi T, Kojima M. Enzymatic characterization of GOAT, ghrelin O-acyltransferase. *Methods Enzymol* (2012) **514**:147–63. doi:10.1016/B978-0-12-381272-8.00010-6
11. Kirchner H, Gutierrez JA, Solenberg PJ, Pfluger PT, Czyzyk TA, Willency JA, et al. GOAT links dietary lipids with the endocrine control of energy balance. *Nat Med* (2009) **15**:741–5. doi:10.1038/nm.1997
12. Nishi Y, Yoh J, Hiejima H, Kojima M. Structures and molecular forms of the ghrelin-family peptides. *Peptides* (2011) **32**:2175–82. doi:10.1016/j.peptides.2011.07.024

13. Nishi Y, Hiejima H, Hosoda H, Kaiya H, Mori K, Fukue Y, et al. Ingested medium-chain fatty acids are directly utilized for the acyl modification of ghrelin. *Endocrinology* (2005) **146**:2255–64. doi:10.1210/en.2004-0695
14. Hiejima H, Nishi Y, Hosoda H, Yoh J, Mifune H, Satou M, et al. Regional distribution and the dynamics of n-decanoyl ghrelin, another acyl-form of ghrelin, upon fasting in rodents. *Regul Pept* (2009) **156**: 47–56. doi:10.1016/j.regpep.2009.05.003
15. Date Y, Kojima M, Hosoda H, Sawaguchi A, Mondal MS, Suganuma T, et al. Ghrelin, a novel growth hormone-releasing acylated peptide, is synthesized in a distinct endocrine cell type in the gastrointestinal tracts of rats and humans. *Endocrinology* (2000) **141**:4255–61. doi:10.1210/en.141.11.4255
16. Rindi G, Necchi V, Savio A, Torsello A, Zoli M, Locatelli V, et al. Characterisation of gastric ghrelin cells in man and other mammals: studies in adult and fetal tissues. *Histochem Cell Biol* (2002) **117**:511–9. doi:10.1007/s00418-002-0415-1
17. Yabuki A, Ojima T, Kojima M, Nishi Y, Mifune H, Matsumoto M, et al. Characterization and species differences in gastric ghrelin cells from mice, rats and hamsters. *J Anat* (2004) **205**:239–46. doi:10.1111/j.0021-8782.2004.00331.x
18. Tomasetto C, Karam SM, Ribieras S, Masson R, Lefebvre O, Staub A, et al. Identification and characterization of a novel gastric peptide hormone: the motilin-related peptide. *Gastroenterology* (2000) **119**:395–405. doi:10.1053/gast.2000.9371
19. Zhao CM, Furnes MW, Stenstrom B, Kulseng B, Chen D. Characterization of obestatin- and ghrelin-producing cells in the gastrointestinal tract and pancreas of rats: an immunohistochemical and electron-microscopic study. *Cell Tissue Res* (2008) **331**:575–87. doi:10.1007/s00441-007-0514-3
20. Toshinai K, Mondal MS, Nakazato M, Date Y, Murakami N, Kojima M, et al. Upregulation of Ghrelin expression in the stomach upon fasting, insulin-induced hypoglycemia, and leptin administration. *Biochem Biophys Res Commun* (2001) **281**:1220–5. doi:10.1006/bbrc.2001.4518
21. Nishi Y, Mifune H, Kojima M. Ghrelin acylation by ingestion of medium-chain fatty acids. *Methods Enzymol* (2012) **514**:303–15. doi:10.1016/B978-0-12-381272-8.00019-2
22. Mifune H, Richter R, Forssmann WG. Detection of immunoreactive atrial and brain natriuretic peptides in the equine atrium. *Anat Embryol (Berl)* (1995) **192**:117–21. doi:10.1007/BF00186000
23. Mayhew TM, Lucocq JM. Multiple-labelling immunoEM using different sizes of colloidal gold: alternative approaches to test for differential distribution and colocalization in subcellular structures. *Histochem Cell Biol* (2011) **135**:317–26. doi:10.1007/s00418-011-0788-0
24. Namba K, Suzuki T, Nakata H. Immunogold electron microscopic evidence of in situ formation of homo- and heteromeric purinergic adenosine A1 and P2Y2 receptors in rat brain. *BMC Res Notes* (2010) **3**:323. doi:10.1186/1756-0500-3-323
25. Hosoda H, Kojima M, Matsuo H, Kangawa K. Ghrelin and des-acyl ghrelin: two major forms of rat ghrelin peptide in gastrointestinal tissue. *Biochem Biophys Res Commun* (2000) **279**:909–13. doi:10.1006/bbrc.2000.4039
26. Nishi Y, Hiejima H, Mifune H, Sato T, Kangawa K, Kojima M. Developmental changes in the pattern of ghrelin's acyl modification and the levels of acyl-modified ghrelins in murine stomach. *Endocrinology* (2005) **146**:2709–15. doi:10.1210/en.2004-0645
27. Yoh J, Nishi Y, Hosoda H, Tajiri Y, Yamada K, Yanase T, et al. Plasma levels of n-decanoyl ghrelin, another acyl- and active-form of ghrelin, in human subjects and the effect of glucose- or meal-ingestion on its dynamics. *Regul Pept* (2011) **167**:140–8. doi:10.1016/j.regpep.2010.12.010
28. Hamada N, Nishi Y, Tajiri Y, Setoyama K, Kamimura R, Miyahara K, et al. Disrupted regulation of ghrelin production under antihypertensive treatment in spontaneously hypertensive rats. *Circ J* (2012) **76**:1423–9. doi:10.1253/circj.CJ-11-1345
29. Mifune H, Nishi Y, Tajiri Y, Masuyama T, Hosoda H, Kangawa K, et al. Increased production of active ghrelin is relevant to hyperphagia in nonobese spontaneously diabetic Torii rats. *Metabolism* (2012) **61**:491–5. doi:10.1016/j.metabol.2011.09.001
30. Nishi Y, Haji M, Takayanagi R, Iguchi H, Shimazoe T, Hirata J, et al. Establishment and characterization of pthrp-producing human pancreatic-cancer cell-line. *Int J Oncol* (1994) **5**:33–9.
31. Kojima M, Kangawa K. Ghrelin: from gene to physiological function. *Results Probl Cell Differ* (2010) **50**:185–205. doi:10.1007/400_2009_28
32. Matsumoto M, Hosoda H, Kitajima Y, Morozumi N, Minamitake Y, Tanaka S, et al. Structure-activity relationship of ghrelin: pharmacological study of ghrelin peptides. *Biochem Biophys Res Commun* (2001) **287**:142–6. doi:10.1006/bbrc.2001.5553

Conflict of Interest Statement: The authors declare that the research was conducted in the absence of any commercial or financial relationships that could be construed as a potential conflict of interest.

*Received: 29 March 2013; accepted: 26 June 2013; published online: 09 July 2013. Citation: Nishi Y, Mifune H, Yabuki A, Tajiri Y, Hirata R, Tanaka E, Hosoda H, Kangawa K and Kojima M (2013) Changes in subcellular distribution of n-octanoyl or n-decanoyl ghrelin in ghrelin-producing cells. Front. Endocrinol. **4**:84. doi: 10.3389/fendo.2013.00084*
This article was submitted to Frontiers in Experimental Endocrinology, a specialty of Frontiers in Endocrinology.

frontiers in
ENDOCRINOLOGY

ORIGINAL RESEARCH ARTICLE
published: 30 August 2013
doi: 10.3389/fendo.2013.00112

Characterization and endocytic internalization of Epith-2 cell surface glycoprotein during the epithelial-to-mesenchymal transition in sea urchin embryos

Norio Wakayama†, Tomoko Katow and Hideki Katow*

Research Center for Marine Biology, Tohoku University, Aomori, Aomori, Japan

Edited by:
Sho Kakizawa, Kyoto University, Japan

Reviewed by:
Ryusuke Niwa, University of Tsukuba, Japan
Gary Wessel, Brown University, USA
David McClay, Duke University, USA

***Correspondence:**
Hideki Katow, Research Center for Marine Biology, Graduate School of Life Sciences, Tohoku University, Asamushi, Aomori, Aomori 039-3501, Japan
e-mail: hkatow@m.tohoku.ac.jp

†Present address:
Norio Wakayama, Research Institute for Integrated Science, Kanagawa University, Tsuchiya, Hiratsuka, Kanagawa 259-1293, Japan
e-mail: wt502522ru@kanagawa-u.ac.jp

The epithelial cells of the sea urchin *Hemicentrotus pulcherrimus* embryo express an Epith-2, uncharacterized glycoprotein, on the lateral surface. Here, we describe internalization of Epith-2 during mesenchyme formation through the epithelial-to-mesenchymal transition (EMT). Epith-2 was first expressed on the entire egg surface soon after fertilization and on the blastomeres until the 4-cell stage, but was localized to the lateral surface of epithelial cells at and after the 16-cell stage throughout the later developmental period. However, primary mesenchyme cells (PMC) and secondary mesenchyme cells (SMC) that ingress by EMT lost Epith-2 from their cell surface by endocytosis during dissociation from the epithelium, which was associated with the appearance of cytoplasmic Epith-2 dots. The cytoplasmic Epith-2 retained a similar relative molecular mass to that of the cell surface immediately after ingression through the early period of the spreading to single cells. Then, Epith-2 was completely lost from the cytoplasm. Tyrosine residues of Epith-2 were phosphorylated. The endocytic retraction of Epith-2 was inhibited by herbimycin A (HA), a protein tyrosine kinase (PTK) inhibitor, and suramin, a growth factor receptor (GFR) inhibitor, suggesting the involvement of the GFR/PTK (GP) signaling pathway. These two GP inhibitors also inhibited PMC and SMC spreading to individual cells after ingression, but the dissociation of PMC and SMC from the epithelium was not inhibited. In suramin-treated embryos, dissociated mesenchyme cells migrated partially by retaining their epithelial morphology. In HA-treated embryos, no mesenchyme cells migrated. Thus, the EMT occurs in relation to internalization of Epith-2 from presumptive PMC and SMC.

Keywords: Epith-2, EMT, cell surface modification, protein tyrosine kinase, growth factor receptor, sea urchin

INTRODUCTION

The epithelial-to-mesenchymal transition (EMT) occurs in various processes found in metazoans, such as normal morphogenesis, the mesoderm formation in rabbit embryos (1), and neural crest cell formation in vertebrates [rev. Ref. (2)]. The EMT also constitutes the basic mechanism of metastasis (3, 4) and endocrine system formation, including the shedding of human fetal pancreatic insulin-producing cells from pancreatic islets (5) and luteinizing hormone-releasing hormone-immunoreactive neurons from the placodal epithelium (6).

In invertebrates, the EMT has been reported in relation to mesenchyme formation, particularly in sea urchin embryos in which the ingression of primary mesenchyme cells (PMC) occurs at the vegetal plate region of late blastulae (7–10). The EMT also produces secondary mesenchyme cells (SMC) at the tip of the archenteron in late gastrulae (8, 10, 11). The EMT is associated with an alteration of cell surface properties such as the retraction of epithelial cell surface-specific Epith-1 protein that is recognized by a monoclonal antibody (mAb), anti-Epith-1 mAb, in the sea urchin *Temnopleurus hardwicki* (10), and the acquisition of PMC surface-specific proteins such as the msp130 protein (12) in the sea urchin *Strongylocentrotus purpuratus* or the P4 protein that is recognized by anti-P4 mAb, in the sea urchin *Hemicentrotus pulcherrimus* (13–15). The EMT is also associated with losing integrin alphaSU2 and an affinity to laminin in the sea urchin *Lytechinus variegatus* (16). Similarly in vertebrate embryos, the EMT occurs by losing epithelial cell marker molecules such as E-cadherin, and the resultant mesenchyme cells acquire mesenchymal cell marker molecules such as vimentin, fibronectin, and type 1 collagen (17, 18).

In the sea urchin *L. variegatus*, β-catenin (19) and cadherin [LvG-cadherin; (20)] are expressed as a complex of these two proteins on the lateral surface of embryonic epithelial cells, particularly near adherence junctions that are dissolved during the early moments of PMC ingression in *L. pictus* (9). These proteins are lost by endocytosis, which results in the dissociation of PMC and SMC from neighboring epithelial cells (19, 20). Whether a similar mechanism is involved in losing cell surface Epith-1 in *T. hardwicki* has remained question (10). Our previous reports indicate that protein tyrosine kinase (PTK) is involved in PMC spreading after the ingression in *H. pulcherrimus* and *Clypeaster japonicus* (21, 22) as well as the retraction of Epith-1 and PMC spreading in *T. hardwicki* (23). PTK signaling pathways also regulate endocytosis (24); therefore, it has been predicted that the retraction of Epith-1 also occurs by endocytosis.

Thus, the present study aimed to elucidate the involvement of endocytosis in losing Epith-2, an epithelial cell surface-specific protein that is recognized by an anti-Epith-2 mAb and its sister mAb, anti-Epith-1 mAb (10), from the epithelial cell surface during PMC ingression. To this end, the experiments used PMCs purified from mesenchyme blastulae using an immunoaffinity column that fixed the magnet-tagged antibody (Ab) against anti-P4 mAb (13, 14), which is specific to PMCs. The potential involvement of PTK was examined using pharmaceutical inhibitors that included the closely related growth factor receptor (GFR) inhibitor. The previous analysis of the epitopic property of the anti-Epith-2 mAb proved that the mAb is an excellent tool to analyze the mechanism of cell surface modification and the function of Epith-2/Epith-1 protein as a cell adhesion molecule instead of the anti-Epith-1 mAb.

MATERIALS AND METHODS

Gametes from the sea urchin *H. pulcherrimus*, *T. hardwicki, S. intermedius, Mespilia globules, C. japonicus, L. pictus,* and *Pseudocentrotus depressus* were obtained by blastocoelic injection of 0.5 M KCl. The inseminated eggs were incubated in filtered sea water (FSW) on a gyratory shaker at 15°C for *H. pulcherrimus* and *S. intermedius*, 17°C for *L. pictus*, 18°C for *T. hardwicki* and *C. japonicus*, 19–25°C for *M. globules*, and 20°C for *P. depressus* until the stage described in the text. The majority of the present study was conducted using *H. pulcherrimus*. The *H. pulcherrimus* zygotes and embryos were collected at 20 min post fertilization (fertilized eggs), at 2 h post fertilization (2-hpf) (2-cells), at 2.5-hpf (4-cells), at 5-hpf (16-cells), at 8-hpf (morula), at 16-hpf (swimming blastula), at 19-hpf (mesenchyme blastula), at 23-hpf (1/2 gastrula, gastrulation half completed), at 25-hpf (late gastrula, gastrulation completed), at 29-hpf (prism), and at 40-hpf (pluteus stages). The *T. hardwicki* embryos were collected at 12-hpf (swimming blastula) and at 14-hpf (mesenchyme blastula).

IMMUNOBLOTTING

The *H. pulcherrimus* and *T. hardwicki* embryos reached the developmental stages described above, and they along with the *S. intermedius* mesenchyme blastulae, the *M. globules, C. japonicus*, and *L. pictus* swimming blastulae, and the *P. depressus* gastrulae were solubilized in lysis buffer (6 M urea, 1% Nonidet P-40, 10 mM Tris-HCl, pH 7.6) and were precipitated in 70% ethanol at −30°C overnight. The samples were lyophilized, dissolved in 2× sample buffer of sodium-dodecyl sulfate acrylamide gel electrophoresis (SDS-PAGE) with or without 2-mercaptoethanol at 500 μg/ml, separated on SDS-PAGE slab gels, and transferred to nitrocellulose filters (Schleicher Schuell, Dassel, Germany) at 400 mA at 4°C for 2 h as previously described (10). The protein-blotted nitrocellulose filters were blocked with 5% bovine serum albumin (BSA, Sigma Chemical Co. St. Louis, MO, USA) or 10% skim milk (Snow Brand Co. Sapporo, Japan) in TBST (25 mM Tris at pH 7.5, 7.5 mM NaCl, 0.025% Tween-20) for 1 h. The blots were probed with anti-Epith-1 mAb or anti-Epith-2 mAb [Ref. (10); diluted at 1:1000 for anti-Epith-1 mAb and 1:100 for anti-Epith-2 mAb in TBST] by incubating for 2 h at ambient temperature. The primary antibodies were detected with alkaline phosphatase-labeled sheep anti-mouse IgG antibodies (Promega, Madison, WI, USA) diluted at 1:7500 in TBST and were visualized with nitroblue tetrazolium/5-bromo-4-chloro-3-indolyl phosphate (Promega) according to the instructions by the manufacturer.

ISOELECTRIC POINTS AND MOLECULAR MASS IN DALTON SEPARATION (ISO-DALT 2D GEL)

The lyophilized swimming blastulae of *H. pulcherrimus* and *T. hardwicki* were dissolved in isoelectric focusing sample buffer [9 M urea, 4% Nonidet P-40, and 2% ampholytes (Sigma Chem. Co.); pH 4–7: pH 3.5–10 = 3:1 (25)] at 1 mg/ml. Undissolved debris in the sample was removed by centrifugation at 10,000 × *g* for 15 min. Fifteen microliters of supernatant was loaded onto each isoelectric focusing gel column [9 M urea, 3.15% acrylamide, 0.6% *N*-*N*′methylene bis acrylamide, 2.05% Nonidet P-40, 5% ampholytes (pH 4–7: pH 3.5–10 = 3:1), 0.038% ammonium peroxydisulfate, 0.063% *N*,*N*,*N*″,*N*″-tetramethylethylenediamine] overlayed with 5 μl of sample overlay solution [8 M urea, 2% ampholytes (pH 4–7: pH 3.5–10 = 3:1)], electrophoresed for 3 h at 400 V and then electrophoresed for 30 min at 500 V as for first dimensional gels. The column gels were equilibrated in an equilibration buffer (0.125 M Tris, 2% SDS, 10% glycerol, pH 6.8) for 30 min with constant agitation and were embedded in agarose gel (0.125 M Tris, 0.5% agarose, 0.1% SDS) on the top of the second dimensional slab gel. The second electrophoresis step was conducted at 25 mA, and the separated proteins were visualized by silver stain using a Silver Stain Plus kit (Bio-Rad, CA, USA). Aliquot gels were analyzed with immunoblotting as described above.

The pH gradient was examined using 5-mm long slices cut from a first dimensional column after initial isoelectric focusing. The ampholytes in the gel slices were eluted by immersing these slices in distilled water with agitation for 1 h. The pH of each eluted ampholyte was examined using a MP220 pH meter (Mettler Toledo International Inc., Tokyo) and the entire pH gradient was calculated in an 8-cm long column.

DETERGENT EXTRACTION OF EPITH-2

To examine whether the epitope of the anti-Epith-2 mAb is embedded in the plasma membrane similar to the epitope of anti-Epith-1 mAb (10), lyophilized *H. pulcherrimus* swimming blastulae were dissolved in a mixture of 0.1 M Tris, 1% Triton X-100, and 1% glycerol at 1 mg/ml as a detergent soluble fraction. The sample aliquots were dissolved in plain distilled water as a water-soluble fraction, both samples were centrifuged at 10,000 × *g* for 15 min and the supernatant was diluted in 2× SDS-PAGE sample buffer to separate on the slab gels as described above. The separated proteins were transferred to the nitrocellulose filters as described above and used for immunoblotting.

CONCANAVALIN A BINDING SITES

To detect α-D-mannosyl and α-D-glucosyl groups that are abundant in sea urchin embryos (26), concanavalin A (Con A; Sigma Chem. Co.) was applied to the lyophilized *H. pulcherrimus* swimming blastulae after separation on 10% SDS-PAGE slab gels. The gels were fixed overnight in a mixture of 25% isopropanol and 10% acetic acid and were washed 17 h with 0.1 M phosphate-buffered saline (PBS) by replacing several times with fresh PBS. The samples were incubated with 0.5 mg/ml Con A for 2 h, washed with PBS

for 17 h as described above and were incubated with 50 μg/ml horseradish peroxidase (Sigma Chem. Co.) in PBS for 2 h. The samples were further washed with 0.1 M PBS and were treated with 0.5 mg/ml 3,3′-diaminobenzidine (Sigma Chem. Co.) dissolved in PBS for color development and were finally treated with 6% hydrogen peroxide.

EPITH-2 ISOLATION FROM ISO-DALT 2D GELS

The location of the anti-Epith-2 mAb-immunopositive spot in the ISO-DALT 2D gel was estimated by immunoblotting. Using ISO-DALT 2D gel aliquots, the estimated anti-Epith-2 mAb-positive spot was cut using a razor blade and was placed in tubes installed in elusion tank of Centriluter (Amicon, Bevery, MA, USA) that was filled with SDS-PAGE tank buffer (25 mM Tris, 192 mM glycine, 0.1% SDS). Epith-2 was eluted from the gels at 4°C for 4 h at 200 V according to the manufacturer's instructions. The elution buffer was replaced with 0.1 M PBS, the samples were concentrated using Centricon YM-10 tubes (Amicon) and were subsequently mixed with an equal volume of 2× non-reducing sample buffer for analysis with SDS-PAGE.

DIGESTION OF EPITH-2 WITH TRYPSIN AND CHYMOTRYPSIN

The lyophilized *T. hardwicki* swimming blastulae were dissolved in trypsin digestion sample buffer (TdSB; 8 M urea, 50 mM Tris-HCl, 1 mM $CaCl_2$, pH 8.0) at 2 mg/ml (sample solution). Trypsin or chymotrypsin (Sigma Chem. Co.) was diluted in TdSB at 2 mg/ml (trypsin or chymotrypsin solution; TCS). TCS was mixed with the sample solution at 1:1, 1:2, 1:10, and 1:25, incubated for 2 h at 37°C, and then diluted 1:1 in 2× SDS-PAGE sample buffer for immunoblotting with anti-Epith-2 mAb as described above. The sample solution without the enzyme was used as a negative control and was incubated for the same period as the solution containing the enzyme.

IMMUNOHISTOCHEMISTRY

The eggs before and 20 min after insemination as well as the embryos at the appropriate developmental stages described in the text were fixed in 4% paraformaldehyde in FSW, dehydrated in ethanol, and embedded in Polywax. Six-micrometer thick sections were examined as described previously by Katow and Komazaki (27). Briefly, dewaxed Polywax sections were blocked with 5% BSA in 0.1 M PBS for 1 h, incubated with anti-Epith-2 mAb diluted 1:100 in PBS for 1 h, and washed with 0.1 M PBS three times (10 min each). These primary antibodies were visualized with goat tetramethylrhodamine-5-(and 6)-isothiocyanate (TRITC)-tagged anti-mouse IgG Ab (Promega; 1:300 diluted in 0.1 M PBS). The samples were embedded in glycerine, examined under an Optiphot fluorescence microscope (Nikon, Tokyo), and photographed with a CAMEDIA C-3030Z digital camera (Olympus Corporation, Tokyo).

For whole-mount immunohistochemistry, the fertilization envelopes of fertilized eggs and embryos before hatching were removed to allow antibody access as previously described (28). The eggs and embryos at the specific developmental stages were fixed in 4% paraformaldehyde, dehydrated in 70% ethanol, and stored at 4°C until use. Before primary Ab application, the stored embryos were hydrated in 0.1 M PBS with 1% Tween-20 (v/v) (PBST), blocked with 1% BSA in 0.1 M PBST for 1 h, and incubated with lyophilized mouse anti-Epith-2 mAb (1:10 in 0.1 M PBST) for 48 h at 4°C. Then, the samples were washed three times with 0.1 M PBST (10 min each). The primary Ab was visualized with Alexa Fluor 488-tagged rabbit anti-mouse IgG Ab (Invitrogen, 1:500 in 0.1 M PBST) for 2 h at ambient temperature. After washing three times with 0.1 M PBST (10 min each), the samples were examined under a Micro Radiance 2000 confocal laser scanning microscope (Bio-Rad, Hercules, CA, USA) with occasional optical sections at 2–4 μm, and the images were analyzed using an ImageJ 1.43u (NIH) and Photoshop CS5 Extended (Adobe Systems Inc., San Jose, CA, USA).

PMC ISOLATION

To examine whether cytoplasmic Epith-2 is modified from its state on the cell surface, PMCs in the blastocoel were isolated from *T. hardwicki* mesenchyme blastulae. Initially, PMCs were separated from the epithelial cells in calcium-magnesium-deprived artificial seawater (CMDASW; 463 mM NaCl, 11 mM KCl, 2.15 mM $NaHCO_3$, 25.5 mM Na_2SO_4). The embryos were incubated in CMDASW for 10 min to remove the hyaline layer, precipitated by centrifugation at 1000 rpm for 10 s, and the discarded supernatant was replaced with fresh CMDASW. The embryos were gently pipetted to dissociate to single cells that were fixed with 4% paraformaldehyde diluted in CMDASW for 1 h, washed with 0.1 M PBST three times (10 min each), and incubated with anti-P4 mAb diluted 1:100 in 0.1 M PBST for 20 min at 4°C. The primary Ab was washed as describe above and incubated with magnetic Microbead-tagged MACS goat anti-mouse IgG Ab (Miltenyi Biotec GmbH, Bergisch Gladbach, Germany) diluted to 1:5 in PBST for 30 min at ambient temperature for magnetic cell separation. To visually test PMC purity, TRITC-tagged goat anti-mouse IgG Ab (diluted 1:300 in 0.1 M PBST) was also applied simultaneously to the magnetic Microbead-tagged secondary Ab. After secondary Ab treatment, the labeled PMCs were diluted at 2×10^8 cells/ml and were applied to the magnetic cell separation column that was set in a MiniMACS cell separation apparatus (Miltenyi Biotec GmbH) according to the manufacturer's instructions. The column was washed once with 0.1 M PBST that contains 0.5% BSA and 2 mM EDTA, and the column was then dismantled to obtain purified PMCs. The purity of the PMCs was examined under an Optiphot fluorescence microscope (Nikon, Tokyo). The purified PMC aliquots were further dissolved in SDS-sample buffer under reducing conditions and were analyzed by immunoblotting as described above. The PMC separation was summarized in a flowchart as shown in **Figure 5F**.

HERBIMYCIN A TREATMENT

Early swimming blastulae were treated with 10 μg/ml herbimycin A (HA), a PTK inhibitor [Ref. (29–31): Wako Pure Chemical Co., Osaka, Japan], until the mesenchyme blastula stage, and then they were fixed and embedded in Polywax (32). The samples were sectioned, probed with anti-Epith-2 mAb, and examined by immunofluorescence microscopy as described above.

Aliquots of embryos were also used for immunoblotting after ISO-DALT 2D gel electrophoresis using anti-Epith-2 mAb, rabbit anti-phosphotyrosine (PT) Ab, rabbit anti-phosphoserine (PS)

Ab, and rabbit anti-phosphothreonine (PY) Ab (Promega) as described above.

SURAMIN TREATMENT

Suramin, a GFR inhibitor [(33–35): Calbiochem Merck KGaA, Darstadt, Germany], was diluted in FSW at 150 mM and was applied to swimming blastulae to the stage when control embryos reached the early gastrula stage. Next, the embryos were fixed in 4% paraformaldehyde for whole-mount immunohistochemistry with anti-Epith-2 mAb and were then examined as described above.

EMBRYONIC CELL REAGGREGATION ASSAY

To examine the potential involvement of Epith-2 in epithelial cell adhesion, anti-Epith-2 mAb IgG in conditioned medium was concentrated 30-fold using Centriprep 10 (Amicon), centrifuged for 10 min at 10,000 × *g* to remove precipitates, and IgG was purified using the HiTrap Protein G affinity column (Amersham Pharmacia Biotech, Buckinghamshire, UK). Thirty milliliters of conditioned medium produced 480 μg IgG.

The dissociated *H. pulcherrimus* swimming blastulae in CMDASW were washed once with fresh CMDASW and diluted at 1.6×10^6 cells/ml. The anti-Epith-2 mAb IgG was added to the cell suspension in 24-well plates at 10 or 50 μg/ml and was placed in an incubator at 15°C for 5 h. The cell suspensions were examined under a light field microscope and photographed. The major axis of randomly chosen 80 cell aggregates was measured manually using printouts of micrographs of each sample, and the statistical significance was examined between the averages of two subjects using the unpaired *t* test by an online GraphPad software, QuickCalcs[1] as shown in **Figures 7E,F**.

RESULTS

IMMUNOCROSSREACTIVITY OF ANTI-EPITH-1 AND -2 mAbs AMONG SEA URCHINS

Prior to onset of immunocrossreactivity assay of anti-Epith-1 mAb and -2 mAb in several species of the sea urchins as will be described below, immunochemical property of antigens of these mAbs was examined by ISO-DALT immunoblotting using *T. hardwicki*. The ISO-DALT immunoblotting showed both mAbs bound to a spot at 160 kDa and pH 4.98 region (**Figures 1A–C**), which is, regarding these two mAbs were raised as sister mAbs, predictable result.

Anti-Epith-1 and -2 mAbs were applied to *T. hardwicki* (**Figure 1B**, lanes 1, 8), *H. pulcherrimus* (**Figure 1B**, lanes 2, 9), *C. japonicus* (**Figure 1B**, lanes 3, 10), *M. globules* (**Figure 1B**, lanes 4, 11), and *L. pictus* swimming blastulae (**Figure 1**, lanes 5, 12), *P. depressus* gastrulae (**Figure 1**, lanes 6, 13), and *S. intermedius* mesenchyme blastulae (**Figure 1B**, lanes 7, 14). Anti-Epith-1 mAb bound only to *T. hardwicki* at the 160 kDa region, whereas anti-Epith-2 mAb bound to *T. hardwicki*, *H. pulcherrimus*, and *S. intermedius*, but not to the other four species examined in this study. The relative molecular mass (M_r) of the anti-Epith-2 mAb-binding band of *H. pulcherrimus* and *S. intermedius* were slightly smaller than in *T. hardwicki* at 143 and 137 kDa, respectively.

[1]http://www.graphpad.com/quickcalcs/ttest1.cfm

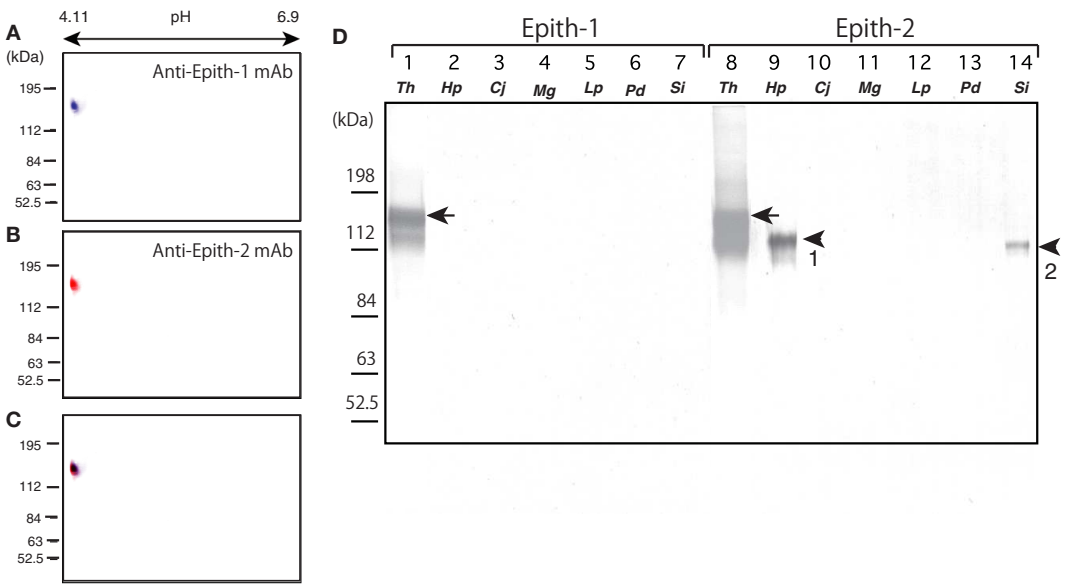

FIGURE 1 | Immunochemical property of antigen of anti-Epith-1 mAb and -2 mAb in *T. hardwicki* using isoelectric points and molecular mass in Daltons separation (ISO-DALT) 2D immunoblotting and immunocrossreactivity of these two mAbs among seven species of sea urchins. **(A)** ISO-DALT 2D immunoblotting with anti-Epith-1 mAb shows an immunopositive spot at 160 kDa region and pH 4.98 (blue). The spot was artificially colored. **(B)** ISO-DALT 2D immunoblotting with anti-Epith-2 mAb shows an immunopositive spot (red) at the same region as **(A)**. The spot was artificially colored. **(C)** Merged image between **(A,B)**. **(D)** Immunocrossreactivity of anti-Epith-1 mAb (lanes 1–7) and anti-Epith-2 mAb (lanes 8–14). Lanes 1, 8; *T. hardwicki* (*Th*) swimming blastulae, lanes 2, 9; *H. pulcherrimus* (*Hp*) swimming blastulae, lanes 3, 10; *C. japonicus* (*Cj*) swimming blastulae, lanes 4, 11; *M. globules* (*Mg*) swimming blastulae, lanes 5, 12; *L. pictus* (*Lp*) swimming blastulae, lanes 6, 13; *P. depressus* (*Pd*) gastrulae, lanes 7, 14; *S. intermedius* mesenchyme blastulae (*Si*). Arrows, 160 kDa region. Arrowhead-1, 143 kDa region. Arrowhead-2, 137 kDa region.

The relative intensity of the immunoreaction was also strongest in *T. hardwicki*, moderate in *H. pulcherrimus*, and weak in *S. intermedius*. This finding showed that the epitopic structures of the two mAbs were not identical but were similar to some extent among the sea urchins examined in the present study. Therefore, anti-Epith-1 mAb was highly specific to *T. hardwicki*, whereas anti-Epith-2 mAb crossreacted with a wider number of sea urchin species.

IMMUNOCHEMICAL PROPERTY OF EPITH-2

To examine the similarities between the epitopes of anti-Epith-2 mAb of *H. pulcherrimus* and *T. hardwicki*, further proteomic analysis was conducted using ISO-DALT 2D immunoblotting using swimming blastulae. The immunoblotting localized an anti-Epith-2 mAb-binding spot at the acidic region [isoelectric point (pI) = 4.7; **Figure 2A**], which is similar to the previous report regarding *T. hardwicki* [pI = 4.98, Ref. (10)]. However, according to silver-stained ISO-DALT separation gel analysis, no positive spot was observed at the equivalent spot to the anti-Epith-2 mAb-binding spot region (**Figure 2B**, arrow), which was confirmed by a merged image (**Figure 2C**). In *T. hardwicki*, however, the 160 kDa region was weakly silver-stained using ISO-DALT 2D gel analysis (10). This weak stain may not be due to the small proportion of peptide but may be due to the highly acid property of Epith-2 (36).

The immunoblotting results using samples that were digested with trypsin and chymotrypsin indicated a decreased immunoreaction intensity according to the increasing concentration of both proteinases, which suggests that the anti-Epith-2 mAb epitope is located near the targets of these proteinases (**Figure 2D**). The sensitivity of the anti-Epith-2 mAb epitope to trypsin was apparently greater than the sensitivity to chymotrypsin, suggesting that the epitope is rich in lysine and/or arginine (targets of trypsin) compared to aromatic residues [target of chymotrypsin; Ref. (37)].

The subcellular localization of Epith-2 was examined using lyophilized swimming blastulae of *H. pulcherrimus*. According to the immunoblotting, Epith-2 was not detected in the water-soluble fraction (**Figure 3A**, lane 1) but was detected in the non-ionic detergent-extract fraction at the 143 kDa region (**Figure 3A**, lane 2), which was consistent with previous Epith-1 analysis in *T. hardwicki* (10). The result suggested that Epith-2 is embedded in the plasma membrane or has a transmembrane domain (38). The Con-A staining of separated gels did not detect a 143 kDa band region (**Figure 3A**, lane 3), suggesting that unlike in the blastocoelar extracellular matrix in sea urchin embryos (26), Epith-2 has few or lacks mannose moieties.

To examine the potential presence of disulfide bonds in the *T. hardwicki* Epith-2 peptide, immunoblotting was conducted under reducing and non-reducing conditions. In non-reducing conditions, the anti-Epith-2 mAb strongly bound to a band at the 160 kDa region (**Figure 3B**, lane 1, arrow) but bound weakly to a band at the 174 kDa region under reducing conditions (**Figure 3B**, lane 2, arrowhead). Thus, Epith-2 was not found to have a subunit structure but was shown to have intra-peptide disulfide bonds that increased the M_r due to stretching of peptide chain under reducing conditions, which resulted in the spatial expansion of the peptide. The weakened immunoreactivity under reducing conditions suggests that the anti-Epith-2 mAb epitope located near the intra-peptide disulfide bonds region or to the region where the epitopic molecular configuration was easily affected by the loss of disulfide bonds.

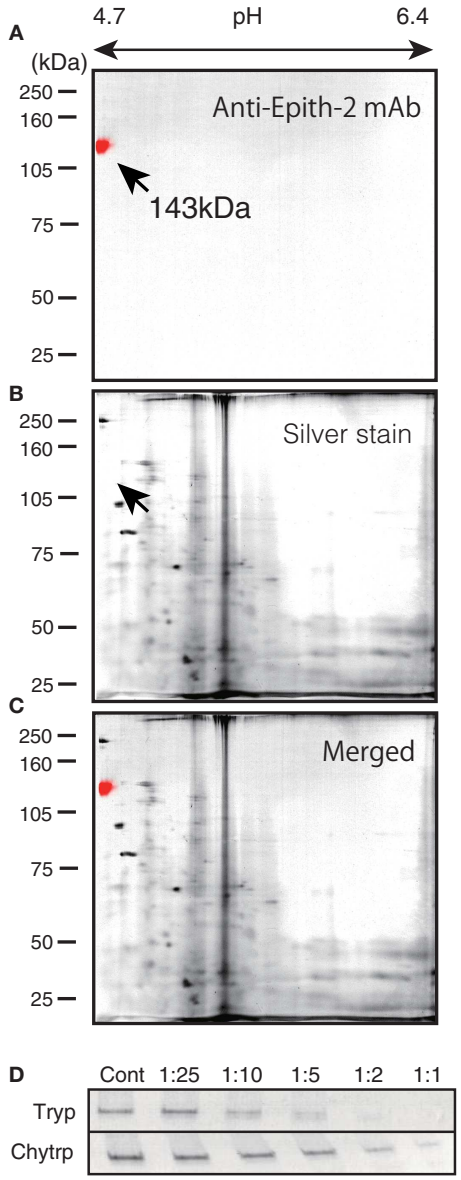

FIGURE 2 | Isoelectric points and molecular mass in Daltons separation (ISO-DALT) analysis of Epith-2 of *H. pulcherrimus* (A–C) and proteinase sensitivity of Epith-2 *T. hardwicki* (D). **(A)** ISO-DALT 2D immunoblotting shows an immunopositive spot at the 143 kDa and pH 4.7 (red) region. The spot is artificially colored. **(B)** ISO-DALT 2D pattern stained with silver. **(C)** Merged image between **(A,B)**. **(D)** Protease digestion of Epith-2 of swimming blastulae. Cont, control; the numbers, dilution ratios of protease, Tryp, trypsin digested. Chytrp, chymotrypsin digested.

THE EPITH-2 EXPRESSION PATTERN DURING EARLY EMBRYOGENESIS IN *H. PULCHERRIMUS*

Based on the immunoblotting using the anti-Epith-2 mAb that was conducted with unfertilized eggs and embryos ranging to the 29-hpf prism stage, the protein was detected consistently at the

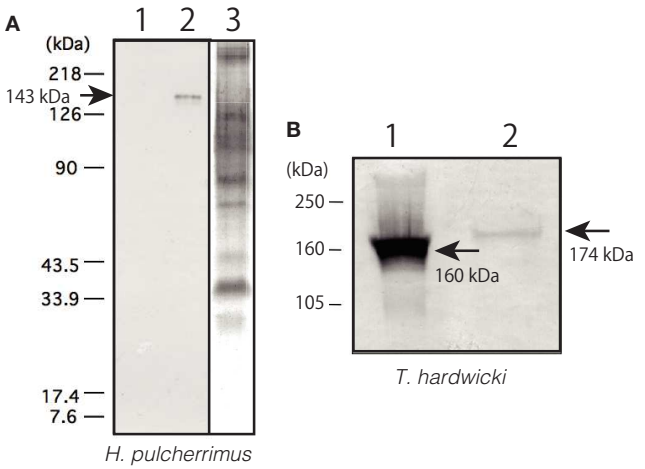

FIGURE 3 | Immunochemical property of Epith-2 of *H. pulcherrimus* (A) and *T. hardwicki* (B) analyzed by immunoblotting. (A) Immunoblotting of Epith-2 extracted in water (lane 1) and in non-ionic detergent 1% Triton X-100 (lane 2) of swimming blastulae. Whole embryo lysate stained with concanavalin A (lane 3). **(B)** M_r of Epith-2 glycoprotein under non-reducing conditions (lane 1; 160 kDa region) and reducing conditions (lane 2; 174 kDa region).

143 kDa region (**Figure 4A**, lanes 1–11). However, at the 40-hpf pluteus stage, the immunoreaction of the 143 kDa band weakened considerably. Instead, a smaller but distinctive new band appeared at the 126 kDa region (**Figure 4A**, lane 12), which is similar to our previous observations in *T. hardwicki* in which the major 160 kDa band shift to a smaller 142 kDa at this stage (10). This finding also suggests that the post-maternal message of the Epith-2 protein was switched on during the period between the 29- and 40-hpf larva stages as was previously reported regarding the Hp-Unc-5 expression pattern in *H. pulcherrimus* (39). However, further elucidative studies ought to be done.

Whole-mount immunohistochemistry faintly detected an anti-Epith-2 mAb-positive area near the egg surface in unfertilized eggs, which was not associated with any particular feature (**Figures 4Ba,a'**, arrow). In the eggs 20 min post fertilization, the mAb detected a thin but distinctively strong positive area near the egg surface (**Figures 4Bb,b'**). At the 2-hpf two-cell stage, the entire surface of the blastomeres was positive to the mAb that included the furrow region (**Figures 4Bc,c'**, arrow). At the 2.5-hpf 4-cell stage, the entire surface of all the blastomeres remained positive to the mAb, including the region that faces the newly formed blastocoel (**Figures 4Bd,d'**, arrow). After following two more cleavages at the 5.5-hpf 16-cell stage, while the entire apical surface of the blastomeres remained positive to anti-Epith-2 mAb (**Figure 4Be**), the basal surface around the vegetal pole area (**Figure 4Be'**, arrow) and the animal hemisphere (**Figure 4Be"**, arrow) lost Epith-2, which was the first sign of the apico-lateral distribution of Epith-2 in the embryogenesis. The apico-lateral distribution remained in the next 6.5-hpf 32-cell stage (**Figures 4Bf,f'**, arrow); however, at the 16-hpf swimming blastula stage, Epith-2 was lost from the apical surface of the epithelial cells (**Figures 4Bg,g'**). Epith-2 remained only on the lateral surface where the protein completely encircled the epithelial cells (**Figure 4Bg"**). At the 19-hpf mesenchyme blastula stage, Epith-2 was not detected on the entire surface of PMCs spread into the blastocoel (arrows in **Figures 4Bh,h'**) and in cellular aggregates at two sessile sites near the blastopore at the 22-hpf early gastrula stage (**Figures 4Bi,i'**). SMC that ingressed around the tip region of the archenteron also lost Epith-2 from their surface at the 25-hpf late gastrula stage (**Figures 4Bj,j'**, arrows). Thus, all the mesenchyme cells lost Epith-2 from their surface after ingression.

THE MECHANISM OF CELL SURFACE EPITH-2 RETRACTION DURING MESENCHYME INGRESSION

According to the immunohistochemistry performed using Polywax sections, PMCs lost Epith-2 from their surface at large while they are still in the vegetal ectoderm (**Figures 5A,A'**), and instead, several anti-Epith-2 mAb-positive dots were detected in the cytoplasm at the 19-hpf early mesenchyme blastula stage (**Figure 5B**, arrows), suggesting the occurrence of Epith-2 internalization. However, cytoplasmic immunoreaction in the PMCs was not detected by the 22-hpf early gastrula stage (**Figures 5C,C'**, arrow). In 25-hpf late gastrulae, ingression of the SMC also initiated at the tip of the archenteron. As in the PMCs, Epith-2 was not detected on the large surface area of the SMC (**Figures 5C,C'**); however, it was present in the cytoplasm and was associated with cytoplasmic dots (**Figure 5D**, arrows), suggesting the occurrence of Epith-2 internalization in SMC ingression.

To examine whether the internalization of the plasma membrane-bound Epith-2 occurs in association with any proteolysis, as has been previously reported regarding LvG-cadherin/β-catenin complex internalization in micromeres in the sea urchin (40), the potential decrease in the M_r of Epith-2 was analyzed by immunoblotting using PMCs isolated from *T. hardwicki* mesenchyme blastulae immediately after ingression. According to immunocytochemistry using anti-P4 mAb, the proportion of PMCs isolated using magnetic cell sorting system was greater than 90% (**Figures 5E,E'**). The sample preparation for the analysis of cytoplasmic Epith-2 in PMCs using immunoblotting is summarized in **Figure 5F**. The immunoblotting showed three anti-Epith-2 mAb-positive major bands at approximately 250, 175, and 160 kDa regions in purified PMCs that were pre-incubated with anti-P4 mAb and magnetic Microbead-tagged MACS goat anti-mouse IgG Ab (**Figure 5G**, lane 1). After separation of the PMCs, the mesenchyme blastulae without PMCs showed two major bands at approximately 250 and 160 kDa regions. A band at the 175 kDa region was significantly weaker compared to the band observed in the PMCs (**Figure 5G**, lane 2). Swimming blastulae that were pre-incubated with anti-Epith-2 mAb showed two bands at approximately 250 and 160 kDa regions (**Figure 5G**, lane 3); however, before combining the two antibodies, the mesenchyme blastulae demonstrated only one band at 160 kDa region (**Figure 5F**, lane 4), as was previously shown (**Figure 1**, lane 8). This finding suggests that the 250 kDa band and, possibly, the 175 kDa band are derived from the anti-P4 mAb IgG, which has been confirmed by a following study of immunoblotting using the anti-P4 mAb alone, which showed a major band at 250 kDa region, a minor band at 175 kDa region and additional smaller minor bands but not at 160 kDa region (**Figure 5G**, lane 5). Because Microbead-tagged anti-mouse

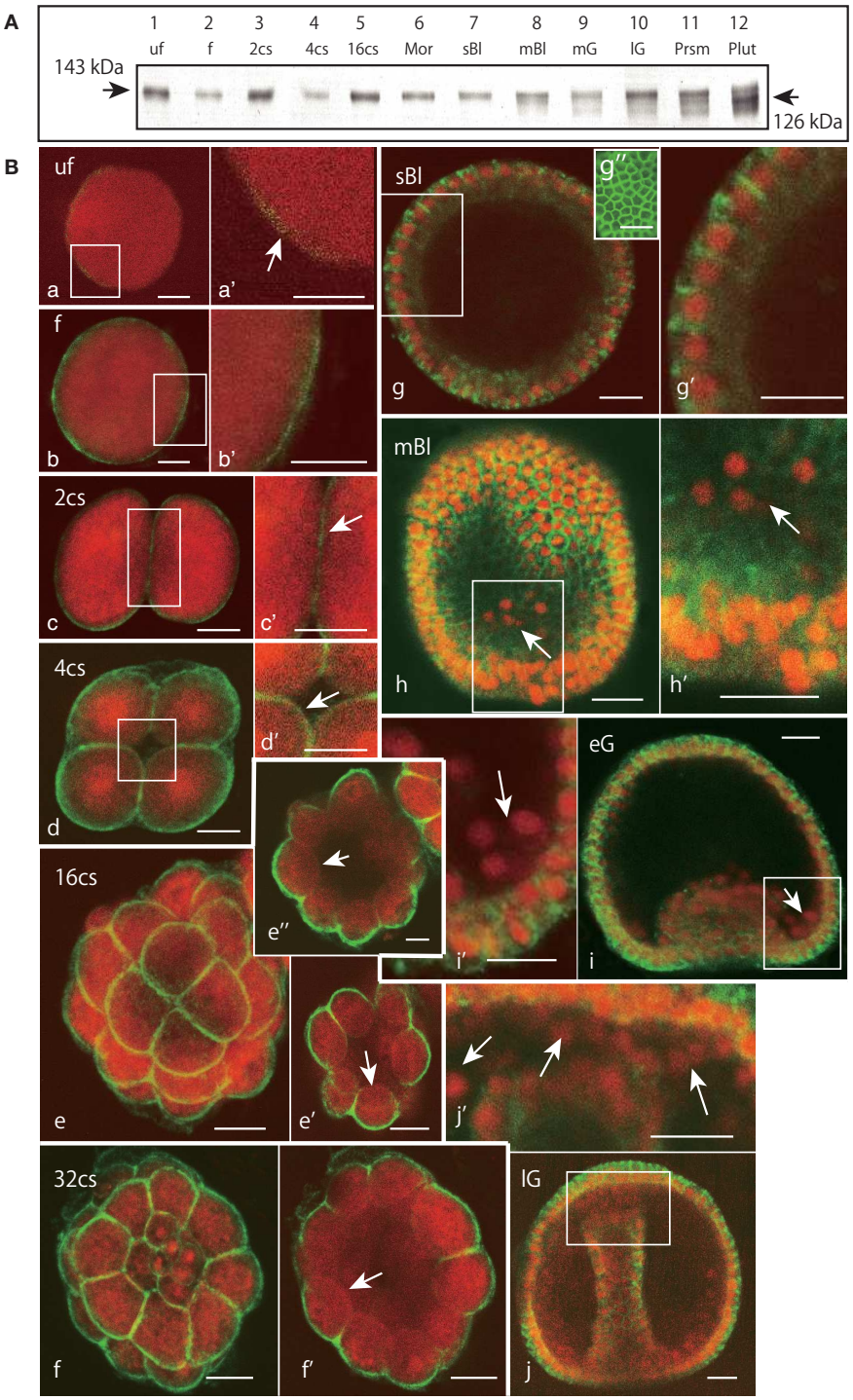

FIGURE 4 | Immunochemical expression pattern of Epith-2 during early development of *H. pulcherrimus*. **(A)** Immunoblotting pattern. Lane 1; unfertilized eggs (uf), lane 2; fertilized eggs (f), lane 3; the 2-cell stage embryos (2cs), lane 4; the 4-cell stage embryos (4cs), lane 5; the 16-cell stage embryos (16cs), lane 6; morulae (Mor), lane 7; swimming blastulae (sBl), lane 8; mesenchyme blastulae (mBl), lane 9; mid-gastrulae (mG), lane 10; late gastrulae (lG), lane 11; prism larvae (Prsm), lane 12; pluteus larvae (Plut). Epith-2 is detected consistently at the 143 kDa region from unfertilized eggs to prism larvae, but a new band is detected at the 126 kDa region at the pluteus stage, which replaced the larger band of relative molecular mass. **(B)** Whole-mount double-stained immunohistochemical expression pattern of Epith-2 (green) and DNA with propidium iodide (red) **(a–j')** and Polywax sagittal 6-μm thick sections **(g")**. **(a)** A 4-μm thick optical section of an unfertilized egg (uf). **(a')** Higher magnification image of the box in **(a)**. Arrow, anti-Epith-2 mAb-positive egg surface. **(b)** A 4-μm thick optical section of a fertilized egg (f). **(b')** Higher magnification image of the box in **(b)**. **(c)** A 4-μm thick optical section of a two-cell embryo (2cs). **(c')** Higher magnification image of the box in **(c)**. **(d)** A 4-μm thick optical section of a 4-cell embryo (4cs). **(d')** Higher magnification image of the box in **(d)**. Arrow, the basal surface of a

(Continued)

FIGURE 4 | Continued
blastomere. **(e)** Stacked image of a whole 16-cell stage embryo (16cs). **(e')** A 3-μm thick optical section at the vegetal hemisphere. Arrow, the basal surface of a blastomere at the vegetal hemisphere. **(e")** A 3-μm thick optical section at the animal hemisphere. Arrow, the basal surface of a blastomere. **(f)** Stacked image of a whole 32-cell embryos (32cs). **(f')** A 3-μm thick optical section at the equator region. Arrow, the blastomere basal surface. **(g)** A 2-μm optical section of swimming blastula (sBl). **(g')** Higher magnification image of the box in **(g)**. **(g")** A 6-μm thick sagittal Polywax section. **(h)** A 2-μm thick optical section of a mesenchyme blastula (mBl). **(h')** Higher magnification image of the box in **(h)**. Arrow, primary mesenchyme cells. **(i)** A 3-μm thick optical section of early mesenchyme blastula (eG). **(i')** Higher magnification image of the box in **(i)**. Arrow, primary mesenchyme cells. **(j)** A 3-μm thick optical section of late gastrula (lG). **(j')** Higher magnification image of the box in **(j)**. Arrows, secondary mesenchyme cells. Scale bars, 20 μm **(a–j')**, 50 μm **(g")**.

IgG Ab does not have anti-mouse IgG Ab or anti-goat IgG Ab epitopes, no immunoreaction was observed (**Figure 5G**, lane 6). Thus, any minor bands detected in the sample that was mixed with Microbead-tagged anti-mouse IgG Ab (**Figure 5G**, lanes 1–3) were not derived from the Ab. The immunoblotting procedure that applied secondary Ab alone to the anti-P4 mAb showed a major band at larger than 250 kDa region and weak smaller extra bands, indicating these bands were of degraded fragments of IgG (**Figure 5G**, lane 7). Again, Microbead-tagged anti-mouse IgG Ab did not show an immunoreaction (**Figure 5G**, lane 8).

Thus, an anti-Epith-2 mAb-positive band at 160 kDa region in the PMCs (**Figure 5G**, lane 1) is Epith-2, which suggests that because the cell surface Epith-2 M_r was retained in the cytoplasm, the protein was not cleaved appreciably during internalization and retained its molecular integrity after internalization.

INHIBITION OF EPITH-2 INTERNALIZATION BY HA AND SURAMIN

The immunohistochemistry experiments conducted in this study suggest that the loss of Epith-2 from the PMC surface may be involved in PMC ingression and/or spreading.

The phosphorylation of tyrosine residues of SUp62, a cytoplasmic homo-dimeric 62 kDa protein, in PMCs that spread after ingression to the blastocoel occur in response to the contact of PMCs with pamlin, a blastocoelar PMC adhesion protein in the basal lamina (32, 41). HA inhibited PMC spreading in mesenchyme blastulae associated with hyperphosphorylation of tyrosine residues of SUp62 in *H. pulcherrimus* (32). In *T. hardwicki*, HA inhibited Epith-1 internalization along with P4 transportation to the cell surface of PMCs (23).

To examine whether the internalization of cell surface Epith-2 is also affected by HA in *H. pulcherrimus*, mesenchyme blastulae were treated with HA, and the Epith-2 expression pattern was analyzed. Consistent with mesenchyme blastulae of *T. hardwicki*, PMC dissociation from the vegetal epithelium of *H. pulcherrimus* was not inhibited by HA, but their spreading was inhibited (**Figure 6A**). However, the dissociated PMCs remained aggregated on the vegetal plate, and substantial PMCs retained cell surface Epith-2, particularly between neighboring PMCs (**Figure 6B**, arrowheads), while interestingly, peripheral complementary faces of PMCs that faced to epithelial cells (PE-border) lost their cell surface Epith-2 (**Figures 6A,B**, red arrowheads). In other than the PE-border region of the epithelium, cell surface Epith-2 remained expressed (**Figure 6A**). This finding suggests the occurrence of a centro-peripheral polarity of Epith-2 internalization in a group of PMCs, as well as the PE-border-restricted Epith-2 internalization in epithelium. In control blastulae, PMCs lost Epith-2 from their entire surface (**Figures 4Bh–i**, **5B**, and **6C**); however, a small number of PMCs retained cytoplasmic Epith-2 after spreading (**Figure 6D**). Thus, Epith-2 internalization appears to be involved in PMC dissociation from the epithelium and the spreading to single cells after ingression.

Primary mesenchyme cells spreading is also perturbed by suramin, which inhibits migration via the mitogen-activated protein kinase (MAPK) pathway (21). To examine whether PMC spreading occurs in relation to Epith-2 internalization, suramin was applied to swimming blastulae for 10 h until the early gastrula stage. In early gastrulae, consistent with our previous report (21), a characteristic aggregate of PMCs was observed on the archenteron tip during the early stage of invagination (**Figure 6E**). The aggregated PMCs retained Epith-2 on their cell surfaces (**Figure 6F**, arrow), indicating that Epith-2 internalization of these PMCs was inhibited by the GFR inhibitor. Other PMC aggregates near the archenteron in the blastocoel were also observed, and Epith-2 was also detected in these PMCs (**Figure 6E'**, arrow), which suggests the occurrence of migration associated with epithelial morphology after dissociation. Furthermore, spread cells were also observed in the blastocoel, but these cells did not display Epith-2 on their cell surface or in the cytoplasm (**Figure 6E**). Our previous report that these spread cells do not form spicules (21) suggests that they may not be PMCs. The suramin-treated embryos failed to complete gastrulation, and pigment cells were not formed (21). Thus, SMC ingression was not confirmed in this study.

Despite highly similar behavior between Epith-1 and Epith-2, whether the perturbation of internalization caused by the PTK inhibitor occurs in relation to phosphorylation of tyrosine, serine, and threonine residues of Epith-1 and Epith-2 has remained unanswered. In this study, an initial examination using immunoblotting detected no apparent anti-Epith-2 mAb-positive band at 143 kDa region (**Figure 6G**, lane 1). Furthermore, Abs against phosphotyrosine (**Figure 6G**, lane 2), phosphoserine (**Figure 6G**, lane 3), and phosphothreonine (**Figure 6G**, lane 4) also did not detect an anti-Epith-2 mAb-positive band at 143 kDa region. However, closer examination with an anti-phosphotyrosine Ab alone detected a positive band at the region quite similar to the anti-Epith-2 mAb-positive region (**Figure 6G** inset, lane PS).

To identify the molecules that bound to anti-phosphotyrosine Ab- and anti-Epith-2 mAb, ISO-DALT 2D immunoblotting analysis was conducted. Consistent with the above immunoblotting results obtained using slab gels, Epith-2 was localized at a region with *p*I and M_r that were 4.7 and 143 kDa, respectively (**Figure 6Ha**). Phosphotyrosine also localized at 143 kDa and the near pH 4.7 region, but it had a stretched tail toward the basic region near pH 5.2 (**Figure 6Hb**, arrows). The tail comprised of a line of dots with the strongest immunoreaction at pH 4.7 region (**Figure 6Hb**, inset, arrows). Merged images localized the region that was positive to both anti-Epith-2 mAb and

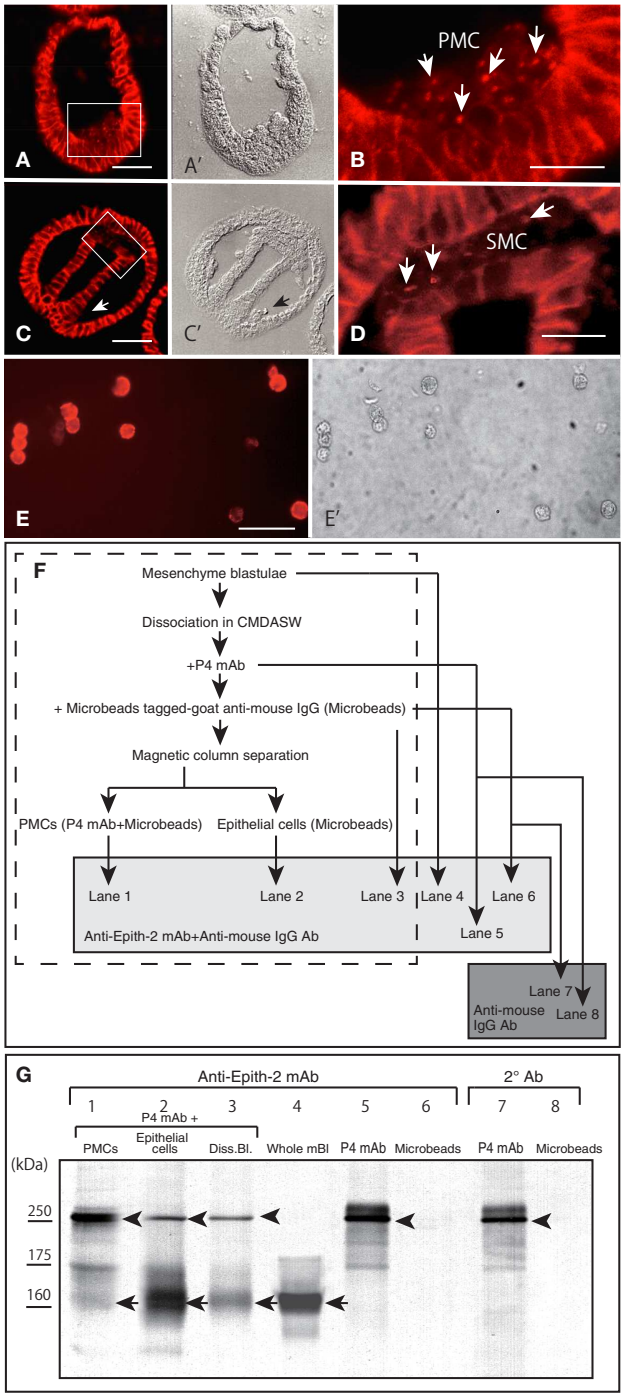

FIGURE 5 | Immunohistochemistry of Epith-2 internalization during mesenchyme ingression in *H. pulcherrimus* [(A–D); 6-μm thick Polywax sections], purified primary mesenchyme cells [PMC; (E,E′)] and the fate of Epith-2 in ingressed PMCs by immunoblotting in *T. hardwicki* (F,G). **(A)** An early mesenchyme blastula. Scale bar, 40 μm. **(A′)** Phase-contrast micrograph of the same section as **(A)**. **(B)** Higher magnification image of the box in **(A)**. Arrows, cytoplasmic anti-Epith-2 mAb-positive dots in primary mesenchyme cells (PMC). Scale bar, 10 μm. **(C)** Late gastrula. Scale bar, 40 μm. **(C′)** Phase-contrast micrograph of the same section as **(C)**. Arrow, PMC aggregate near the blastopore. **(D)** Higher magnification

(Continued)

FIGURE 5 | Continued
image of the box in **(C)**. Arrows, anti-Epith-2 mAb-positive dots in secondary mesenchyme cells (SMC). Scale bar, 10 μm. **(E)** Isolated PMCs stained with anti-P4 mAb. Scale bar, 30 μm. **(E′)** Phase-contrast micrograph of the same cells as **(E)**. **(F)** A chart showing the sample preparation of the immunoblotting shown in **(G)**. Samples in the broken-line box contain anti-P4 mAb and anti-mouse IgG Ab-tagged-magnetized Microbeads. Samples in the shaded box were examined with anti-Epith-2 mAb and anti-mouse IgG Ab. Samples in dark box were examined only with anti-mouse IgG Ab. **(G)** Epith-2 in the cytoplasm of PMCs analyzed with anti-Epith-2 mAb (lanes 1–6) and secondary antibody (Ab) alone (lanes 7, 8). Lane 1; anti-P4 mAb and anti-mouse IgG Ab-tagged-magnetized Microbeads-treated PMC fraction (PMCs), lane 2; anti-P4 mAb-treated epithelial cell fraction (Epithelial cells), lane 3; anti-P4 mAb-treated dissociated mesenchyme blastulae (Diss. Bl.), lane 4; whole mesenchyme blastulae (Whole mBl), lanes 5, 7; anti-P4 mAb alone (P4 mAb), lanes 6, 8; anti-mouse IgG Ab-tagged magnetic Microbeads alone (Microbeads). Arrows, Epith-2 at 160 kDa region. Arrowheads, IgG of primary Ab.

anti-phosphotyrosine Ab at approximately 143 kDa and $pI = 4.7$ region (**Figure 6Hc**, arrow). This finding suggests the occurrence of tyrosine phosphorylation in Epith-2.

THE POTENTIAL ROLE OF EPITH-2 IN CELL ADHESION

The close association of Epith-2 internalization with mesenchyme cell ingression suggests that Epith-2 may be involved in cell–cell adhesion. Although Epith-1 association with cell-cell adhesion using anti-Epith-1 mAb in *T. hardwicki* was shown to be negative (10), based on the present result suggesting that the epitopic structure of anti-Epith-1 mAb and anti-Epith-2 mAb was different (**Figure 1**), the apparently close relationship between Epith-2 behavior with mesenchyme cell ingression suggested the potential involvement of the anti-Epith-2 mAb epitope in cell-cell adhesion.

To examine this possibility, the anti-Epith-2 mAb IgG was purified and applied to the dissociated embryonic cells *in vitro* to examine whether the epitope of the mAb interferes with the reaggregation of these cells. Dissociated embryonic cells (**Figure 7A**) reaggregated in 5 h and formed large aggregates with various smaller sizes in ASW without IgG of anti-Epith-2 mAb (**Figure 7B**). The presence of 10 μg/ml of IgG did not visibly affect the size of the cell aggregates (**Figure 7C**). However, an apparent decrease in the size of the cell aggregates was observed in cells treated with 50 μg/ml of IgG (**Figure 7D**). To examine this morphological observation further, the major diameter of 80 cell aggregates chosen at random was measured in each experimental cell culture group. The average size of the cell aggregates decreased based on IgG treatment in a dose-dependent manner (10–50 μg/ml), which was found to be statistically significant between the control ASW groups (no IgG included) and the 10 μg/ml IgG-treated group ($P = 0.0344$) and between the 10 μg/ml IgG-treated and 50 μg/ml IgG-treated groups ($P = 0.0001$) (**Figure 7E**). According to the analysis of the proportion of the cell aggregates that were artificially sorted into three groups based on the size of the major axis of the aggregate, the group with the smallest aggregate size (10–40 μm) increased in size based on IgG treatment in a dose-dependent manner. However, the group with the largest size (71–140 μm) decreased based on IgG treatment in a dose-dependent manner; $P = 0.0055$ in 10 μg/ml IgG and $P = 0.0231$ in 50 μg/ml IgG (**Figure 7F**). In 50 μg/ml IgG-treated cell suspensions, the proportion of the medium-sized

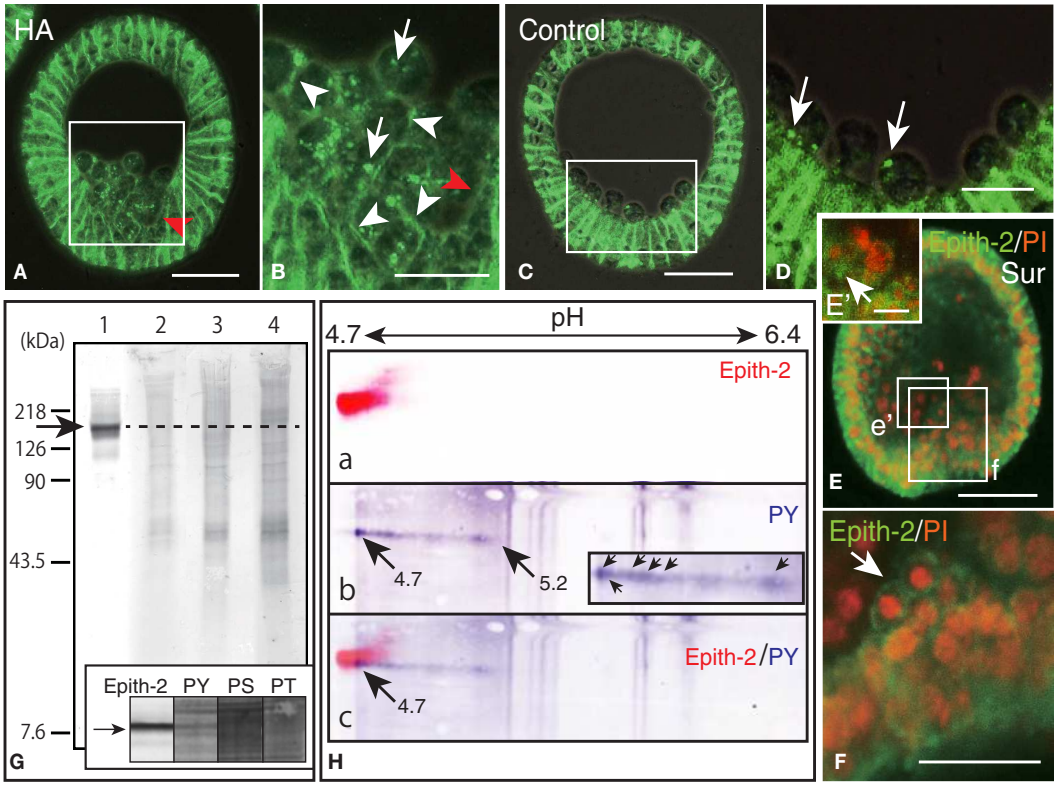

FIGURE 6 | Inhibition of Epith-2 endocytosis and PMC spreading by herbimycin A (HA) and suramin and the analysis of phosphorylation site of Epith-2 of *H. pulcherrimus*. **(A)** Immunohistochemistry of HA-treated mesenchyme blastula using 6-μm thick Polywax section. Red arrow, lack of Epith-2 on the cell surfaces of PMCs and neighboring epithelial cells. Scale bar, 40 μm. **(B)** Higher magnification of box in **(A)**. Arrowheads, cell-surface-associated Epith-2. Arrows, dots of cytoplasmic Epith-2. Red arrow, lack of Epith-2 on the cell surface of PMC and neighboring epithelial cell. Scale bar, 20 μm. **(C)** Immunohistochemistry of control mesenchyme blastula using 6-μm thick Polywax section. Scale bar, 40 μm. **(D)** Higher magnification of the box in **(C)**. Arrows, cytoplasmic Epith-2. Scale bar, 20 μm. (**E**) A 2-μm thick optical section of a confocal laser scanning micrograph of a suramin-treated early gastrula. Epith-2 expressed in an aggregate of PMCs near the archenteron [box **(e')**]. Epith-2 (green) expressed in aggregated-PMCs on top of the archenteron [box **(f)**]. Scale bar, 40 μm. **(E')** Higher magnification of the box **(e')** in **(E)**. Arrow, Epith-2 cell. Scale bar, 5 μm **(F)** Higher magnification image of the box **(f)** in **(E)**. Arrow, aggregated PMCs. Scale bar, 20 μm. (**G**) Epith-2 phosphorylation in swimming blastulae by immunoblotting. Lane 1; anti-Epith-2 mAb, lane 2; anti-phosphotyrosine (PY) antibody (Ab), lane 3; anti-phosphoserine (PS) Ab, and lane 4; anti-phosphothreonine (PT) Ab. Arrow and dotted line denote the 143 kDa region. Inset; immunoblotting with antibodies against Epith-2, phosphotyrosine (PY), phosphoserine (PS), and phosphothreonine (PT) using single-lane SDS-PAGE gel. Arrow, 143 kDa region. **(H)** Phosphotyrosine detection by immunoblotting in Epith-2 of swimming blastulae by isoelectric points and molecular mass in Daltons. **(a)** Anti-Epith-2 mAb. Artificially colored with red. **(b)** Anti-PY Ab. Artificially colored with blue. Inset, higher magnification of tail region. Arrows, anti-PY Ab-positive dots. **(c)** Merged image between **(a,b)**. Numbers on the top show the pH gradient from the left (4.7) to right (6.4).

group (41–70 μm) was significantly smaller than that of the group with the smallest size ($P = 0.0588$). Thus, unlike the anti-Epith-1 mAb epitope, anti-Epith-2 mAb epitope was involved in cell–cell adhesion.

DISCUSSION

ANTI-EPITH-1 mAb AND ANTI-EPITH-2 mAb EPITOPES

The anti-Epith-2 mAb was first generated in *T. hardwicki* as a sister mAb of anti-Epith-1 mAb. The mAb recognizes an Epith-1glycoprotein that contains *N*-glycosylated oligosaccharide, and the glycoprotein is present specifically in epithelial cells (10). Thus, the overall properties of the anti-Epith-2 mAb were similar to that of the anti-Epith-1 mAb as described in this study. However, the present study revealed a significantly different epitopic property of anti-Epith-2 mAb as well. The anti-Epith-2 mAb cross-reacts with two other sea urchin species, *H. pulcherrimus* and *S. intermedius*, in addition to *T. hardwicki*. Thus, although the evolutionary concept of Epith-2 is not the subject of the present study, the anti-Epith-2 mAb-binding epitope of these sea urchins that belong to Echinoidea and Temnopleuroida of Echinoidea (42) is similar, which may shed new insights into the evolutional significance of cell surface properties in future studies.

Although relevance of using intact divalent Abs against cell surface proteins in attempt to inhibit cell–cell adhesion is not generalized (43), consistent with previous reports (44–46), the present mAb utilization apparently worked. Thus, regardless whether the Ab is applied as an intact divalent form or a monovalent form, the validity would be dependent on their molecular property in antigen/Ab interaction.

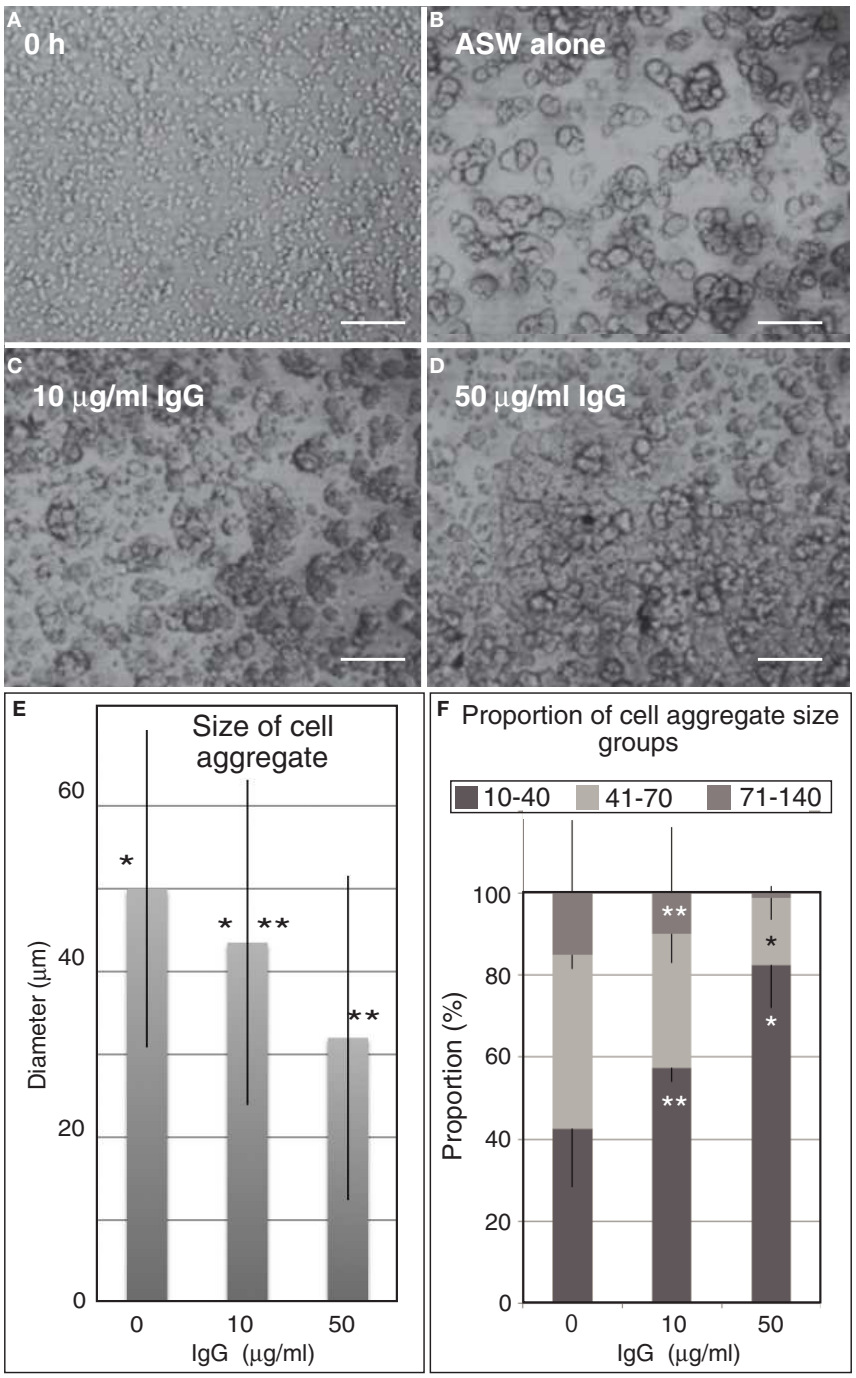

FIGURE 7 | Embryonic cell reaggregation assay in the presence of IgG of anti-Epith-2 monoclonal antibody in *H. pulcherrimus*. **(A)** Whole embryonic cells of swimming blastulae immediately after dissociation (0 h). **(B–D)** Re-aggregated embryonic cells at 5 h after dissociation. **(B)** In plain artificial seawater (ASW alone). **(C)** With 10 μg/ml IgG (10 μg/ml IgG). **(D)** With 50 μg/ml IgG (50 μg/ml IgG). Scale bars, 100 μm. **(E)** Average size of cell aggregates with no IgG (0), 10 μg/ml (10) and 50 μg/ml (50) IgG. Bars, SD ($n = 80$). $^{*}P = 0.0344$, $^{**}P = 0.0001$. Unpaired t test. **(F)** Proportion of three cell aggregate sizes in 0 μg/ml (0), 10 μg/ml (10), and 50 μg/ml (50) anti-Epith-2 mAb IgG. Bars, SD ($n = 80$). $^{*}P = 0.0055$, $^{**}P = 0.0588$. Unpaired t test.

The immunoreaction of Epith-2 to its mAb was significantly weakened by digestion with trypsin and not chymotrypsin, suggesting the presence of lysine and/or arginine-rich regions (L/R-rich region) in the peptide (37) near the anti-mAb epitope. Furthermore, the present cell reaggregation assay conducted in the presence of anti-Epith-2 mAb IgG indicates that the mAb epitope is located in the extracellular region of the protein and is involved in cell adhesion activity. The L/R-rich region of the protein may be

involved in the cell adhesion activity of Epith-2. Interestingly the lysine-rich region is reported in the junction-associated protein, zonula occludens-1, in mammalian cells (47) and the arginine-rich region in vitronectin, a major cell adhesion protein (48). This region in vitronectin stimulates the activity of TGFβ (49). Further proteomic analysis will enable to determine the functional significance of the L/R-rich region of Epith-2 in the GFR signaling pathway.

ENDOCYTIC RETRACTION OF EPITH-2 FROM THE SURFACE OF MESENCHYME PRECURSOR CELLS DURING EMT

The present immunohistochemical detection of Epith-2 in the cytoplasm of mesenchyme cells and the observation of apparent GFR/PTK-dependent Epith-2 internalization suggest the involvement of growth factor(s). In *S. purpuratus*, an FGF receptor (SpFGFR1) possesses conserved tyrosine kinase domain, and the transcripts accumulate when mesenchyme cell ingression and gastrulation occurs (50). Thus, the present and the previous observations suggest that the cell surface modification is carried out by endocytosis. The presently shown non-ionic detergent solubility of Epith-2 suggests that the protein is anchored to the plasma membrane via a transmembrane domain. Thus, the endocytic retraction of Epith-2 from the cell surface is reminiscent of a similar retraction of the LvG-cadherin/β-catenin complex in the micromere specification in *L. variegatus* (19, 20). The complex was removed from the cell surface by endocytosis (51), which was followed by the cleavage of β-catenin from LvG-cadherin and movement into the nucleus (40). According to the NCBI database[2] and proteomic analysis using an open proteomic database ExPASy Compute pI/Mw (SIB Swiss Institute of Bioinformatics)[3], the calculated M_r of *H. pulcherrimus* β-catenin was approximately 89.9 kDa, and the *p*I was 5.72 (BAN 13547). The M_r of LvG-cadherin (AAC06341.1) was 303 kDa, and the *p*I was 3.88, whereas the M_r of Epith-2 was 143 kDa, and the *p*I was 4.7. Thus, Epith-2 is different from both proteins. Nevertheless, it is evident that the endocytic retraction of at least two cell surface proteins, Epith-2 and LvG-cadherin, are involved in the EMT and the acquisition of the mesenchymal property during and/or at the end of the EMT in sea urchin embryos.

The present isolated Epith-2 immunoblotting experiments of the ingressed PMCs indicated no detectable decrease in the M_r, suggesting the occurrence of little or no Epith-2 degradation following endocytosis; however, later in the PMCs that spread into the blastocoels, cytoplasmic Epith-2 was not detected by immunohistochemistry. Thus, at least during the early period after endocytosis, Epith-2 retained its initial molecular configuration, including the anti-Epith-2 mAb epitopic structure, which suggests the potential occurrence of the prolonged activation of the Epith-2-mediated signaling pathway by constituting "signaling endosomes" [rev. (52)]. The present study did not determine whether tyrosine residues of Epith-2 were dephosphorylated in the endosomes as has been previously reviewed by Kholodenko (53). There are two major mechanisms of internalization of cell surface proteins: clathrin-mediated endocytosis and clathrin-independent lipid-raft-dependent endocytosis, and this latter mechanism includes the TGFβ receptor pathways [rev. (54)]. TGFβ contributes to numerous morphogenetic processes in sea urchin embryos (55, 56). According to immunoelectron microscopy images of bovine kidney epithelium, endocytosed cadherin was found to be associated with the zonula adherens plaque and the attached actin filaments in the juxtanuclear cytoplasm (57). Using *in vitro* astrocytes, immunoprecipitation studies indicated that neural cell adhesion molecules are endocytosed via a clathrin-dependent pathway (58). The endocytosis of DM-GRASP, a cell adhesion molecule of the immunoglobulin superfamily that promotes the growth and the navigation of axons in chick embryos, is dependent on clathrin. Immunoprecipitation studies have shown that internalized DM-GRASP enters the degradation pathway after ubiquitination with one or two ubiquitin(s) (59). Thus, substantial cell adhesion molecules are endocytosed via a clathrin-dependent pathway. However, whether Epith-2 is endocytosed via the clathrin pathway needs to be further addressed by immunoprecipitation experiments that will also clarify whether Epith-2 is ubiquitinated during immunochemical disappearance during the early gastrula stage as observed in PMCs. Whether LvG-cadherin is digested in the cytoplasm remains currently unknown.

The sea urchin genome contains at least 20 receptor tyrosine kinase genes, and among these genes, the accumulation of the FGFR1 transcripts is localized at the PMC and the SMC around the swimming blastula stage and the late gastrula stage, respectively, in *S. purpuratus* (56). This finding suggests the involvement of FGFR1 in mesenchyme differentiation or more precisely the ingression process. Tyrosine kinase induces endocytosis in bovine adrenal chromaffin cells (24), and gp60 induces endocytosis in pulmonary micro-vascular endothelial cells (60).

The apparent GFR/PTK-dependent Epith-2 endocytosis suggests the presence of an upstream growth factor(s), which is consistently reported in the vast EMT. TGFβ is known to be involved in the vast EMT (61–63) along with HGF, FGF, and EGF [rev. (64)], which is initiated by Notch signaling (3). The source of the growth factors in the sea urchin embryo [rev. (22)] and in vast animals (65, 66) is the extracellular matrix. The sea urchin genome contains numerous TGFβ (56), and its involvement in PMC skeletogenesis has been reported (67). TGFβ activates Ras (68), which is required for cell dissociation and spreading during the EGF-induced EMT of the *in vitro* NBT-II rat carcinoma cell line. The overexpression of the activated forms of c-Raf and MEK1 leads to cell dissociation. Consistently, the MEK1 inhibitor PD98059 inhibits EGF- and Ras-induced cell dispersion (69). Likewise, in *H. pulcherrimus*, PD98059 delays PMC ingression and inhibits SMC ingression as well as inhibits the phosphorylation of ERK that comprises a factor in the MAPK pathway (21). Thus, the MAPK pathway is essentially involved in mesenchyme cell dispersion or spreading. The phosphorylation by ERK activates the transcription factor Ets1 that is required for PMC specification (70), suggesting that endocytic internalization of Epith-2 initiates the activation of genes that are involved in the acquisition of mesenchymal properties. TGFβ also upregulates Snail (71), which plays an essential role in the EMT accompanied with the downregulation of E-cadherin and the upregulation of N-cadherin, known

[2]http://www.ncbi.nlm.nih.gov/
[3]http://web.expasy.org/compute_pi/

as "cadherin switch" in cancer metastasis [rev. (64)]. Likewise, in the sea urchin embryo, Snail is required for the endocytosis of cadherin downstream of Pmar1 and Alx1 through several downstream PMC-expressed proteins (72).

THREE-STEP PROCESS OF MESENCHYME INGRESSION

Herbimycin A and suramin differently affected the ingression process of the mesenchyme. HA moderately inhibited, whereas suramin severely inhibited Epith-2 endocytosis. In particular, PMCs not only retained their epithelial morphology but also migrated after dissociation en masse, which caused PMCs to undergo "collective migration" as observed in several cancer cells that maintain cell–cell adhesions and epithelial morphology during metastasis (64). PMCs that undergo "collective migration" appear to support the present observation that Epith-2 retracted at the PE-border, while Epith-2 remained on the cell surface among PMCs. This finding suggests the occurrence of a centro-peripheral polarity in cell surface Epith-2 endocytic retraction during the early stage of ingression. Likewise, during the "collective migration" of several cancer cells such as L-10 human rectal adenocarcinoma cells, the cellular properties are different depending on the location of each cell (73). Thus, the centro-peripheral polarity of Epith-2 expression or endocytosis in the ingressed PMCs suggests that the GFR/PTK pathway is not involved in Epith-2 endocytosis at the PE-border. Further several control studies would further ensure the present inhibitory effects of HA and suramin.

Along with the present observation of the normal ingression process, the inhibition of EMT by HA and suramin suggest that at least three steps of the mesenchyme ingression process relates to GFR/PTK signaling: (1) GFR/PTK-dependent endocytic retraction of cell surface Epith-2; (2) GFR/PTK-independent dissociation from the epithelium; and (3) GFR-independent/TPK-dependent spreading to single cells and the acquisition of cell motility.

POST-ENDOCYTOSIS OF CELL ADHESION MOLECULES

The endocytosis of cell surface adhesion proteins in the EMT results in the sole dissolution of the epithelial phenotype and in the activation of new sets of mesenchyme-specific genes. In sea urchin embryos, LvG-cadherin/β-catenin endocytosis triggers the activation of a substantial number of PMC-specific genes, including *Hp-ets* (74), *pmar1*, *alx1*, *ets1*, and *tbr* (72, 75). Based on perturbation studies, *pmar1* and *alx1* are positioned at upstream of *snail*, and their activation is a prerequisite of β-catenin endocytosis (72). In addition, PMC-specific gene activation cannot be regulated by the cell adhesion molecules. In Madin–Darby canine kidney cells, TGFβ1 induces *snail* expression, which triggers the EMT via a MAPK-dependent mechanism (76). However, conversely in breast cancer, Snail appears to activate the TGFβ pathway with Slug by increasing histone acetylation at the promoter region of TGFβ and the inhibition of the signaling pathway consequently decreases cell migration with no impact on cell junction molecules by Snail and Slug. These observations propose a dual regulatory system in the EMT: (1) the repression of the cell junction and (2) the cell migration through TGFβ and/or other pathways (77), which appears comparable to the present hypothesis suggesting a three-step process of mesenchyme ingression.

SMC-specific genes, such as *glial cells missing* (*gcm*), the *polyketide synthase* gene cluster (*pks-gc*), the *flavin-containing monooxygenases* multigene family (*fmo*), and *sulfotransferase* (*sult*), are isolated from the pigment cell lineage, and they are downstream of the Notch signaling pathway (78). Several of these genes may also be activated after endocytic retraction of the cell surface LvG-cadherin/β-catenin complex (19, 20) and, possibly, Epith-2.

ACKNOWLEDGMENTS

We thank M. Washio and S. Tamura (Research Center for Marine Biology, Tohoku University) for obtaining conditioned Epith-2 hybridoma medium and for collecting *T. hardwicki* and *H. pulcherrimus*. We thank the Akkeshi Marine Station, Hokkaido University for providing us with *S. intermedius*, Dr. M. Kiyomoto (Marine and Coastal Research Center, Ochanomizu University) for *C. japonicus,* Misaki Marine Biological Station, University of Tokyo for *P. depressus,* the Seto Marine Biological Laboratory, Kyoto University for *M. globules*, and the Hopkins Marine Station, Stanford University for *L. pictus* for the study. We also thank Dr. R. Matsuda, University of Tokyo, for providing anti-P4 mAb.

REFERENCES

1. Viebahn C, Mayer B, Miething A. Morphology of incipient mesoderm formation in the rabbit embryo: a light- and retrospective electron-microscopic study. *Acta Anat* (1995) **154**:99–110. doi:10.1159/000147756
2. Hall BK. *The Neural Crest in Development and Evolution.* New York: Springer (1999).
3. Timmerman LA, Grego-Bessa J, Raya A, Bertran E, Perez-Pomares JM, Diez J, et al. Notch promotes epithelial-mesenchymal transition during cardiac development and oncogenic transformation. *Genes Dev* (2004) **18**:99–115. doi:10.1101/gad.276304
4. Kong D, Li Y, Wang Z, Sarkar FH. Cancer stem cells and epithelial-to-mesenchymal transition (EMT)-phenotypic cells: are they cousins or twins? *Cancers* (2011) **3**:716–29. doi:10.3390/cancers30100716
5. Joglekar MV, Joglekar VM, Joglekar SV, Hardikar AA. Human fetal pancreatic insulin-producing cells proliferate *in vitro*. *J Endocrinol* (2009) **201**:27–36. doi:10.1677/JOE-08-0497
6. Schwanzel-Fukuda M. Origin and migration of luteinizing hormone-releasing hormone neurons in mammals. *Microsc Res Tech* (1999) **44**:2–10. doi:10.1002/(SICI)1097-0029(19990101)44:1<2::AID-JEMT2>3.0.CO;2-4
7. Dan K. Cyto-embryology of echinoderm and amphibian. In: Bourne GH, Danielli JK editors. *International Review of Cytology*. (Vol. 6), New York: Academic Press (1960). p. 321–67.
8. Okazaki K. Normal development to metamorphosis. In: Czihak G editor. *The Sea Urchin Embryo: Biochemistry and Morphogenesis.* Berlin: Springer-Verlag (1975). p. 177–232.
9. Katow H, Solursh M. Ultrastructure of primary mesenchyme cell ingression in the sea urchin *Lytechinus pictus*. *J Exp Zool* (1980) **213**:231–46. doi:10.1002/jez.1402130211
10. Kanoh K, Aizu G, Katow H. Disappearance of an epithelial cell surface-specific glycoprotein (Epith-1) associated with epithelial-mesenchymal conversion in sea urchin embryogenesis. *Dev Growth Differ* (2001) **43**:83–95. doi:10.1046/j.1440-169x.2001.00548.x
11. Hörstadius S. The mechanics of sea urchin development, studied by operative methods. *Biol Rev* (1939) **14**:132–79. doi:10.1111/j.1469-185X.1939.tb00929.x
12. Anstrom JA, Chin JE, Leaf DS, Parks AL, Raff RA. Localization and expression of msp130, a primary mesenchyme lineage-specific cell surface protein of the sea urchin embryo. *Development* (1987) **101**:255–65.

13. Shimizu K, Noro N, Matsuda R. Micromere differentiation in the sea urchin embryo: expression of primary mesenchyme cell specific antigen during development. *Dev Growth Differ* (1988) **30**:35–47. doi: 10.1111/j.1440-169X.1988.00035.x
14. Shimizu K, Katow H, Matsuda R. Micromere differentiation in the sea urchin embryo: immunochemical characterization of primary mesenchyme cell-specific antigen and its biological role. *Dev Growth Differ* (1990) **32**:629–36. doi:10.1111/j.1440-169X.1990.00629.x
15. Katow H. Role of a primary mesenchyme cell surface specific antigen during early morphogenesis in sea urchin embryos. In: Yanagisawa K, Yasumasu I, Oguro C, Suzuki N, Motokawa T editors. *Biology of Echinodermata*. Rotterdam: Balkema (1991). p. 453–9.
16. Hertzler PL, McClay DR. AlphaSU2, an epithelial integrin that binds laminin in the sea urchin embryo. *Dev Biol* (1999) **207**:1–13. doi:10.1006/dbio.1998.9165
17. Chagraoui J, Lepage-Noll A, Anjo A, Uzan G, Charbord P. Fetal liver stroma consists of cells in epithelial-to-mesenchymal transition. *Blood* (2003) **101**:2973–82. doi:10.1182/blood-2002-05-1341
18. Shimizu Y, Yamamichi N, Saitoh K, Watanabe A, Ito T, Yamamichi-Nishina M, et al. Kinetics of v-src-induced epithelial-mesenchymal transition in developing glandular stomach. *Oncogene* (2003) **22**:884–93. doi:10.1038/sj.onc.1206174
19. Miller JR, McClay DR. Changes in the pattern of adherens junction-associated β-catenin accompany morphogenesis in the sea urchin embryo. *Dev Biol* (1997) **192**:310–22. doi:10.1006/dbio.1997.8739
20. Miller JR, McClay DR. Characterization of the role of cadherin in regulating cell adhesion during sea urchin development. *Dev Biol* (1997) **192**:323–39. doi:10.1006/dbio.1997.8740
21. Katow H, Aizu G. Essential role of growth factor receptor-mediated signal transduction through the mitogen-activated protein kinase pathway in early embryogenesis of the echinoderm. *Dev Growth Differ* (2002) **44**:437–55. doi:10.1046/j.1440-169X.2002.00657.x
22. Katow H. Extracellular signal transduction in sea urchin embryogenesis: from extracellular matrix to MAP kinase pathway. *Curr Top Peptide Protein Res* (2003) **5**:149–60.
23. Wessel GM, Katow H. Regulation of the epithelial-to-mesenchymal transition in sea urchin embryos. In: Savagner P editor. *Rise and Fall of Epithelial Phenotype: Concepts of Epithelia-Mesenchyme Transition Molecular Biology Intelligence Unit*. New York: Eureka.com/Landes Bioscience, Kluwer Academic/Plenum Publishers (2005). p. 77–100.
24. Nucifora PG, Fox AP. Tyrosine phosphorylation regulates rapid endocytosis in adrenal chromaffin cells. *J Neurosci* (1999) **19**:9739–46.
25. Rickwood D, Chambers JAA, Spragg SP. Two-dimentional gel electrophoresis. 2nd ed. In: Hames BD, Rickwood D editors. *Gel Electrophoresis of Proteins: A Practical Approach*. Oxford: IRL Press (1990). p. 217–72.
26. Katow H, Solursh M. In situ distribution of concanavalin A binding sites in mesenchyme blastulae and early gastrulae of the sea urchin *Lytechinus pictus*. Exp Cell Res (1982) **139**:171–80. doi:10.1016/0014-4827(82)90330-5
27. Katow H, Komazaki S. Spatiotemporal expression of pamlin during early embryogenesis in sea urchin and importance of N-linked glycosylation for the glycoprotein function. *Roux's Arch Dev Biol* (1996) **205**:371–81. doi:10.1007/BF00377217
28. Katow H, Suyemitsu T, Ooka S, Yaguchi J, Jin-nai T, Kuwahara I, et al. Development of a dopaminergic system in sea urchin embryos and larvae. *J Exp Biol* (2010) **213**:2808–19. doi:10.1242/jeb.042150
29. Honma Y, Okabe-Kado J, Kasukabe T, Hozumi M, Kodama H, Kijigaya S, et al. Herbimycin A, an inhibitor of tyrosine kinase, prolongs survival of mice inoculated with myeloid leukemia C1 cells with high expression of *v-abl* tyrosine kinase. *Cancer Res* (1992) **52**:4017–20.
30. Turturro F, Arnold MD, Frist AY, Pulford K. Model of inhibition of the NPM-ALK kinase activity by herbimycin A. *Clin Cancer Res* (2002) **8**:240–5.
31. Gudi S, Huvar I, White CR, McKnight NL, Dusserre N, Boss GR, et al. Rapid activation of Ras by fluid flow is mediated by Gaq and Gbg subunits of heterotrimeric G proteins in human endothelial cells. *Arterioscler Thromb Vasc Biol* (2003) **23**:994–1000. doi:10.1161/01.ATV.0000073314.51987.84
32. Katow H, Washio M. Pamlin-induced tyrosine phosphorylation of SUp62 protein in primary mesenchyme cells during early embryogenesis in the sea urchin, *Hemicentrotus pulcherrimus*. *Dev Growth Differ* (2000) **42**:519–29. doi:10.1046/j.1440-169x.2000.00533.x
33. Coffey RJ Jr., Leof EB, Shipley GD, Moses HL. Suramin inhibition of growth factor receptor binding and mitogenicity in AKR-2B cell. *J Cell Physiol* (1987) **132**:143–8. doi:10.1002/jcp.1041320120
34. Zhang Y-L, Keng Y-F, Zhao Y, Wu L, Zhang Z-Y. Suramin is an active site-directed, reversible, and tight-binding inhibitor of protein-tyrosine phosphatases. *J Biol Chem* (1998) **273**:12281–7. doi:10.1074/jbc.273.20.12281
35. Nakata H. Stimulation of extracellular signal-regulated kinase pathway by suramin with concomitant activation of DNA synthesis in cultured cells. *J Pharmacol Exp Ther* (2004) **308**:744–53. doi:10.1124/jpet.103.058230
36. Allen RC, Saravis CA, Maurer HR. *Gel Electrophoresis and Isoelectric Focusing of Proteins. Selected Techniques*. Berlin: Walter de Gruyter (1984).
37. Vajda T, Szabo T. Specificity of trypsin and alpha-chymotrypsin towards neutral substrates. *Acta Biochim Biophys Acad Sci Hung* (1976) **11**:287–94.
38. Mayor S, Maxfield FR. Insolubility and redistribution of GPI-anchored proteins at the cell surface after detergent treatment. *Mol Biol Cell* (1995) **6**:929–44.
39. Abe K, Katow T, Ooka S, Katow H. Unc-5/netrin-mediated axonal projection during larval serotonergic nervous system formation in the sea urchin, *Hemicentrotus pulcherrimus*. *Int J Dev Biol* (2013) **57**:415–25. doi:10.1387/ijdb.120256hk
40. Logan CY, Miller JR, Ferkowicz MJ, McClay DR. Nuclear β-catenin is required to specify vegetal cell fates in the sea urchin embryo. *Development* (1999) **126**:345–57.
41. Katow H. Pamlin, a primary mesenchyme cell adhesion protein, in the basal lamina of the sea urchin embryo. *Exp Cell Res* (1995) **218**:469–78. doi:10.1006/excr.1995.1180
42. Barnes RSK, Calow P, Olive PJW, Galding DW, Spicer JI. *The Invertebrates: A Synthesis*. 3rd ed. Tokyo: Blackwell Science KK (2001).
43. Mao X, Chol EJ, Payne AS. Disruption of desmosome assembly by monovalent human pemphigus vulgaris monoclonal antibodies. *J Invest Dermatol* (2009) **129**:908–18. doi:10.1038/jid.2008.339
44. Springer WR, Baronde SH. Cell adhesion molecules: detection with univalent second antibody. *J Cell Biol* (1980) **87**:703–7. doi:10.1083/jcb.87.3.703
45. Damsky CH, Richa J, Solter D, Knudsen K, Buck CA. Identification and purification of a cell surface glycoprotein mediating intercellular adhesion in embryonic and adult tissue. *Cell* (1983) **34**:455–66. doi:10.1016/0092-8674(83)90379-3
46. Springer WR, Haywood-Reid PL. Antibodies specific for gp40 inhibit cell-cell adhesion by cross-linking the protein on the surface of *Dictyostelium purpureum*. *J Cell Biochem* (1993) **53**:85–97. doi:10.1002/jcb.240530202
47. Gottardi CJ, Arpin M, Fanning AS, Louvard D. The junction-associated protein, zonula occludens-1, localizes to the nucleus before the maturation and during the remodeling of cell-cell contacts. *Proc Natl Acad Sci U S A* (1996) **93**:10779–84. doi:10.1073/pnas.93.20.10779
48. Kost C, Stuber W, Ehrlich HJ, Pannekock H, Preissner KT. Mapping of binding sites for heparin, plasminogen activator inhibitor-1 and plasminogen to vitronectin's heparin binding region reveals a novel vitronectin-dependent feedback mechanism for the control of plasmin formation. *J Biol Chem* (1992) **267**:12098–105.
49. Ribeiro SMF, Schultz-Cherry S, Murphy-Ullrich JE. Heparin-binding vitronectin up-regulates latent TGF-β production by bovine aortic endothelial cells. *J Cell Sci* (1995) **108**:1553–61.
50. McCoon PE, Angerer RC, Angerer LM. SpFGFR, a new member of the fibroblast growth factor receptor family, is developmentally regulated during early sea urchin development. *J Biol Chem* (1996) **271**:20119–25. doi:10.1074/jbc.271.33.20119
51. Nelson WJ. Regulation of cell–cell adhesion by the cadherin–catenin complex. *Biochem Soc Trans* (2008) **36**:149–55. doi:10.1042/BST0360149
52. Pálfy M, Reményi A, Korcsmáros T. Endosomal crosstalk: meeting points for signaling pathways. *Trends Cell Biol* (2012) **22**:447–56. doi:10.1016/j.tcb.2012.06.004
53. Kholodenko BN. Four-dimensional organization of protein kinase signaling cascades: the roles of diffusion, endocytosis and molecular motors. *J Exp Biol* (2003) **206**:2073–82. doi:10.1242/jeb.00298
54. Le Roy C, Wrana JL. Clathrin- and non-clathrin mediated endocytic regulation of cell signaling. *Nat*

Rev Mol Cell Biol (2005) **6**:112–26. doi:10.1038/nrm1571
55. Flowers VL, Courteau GR, Poustka AJ, Weng W, Venuti JM. Nodal/activin signaling establishes oral-aboral polarity in the early sea urchin embryo. *Dev Dyn* (2004) **231**:727–40. doi:10.1002/dvdy.20194
56. Lapraz F, Röttinger E, Duboc V, Range R, Duloquin L, Walton K, et al. RTK and TGF-β signaling pathways genes in the sea urchin genome. *Dev Biol* (2006) **300**:132–52. doi:10.1016/j.ydbio.2006.08.048
57. Kartenbeck J, Schmelz M, Franke WW, Geiger B. Endocytosis of junctional cadherins in bovine kidney epithelial (MDBK) cells cultured in low Ca^{2+} ion medium. *J Cell Biol* (1991) **113**:881–92. doi:10.1083/jcb.113.4.881
58. Miñana R, Duran JM, Tomas M, Renau-Piqueras J, Guerri C. Neural cell adhesion molecule is endocytosed via a clathrin-dependent pathway. *Eur J Neurosci* (2001) **13**:749–56. doi:10.1046/j.0953-816x.2000.01439.x
59. Thelen K, Georg T, Bertuch S, Zelinal P, Pollerberg GE. Ubiquitination and endocytosis of cell adhesion molecule DM-GRASP regulate its cell surface presence and affect its role for axon navigation. *J Biol Chem* (2008) **283**:32792–801. doi:10.1074/jbc.M805896200
60. Minshall RD, Tiruppathi C, Vogel SM, Malik AB. Vesicle formation and trafficking in endothelial cells and regulation of endothelial barrier function. *Histochem Cell Biol* (2002) **117**:105–12. doi:10.1007/s00418-001-0367-x
61. Miettinen PJ, Ebner R, Lopez AR, Derynck R. TGF-beta induced transdifferentiation of mammary epithelial cells to mesenchymal cells: involvement of type I receptors. *J Cell Biol* (1994) **127**:2021–36. doi:10.1083/jcb.127.6.2021
62. Runyan R, Heimark RL, Camenisch TD, Klewer SE. Epithelial-mesenchymal transformation in the embryonic heart. In: Savagner P editor. *Rise and Fall of Epithelial Phenotype: Concepts of Epithelia-Mesenchyme Transition Molecular Biology Intelligence Unit.* New York: Eureka.com/Landes Bioscience, Kluwer Academic/Plenum Publishers (2005). p. 40–55.
63. Vignalis M-L, Fafet P. TGF-β dependent epithelial-mesenchymal transition. In: Savagner P editor. *Rise and Fall of Epithelial Phenotype: Concepts of Epithelia-Mesenchyme Transition Molecular Biology Intelligence Unit.* New York: Eureka.com/Landes Bioscience, Kluwer Academic/Plenum Publishers (2005). p. 236–44.
64. Kawauchi T. Cell adhesion and its endocytic regulation in cell migration during neural development and cancer metastasis. *Int J Mol Sci* (2012) **13**:4564–90. doi:10.3390/ijms13044564
65. Macri L, Silverstein D, Clark RAF. Growth factor binding to the pericellular matrix and its importance in tissue engineering. *Adv Drug Deliv Rev* (2007) **59**:1366–81. doi:10.1016/j.addr.2007.08.015
66. Clark RAF. Synergistic signaling from extracellular matrix-growth factor complex. *J Invest Dermatol* (2008) **128**:1354–5. doi:10.1038/jid.2008.75
67. Zito F, Costa C, Sciarrino S, Poma V, Russo R, Angerer LM, et al. Expression of *univin*, a TGF-β growth factor, requires ectoderm–ECM interaction and promotes skeletal growth in the sea urchin embryo. *Dev Biol* (2003) **264**:217–27. doi:10.1016/j.ydbio.2003.07.015
68. Janda E, Nevolo M, Lehmann K, Downward J, Beug H, Grieco M. Raf plus TGFbeta-dependent EMT is initiated by endocytosis and lysosomal degradation of E-cadherin. *Oncogene* (2006) **25**:7117–30. doi:10.1038/sj.onc.1209701
69. Edme N, Downward J, Thiery JP, Boyer B. Ras induces NBT-II epithelial cell scattering through the coordinate activities of Rac and MAPK pathways. *J Cell Sci* (2002) **115**:2591–601.
70. Rottinger E, Besnardeau L, Lepage T. A Raf/MEK/ERK signaling pathway is required for development of the sea urchin embryo micromere lineage through phosphorylation of the transcription factor Ets. *Development* (2004) **131**:1075–87. doi:10.1242/dev.01000
71. Peinado H, Quintanilla M, Cano A. Transforming growth factor β-1 induces snail transcription factor in epithelial cell lines: mechanisms for epithelial mesenchymal transitions. *J Biol Chem* (2003) **278**:21113–23. doi:10.1074/jbc.M211304200
72. Wu SY, McClay DR. The Snail repressor is required for PMC ingression in the sea urchin embryo. *Development* (2007) **134**:1061–70. doi:10.1242/dev.02805
73. Nabeshima K, Inoue T, Shimao Y, Okada Y, Itoh Y, Seiki M, et al. Front-cell-specific expression of membrane-type 1 matrix metalloproteinase and gelatinase a during cohort migration of colon carcinoma cells induced by hepatocyte growth factor/scatter factor. *Cancer Res* (2000) **60**:3364–9.
74. Kurokawa D, Kitajima T, Mitsunaga-Nakatsubo K, Amemiya S, Shimada H, Akasaka K. HpEts, an ets-related transcription factor implicated in primary mesenchyme cell differentiation in the sea urchin embryo. *Mech Dev* (1999) **80**:41–52. doi:10.1016/S0925-4773(98)00192-0
75. Rho HK, McClay DR. The control of *foxN2/3* expression in sea urchin embryos and its function in the skeletogenic gene regulatory network. *Development* (2011) **138**:937–45. doi:10.1242/dev.058396
76. Pierce KL, Maudsley S, Daaka Y, Luttrell LM, Lefkowitz RJ. Role of endocytosis in the activation of the extracellular signal regulated kinase cascade by sequestering and non sequestering G protein coupled receptors. *Proc Natl Acad Sci U S A* (2000) **97**:1489–94. doi:10.1073/pnas.97.4.1489
77. Dhasarathy A, Phadke D, Deepak Mav D, Shah RR, Wade PA. The transcription factors snail and slug activate the transforming growth factor-beta signaling pathway in breast cancer. *PLoS One* (2011) **6**:e26514. doi:10.1371/journal.pone.0026514
78. Calestani C, Rast JP, Davidson EH. Isolation of pigment cell specific genes in the sea urchin embryo by differential macroarray screening. *Development* (2003) **130**:4587–96. doi:10.1242/dev.00647

Conflict of Interest Statement: The authors declare that the research was conducted in the absence of any commercial or financial relationships that could be construed as a potential conflict of interest.

Received: 31 May 2013; accepted: 14 August 2013; published online: 30 August 2013.
*Citation: Wakayama N, Katow T and Katow H (2013) Characterization and endocytic internalization of Epith-2 cell surface glycoprotein during the epithelial-to-mesenchymal transition in sea urchin embryos. Front. Endocrinol. **4**:112. doi: 10.3389/fendo.2013.00112*
This article was submitted to Experimental Endocrinology, a section of the journal Frontiers in Endocrinology.

frontiers in
ENDOCRINOLOGY

ORIGINAL RESEARCH ARTICLE
published: 03 September 2013
doi: 10.3389/fendo.2013.00117

Determination of ghrelin structure in the barfin flounder (*Verasper moseri*) and involvement of ingested fatty acids in ghrelin acylation

Hiroyuki Kaiya[1]*, Tadashi Andoh[2], Takashi Ichikawa[3], Noriko Amiya[4], Kouhei Matsuda[5], Kenji Kangawa[6] and Mikiya Miyazato[1]

[1] *Department of Biochemistry, National Cerebral and Cardiovascular Center, Suita, Japan*
[2] *Seikai National Fisheries Research Institute, Fisheries Research Agency, Nagasaki, Japan*
[3] *Hokkaido National Fisheries Research Institute, Fisheries Research Agency, Akkeshi, Japan*
[4] *School of Marine Biosciences, Kitasato University, Sagamihara, Japan*
[5] *Laboratory of Regulatory Biology, Graduate School of Science and Engineering, University of Toyama, Toyama, Japan*
[6] *National Cerebral and Cardiovascular Center, Suita, Japan*

Edited by:
Sho Kakizawa, Kyoto University, Japan

Reviewed by:
Suraj Unniappan, York University, Canada
Yung-Hsi Kao, National Central University, Taiwan

****Correspondence:***
Hiroyuki Kaiya, Department of Biochemistry, National Cerebral and Cardiovascular Center Research Institute, 5-7-1 Fujishirodai, Suita, Osaka 565-8565, Japan
e-mail: kaiya@ncvc.go.jp

Ghrelin is a peptide hormone that is acylated with a fatty acid, usually *n*-octanoic acid, at the third amino acid (aa) residue (usually a serine or threonine), and this acylation is known to be essential for ghrelin activity not only in mammals but also in non-mammals, such as fish. However, the modification mechanisms of ghrelin modification in fish are not known. In this study, we elucidated the structure of ghrelin in a teleost, the barfin flounder (*Verasper moseri*), and determined whether ingested free fatty acids of various chain lengths participated in ghrelin acylation. Complementary DNA cloning revealed the barfin flounder prepro-ghrelin to be a 106-aa peptide and the mature ghrelin to be a 20-aa peptide (GSSFLSPSHKPPNKGKPPRA). However, purification of ghrelin peptides from stomach extracts demonstrated that the major form of the hormone was a 19-aa decanoylated peptide [GSS(C10:0)FLSPSHKPPNKGKPPR] missing the last alanine of the 20-aa peptide. Ingestion of feed enriched with *n*-heptanoic acid (C7), *n*-octanoic acid (C8), or *n*-non-anoic acid (C9) changed the modification status of the peptide: ingestion of C8 or C9 increased the amount of C8:0 or C9:0 19-aa ghrelin, respectively, but no C7:0 ghrelin was isolated after ingestion of C7. These results indicate that ingested free fatty acids are substrates for ghrelin acylation in the barfin flounder, but the types of free fatty acids utilized as substrates may be limited.

Keywords: acyl modification, barfin flounder, cDNA cloning, feed, fatty acid, ghrelin, ingestion

INTRODUCTION

Ghrelin, a peptide hormone produced in gastric ghrelin cells (called X/A-like cells in rats and P/D cells in humans), is acylated at the third amino acid (aa) residue, usually a serine or threonine (1, 2). Acylation is essential for binding of the hormone to its receptor [growth hormone secretagogue receptor type 1a (GHS-R1a)] and for eliciting its activities (1). Acylation, usually with *n*-octanoic acid (C8), occurs post-transcriptionally; but des-acyl ghrelin, which lacks a fatty acid side chain and does not activate GHS-R1a, is also produced in the same ghrelin cells. Ghrelin acylation is catalyzed by ghrelin *O*-acyltransferase [GOAT; (3, 4)], a member of the membrane-bound *O*-acyltransferase superfamily. The expression pattern of the enzyme overlaps that of ghrelin in gastric mucosal cells, suggesting that these cells play a key role in ghrelin synthesis (5, 6).

Ghrelin can be acylated by fatty acids other than C8, as is the case in cats, rats, and humans (7, 8). Several studies have investigated the source of substrates for ghrelin acylation. Nishi et al. (9) demonstrated that in mice, dietary lipids (free fatty acids or medium-chain triacylglycerols) contribute to ghrelin acylation. Subsequent studies demonstrated that these triacylglycerols are substrates for GOAT-mediated acylation of ghrelin (3), and GOAT plays an important role in the acylation [(10); see also the review by Shlimun and Unniappan (11)].

Ghrelin is also present in a wide variety of non-mammalian vertebrates (12, 13), and ghrelins acylated by fatty acids other than C8 have also been identified in various animals from birds to elasmobranchs, including chickens (14), red-eared slider turtles (15), bullfrogs (2), rainbow trout (16), Japanese eels (17), Mozambique tilapia (18), channel catfish (19), goldfish (20), and sharks (21). In Mozambique tilapia, decanoylated ghrelin (C10) is the major form of the peptide, and the physiological actions of C8- and C10-ghrelin are different (22, 23), suggesting that the type of fatty acid modification is an important determinant of ghrelin's actions.

The source of fatty acids for ghrelin acylation has been investigated in neonatal chicks (24): oral or intraperitoneal administration of *n*-octanoic acid increases the amount of C8-ghrelin in the proventriculus (a glandular portion of the stomach of chickens) and in plasma. However, whether such a mechanism for ghrelin acylation exists in other non-mammalian vertebrates is not known.

Our goal in this study was to determine whether exogenous free fatty acids contribute to ghrelin acylation in fish. We used a cultured flatfish, the barfin flounder (*Verasper moseri*). This species is distributed over the Hokkaido Pacific coast. At one point, hauls of the fish had decreased so substantially that it was referred to as "the rarely seen fish," but catches have been increasing as a result of the release of aquacultured fish. First, we determined the structure of ghrelin in the barfin flounder by means of both cDNA cloning and peptide purification. Then we determined the modification status of ghrelin peptides purified from the stomach extracts of fish that were given feed enriched in *n*-heptanoic (enanthic) acid (C7), *n*-octanoic (caprylic) acid (C8), or *n*-nonanoic acid (pelargonic) acid (C9). The results of the feeding experiment indicate that ingested free fatty acids were substrates for ghrelin acylation in the barfin flounder, as has been demonstrated in mice and chickens, but the type of fatty acid utilized as substrate is likely to be limited.

MATERIALS AND METHODS

CLONING OF GHRELIN cDNA IN BARFIN FLOUNDER

Adult male barfin flounder (*V. moseri*) were obtained from the Iwate Fisheries Technology Center (Kamaishi, Iwate, Japan). The fish were reared under natural photoperiod and temperature conditions in seawater. Stomach and intestine were dissected out of fish anesthetized by immersion in 0.05% 2-phenoxyethanol, and the organs were frozen in liquid nitrogen and stored at −85°C until use. Total RNA was obtained from stomach and intestine of two individuals by means of a QIAcube (QIAGEN, Hilden, Germany) and an RNeasy Mini Kit (QIAGEN); and poly(A)$^+$ RNA was purified using an Oligotex dT30 Super (TaKaRa Bio Inc., Shiga, Japan). First-strand cDNA was synthesized from 132 ng of poly(A)$^+$ RNA (half from the pooled stomach RNA and the other half from the pooled intestinal RNA) by means of a First-Strand cDNA Synthesis Kit (Amersham Pharmacia Biotech, Buckinghamshire). Reverse transcription was performed at 25°C for 10 min, at 42°C for 1 h, and at 51°C 30 min, followed by 5 min at 99°C with an adaptor primer (ATTCTAGAGGCCGAGGCGGCCGACATG-d(T) $_{30}$-VN).

3′-Rapid amplification of cDNA ends (RACE) PCR was conducted using a degenerate sense primer based on known ghrelin sequences (5′-TNG GNM GNC ARA CNA TGG ARG-3′) and the adaptor primer described above with preheating at 94°C for 2 min followed by 35 cycles at 94°C for 40 s, 60°C for 40 s, and 72°C for 1 min in a thermocycler (Whatman Biometra, Göttingen, Germany). The PCR products were electrophoresed on 3% agarose gel (Agarose S, Nippon Gene, Tokyo, Japan) containing 0.005% ethidium bromide. The cDNA fragment of the expected size was cut out, purified by means of a Wizard SV Gel and PCR Clean-Up System (Promega, Madison, WI, USA), and ligated into the pT7Blue T-Vector (Novagen, San Diego, CA, USA). Plasmid DNA containing the expected insert was extracted from bacterial culture with a High Pure Plasmid Isolation Kit (Roche Diagnostics, Mannheim, Germany). The sequencing reaction was performed with a BigDye Terminator Cycle Sequencing Kit (Applied Biosystems, Foster City, CA, USA).

5′-RACE PCR was performed with gene-specific antisense primers based on the sequence determined by 3′-RACE PCR, as well as a 5′-primer. Primary and nested PCRs were performed with GSP-BF-ghrelin R1 (5′-GGC AAC TGA CAC TTT TAC TC-3′) and GSP-BF-ghrelin R2 (5′-TTC AAT GAT CAC TAT CTA ATG-3′) primers, respectively. To confirm the total nucleotide sequence, we amplified the full-length cDNA with a sense primer (BarfinGHRL-full-s: 5′-GTT TAA GGT CCA CTA ACT CAG GGG-3′) and a 3′-primer.

PURIFICATION OF GHRELIN FROM STOMACH EXTRACTS OF BARFIN FLOUNDER FED NORMAL FEED

Frozen stomach (12.4 g) collected from a fish that ate normal feed, as described in the next section, was used for the starting material.

To follow ghrelin activity during the purification process, we measured changes in intracellular Ca^{2+} concentration in CHO-GHSR62 cells, a cell line stably expressing rat GHS-R1a (1). Samples (1/40 to 1/200 volume of collected fraction) were used for this assay. The cells were plated onto a 96-well black plate at a density of 5×10^4 cells per well. Twenty hours after plating, the culture medium was aspirated, and 100 μl of fluorescent dye solution containing 4.4 μM Fluo-4AM (Life Technologies, Foster City, CA, USA), 1% fetal calf serum, and 1% PowerLoad solution (Life Technologies) in a working buffer was loaded onto each well. After the plate was incubated for 1 h at 37°C, the cells were washed three times with the working buffer. Sample was dissolved with the working buffer containing 0.001% Triton X-100, and an intracellular Ca^{2+} mobilization assay was performed automatically with a fluorometric imaging plate reader (FLIPR Tetra, Molecular Devices, Menlo Park, CA, USA).

Stomach tissues were boiled for 10 min with five volumes of Milli-Q water, cooled, and then acidified with 1 M acetic acid. The tissues were homogenized, and the supernatant was obtained by centrifugation at 13,400 × *g* for 30 min. The crude acidic extracts were loaded onto a Sep-Pak Plus C18 cartridge (Waters, Milford, MA, USA), and adsorbed peptides were eluted first with 30% and then with 60% acetonitrile containing 0.1% trifluoroacetic acid (TFA). The solution eluted with 60% acetonitrile containing 0.1% TFA was subjected to cation-exchange chromatography (SP-Sephadex C-25, H^+-form, GE Healthcare Bio-Science Corp., Piscataway, NJ, USA), and successive elution with 1 M acetic acid, 2 M pyridine, and 2 M pyridine/acetic acid (pH 5.0) yielded three fractions: SP-I, SP-II, and SP-III, respectively. The strongly basic peptide-enriched SP-III fraction was purified with a Sep-Pak Plus C18 cartridge, and the evaporated sample was subjected to gel-filtration high-performance liquid chromatography (HPLC) on a TSKgel G2000 SWxL column (21.5 mm × 300 mm, custom order, Tosoh, Tokyo, Japan) with 35% acetonitrile containing 0.1% TFA as the eluent at a flow rate of 2 ml/min. Fractions showing ghrelin activity were lyophilized, loaded onto a carboxymethyl (CM) ion-exchange HPLC column (TSKgel CM-2SW, 4.6 mm × 250 mm, Tosoh), and eluted at 1 ml/min with a four-step solvent gradient consisting of mixtures of solution A (9:1 mixture of 10 mM $HCOONH_4$ and acetonitrile, pH 4.8) and solution B (9:1 mixture of 1 M $HCOONH_4$ and acetonitrile, pH 4.8) as follows: increase from 0 to 25% B over 5 min (step 1), increase from 25 to 65% B over 60 min (step 2), increase from 65 to 100% B over 5 min (step 3), and hold at 100% B for 10 min (step 4). Fractions (1 ml/tube) were collected every minute for 80 min. Fractions showing ghrelin activity were separated by reverse-phase HPLC

on a Symmetry300 C18 column (3.9 mm × 150 mm, Waters, Milford, MA, USA); the eluent was a linear gradient of acetonitrile containing 0.1% TFA (10–60% over 40 min; flow rate, 1 ml/min). Fractions (0.5 ml/tube) were collected starting 15 min after injection. Fractions showing ghrelin activity were further purified by reverse-phase HPLC on a diphenyl column (2.1 mm × 150 mm, 219TP5125, GRACE Vydac, ChemcoPlus Scientific Co., Osaka, Japan); the eluent was a linear gradient of acetonitrile containing 0.1% TFA (10–60% over 40 min; flow rate, 0.2 ml/min). The eluate corresponding to each absorbance peak was collected.

The sequences of isolated peptides were analyzed with a protein sequencer (model 494HT, Life Technologies). The molecular weights of all isolated peptides were measured with an AB SCIEX TOF/TOF 5800 system (AB SCIEX, Tokyo, Japan) with α-cyano-4-hydroxycinnamic acid (Sigma-Aldrich Co., St. Louis, MO, USA) as a matrix.

FEEDING EXPERIMENT WITH FATTY ACID-ENRICHED FEED

The barfin flounder used in the feeding experiment were bred at Akkeshi Station, Hokkaido National Fisheries Research Institute, Fisheries Research Agency, Japan. Two-year-old flounder were kept in 2000 l aquaria with running seawater controlled at 17.0 ± 0.5°C. Flounder were fed apparent satiation with commercial dry pellets (P-8 for flounders, diameter 1.5 cm, Higashimaru, Kagoshima, Japan) once daily every business day for 2 months until the start of the feeding experiment. Regarding the fatty acid compositions in the diet, there were the data about the long-chain fatty acids but not the data of the middle-chain fatty acids. In the long-chain fatty acids, palmitic acid, oleic acid, icosapentaenoic acid, and docosahexaenoic acid predominated.

We divided the fish into four experimental groups consisting of three fish each: group 1 was fed normal feed, group 2 was fed C7-enriched feed, group 3 was fed C8-enriched feed, and group 4 was fed C9-enriched feed. The total body lengths and body weights (means ± SDs) of each group were 479.8 ± 12.7 mm and 1729.8 ± 222.6 g for group 1, 436.5 ± 43.8 mm and 1356.5 ± 675.6 g for group 2, 417.8 ± 54.8 mm and 1155.5 ± 461.9 g for group 3, and 441.3 ± 11.9 mm and 1217.8 ± 189.4 g for group 4; there were no significant differences in either body length or weight among the groups.

The enriched feeds were prepared by manually pipetting 20 μl of either *n*-heptanoic, *n*-octanoic, or *n*-non-anoic acid onto each feed pellet, and then 20 μl of 10% (v/w) aqueous L-alanine was added dropwise as a feeding attractant. The feed for the control group was treated only with the L-alanine solution. The feeding experiment was started on a Monday, and fish were fed every Monday, Wednesday, and Friday for a total of seven feedings at a rate of 2% of body weight per day; as a result, each fish ingested approximately 140 μl per individual per day of each fatty acid. The experiment was performed twice, and the total number of fish in each group ranged from four to six individuals. Sampling was conducted 24 h after the final feeding (day 16, which was the third Tuesday morning). The fish were anesthetized in 0.01% aqueous ethyl *p*-aminobenzoate (Wako Pure Chemical Industries, Osaka, Japan), and stomach were dissected out, rinsed with saline (0.9% NaCl), cut longitudinally, and frozen. The stomach samples were kept at −80°C until use. The stomach samples collected as described in this section were used for purification of ghrelin (stomach weights: normal feed, 12.4 g; C7-enriched feed, 7.6 g; C8-enriched feed, 10.5 g; C9-enriched feed, 14.5 g) as described above and for profiling of ghrelin in each stomach by reverse-phase HPLC as described below.

PROFILING OF BARFIN FLOUNDER GHRELIN IN STOMACH SAMPLES

Peptide components were extracted from frozen stomach samples, approximately 1 g, from each fish (normal feed, $n = 4$; C7-enriched feed, $n = 4$; C8-enriched feed, $n = 6$; C9-enriched feed, $n = 6$) as described earlier. Each resulting stomach extract (equivalent to 100 mg of tissue) was placed on a Sep-Pak Plus C18 column and eluted with 60% acetonitrile containing 0.1% TFA. The eluate was subjected to reverse-phase HPLC on a Symmetry300 C18 column; the eluent was a linear gradient of acetonitrile containing 0.1% TFA (10–60% over 80 min; flow rate, 1 ml/min). To confirm the elution times of the isolated peptides, we also subjected representative isolated native barfin flounder ghrelin to reverse-phase HPLC under the same conditions used for the stomach extracts. Fractions (1 ml/tube) were collected starting 30 min after injection, and ghrelin activity in the fractions was measured by means of Ca^{2+} mobilization assay with CHO-GHSR62 cells.

QUANTITATIVE PCR FOR BARFIN FLOUNDER GHRELIN mRNA IN THE STOMACH

To evaluate the effect of fatty acid ingestion on ghrelin mRNA expression in the stomach, we conducted quantitative PCR for ghrelin. A ghrelin fragment (337 bp) was amplified from stomach cDNA by means of reverse-transcription PCR with a primer pair for ghrelin (BarfinGHRL Q-s: 5′-AGC TGC TGG TTT TTC TAC TCT GTT-3′; BarfinGHRL Q-AS: 5′-AAA GGT AAA TCT GCC ATT CTT GTC-3′). As an internal control, β-actin (629 bp) was quantified with a primer pair (BarfinB-actin-s: 5′-TGA AGT ACC CCA TCG AGC AC-3′; BarfinB-actin-AS: 5′-TAC AGG TCC TTA CGG ATG TC-3′). Quantitative PCR was performed with a LightCycler 480 instrument (Roche Applied Science, Mannheim, Germany) and a QuantiFast SYBR Green PCR Kit (QIAGEN). The amplification conditions were as follows: 95°C for 5 min followed by 40 cycles at 95°C for 10 s and 60°C for 30 s. The reaction mixture consisted of 1× master mix, the two primers (250 nM each), and a template (equivalent to 100 ng of total RNA) prepared by QuantiTect Reverse-Transcription Kit (QIAGEN). For quantification of mRNA copy numbers, a linear regression line was generated using a serially diluted pCRII vector containing each cloned cDNA fragment that was linearized by restriction with *Xba*I.

STATISTICAL ANALYSES

In the experiment on profiling of ghrelin in stomach extracts, the values for each group were compared to the control values by analysis of variance followed by Fisher's protected least significant difference test. For comparison of ghrelin mRNA expression in the stomach, non-parametric Mann–Whitney *U* test was applied. Differences were considered significant at $P < 0.05$.

RESULTS

STRUCTURE OF BARFIN FLOUNDER GHRELIN

By means of cDNA cloning, we isolated four different barfin flounder ghrelin cDNAs (**Figure 1**): (1) a 948-bp cDNA that

A

```
        10        20        30        40        50        60        70        80        90
GTTTAAGGTCCACTAACTCAGGGGATCAAACCACCAACCTTTTGGCCCGTGGACGACCCACTTATCCACAGCCGCCCCCTTATATGCCTC
       100       110       120       130       140       150       160       170       180
AGTGTAAATTCAAATGCGGAGACTCTGGTTCCACCATGTTTTTGAAAAGAAACACCCAGCTGCTGGTTTTTCTACTCTGTTCTCTGACCT
                                    M  F  L  K  R  N  T  Q  L  L  V  F  L  L  C  S  L  T
       190       200       210       220       230       240       250       260       270
TGTGGTGCAAGTCGACCAGCGCAGGCTCCAGTTTCCTCAGCCCTTCACACAAACCTCCGAACAAGGGGAAACCTCCGAGAGCCGGCCGCC
L  W  C  K  S  T  S  A  G  S  S  F  L  S  P  S  H  K  P  P  N  K  G  K  P  P  R  A  G  R
       280       290       300       310       320       330       340       350       360
AAATCACGGAGGAGCAGAGTCAACCCACTGAGGACCACCCCATCACTcagGTGAGTGCCCCATTTGAAATTGGCATCACCATGACACCGG
Q  I  T  E  E  Q  S  Q  P  T  E  D  H  P  I  T  Q  V  S  A  P  F  E  I  G  I  T  M  T  P
       370       380       390       400       410       420       430       440       450
AGGACTTTGAGGAGTACGGCGCGTTGCTGCAAGAGATCGTTCAGCGTCTGCTGGGAAACACGGAGGCAGCAGAGAGACCATCTTAACTTT
E  D  F  E  E  Y  G  A  L  L  Q  E  I  V  Q  R  L  L  G  N  T  E  A  A  E  R  P  S  *
       460       470       480       490       500       510       520       530       540
GAATATTATGGACAAGAATGGCAGATTTACCTTTTCATTTCTTTAAATTTCTACTTCATTAGATAGTGATCATTGAAATATGAGTAAAAG
       550       560       570       580       590       600       610       620       630
TGTCAGTTGCCTTAAAA CATTGTTACTCACACTGTTGGTAGTTAATCTGTTCATCAAGTGAAACTATGAGTAAGTCTATTTTCAGAGCTT
       640       650       660       670       680       690       700       710       720
TCAACCACATCTCAGTGCCACCATCAGTGATGGAGATGGTTGTGTTAAAAATAATAAAGAAGTTAATATCAATTCAATATTGATATATAT
       730       740       750       760       770       780       790       800       810
ATAAAACTTGAGTTTGAATTAATTTGTCAAACTATGGTTCTCATTCATAAACTTAGTGATGAGATTTAAGTCTCACATAGGCTTCCATTA
       820       830       840       850       860       870       880       890       900
TTAGGTCACCGTCATCTGACATTTAACACATTTAAATATTTAAAGATCTACACCCACTCTGCAGTATAGAATATAACTTAAGTCTTTATT
       910       920       930       940
TGTCTTCAGAGACTTACATGTAGTGGTAAAAATAAAGCATCAACTGAC
```

B

```
        10        20        30        40        50        60        70        80        90
GTTTAAGGTCCACTAACTCAGGGGATCAAACCACCAACCTTTTGGCCCGTGGACGACCCACTTATCCACAGCCGCCCCCTTATATGCCTC
       100       110       120       130       140       150       160       170       180
AGTGTAAATTCAAATGCGGAGACTCTGGTTCCACCATGTTTTTGAAAAGAAACACCCAGCTGCTGGTTTTTCTACTCTGTTCTCTGACCT
                                    M  F  L  K  R  N  T  Q  L  L  V  F  L  L  C  S  L  T
       190       200       210       220       230       240       250       260       270
TGTGGTGCAAGTCGACCAGCGCAGGCTCCAGTTTCCTCAGCCCTTCACACAAACCTCCGAACAAGGGGAAACCTCCGAGAGCCGGCCGCC
L  W  C  K  S  T  S  A  G  S  S  F  L  S  P  S  H  K  P  P  N  K  G  K  P  P  R  A  G  R
       280       290       300       310       320       330       340       350       360
AAATCACGGAGGAGCAGAGTCAACCCACTGAGGACCACCCCATCACTcagGTGAGTGCCCCATTTGAAATTGGCATCACCATGACACCGG
Q  I  T  E  E  Q  S  Q  P  T  E  D  H  P  I  T  Q  V  S  A  P  F  E  I  G  I  T  M  T  P
       370       380       390       400       410       420       430       440       450
AGGACTTTGAGGAGTACGGCGCGTTGCTGCAAGAGATCGTTCAGCGTCTGCTGGGAAACACGGAGGCAGCAGAGAGACCATCTTAACTTT
E  D  F  E  E  Y  G  A  L  L  Q  E  I  V  Q  R  L  L  G  N  T  E  A  A  E  R  P  S  *
       460       470       480       490       500       510       520       530       540
GAATATTATGGACAAGAATGGCAGATTTACCTTTTCATTTCTTTAAATTTCTACTTCATTAGATAGTGATCATTGAAATATGAGTAAAAG
       550
TGTCAGTTGCCTTAAAA
```

FIGURE 1 | Nucleotide and deduced amino acid sequences of barfin flounder ghrelins. The asterisk indicates the termination codon, the box indicates the sequence of the mature ghrelin, and the underlining indicates the polyadenylation signal (AATAAA). Four different cDNAs were obtained: **(A)** a 948-bp cDNA (acc. no. AB823534) and a 945-bp variant missing the codon for Q65 (acc. no. AB824842) and **(B)** a 557-bp cDNA missing the nucleotides italicized in **(A)** (acc. no. AB824843) and a 554-bp cDNA missing the italicized nucleotides and the codon for Q65 (acc. no. AB824844).

encodes a 106-aa prepro-ghrelin (acc. no. AB823534, **Figure 1A**); (2) a 945-bp cDNA that encodes des-Q65 prepro-ghrelin, which has 105 aa and lacks the 65th glutamine of the 106-aa prepro-ghrelin (acc. no. AB824842, **Figure 1A**); (3) a 557-bp cDNA that encodes a 106-aa prepro-ghrelin but lacks part of the 3′-untranslated region of AB823534 (acc. no. AB824843, **Figure 1B**), and (4) a 554-bp cDNA that encodes des-Q65 prepro-ghrelin but lacks part of the 3′-untranslated region of AB823534 (acc. no. AB824844, **Figure 1B**). These cDNAs encoded identical mature ghrelins.

On the basis of sequence homology with the ghrelins of other fish, the barfin flounder ghrelin was predicted to be a 20-aa peptide (GSSFLSPSHKPPNKGKPPRA) with a C-terminal amide structure. Phylogenetic analysis revealed that the barfin flounder ghrelin belongs to the evolutionarily most advanced group of Teleostei, which includes Perciformes and Gasterosteiformes (**Figure 2**), and shows the highest identity (93.4%) to Atlantic halibut ghrelin.

IDENTIFICATION OF GHRELIN IN THE STOMACH OF FISH FED A NORMAL FEED

Fractions obtained by means of CM ion-exchange HPLC of stomach extracts of barfin flounder fed a normal feed were divided into seven groups (a–g) on the basis of their ghrelin activity

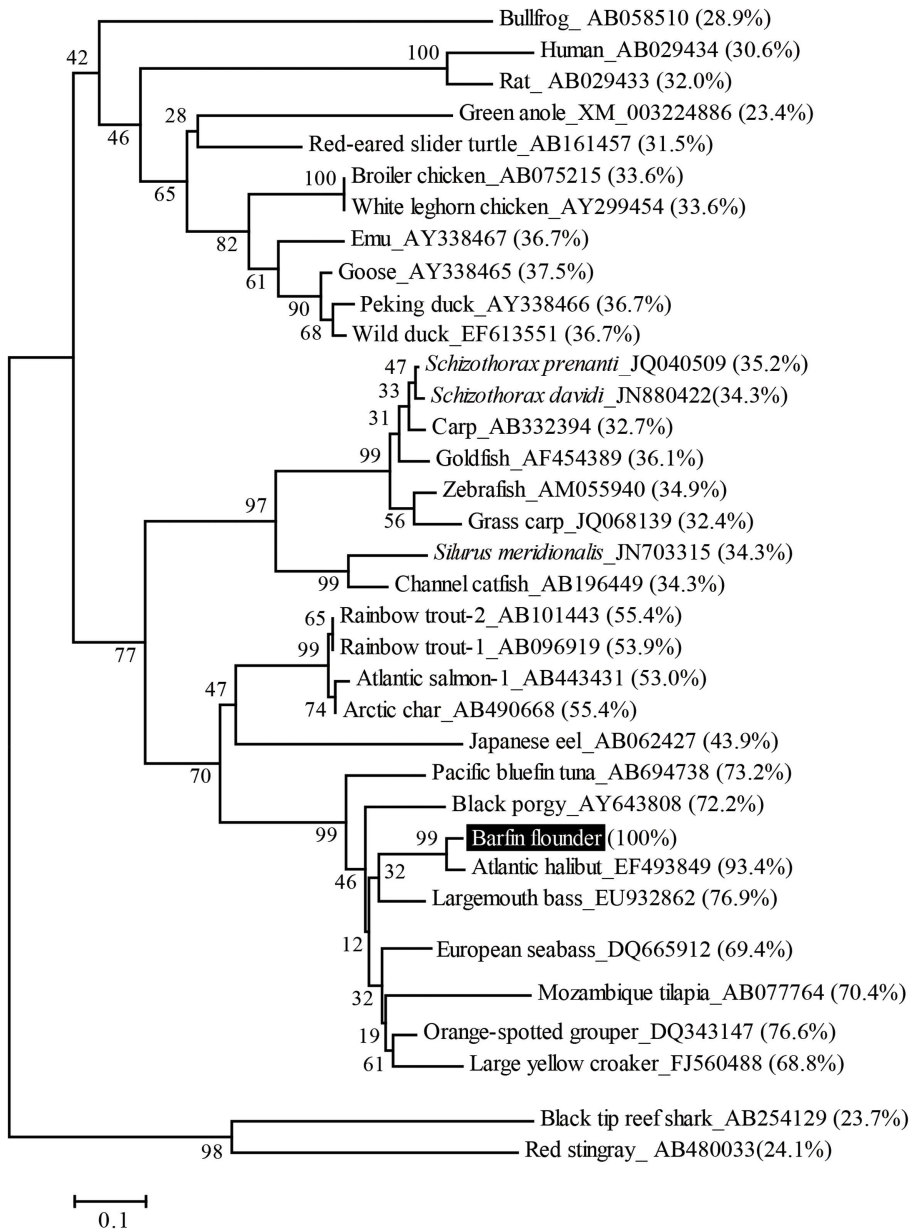

FIGURE 2 | Phylogenetic analysis of the barfin flounder prepro-ghrelin. The phylogenetic tree was generated by means of the NJ method of the MEGA4 software package (http://www.megasoftware.net/). The GenBank accession numbers follow the species names, the percentages in parentheses indicate amino acid identities to the barfin flounder prepro-ghrelin, and the numbers at the branch points represent bootstrap values (1000 repetitions).

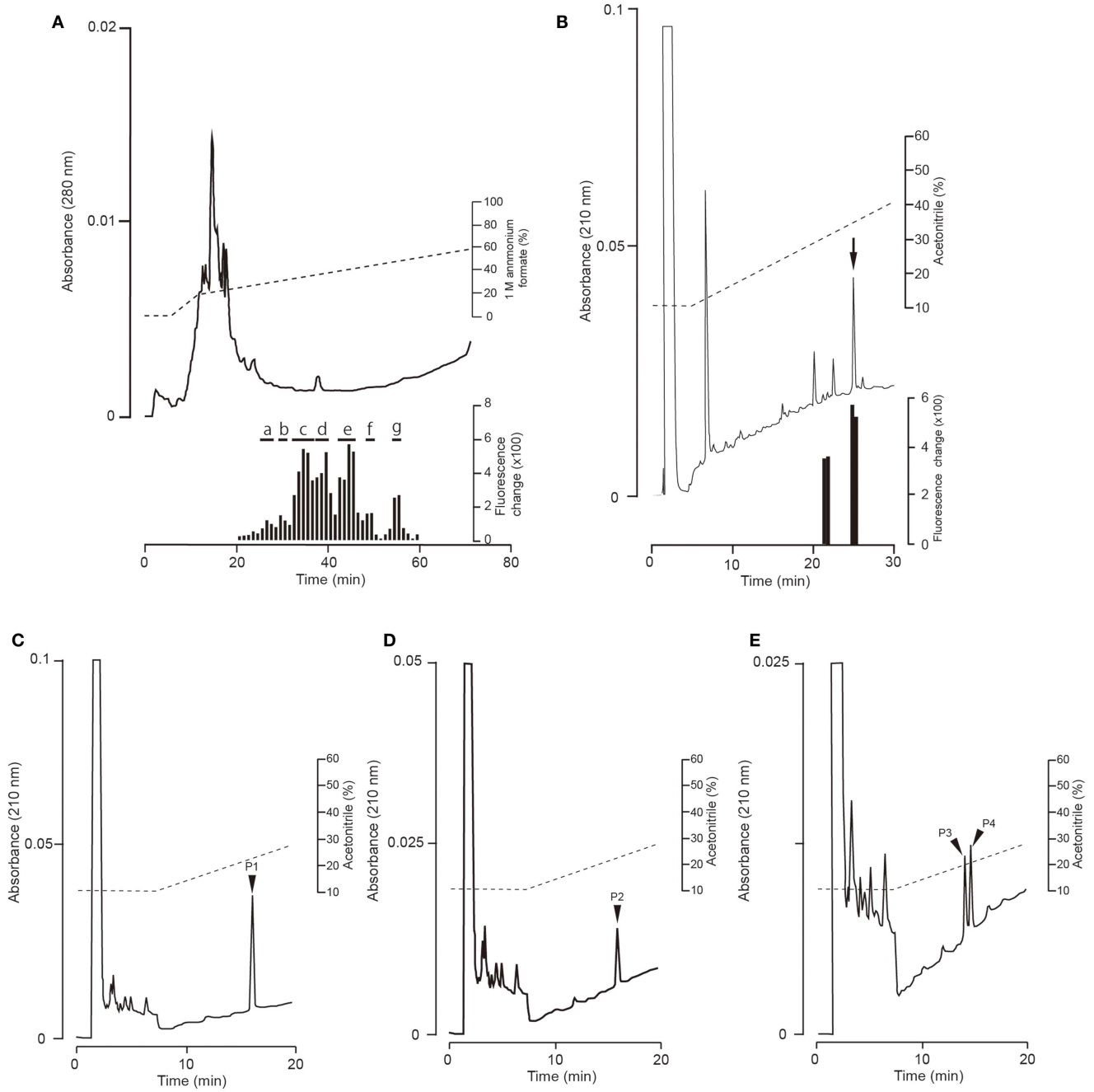

FIGURE 3 | Representative absorption spectra and activity data obtained at various points during the purification of ghrelin from the stomach of barfin flounder fed normal feed. **(A)** Carboxyl methyl ion-exchange HPLC. Black bars indicate ghrelin activity measured using CHO cells expressing rat GHS-R1a. The fractions were divided into groups a–g on the basis of ghrelin activity. **(B)** Reverse-phase HPLC of group "e" on a symmetry 300 C18 column. The arrow indicates the major peak. **(C)** Reverse-phase HPLC of group "e" on a diphenyl column. The peak labeled P1 corresponds to the peak indicated by the arrow in **(B)**; this peak corresponds to the peptide obtained in the highest yield from the stomach of fish fed normal feed. **(D)** The peptide (P2) obtained in the second highest yield (isolated from group "g"). **(E)** The peptides (P3 and P4) obtained in the third and fourth highest yields (isolated from group "c").

(**Figure 3A**). The group "e" fractions were subjected to preparative reverse-phase HPLC on a symmetry column (**Figure 3B**) and then to reverse-phase HPLC on a diphenyl column (**Figure 3C**) to afford peptide P1, which was the peptide obtained in the highest yield. The peptides obtained in the second (P2) and the third and fourth highest yields (P3 and P4, respectively) were isolated from the group "g" and group "c" fractions, respectively (**Figures 3D,E**, respectively).

The amino acid sequence of peptide P1 was determined to be GSXFLSPSHKPPNKGKP (X was not detected). This sequence corresponded to 17 of the amino acid residues in the 20-aa sequence of the barfin flounder ghrelin (GSSFLSPSHKPPNKGKP^{17}PRA) deduced from cDNA. Thus, we concluded that the isolated peptide was the barfin flounder ghrelin and that the undetected third aa was a serine. Subsequent mass spectrometric analysis of peptide P1 revealed that its molecular weight $[M+H]^+$ was 2172.06, and the molecular form corresponded to decanoylated ghrelin with 19 aas [GSS(C10:0)FLSPSHKPPNKGKPPR]; the last alanine from the 20-aa peptide was missing. This result indicates that the major form of ghrelin isolated from the barfin flounder stomach extracts was slightly different from the form deduced from the cDNA sequence. The molecular forms of the other peptides isolated from in the stomach of fish fed a normal feed (Cont) are summarized in **Table 1**. Peptide P2 was determined to be a C-terminal amidated 20-aa peptide with C10 modification, and P3 and P4 were determined to be, respectively, a C8-modified 19-aa peptide and an adduct of a C8-modified 19-aa peptide and sodium-like ion with a 24 *m*/*z*.

DETERMINATION OF MOLECULAR FORM OF GHRELIN IN THE STOMACH OF FISH FED FATTY ACID-CONTAINING FEED

We found that gastric expression of ghrelin in fish fed fatty acid-containing feed was not significantly different from expression in control fish that were fed normal feed; the mean mRNA copy numbers $\times 10^4 \pm$ SEMs were as follows: controls, 6.57 ± 2.91 ($n = 4$); C7-enriched feed, 3.31 ± 0.77 ($n = 4$); C8-enriched feed, 4.29 ± 0.91 ($n = 6$); C9-enriched feed, 5.17 ± 1.48 ($n = 6$).

We compared the distributions of ghrelin activity in CM ion-exchange HPLC fractions obtained from fish that were fed C7-, C8-, and C9-enriched feeds (**Figure 4**). Fish that ingested C7 showed lower total ghrelin activity (**Figure 4B**) than control fish (**Figure 4A**), but the two distribution profiles differed only slightly. In contrast, in fish that ingested C8, ghrelin activities of the fractions that eluted from 33 to 36 min (group o) and from 43 to 46 min (group q) were much higher than activities of the corresponding fractions for the control fish, whereas the activities of the fractions that eluted from 55 to 56 min (group r) were lower (**Figure 4C**). The greatest change in the distribution profile was observed for fish that ingested C9 (**Figure 4D**); the ghrelin activities in the fractions that eluted from 30 to 31 min (group s), from 38 to 41 min (group u), and from 49 to 50 min (group w) were substantially higher than the activities for the controls, but activities in the fractions that eluted from 35 to 37 min (group t) and from 45 to 46 min (group v) were lower than the activities for the controls.

Table 1 summarizes the molecular weights and expected forms of the ghrelin peptides isolated from the groups of fractions shown in **Figure 4**. From the fish that ingested the C7-enriched feed, the peptide obtained in the highest yield was a 19-aa peptide with a C10 modification, as was the case for the control fish. The purified peptide eluted from 45 to 47 min (group k), which was nearly the same as the elution time for the peptide obtained in the highest yield from the control fish (group e). We looked for different groups, but were unable to identify a peptide modified by C7. From the fish that ingested the C8-enriched feed, the most abundant peptide was a 19-aa peptide with a C8 modification, which was isolated from fractions that eluted from 33 to 37 min (group o). From the fish that ingested the C9-enriched feed, the most abundant peptide was a 19-aa peptide with a C9 modification, which was isolated from fractions that eluted from 38 to 41 min (group u).

DISTRIBUTION OF GHRELIN ACTIVITY IN FRACTIONS OBTAINED FROM STOMACH EXTRACTS OF CONTROL FISH AND FISH FED FATTY ACID-CONTAINING FEED

In this experiment, stomach extracts (equivalent to 100 mg of tissue) from control fish or fish fed fatty acid-enriched feed was subjected to reverse-phase HPLC only, without further purification, and ghrelin activities in the separated fractions were compared (**Figure 5**). Ghrelin activities were significantly higher in the 32-min fraction of the C7-enriched group, the 35-min fraction of the C8-enriched group, and the 37-, 39-, 40-, and 43-min fractions of the C9-enriched group compared to the activities in the corresponding fractions of the control fish. These elution times correspond to the elution time of the most abundant molecular form of ghrelin isolated from each group.

DISCUSSION

We determined the nucleotide sequence of ghrelin cDNA in the barfin flounder for the first time. From the cDNA sequence, the mature peptide was predicted to be a 20-aa peptide (GSSFLSPSHKPPNKGKPPRA) with an amide structure at the C-terminus, and the expected 20-aa peptide was in fact isolated from the stomach extracts of fish fed a normal diet. However, the peptide isolated in the highest yield was a 19-aa peptide (GSSFLSPSHKPPNKGKPPR) lacking the last alanine. This result is similar to results reported for goldfish ghrelin (20). A possible mechanism for the lack of alanine is due to an effect of arginine endopeptidase, trypsin, for the proteolytic processing. However, the detail mechanisms are unclear.

The 19-aa ghrelin was modified not with C8, which is the usual acyl modification of ghrelin, but with C10 (1). This result is not completely unprecedented: C10-modified ghrelin has occasionally been identified in non-mammalian vertebrates (14–17, 19, 21), and a C10-modified ghrelin is the major form in Mozambique tilapia (18). C10-modified ghrelin is also present in mammals (25, 26). In this study, we also detected ghrelin peptides acylated with C8, C9, and unsaturated decanoic acids (C10:1 and C10:2). Modification of ghrelin with various fatty acids has been known in other fish and animals not having been limited to barfin flounder. In the barfin flounder, however, C9 appears to be a substrate for ghrelin acylation, even though acylation with C9 is rare in other vertebrates, except cats and goats (27, 28).

In previous studies of neonatal chicks that had not yet begun to eat feed, the expression of ghrelin mRNA was detected, while the production of acylated ghrelin was not (24, 29). This result strongly suggests that expression of the ghrelin gene is unaffected by feeding, and that fatty acids (substrates) in feed are involved in ghrelin acylation. In the present study, we found that expression of the ghrelin gene was unaffected by the addition of fatty acids to feed. Similar results have been reported in mice (9) and chickens (24). It is likely that intake of fatty acid does not affect the gastric expression of the ghrelin gene in vertebrates.

Table 1 | Masses and expected molecular forms of ghrelins purified from barfin flounder stomach extracts by carboxymethyl ion-exchange HPLC.

Feed group[1]	HPLC fraction group (elution time, min)[2]	Actual mass $[M+H]^+$	Expected ghrelin form	Abundance[3]
Cont	c (33–37)	2144.12	19-(C8:0)	△
		2272.17	21-(C8:0)	
		2168.03	19-(C8:0) + 24	△
		2296.07	21-(C8:0) + 24	
	d (38–40)	2158.04	19-(C9:0)	
		2170.04	19-(C10:1)	
		2286.09	21-(C9:0)	
		2298.09	21-(C10:1)	
		2170.04	19-(C10:1)	
		2298.09	21-(C10:1)	
	e (43–46)	2214.19	20-(C8:0)-amide	
		2238.10	20-(C10:2)-amide	
		2172.06	19-(C10:0)	◎
	f (49–50)	2228.09	20-(C9:0)-amide	
		2240.09	20-(C10:1)-amide	
		2240.10	20-(C10:1)-amide	
	g (55–56)	2242.12	20-(C10:0)-amide	◯
C7	h (35–37)	2144.02	19-(C8:0)	
		2188.05	19-(C10:1) + 17	
	i (38–40)	2170.03	19-(C10:1)	△
		2298.07	21-(C10:1)	
	j (42–45)	2300.08	21-(C10:0)	◯
	k (45–47)	2172.04	19-(C10:0)	◎
	l (48–50)	2240.09	20-(C10:1)-amide	
	m (55–56)	2242.09	21-(C10:0)-amide	◯
C8	o (33–37)	2146.02	19-(C8:0)	◎
		2272.06	21-(C8:0)	
	p (39–41)	2157.98	19-(C9:0)	
		2170.03	19-(C10:1)	
		2170.03	19-(C10:1)	
	q (43–46)	2242.09	20-(C10:0)-amide	△
	r (55–56)	2214.07	20-(C8:0)-amide	◯
		2172.03	19-(C10:0)	◯
C9	s (30–31)	2159.02	19-(C9:0) + 1	
		2001.95	18-(C9:0)	
	t (35–37)	2144.02	19-(C8:0)	
		2168.02	19-(C10:2)	
		2286.09	21-(C9:0)	△
	u (38–41)	2158.03	19-(C9:0)	◎
	v (45–46)	2172.04	19-(C10:0)	◯
	w (49–50)	2228.07	20-(C9:0)-amide	◯

[1] Cont, normal feed; C7, feed enriched with n-heptanoic acid; C8, feed enriched with n-octanoic acid; C9, feed enriched with n-non-anoic acid.

[2] Carboxymethyl ion-exchange HPLC fractions were grouped on the basis of ghrelin activity.

[3] Fractions containing the peptides obtained in the (◎) highest, (◯) second highest, and (△) third highest yields.

Different fatty acids cause alteration in the ghrelin protein levels of the stomach as observed by analyses used reverse-phase HPLC or ion-exchange HPLC of stomach extracts (**Figures 4** and **5**), and the use of different fatty acids in the feed resulted in the identification of different ghrelin molecules (**Table 1**). The present study showed that in fish given feed containing C8 or C9, ghrelins modified with these fatty acids were the major form in the stomach. In contrast, C10-ghrelin was the major form in fish fed normal feed. This result clearly indicates that dietary fatty acids were substrates for ghrelin acylation in fish, as is the case for mice and chickens.

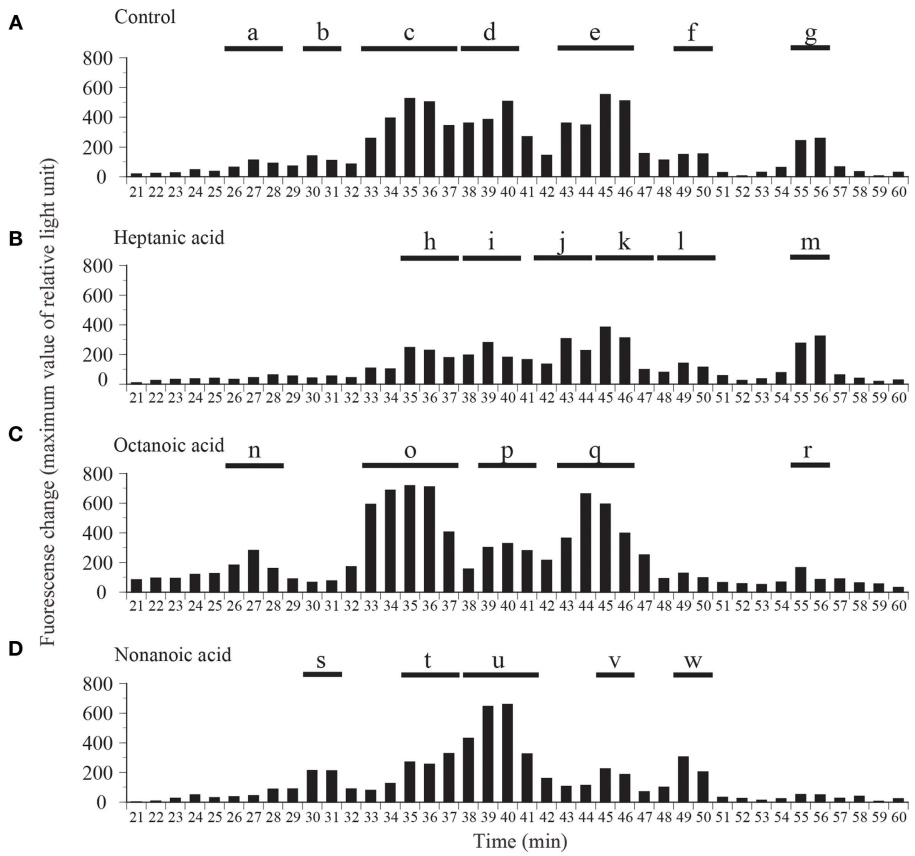

FIGURE 4 | Distribution of ghrelin activity in fractions separated by ion-exchange HPLC of samples obtained from fish fed (A) normal feed, (B) *n*-heptanoic acid (C7)-enriched feed, (C) *n*-octanoic acid (C8)-enriched feed, and (D) *n*-non-anoic acid (C9)-enriched feed. The fractions were assigned to groups a–w on the basis of their ghrelin activity. Ghrelin activity in the equivalent of 400 mg stomach tissue is expressed in terms of fluorescence change in CHO cells expressing rat GHS-R1a The maximum changes in fluorescence are plotted.

In a previous study by Nishi et al. (9), *n*-heptanoyl ghrelin, an unnatural form of ghrelin, has been isolated in the stomach of mice after ingestion of either *n*-heptanoic acid or glyceryl triheptanoate. In the present study, ghrelin modified by C7 did not identify in the stomach of fish fed control diet, indicating that C7-ghrelin is an unnatural form. In this study, C7-enriched diet was given to barfin flounder, and all the fish ate the same amount of food. However, we could not isolate ghrelin modified with C7. A possible reason is that hat there was not enough C7-ghrelin content to isolate. Meanwhile, C7-ghrelin-like activity could be detected in the analysis of the stomach extract ingested C7 that used reverse-phase HPLC. The reason of the success is probably that this analysis was not subjected to any purification processes other than reverse-phase HPLC, and it prevented a loss of peptide in the purification processes. The result detected an unnatural form C7-ghrelin in this study further supports that dietary fatty acids were substrates for ghrelin acylation in fish. In this study, C9-ghrelin was purified not only in fish fed C9-enriched feed but also in fish fed normal feed. As described earlier, ghrelin acylation with C9 is rare in other vertebrates. Therefore, this result observed in the barfin flounder came from the reason that C9 could be basically used for ghrelin acylation.

It would be helpful if the effect of the diets with increasing the chain length of fatty acids (e.g., C16 and C18) on acylation of ghrelin was tested. We did not perform such an experiment in this study. Nishi et al. (9) observed that neither *n*-butyryl (C4) nor *n*-palmitoyl (C16) ghrelin is detected when mice are given short-chain triacylglyceride glyceryl tributyrate or glyceryl tripalmitate, suggesting short- or long-chain fatty acids are not used for ghrelin acylation. Ohgusu et al. (30) used recombinant GOAT and demonstrated that GOAT did not modify des-acyl ghrelin with long-chain fatty acids such as *n*-palmitoyl-CoA, and *n*-myristoyl-CoA *in vitro*. This result also shows that middle-chain fatty acids derived from the degradation of C16 or C18 fatty acids do not involve in ghrelin acylation.

In CM ion-exchange HPLC, we observed that when the ghrelin activity in one fraction increased, the activity in other fractions decreased. For example, we observed a substantial difference between the distribution of ghrelin activity in fish that ingested C9 (**Figure 4D**) and the distribution in control fish (**Figure 4A**). Similar results have been observed in mice: ingestion of C6:0-medium-chain triacylglycerols increases the amount of C6-ghrelin but decreases the amount of C8-ghrelin (9). This result suggests that GOAT has a finite catalytic capacity. In addition, we observed

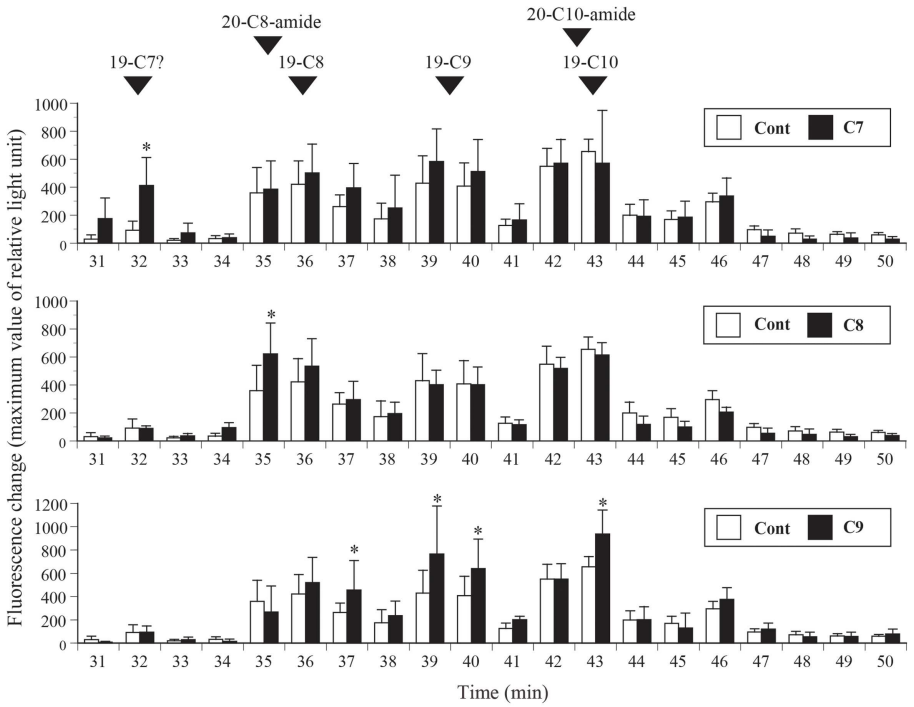

FIGURE 5 | Distribution of ghrelin activity in fractions separated by reverse-phase HPLC. Ghrelin activity in the equivalent of 100 mg stomach tissue is expressed in terms of fluorescence change in CHO cells expressing rat GHS-R1a. The maximum changes in fluorescence are plotted. The numbers of samples used are as follows: control (Cont, $n = 4$); *n*-heptanoic acid (C7)-enriched feed ($n = 4$); *n*-octanoic acid (C8)-enriched feed ($n = 6$); and *n*-non-anoic acid (C9)-enriched feed ($n = 6$). The values for each group were compared to the control values by analysis of variance followed by Fisher's protected least significant difference test. Differences were considered significant at $P < 0.05$. The elution times of isolated native barfin flounder ghrelin, C8-ghrelin with 19 amino acids (aas) (19-C8), C9-ghrelin with 19 aas (19-C9), C10-ghrelin with 19 aas (19-C10), C8-ghrelin with 20 aas and C-terminal amidation (20-C8-amide), and C10-ghrelin with 20 aas and C-terminal amidation (20-C10-amide) are indicated by arrowheads. The expected elution time of C7-ghrelin with 19 aas (19-C7) is also indicated; the time is based on the results for 19-C8, 19-C9, and 19-C10.

that total ghrelin activity decreased when C7 was given to fish, suggesting that C7 might inhibit enzymatic activity.

Currently, the only fish for which the GOAT sequence is available is the zebrafish. Shlimun and Unniappan (11) have indicated which aa are essential for the catalytic activity of GOAT in mammals and fish. Ohgusu et al. (30) reported that the four aa at the N-terminal of ghrelin (GSSF) constitute the minimum core motif required for substrate recognition of GOAT. Because this core sequence is conserved in the ghrelin of the barfin flounder, it is likely that a GOAT-like enzyme plays a role in ghrelin acylation, although the detailed mechanisms remain to be elucidated.

In summary, we determined for the first time the primary structure of ghrelin peptides in the barfin flounder and found that ingestion of various fatty acids affected ghrelin acylation in these fish, as is the case in mice and chickens. This result indicates that the mechanism by which fatty acids in foods are used for post-transcriptional modification of ghrelin peptides and the mechanism by which modification regulates the biological activity of the peptide are conserved between fish and mammals. The possession of this post-transcriptional mechanism in vertebrates may explain why they were able to acquire ingenious and complicated processes for strict regulation of lipids and glucose.

ACKNOWLEDGMENTS

We thank Ms. K. Nakaya for assistance with feeding fish, sampling, and taking measurements, and Mrs. Azumi Ooyama for excellent technical assistance. Hiroyuki Kaiya, Kenji Kangawa, and Mikiya Miyazato were supported by a Grant-in-Aid for Scientific Research (KAKENHI) from MEXT of Japan, and by the Takeda Science Foundation.

REFERENCES

1. Kojima M, Hosoda H, Date Y, Nakazato M, Matuso H, Kangawa K. Ghrelin is a growth-hormone-releasing acylated peptide. *Nature* (1999) **402**:656–60. doi:10.1038/45230
2. Kaiya H, Kojima M, Hosoda H, Koda A, Yamamoto K, Kitajima Y, et al. Bullfrog ghrelin is modified by *n*-octanoic acid at its third threonine residue. *J Biol Chem* (2001) **276**:40441–8. doi:10.1074/jbc.M105212200
3. Gutierrez JA, Solenberg PJ, Perkins DR, Willency JA, Knierman MD, Jin Z, et al. Ghrelin octanoylation mediated by an orphan lipid transferase. *Proc Natl Acad Sci U S A* (2008) **105**:6320–5. doi:10.1073/pnas.0800708105
4. Yang J, Brown MS, Liang G, Grishin NV, Goldstein JL. Identification of the acyltransferase that octanoylates ghrelin, an appetite-stimulating peptide hormone. *Cell* (2008) **132**:387–96. doi:10.1016/j.cell.2008.01.017

5. Sakata I, Yang J, Lee CE, Osborne-Lawrence S, Rovinsky SA, Elmquist JK, et al. Colocalization of ghrelin *O*-acyltransferase and ghrelin in gastric mucosal cells. *Am J Physiol Endocrinol Metab* (2009) **297**:E134–41. doi:10.1152/ajpendo.90859.2008
6. Kang K, Zmuda E, Sleeman MW. Physiological role of ghrelin as revealed by the ghrelin and GOAT knockout mice. *Peptides* (2011) **32**:2236–41. doi:10.1016/j.peptides.2011.04.028
7. Kojima M, Ida T, Sato T. Structure of mammalian and nonmammalian ghrelins. *Vitam Horm* (2008) **77**:31–46. doi:10.1016/S0083-6729(06)77003-0
8. Hosoda H, Kojima M, Mizushima T, Shimizu S, Kangawa K. Structural divergence of human ghrelin. Identification of multiple ghrelin-derived molecules produced by post-translational processing. *J Biol Chem* (2003) **278**:64–70. doi:10.1074/jbc.M205366200
9. Nishi Y, Hiejima H, Hosoda H, Kaiya H, Mori K, Fukue Y, et al. Ingested medium-chain fatty acids are directly utilized for the acyl modification of ghrelin. *Endocrinology* (2005) **146**:2255–64. doi:10.1210/en.2004-0695
10. Kirchner H, Gutierrez JA, Solenberg PJ, Pfluger PT, Czyzyk TA, Willency JA, et al. GOAT links dietary lipids with the endocrine control of energy balance. *Nat Med* (2009) **15**:741–5. doi:10.1038/nm.1997
11. Shlimun A, Unniappan S. Ghrelin *O*-acyl transferase: bridging ghrelin and energy homeostasis. *Int J Pept* (2011) **2011**:217957. doi:10.1155/2011/217957
12. Kaiya H, Miyazato M, Kangawa K, Peter RE, Unniappan S. Ghrelin: a multifunctional hormone in non-mammalian vertebrates. *Comp Biochem Physiol A Mol Integr Physiol* (2008) **149**:109–28. doi:10.1016/j.cbpa.2007.12.004
13. Kaiya H, Miyazato M, Kangawa K. Recent advances in the phylogenetic study of ghrelin. *Peptides* (2011) **32**:2155–74. doi:10.1016/j.peptides.2011.04.027
14. Kaiya H, Van der Gayten S, Kojima M, Hosoda H, Kitajima Y, Matsumoto M, et al. Chicken ghrelin: purification, cDNA cloning, and biological activity. *Endocrinology* (2002) **143**:3445–63. doi:10.1210/en.2002-220255
15. Kaiya H, Sakata I, Kojima M, Hosoda H, Sakai T, Kangawa K. Structural determination and histochemical localization of ghrelin in the red-eared slider turtle, *Trachemys scripta elegans*. *Gen Comp Endocrinol* (2004) **138**:50–7. doi:10.1016/j.ygcen.2004.05.005
16. Kaiya H, Kojima M, Hosoda H, Moriyama S, Takahashi A, Kawauchi H, et al. Peptide purification, cDNA and genomic DNA cloning, and functional characterization of ghrelin in rainbow trout. *Endocrinology* (2003) **144**:5215–26. doi:10.1210/en.2003-1085
17. Kaiya H, Kojima M, Hosoda H, Riley LG, Hirano T, Grau EG, et al. Amidated fish ghrelin: purification, cDNA cloning in the Japanese eel and its biological activity. *J Endocrinol* (2003) **176**:415–23. doi:10.1677/joe.0.1760415
18. Kaiya H, Kojima M, Hosoda H, Riley LG, Hirano T, Grau EG, et al. Identification of tilapia ghrelin and its effects on growth hormone and prolactin release in the tilapia, *Oreochromis mossambicus*. *Comp Biochem Physiol B Biochem Mol Biol* (2003) **135**:421–9. doi:10.1016/S1096-4959(03)00109-X
19. Kaiya H, Small BC, Lelania Bilodeau A, Shepherd BS, Kojima M, Hosoda H, et al. Purification, cDNA cloning, and characterization of ghrelin in channel catfish, *Ictalurus punctatus*. *Gen Comp Endocrinol* (2005) **143**:201–10. doi:10.1016/j.ygcen.2005.03.012
20. Miura T, Maruyama K, Kaiya H, Miyazato M, Kangawa K, Uchiyama M, et al. Purification and properties of ghrelin from the intestine of the goldfish, *Carassius auratus*. *Peptides* (2009) **30**:758–65. doi:10.1016/j.peptides.2008.12.016
21. Kawakoshi A, Kaiya H, Riley LG, Hirano T, Grau EG, Miyazato M, et al. Identification of a ghrelin-like peptide in two species of shark, *Sphyrna lewini* and *Carcharhinus melanopterus*. *Gen Comp Endocrinol* (2007) **151**:259–68. doi:10.1016/j.ygcen.2006.10.012
22. Fox BK, Riley LG, Dorough C, Kaiya H, Hirano T, Grau EG. Effects of homologous ghrelins on the growth hormone/insulin-like growth factor-I in the tilapia, *Oreochromis mossambicus*. *Zoolog Sci* (2007) **24**:391–400. doi:10.2108/zsj.24.391
23. Schwandt SE, Peddu SC, Riley LG. Differential roles for octanoylated and decanoylated ghrelins in regulating appetite and metabolism. *Int J Pept* (2010) **2010**:275804.
24. Yamato M, Sakata I, Wada R, Kaiya H, Sakai T. Exogenous administration of octanoic acid accelerates octanoylated ghrelin production in the proventriculus of neonatal chicks. *Biochem Biophys Res Commun* (2005) **333**:583–9. doi:10.1016/j.bbrc.2005.05.107
25. Nishi Y, Yoh J, Hiejima H, Kojima M. Structures and molecular forms of the ghrelin-family peptides. *Peptides* (2011) **32**:2175–82. doi:10.1016/j.peptides.2011.07.024
26. Yoh J, Nishi Y, Hosoda H, Tajiri Y, Yamada K, Yanase T, et al. Plasma levels of *n*-decanoyl ghrelin, another acyl- and active-form of ghrelin, in human subjects and the effect of glucose- or meal-ingestion on its dynamics. *Regul Pept* (2011) **167**:140–8. doi:10.1016/j.regpep.2010.12.010
27. Ida T, Miyazato M, Naganobu K, Nakahara K, Sato M, Lin XZ, et al. Purification and characterization of feline ghrelin and its possible role. *Domest Anim Endocrinol* (2007) **32**:93–105. doi:10.1016/j.domaniend.2006.01.002
28. Ida T, Miyazato M, Lin XZ, Kaiya H, Sato T, Nakahara K, et al. Purification and characterization of caprine ghrelin and its effect on growth hormone release. *J Mol Neurosci* (2010) **42**:99–105. doi:10.1007/s12031-010-9379-0
29. Wada R, Sakata I, Kaiya H, Nakamura K, Hayashi Y, Kangawa K, et al. Existence of ghrelin-immunopositive and -expressing cells in the proventriculus of the hatching and adult chicken. *Regul Pept* (2003) **111**:123–8. doi:10.1016/S0167-0115(02)00265-3
30. Ohgusu H, Shirouzu K, Nakamura Y, Nakashima Y, Ida T, Sato T, et al. Ghrelin *O*-acyltransferase (GOAT) has a preference for n-hexanoyl-CoA over *n*-octanoyl-CoA as an acyl donor. *Biochem Biophys Res Commun* (2009) **386**:153–8. doi:10.1016/j.bbrc.2009.06.001

Conflict of Interest Statement: The authors declare that the research was conducted in the absence of any commercial or financial relationships that could be construed as a potential conflict of interest.

Received: 16 July 2013; paper pending published: 01 August 2013; accepted: 20 August 2013; published online: 03 September 2013.
*Citation: Kaiya H, Andoh T, Ichikawa T, Amiya N, Matsuda K, Kangawa K and Miyazato M (2013) Determination of ghrelin structure in the barfin flounder (Verasper moseri) and involvement of ingested fatty acids in ghrelin acylation. Front. Endocrinol. **4**:117. doi: 10.3389/fendo.2013.00117*
This article was submitted to Experimental Endocrinology, a section of the journal Frontiers in Endocrinology.